THE UNIVERSITY OF CHICAGO

IMPACT OF THE MICROBIOTA AND DERIVED METABOLITES ON SOLID ORGAN TRANSPLANT OUTCOME

A DISSERTATION SUBMITTED TO
THE FACULTY OF THE DIVISION OF THE BIOLOGICAL SCIENCES
AND THE PRITZKER SCHOOL OF MEDICINE
IN CANDIDACY FOR THE DEGREE OF
DOCTOR OF PHILOSOPHY

COMMITTEE ON IMMUNOLOGY

BY

MARTIN NICOLAS SEPULVEDA

CHICAGO, ILLINOIS

JUNE 2024

TABLE OF CONTENTS

List of Figures vi
Acknowledgements ix
Abstract xii
Chapter 1: Introduction 1
1.1 Alloimmune response: 1
1.1.1 Priming 1
1.1.2 Requirement of secondary lymphoid organs 2
1.1.3 Direct, indirect, semi-direct presentation 5
1.1.4 $CD4^+$ T cells and rejection 7
1.1.5 $CD8^+$ T cells and rejection 9
1.1.6 Monocytes and Macrophages 11
1.2 Microbiota 15
1.2.1 Impact of the microbiota on the immune system 16
1.2.2 Impact of the microbiota on alloimmunity and transplant outcome 19
1.2.3 Influence of microbial metabolites in organ transplantation 23
1.2.4 The microbiota and immunosuppressive drugs 26
1.2.5 The microbiota as a biomarker of transplant outcome or responsiveness to therapy 27
1.2.6 The microbiota as immunomodulating therapy 29
1.3 Conclusion 31
Chapter 2: Materials and Methods 32
2.1 Bacterial cultures 32
2.2 Mice 33
2.3 Antibiotic pre-treatment 34
2.4 *S. epi* painting 34
2.5 Short-chain fatty acid metabolomic profiling 35
2.6 DNA extraction and quantitative polymerase chain reaction 35
2.7 16S rDNA sequencing 37
2.8 Skin transplantation 38
2.9 Recipient bacteria immunizations 38
2.10 Butyrate treatment 38
2.11 Depleting antibody injections 39
2.12 Lymphocyte isolation 39
2.13 FTY720 injections 40
2.14 CFSE labeling 41
2.15 Adoptive transfer of Marilyn T cells 41
2.16 Ex vivo stimulation of T cells 41
2.17 Serum LPS measurement 42
2.18 LPS stimulation 42
2.19 Histology 43
2.20 Antibody staining and flow cytometry analysis 43
2.21 Metagenome analysis 44
2.22 Alpha Diversity Analysis 45
2.23 Beta Diversity Analysis 45
2.24 Bulk RNA-Seq acquisition and analysis 45
2.25 Statistical analysis 46

Chapter 3: Influence of the commensal microbiota on solid organ transplant outcome 47
3.1 Coordinated elimination of bacterial taxa optimally attenuates alloimmunity and prolongs allograft survival 47
3.1.1 Abstract..... 47
3.1.2 Introduction 48
3.1.3 Results 51
3.1.3.1 Targeting of distinct bacterial subgroups with various Abx combinations additively prolongs graft survival 51
3.1.3.2 Alloimmunity is most decreased by the broadest spectrum Abx cocktail 53
3.1.3.3 Microbial diversity is most reduced by VM and VMGKC..... 54
3.1.3.4 Targeting different bacterial subgroups with Abx combinations modifies microbial metabolic pathways..... 56
3.1.3.5 P. distasonis strain DFI 5.70 prolongs graft survival..... 59
3.1.4 Discussion..... 62
3.2 Oral administration of the commensal *Alistipes onderdonkii* prolongs allograft survival.. 65
3.2.1 Abstract..... 65
3.2.2 Introduction 65
3.2.3 Results 67
3.2.3.1 Intestinal presence of *A. onderdonkii* is associated with prolonged survival of minor mismatched skin grafts..... 67
3.2.3.2 Oral administration of *A. onderdonkii* DSM19147 is sufficient to prolong skin allograft survival in conventional mice..... 68
3.2.3.3 Gavage of *A. onderdonkii* DSM19147 reduces TNFα production in T cells, and antigen-presenting cells (APCs) and TNFα neutralization prolongs skin graft survival .. 70
3.2.3.4 *A. onderdonkii* DSM19147 harbors unique genes 72
3.2.4 Discussion..... 76
Chapter 4: Influence of skin-restricted microbiota on solid organ transplant outcome..... 79
4.1 Skin-restricted commensal colonization accelerates skin graft rejection..... 79
4.1.1 Abstract..... 79
4.1.2 Introduction 80
4.1.3 Results 81
4.1.3.1 Cutaneous *S. epi* colonization is sufficient to accelerate skin allograft rejection.. 81
4.1.3.2 *S. epi* colonization does not enhance the priming phase of the alloimmune response in the skin-draining LNs. 83
4.1.3.3 *S. epi* colonization enhances the effector phase of the alloimmune response in the allograft. 86
4.1.4 Discussion..... 91
4.2 Host-versus-commensal immune responses participate in the rejection of colonized solid organ transplants 93
4.2.1 Abstract..... 93
4.2.2 Introduction 93
4.2.3 Results 95

4.2.3.1 Skin graft recipients mount a T cell response to commensals on donor organs that is independent from the alloresponse. 95
4.2.3.2 Hosts with memory against commensals present on donated organs display strong damage of syngeneic skin grafts. 100
4.2.3.3 Anti-commensal memory T cells are required to damage colonized syngeneic skin grafts. 105
4.2.3.4 Host tissue-resident memory cells are sufficient to damage colonized syngeneic skin grafts. 108
4.2.4 Discussion 110
Chapter 5: Influence of microbial-derived metabolites on solid organ transplant outcome 115
5.1 Oral butyrate prolongs survival of distal skin allografts 115
5.1.1 Abstract 115
5.1.2 Introduction 115
5.1.3 Results 120
5.1.3.1 Oral ButM administration prolongs the survival of a distal skin allograft and modifies the microbiota composition 120
5.1.3.2 Butyrate micelle treatment results in a quantitative impact on the myeloid cell compartment at steady-state 124
5.1.3.3 ButM treatment reduces graft-infiltrating myeloid cells 134
5.1.3.4 Butyrate treatments results in a qualitative impact of the myeloid cell compartment at steady-state 135
5.1.3.5 CCR2 depletion protects allograft survival similar to ButM treatment 140
5.1.4 Discussion 144
Chapter 6: Discussion & Future Directions 148
6.1 Influence of the commensal microbiota on solid organ transplant outcome 148
6.2 Influence of skin-restricted microbiota on solid organ transplant outcome 162
6.3 Influence of the SCFA butyrate on solid organ transplant outcome 166
References 180

LIST OF FIGURES

SECTION 3.1

Figure 3.1. 1. Additive prolongation of graft survival and reduction of alloimmunity by cumulative targeting of different bacterial subgroups. 52
Figure 3.1. 2. Abx cocktails do not reduce TNFα production by Marilyn T cells. 54
Figure 3.1. 3. *P. distasonis* fecal bloom is common to all Abx cocktails. 55
Figure 3.1. 4. Coordinated elimination of major bacterial groups reshapes microbial metabolic pathways. 58
Figure 3.1. 5. Oral administration of *P. distasonis* strain DFI 5.70 prolongs skin allograft survival. 60
Figure 3.1. 6. Gavage of *P. distasonis* strain DFI 5.70 does not increase fecal bacterial load or *P. distasonis* abundance. 61

SECTION 3.2

Figure 3.2. 1. Enriched abundance of two taxa correlates with slower skin graft rejection in JAX compared with TAC mice. 68
Figure 3.2. 2. Oral administration of *Alistipes onderdonkii* DSM19147 prolongs skin allograft survival and reduces alloimmunity. 70
Figure 3.2. 3. Oral administration of *Alistipes onderdonkii* DSM19147 results in reduced tumor necrosis factor a (TNFα) production by immune cells. 72
Figure 3.2. 4. Heat-killed *A. oderdonkii* DSM19147 does not prolong skin graft survival. 73
Figure 3.2. 5. Comparison of fecal metabolomics. 74
Figure 3.2. 6. *Alistipes onderdonkii* DSM19147 harbors unique genes when compared with strains that do not prolong graft survival. 75

SECTION 4.1

Figure 4.1. 1. Cutaneous *S. epi* colonization is sufficient to accelerate skin allograft rejection. . 81
Figure 4.1. 2. *S. epi* colonized the skin but not the gut of oral vancomycin-treated gnotobiotic mice. 82
Figure 4.1. 3. Donor skin *S. epi* trends towards accelerating rejection of a fully mismatched skin graft. 83
Figure 4.1. 4. *S. epi* skin colonization does not change the composition or costimulatory molecule expression of LN APCs relative to GF APCs. 84
Figure 4.1. 5. Skin *S. epi* colonization does not enhance the proliferation of alloreactive T cells in the skin-draining LNs. 86
Figure 4.1. 6. *S. epi* skin colonization does not change the composition or costimulatory molecule expression of skin APCs relative to GF APCs. 87
Figure 4.1. 7. Skin *S. epi* colonization enhances skin APC activation of alloreactive T cells. (A and B) GF or *S. epi*–colonized skin-draining LNs 89
Figure 4.1. 8. Exogenous addition of inflammatory cytokines results in augmented effector function by donor-reactive T cells. 90

Figure 4.1. 9. Trend toward increased numbers of donor-reactive T cells in *S. epi* colonized skin grafts. 91

SECTION 4.2

Figure 4.2. 1. Skin graft recipients mount a T cell response to commensals on syngeneic donor organs. 96
Figure 4.2. 2. The protocol for *S. epi* painting of GF mice induces selective colonization of mouse skin that is stable for at least two weeks. 97
Figure 4.2. 3. *S. epi* does not colonize skin of SPF mice housed in our mouse facility. 98
Figure 4.2. 4. Addition of naïve CD8+ graft-commensal-reactive T cells does not perpetuate major damage to colonized, syngeneic skin grafts. 100
Figure 4.2. 5. Hosts with memory against commensals present on donated organs damage colonized syngeneic skin grafts. 102
Figure 4.2. 6. Both $CD4^+$ and $CD8^+$ host memory T cells are required to damage colonized, syngeneic skin grafts. 106
Figure 4.2. 7. Host tissue-resident memory cells are sufficient to damage colonized, syngeneic skin grafts. 109

SECTION 5.1

Figure 5.1. 1. Butyrate micelles treatment prolongs allograft survival, increases cecal butyrate levels, and modifies the intestinal microbiota. 121
Figure 5.1. 2. Different butyrate micelle regimens of administration result in suboptimal allograft prolongation. 123
Figure 5.1. 3. Butyrate micelle treatment alters the skin microbiota. 124
Figure 5.1. 4. Butyrate micelle treatment does not modify systemic levels of Tregs. 126
Figure 5.1. 5. Butyrate micelle treatment does not modify the priming phase of the alloimmune response 127
Figure 5.1. 6. Butyrate micelle treatment does not modify the migration and accumulation of endogenous alloreactive T cells into the graft. 128
Figure 5.1. 7. Butyrate micelle treatment does not modify the capacity of graft-infiltrating T cells to produce Th1 pro-inflammatory 129
Figure 5.1. 8. ButM does not decrease the levels of serum LPS at steady state and after transplantation. 130
Figure 5.1. 9. Butyrate micelles decrease the myeloid cell compartment at steady-state 131
Figure 5.1. 10. Tracking of monocyte frequency during butyrate micelle treatment. 132
Figure 5.1. 11. Butyrate micelles treatment does not impact bone marrow monocytes and expression of CCR2. 133
Figure 5.1. 12. Butyrate micelle treatment results in decreased graft-infiltrating myeloid cells. 135
Figure 5.1. 13. Butyrate micelle treatment enhances monocyte mitochondrial metabolism at the transcriptional level. 137
Figure 5.1. 14. Butyrate micelle treatment homogenizes monocyte transcriptional profile and upregulates genes related to aerobic cellular respiration. 138
Figure 5.1. 15. Butyrate micelle treatment impairs myeloid cell function. 140
Figure 5.1. 16. CCR2 depletion prolongs allograft survival similar to butyrate micelle treatment. 141

Figure 5.1. 17. CCR2 depletion impact on monocytes and T cells. 143
Figure 5.1. 18. DT treatment in CCR2-DTR mice prolongs graft survival. 144

SECTION 6.

Figure 6. 1. Working model on how the microbiota diversity calibrates alloimmune responses. 149
Figure 6. 2. Working model for how the microbiota and derived metabolites can impact alloimmune responses. 161

ACKNOWLEDGEMENTS

It is clear that the work presented in this thesis is not solely my own but, rather, a result of help, collaboration, and support that started many years ago.

From a young age, I was always interested in the sciences. There are several teachers that helped foster that curiosity but I think my particular interest in biology began in Mrs. Juica's high school class. She taught with such skill and passion that it made biology enticing. She encouraged me to always ask questions. It was her class that made me want to pursue scientific research as a career. Then, in college, when I took the introductory course on Immunology by Maria Rosa Bono, I confirmed my love of science. During my undergraduate thesis project in the Hetz lab, the mentorship of Danilo Bilches Medinas was paramount for my scientific training. I am very grateful for his support and the good talks we had about science, life, and family.

After college, my colleagues at TCR^2, Robert Hofmeister, Jian Ding, Ekta Patel, and Eva Quinn, were also influential. They believed in me and encouraged me to pursue graduate school. Without their guidance, I would not have applied.

During my application process to the Immunology program at UChicago, there were two professors that always vouched for me: Pete Savage and Albert Bendelac. They genuinely cared about me and were accommodating and helpful during my transition to UChicago.

I am eternally grateful to have had a great COI cohort that supported me so much during the first two years of classes: Jen Allocco, Jordan Voisine, and Emily Higgs. They are brilliant people, and I was fortunate to see them become brilliant scientists.

And then there's Marisa: I would like to thank Marisa for all her help throughout these years. I am privileged to have her support and mentorship during my graduate training. This academic journey could not have happened without her constant feedback, guidance, and advice.

I am fortunate to have been trained by a very talented scientist. I don't think I can ever truly thank her enough for the opportunity she provided and the impact she has had on me as a scientist. In college, I heard that the main thing you get from a PhD is "how to think" more than the raw information or data. I didn't really believe it, but I now realize that was true. I think Marisa is the single person who has had the greatest impact on my approach to science and I feel fortunate to be mentored by one of the best in this regard.

In Marisa's lab, there have been so many people who have helped me in a myriad of ways. When I first joined the lab, Kevin Lei taught me a lot about techniques and about how to be a productive scientist. There were others who were instrumental in teaching me techniques: Christine McIntosh, Peter Wang, and Zhipeng Li, and helping with the immeasurable number of transplants: Liqiu Chen and Ying Wang. Others were a lot of fun to talk about scientific ideas, such as Isabella Pirozzolo, Ricardo Mora, Jen Allocco, Monty Kwan, Lexi Cassano, Domenic Abbondanza, and Stevie Xie.

I also couldn't have done this without mentorship from my thesis committee: Anne Sperling, Bana Jabri, Anita Chong, and Eric Pamer. I am privileged to have had their help and guidance. The support Jeff Hubbell, Cathy Nagler, and Shijie Cao gave me was also instrumental and I am very grateful for their feedback.

My extended family has always been there for me and I am lucky to have such a large support network. In particular, my parents are truly amazing. They shaped me as a kid and instilled in me the values I have today. They taught me honesty, fostered my curiosity, and taught me the importance of always giving your best in anything you pursue. Moreover, they provided me with a level of love and support that I know is not common and will never take for granted. I love you guys. I am lucky to have had three siblings to grow up with and will always

love them. I am also fortunate to have two beautiful nephews. They are younger than my graduate training and I enjoy so much spending time with them.

Two years ago, we adopted Shiva, and my life has not been the same since. Shiva arrived when I needed her the most, and helped me through some very hard times. She is sweet, playful, and funny and makes life happier.

Finally, there's Giani. I am privileged to have been by your side for the past 13 years. I am lucky to have grown by your side. I have learned so much from you, and I am eternally grateful for your constant support. You followed me to a different country, you moved 9000km to be with me, and have always been by my side to strengthen me. I am lucky to have had someone that was there for me when I needed the most. Thank you for filling my life with laughter and joy. Love you

ABSTRACT

This study aimed to elucidate the complex interplay between microbiota diversity, microbial-derived signals, and alloimmune responses in the context of allograft rejection. At the whole-body microbiome level, a diverse microbial community fine-tuned the capacity of systemic antigen-presenting cells (APCs) to prime alloreactive T cells and orchestrate potent alloimmune responses. Targeting bacterial groups with broad-spectrum antibiotics diminished the microbiota diversity, dampened APC poising status, and weakened alloimmune responses, ultimately prolonging allograft survival. Furthermore, at the individual bacterium level, administration of *Alistipes oderdonkii* and *Parabacteroides distasonis* strains was sufficient to prolong allograft survival, suggesting their potential as probiotic candidates to enhance transplant outcomes. Conversely, colonization with a skin-restricted commensal, *Staphylococcus epidermidis* accelerated allograft rejection by augmenting the effector phase of the alloimmune response. This was achieved through enhancing skin APC activation of alloreactive T cells and triggering a host-versus-commensal T cell response. Lastly, at the microbial metabolite level, administration of butyrate inhibited quantitatively and qualitatively the myeloid cell compartment systemically, reducing the innate immune cell execution of the effector phase. These findings underscore the pivotal role of microbiota-derived signals and microbial modulation in alloimmune responses and graft outcomes.

Chapter 1: Introduction

Transplantation is a commonly used treatment for end-stage organ failure, but the recipient's immune system recognizes the graft as foreign due to genetic disparities with the donor. The host's immune response towards the graft is termed alloimmune response (allo, from the Greek word *allos*, which means 'other') and leads to destruction and rejection of the organ by acute or chronic targeting of the allograft. Germline polymorphisms between the organ donor and the recipient are the main drivers of the strength of this immune response as several are usually recognized by the recipient's adaptive immune system, including T and B cells. Current therapies that aim to prolong the survival of grafts rely on global immunosuppression of the recipient rather than on selective inhibition of donor-reactive adaptive immune cells, which can leave graft recipients more prone to infection and cancer. Developing therapies that establish donor organ-specific tolerance has proven challenging. Despite the use of immunosuppressive therapies, transplant patients still have acute rejection episodes and most will develop chronic allograft rejection. Consequently, finding environmental factors that can calibrate the strength of the alloimmune response and can be targeted therapeutically is a promising avenue to complement current immunosuppressive regimens.

1.1 Alloimmune response:

1.1.1 Priming

When a solid organ is transplanted into a recipient, the host mounts an alloimmune response against the graft, due to genetic differences like major and minor histocompatibility mismatches (MHC and mHC), that can lead to its rejection. For this to happen, the host's adaptive immune system must become activated in a process called priming. T cells are essential

for allograft rejection and their activation is considered the rate-limiting step for rejection. Allorecognition *per se* has been considered a paradox because T cells are positively selected to recognize self-MHC/peptide with moderate affinity and should be unable to recognize non-self MHC. As T cells are not negatively selected for non-self-MHC and T cell receptor (TCR) structures are flexible, cross-reactivity with non-self MHC can occur. It is thought that flexibility within the TCR structure allows cross-reactivity onto distinct MHCs, resulting in 1-10% of T cells reacting to allogeneic MHC molecules[1]. The priming of alloreactive T cells is initiated in secondary lymphoid organs (SLOs), including lymph nodes (LN) that drain the allograft in the case of non-vascularized grafts, or the spleen in vascularized grafts as the lymphatics of the allograft are not re-sutured[2]. Graft-reactive T cells require cognate interaction with antigen-presenting cells (APCs) through TCR-MHC/peptide interaction. Depending on the origin of the APC, donor- or host-derived, allorecognition can be classified as direct or indirect, respectively. Indirect recognition accounts for host APC acquisition of donor-derived antigens, followed by processing and presentation of peptides derived from those antigens on self-MHC, whereas direct recognition occurs when a host TCR cross-reacts on donor MHC presenting donor-derived self-antigens. A third type of presentation has been described and termed semi-direct presentation, when donor cells shed intact MHC-containing exosomes and host cells display this intact donor MHC on their surface and activate cross-reactive T cells directly (semi-directly)[3].

1.1.2 Requirement of secondary lymphoid organs

Where the alloimmune response is primed has been a source of controversy for a long time. The adaptive immune response to infections starts in SLOs that drain the site of infection, prompting investigators to propose that alloimmunity is primed in allograft-draining SLOs, but some studies oppose this hypothesis. Initial work showed that the requirements for rejection of

different organs varied depending on their access to the host's lymphatic vasculature, the antigenic load, or if they were vascularized. For example, non-vascularized skin graft survival was found to be influenced by its connection to the host's lymphatic system[4]. Here, the investigators used an experimental model that used a vascularized skin pedicle and limited lymphatic development to skin allografts by covering the basal surface of the skin graft to impede attachment and lymphatic vessel growth. Skin rejection was delayed if there was no lymphatic drainage. In contrast, the rejection of vascularized organs, such as kidneys and hearts, appears to have different requirements. Vascularized allografts were not required to have lymphatic connections to their hosts for rejection[5]. To ensure no host lymphatic access to transplanted kidneys, allografts were maintained in a separate container with a blood supply. Almost all kidneys were rejected only by diffusion of blood, which suggested that the antigens from the donor endothelium of the graft were sufficient to initiate an alloimmune response. These studies led to the peripheral sensitization hypothesis, which stated that donor endothelial cells that accompany an allograft can mediate the priming of alloimmune responses and contribute to rejection[6,7].

The peripheral sensitization concept was supported by studies that showed that MHC class I and II antigens and costimulatory molecules were expressed on endothelial cells during rejection[8,9]. A study from Kreisel et al., 2009[10], showed that non-hematopoietic cells from allografts can directly activate the host's $CD8^+$ T cells and mediate rejection. The authors used the Bm3 TCR Tg mouse model ($H\text{-}2^k$) which develops cross-reactive $CD8^+$ T cells that recognize peptides presented in $H\text{-}2\text{-}K^b$. They generated bone marrow chimeras by transferring CBA ($H\text{-}2^k$) bone marrow into lethally irradiated B6 ($H\text{-}2^b$) mice. This resulted in hearts that lacked the MHC class I haplotype $H\text{-}2^b$ in their hematopoietic compartment but expressed it in

their radioresistant compartment. These hearts were transplanted into $CD4^+$ T cell-depleted Bm3 mice. These mice were able to reject the hearts, which suggested that the $CD8^+$ T cells were being directly activated by the non-hematopoietic MHC class I from the $H\text{-}2^b$ haplotype in the graft and mediating rejection, supporting the peripheral sensitization hypothesis.

Opposing studies show the importance of SLO in the priming of alloimmune responses and give conflicting evidence against the peripheral sensitization model. These studies have taken advantage of an alymphoblastic mouse model, termed *aly/aly* mice[11], that does not develop lymph nodes and Peyer's Patches because of a spontaneous mutation in the NF-κB-inducing kinase (NIK). Lakkis and colleagues[12] analyzed the importance of SLOs in transplantation by using *aly/aly* mice, Hox11-KO mice, which do not develop a spleen, and splenectomized *aly/aly* mice, which are devoid of all SLOs. Skin grafts were not rejected in *aly/aly* mice, but were rejected in Hox11-KO mice, suggesting a requirement of draining LNs for skin initiation of rejection. The skin grafts used were of split thickness, which accounts for lower antigenic load, and is a possible reason for their long-term acceptance. Vascularized heart allografts were rejected in *aly/aly* and Hox11-KO mice, but not rejected in splenectomized aly/aly mice, supporting the requirement of SLOs for the rejection of vascularized organs.

Results were slightly different in another model of alymphoplastic mice, splenectomized LTα-KO or LTβR-KO mice which do not develop LNs[13]. Full-thickness skin and heart allografts survived much longer in these hosts than in wild-type (WT) control mice, but were eventually rejected. The authors were able to demonstrate that there was priming of alloreactive T cells in the absence of SLOs in C57Bl/6 mice, by performing BALB/c major mismatched skin transplantation in splenectomized LTβR-KO mice, and rechallenging with BALB/c hearts[13]. The heart rejection kinetics were accelerated compared to non-sensitized mice, suggesting the

priming of T cells occurred without SLOs. LTα-KO and LTβR-KO mice have been shown to have a higher level of circulating activated T cells and T cells infiltrating non-lymphoid tissue[14], which may contribute to the rejection of allografts found in these mice. Indeed, antigen-experienced alloreactive memory T cells were capable of mediating heart rejection in splenectomized *aly/aly* mice[15], supporting the concept that SLOs are important for the priming of naïve T cells, but not required for subsequent activation of memory T cells. Altogether, these studies suggest that SLOs are important for alloreactive T cell priming but differ in their absolute requirement to initiate rejection.

Some allografts carry their own SLOs, like in the case of intestinal transplantation, which have been shown to be important for rejection. Wang and colleagues demonstrated the importance of donor SLOs that are associated with the intestine and showed that the donor lymphoid organs are quickly infiltrated by recipients' T cells[16]. Splenectomized LTα-KO mice rejected WT intestine faster than *aly/aly* intestine, suggesting that SLOs only in the donor organ are enough to amplify intestinal allograft rejection.

1.1.3 Direct, indirect, semi-direct presentation

Direct and indirect allorecognition by the donor or host dendritic cells (DCs), respectively, both play important roles in allograft rejection[17]. The direct pathway, where donor passenger DCs are recognized directly by the recipient's T cells, is thought to be involved early post-transplantation. T cells that recognize non-self MHC molecules are found at a high precursor frequency[1], and lead to strong mixed-lymphocyte reactions, suggesting direct recognition may lead to strong responses post-transplantation. Lafferty et al., 1976[18] demonstrated that fully allogeneic thyroid grafts survived longer if transplanted following in vitro culture of the graft, which resulted in the death of donor APCs in the thyroid gland. This led

to the conclusion that passenger hematopoietic cells are an important mediator of rejection via the direct pathway. The direct pathway can activate $CD4^+$ T cells, as described by Pietra and colleagues[19], as MHC II-KO allogeneic hearts were not acutely rejected by SCID recipients with transferred CD4 T cells. It is thought that direct allorecognition phases out over time, due to the short half-life of DCs or their elimination by host T cells and NK cells[20,21]. In contrast to the direct pathway, indirect allorecognition T cells start from a lower precursor frequency and account for later phases of alloimmune responses. Early studies using MHC II-KO skin grafts determined that host $CD4^+$ T cells can reject these grafts, via indirect recognition of alloantigens[22]. Moreover, both $CD4^+$ and $CD8^+$ T cells have been shown to reject skin grafts via indirect pathways[23–25]. These studies confirm that different types of allografts (skin versus heart) have different requirements of direct vs indirect allorecognition to mediate rejection.

The participation in rejection of the semi-direct pathway, based on host DCs being coated with intact donor-MHC shed by the graft and activating host alloreactive T cells with direct donor MHC reactivity, has been recognized more recently. DCs cross-decorated in this manner with allogeneic MHC, in addition to expressing their self-MHC, can thus theoretically activate T cells via both the direct and indirect pathways[26]. This may be a way by which $CD4^+$ T cells with direct specificity can give help to $CD8^+$ T cells with indirect specificity, in a 3-cell scenario. Allogeneic MHC is acquired by host DCs following secretion by donor cells of exosomes that carry donor-derived MHC molecules[27]. Using microscopy, Liu et al., 2016[3] showed that DCs from C57BL/6 recipient mice ($H\text{-}2^b$) were cross-decorated with whole $H\text{-}2K^d$ molecules after BALB/c fully mismatched heart transplantation, were able to directly activate alloreactive T cells, and confirmed the relevance of exosome-mediated semi-direct pathways in transplantation.

1.1.4 $CD4^+$ T cells and rejection

Alloreactive $CD4^+$ T cells are important mediators of adaptive immunity and are key players during allograft rejection. Following priming, T cells acquire effector functions and migrate to the allograft to orchestrate rejection. $CD4^+$ T helper 1 cells (Th1) are considered to be the major drivers of rejection and secrete IFNγ and TNFα, key proinflammatory cytokines that mediate rejection by recruiting and activating monocytes and macrophages, creating an inflamed environment[28]. Th1-related cytokines have been studied in the context of transplantation, including IL-2[29,30], IL-12[31], and IFNγ[30,32]. All of them were dispensable for acute rejection, by using germline KO as recipients. Further experiments remain to understand the importance of Th1 differentiation in alloreactive T cells in allograft damage and rejection.

Many studies have been performed in order to understand the mechanisms by which $CD4^+$ T cells contribute to graft rejection. Adoptive transfer of $CD4^+$ T cells from CD8-KO mice into severe combined immunodeficient (SCID) mice was sufficient to reject MHC class I- and II-mismatched skin grafts and resulted in higher levels of total graft TNFα mRNA levels following $CD4^+$ acquisition of a Th1 phenotype[33]. Similarly, the transfer into SCID mice of alloreactive TCR-Tg $CD4^+$ T cells that recognize I-A^k58-71 via an indirect pathway (clone SH10) was sufficient to reject H-2^k skin grafts and correlated with expression of Th1 cytokines, enhanced macrophage infiltration and fibrosis[34]. Screening for an alloantigen that can mediate heart transplant rejection via an indirect pathway[35], Honjo and colleagues generated a TCR-Tg mouse line specific for a peptide from K^d presented on I-A^b and bred these founders to a recombination activating gene (RAG)1-KO background, to produce the TCR75 mouse line[36]. When injected in large numbers into lymphopenic hosts, these T cells infiltrated the graft and were capable of rejecting H-2^d-expressing hearts, suggesting that host-derived APCs capable of presenting the

TCR75-activating peptide were present in the graft. Whether homeostatic proliferation of the transferred T cells into lymphopenic hosts and ensuing acquisition of virtual memory was necessary for rejection to occur remains to be evaluated. Nevertheless, these experiments raised the question of how exactly $CD4^+$ T cells that cannot recognize donor cells directly can mediate rejection.

Acute rejection by $CD4^+$ T cell direct allorecognition has been proposed to occur in a two-step manner. First, donor-derived DCs directly prime alloreactive T cells. Next, donor-derived somatic cells (including endothelial cells) act as direct targets of these $CD4^+$ T cells[37]. This was demonstrated by Grazia and colleagues, using donor hearts from bone marrow chimeras, where MHC II was expressed either on somatic or hematopoietic cells. MHC II deficiency in both compartments prevented $CD4^+$ T cell-mediated rejection, which could only occur if donor MHC II-expressing APCs were transferred into the graft recipients[37]. This suggests that endothelial cells can act as APCs during inflammatory events, as IFNγ can drive the upregulation of MHC II[38]. The targeting of the graft can also occur by crossed-decorated host DCs that are located within grafts and present donor MHC via a semi-direct pathway. Hughes and colleagues demonstrated this using mouse islet and kidney transplantation models. They showed that host DCs presenting intact donor MHC occurred frequently and during early stages post-transplantation, and were sufficient to induce acute rejection by T cells[39]. The loss of direct recognition over time and the maintenance of indirect alloresponses are associated with chronic rejection. In kidney transplant patients, chronic allograft nephropathy was found in graft recipients who maintained high levels of indirectly activated $CD4^+$ T cells, whereas T cells activated by direct recognition, decreased over time[40]. In a chronic bm12.K^d.I-E^d heart transplant model, these phases were studied in detail, using different TCR-Tg T cells[41]. Early after

transplantation, ABM TCR-Tg T cells, which directly recognize I-A^{bm12}, could proliferate only if transferred the first week after surgery, but could not when transferred 5 weeks later, suggesting direct allorecognition is not long-lived. TCR75 TCR-Tg T cells could proliferate both early and late after transplantation, confirming that indirect MHC I allorecognition can happen throughout the early and later stages. Conversely, TEa TCR-Tg cells, which recognize an I-E^d peptide presented in host I-A^b MHC II, could only proliferate early after transplantation, due to a rapid elimination of donor-derived APCs. This confirms that direct alloresponses occur early after transplantation and that indirect allorecognition is heterogenous, dependent on whether the donor-derived alloantigen recognized is expressed on/in graft cells for a short or long duration post-transplantation[41].

There are still mechanistic questions that remain to be answered regarding the effector function of $CD4^+$ T cells once they are within the allograft. It has largely been assumed that rejection is driven by Th1 cells, due to the phenotypic characterization of intra-graft alloreactive T cells present, but the ability of STAT4-deficient mice, which have reduced Th1 responses, to drive rejection[42–44], suggests that Th1 cells are not required for the effector phase of acute rejection. Whether IFNγ- and TNFα-deficient alloreactive $CD4^+$ T cells can drive the effector phase of graft rejection remains to be determined. Also, the utilization of macrophage-deficient mouse models may help elucidate the requirement for Th1-dependent innate amplification of alloimmune responses mediated by IFNγ and TNFα.

1.1.5 $CD8^+$ T cells and rejection

Activation of alloreactive $CD8^+$ T cells is considered a main driver of effector mechanisms in allograft rejection. Upon antigen stimulation by specific interaction of their TCRs and MHC I, these cells differentiate into cytotoxic T lymphocytes (CTLs)[45] and are thought to

mediate graft damage[28]. Early studies determined that the adoptive transfer of $CD8^+$ T cells enriched from the spleen was sufficient to induce rejection of major-mismatched MHC I-disparate skin grafts using B10 nude mice as recipients[46].

The molecular mechanisms by which CTLs mediate graft damage involve the release of cytotoxic granules and the upregulating of death receptors[28]. Granules containing granzyme B, perforin, serglycin, calreticulin, granulysin, and Fas ligand (FasL) are released by the CTLs in a process called granzyme exocytosis. Perforin assembles into polyperforin and inserts into the target cell membrane to facilitate the internalization of granzyme B. FasL-containing granules also play a role in cell death by interacting with target cells that express Fas. Both pathways result in cytotoxicity by inducing apoptosis via caspase activation[47–49]. Annexin V staining positively correlated with rejection in a human cardiac allograft study[50], and zinc chloride, a caspase-3 inhibitor, reduced cell death and prolonged graft survival in a rat heart transplant model[51].

In vitro experiments using perforin-deficient CTLs resulted in ablated capacity to mediate cytotoxicity in virus-infected and allogeneic fibroblasts[52], but the CTLs were still able to mediate cell death in FasL-expressing target cells[53]. These experiments demonstrated that perforin cytotoxicity was independent of FasL-Fas interaction and that both mechanisms were important for cell death. Nevertheless, incubating graft-infiltrating T cells from human renal allografts undergoing rejection with a granzyme exocytosis inhibitor (concanamycin A) substantially reduced in vitro lysis and apoptosis of proximal tubular epithelial cells, whereas incubation with a Fas blocking antibody did not, suggesting a predominant effect of the former mechanism in vitro[54]. Ultimately, Sleater et al, 2007 confirmed that both mechanisms were required for in vivo graft damage using an islet allograft rejection model[55]. Either adoptively transferring perforin-

deficient CTLs or using Fas-KO allografts only resulted in limited graft damage. Only when both pathways were ablated was allograft rejection prevented, confirming a requirement of both mechanisms for graft damage[55].

Another essential contributor to graft damage is $CD8^+$ T cell expression of the pro-inflammatory cytokine IFNγ. To study their importance in graft rejection, Diamond et al, 2000 performed an adoptive transfer of in vitro-primed alloreactive $CD8^+$ T cells from IFNγ-KO mice into SCID mice with established pancreatic allografts[56]. IFNγ-deficient $CD8^+$ T cells were not capable of rejecting the allografts, confirming the cytokine can drive a graft-damaging role during allograft rejection[56]. Further experiments remain to be performed to identify the cell target and mechanisms of graft destruction in this model.

1.1.6 Monocytes and Macrophages

During solid organ transplantation, allografts are damaged as they are cut from their blood supply, suffering a loss of oxygenation in a process called ischemia. When the allograft is transplanted in the recipients, perfusion and reoxygenation are restored. This process is called ischemia and reperfusion injury (IRI) and generates inflammation, oxidative damage, and the release of DAMPS in the organ, leading to the activation of the recipient's immune system[57]. Early after IRI, graft endothelial and parenchymal cells express TNFα and IL-1β, promoting the expression of the monocyte chemoattractant MCP-1. High levels of MCP-1 mediate the egress of monocytes from the bone marrow and the infiltration to inflamed allografts, in a CCR2- and CX3CR1-dependant manner[58–60]. Other chemoattractants that are important for monocyte recruitment are CCR1 (with its ligand CX3CL1) and MIP-1α, and help attract monocytes located in the blood, bone marrow, and spleen[61]. CCR2-deficient and CX3CL1-deficient monocytes infiltrated ischemic kidneys less than WT monocytes and induced less tissue injury in a kidney

IRI model[60], confirming the relevance of these molecules in the initiation of the innate immune response after reperfusion.

As monocytes infiltrate the allografts, they are exposed to an inflamed microenvironment, which mediates their differentiation into inflammatory macrophages, characterized by their pro-inflammatory phenotype, also denoted as M1-like[62]. Macrophage accumulation is associated with worse clinical outcomes for kidney and heart transplant patients[63,64] and graft-infiltrating macrophages can account for 38-60% of the total leukocytes in grafts[65]. Human transplant data has shown that there is an initial accumulation of monocytes in all grafts, whether rejecting or non-rejecting[66]. Schreiner et al, 1993 confirmed that in a rat renal transplant model, there is an initial macrophage accumulation seen in both transplanted kidney allografts and isografts in the first 1-2 days, but only allografts display a marked increase in macrophage levels at day 4 post-transplantation[67]. This is probably due to surgery-related damage or IRI happening in both isografts and allografts, but only in the case of the allograft does the alloimmune response cooperate to further attract a higher influx of myeloid cells. Moreover, experimental depletion of macrophages has proven to attenuate graft injury. In a rat renal allograft model[68] and a heart-lung transplant model[69], the use of liposomal-clodronate was effective at depleting infiltrating macrophages and resulted in lower acute rejection[68]. Likewise, the depletion of $CD11b^+$ myeloid cells in CD11b-DTR mice resulted in less kidney damage to the microvasculature in a mouse renal transplant model[70]. Lastly, depletion of monocytes/macrophages with a c-Fms kinase inhibitor resulted in less renal allograft dysfunction and structural damage[71], confirming that these myeloid cells are major mediators of graft damage and destruction.

Inflammatory macrophage (M1-like) polarization occurs when monocytes sense the extracellular signals CSF-2, TNFα, LPS, and IFNγ, and these macrophages are characterized by the expression of Ly6C^{hi}, Nos2, and Gzmb[72]. M1-like macrophages act as the primary source of reactive oxygen species (ROS), by producing inducible nitric oxide synthase 2 (iNOS2) enzyme, which helps mediate graft injury[68,73]. Moreover, inhibition of iNOS with carbon monoxide[74] or pharmaceutical inhibitors[75] resulted in low levels of NO production, and reduced tissue damage and improved graft survival in mouse models of hepatic injury and rat kidney transplantation, respectively.

M1-like macrophages secrete a wide variety of pro-inflammatory cytokines, including IL-1, IL-6, IL-12, TNFα, and IFNγ, which damage the allograft by different mechanisms[73]. Inflammatory macrophages rely mainly on glycolysis and inhibit the Krebs cycle, blocking oxidative phosphorylation (OXPHOS)[76]. They also express inflammatory chemokines like CXCL9, CXCL10 and CXCL16[72]. Finally, macrophages can also act as APCs in the allograft, amplifying T cell responses via expression of MHC II and co-stimulatory molecules CD40, CD80, and CD86, which in turn, further activate macrophages. Early after transplantation, the bone marrow has an egress of M1-like monocytic precursors that infiltrate heart allografts[77], and under acute rejection, they become M1-like macrophages that damage allografts[78]. Interestingly, under co-stimulation blockade treatment with αCD154 mAb, these M1-like macrophages convert into DC-SIGN^{+} M2-like macrophages that are required for tolerance induction[78]. Although their exact contribution to graft rejection requires additional study, infiltrating macrophages account for the first line of effector cells targeting transplanted organs and are an important source of inflammation and damage during acute rejection.

Chronic rejection of transplanted organs is associated with the differentiation of intra-graft macrophages that acquire an M2-like phenotype. M2-like polarization occurs when monocytes sense the extracellular signals IL-4, Il-10, TGFβ, and CSF-1, and these macrophages are characterized by the expression of Ly6C^{lo}, CX3CR1, CD169, CSF-1R, and CD206[72]. The main characteristics of a chronically rejected allograft are tissue fibrosis and graft vasculopathy, and extensive studies have associated M2-like macrophages with being involved in the development of these processes. M2-like macrophages promote smooth muscle proliferation by producing growth factors that exert pro-fibrotic functions, like TGFβ and vascular endothelial growth factor (VEGF) production[72]. M2-like metabolism is more dependent on OXPHOS, having an intact Krebs cycle, and high levels of mitochondrial electron transport chain (ETC) respiration. Macrophages accumulate in great numbers in transplanted organ vessels[79] and have been shown to correlate with the degree of graft fibrosis[80] and with worse graft outcomes[81]. They produce the immunosuppressive molecules IL-10 and express arginase-1 (Arg1)[72].

Recent studies have unveiled possible innate allorecognition by monocytes and macrophages. Dai and colleagues determined that recipient monocytes and macrophages can respond to allogeneic grafts via CD47 interaction with donor SIRPα[82]. The polymorphisms found on SIRPα allow for different affinities of interaction with CD47, leading to their activation and graft damage. Innate immune memory to non-self has also been studied[83]. Recipient-derived monocytes and macrophages were found to recognize donor MHC I via interaction with the paired Ig-like receptor (PIR) PIR-A. PIR-A in the recipient was necessary for memory formation, and its deletion or blocking prolonged kidney and heart graft survival. These findings provide evidence that the innate immune system plays a role during the alloimmune response and mirrors aspects of the adaptive immune system.

1.2 Microbiota

The microbiota, the communities of microorganisms that colonize mucosal and epithelial surfaces in contact with the outside world, live in symbiosis with their hosts. Hosts become colonized at birth, with microbial diversity increasing in the first few years of life[84]. Each individual carries their microbial community structures, shaped by birth mode, diet, environmental exposures, host genetics, and immune constraints[85]. In turn, the microbiota is essential for health. For instance, the gut microbiota synthesizes essential metabolites such as vitamin K, breaks down otherwise indigestible dietary plant fibers, inactivates toxic substances, and prevents pathogen colonization. The skin microbiota helps prevent cutaneous infections and accelerates wound healing. In addition, both intestinal and extra-intestinal microbiota have intimate reciprocal relationships with the immune system, with the microbiota promoting the maturation of the immune system and the immune system shaping microbial composition.

The microbiota and transplantation intersect in different ways. First, the microbiota modulates alloreactivity. Indeed, although the strength of the immune response against a transplanted organ is primarily determined by the genetic disparities between the donor and recipient of the allograft, mouse models of skin, aortic, heart, and lung allografts show that the microbiota can also modify this response, potentially enhancing or dampening alloimmunity. It is possible that this occurs because of systemic immune regulation modulated by the gut microbiota, and/or because of local effects dictated by the transplanted-organ-specific microbiota. In both cases, the microbiota may be mediating its effects via microbe-produced microbial-associated molecular patters (MAMPS) and/or via generation of metabolites. An effect of graft-associated microbiota may partly explain why colonized organs like the lung have worse outcomes after transplantation than non-colonized organs like the heart or kidney. Second, the

gut microbiota may also alter the metabolism of some immunosuppressive drugs and consequently affect their dosing or cause some of their side effects. Third, because of its dynamic status and rapid response to environmental changes, the gut microbiota might become useful as a predictive biomarker, for instance for allograft outcome, responsiveness to immunosuppression, or post-transplant complications. Fourth, the microbiota might be harnessed therapeutically to improve transplant outcomes.

1.2.1 Impact of the microbiota on the immune system

The hypothesis that the intestinal microbiota might modulate alloimmunity derives from observations outside the transplant field that the microbiota matures and shapes the immune system. For instance, colonization of germ-free (GF) mice with the bacterium *Bacteroides fragilis*, promoted lymphoid organogenesis and corrected immune deficits[86]. Along the same lines, mice treated with antibiotics and GF mice have a reduced number of lacteals, lymphatic-like structures that originate from each intestinal villus and help absorb dietary lipids, whereas conventionalization of GF mice restores lacteal maturation and integrity[87].

The intestinal microbiota also directs the differentiation of innate and adaptive immune cells in the gut and lamina propria. Bacterial species colonize specific niches in the gut, creating microenvironments and providing signals that dictate DC licensing to orchestrate highly specialized T cell responses[88]. For example, segmented-filamentous bacterium (SFB) attaches to the lining of the ileum and promotes T cell-dependent IgA responses[89], Th17[90,91], and Th1[90] differentiation. On the other hand, intestinal *Clostridial* consortia[92,93] and *Bacteroides fragilis*[94] promote the induction of T regulatory cells (Tregs), whereas *Bacteroides thetaiotaomicron* drives both Th1 and Treg differentiation[95]. The gut microbiota can also modulate immunity systemically, impacting immune responses distal to the gut. For example, Abt et al, 2012[96]

showed reduced anti-viral responses in mice upon oral antibiotic treatment that affected the gut microbiota, resulting in impaired viral clearance and enhanced viral susceptibility. However, it should be noted that antibiotic treatment not only impacts the gut communities but also alters other commensal-containing compartments including the skin[97]. Colonization of GF mice with gut-tropic commensals that cannot colonize other compartments may more conclusively address whether gut commensals can have systemic immune effects. Indeed, compared with uncolonized mice, SFB mono-colonized GF mice displayed enhanced pathological score and proinflammatory T cell induction in the brain in an experimental mouse model of autoimmune encephalomyelitis (EAE)[98], and also developed exacerbated joint thickening and autoantibody production in a rheumatoid arthritis mouse model[99]. Outstanding questions remain as to how gut-resident bacteria can impact immune responses at locations distal to the gut. Possible mechanisms include the production of microbial products or metabolites that circulate systemically or induction of signaling in gut epithelial cells or intestinal immune cells that then either relay these signals to other cells or travel systemically. The intestinal microbiota's ability to modulate immunity in distal, sterile sites like the brain and joints suggests that the gut microbiota may affect transplantation by altering alloimmunity to non-intestinal allografts, whether colonized or sterile, as suggested by the ability of oral antibiotics to prolong survival of skin, heart and lung allografts in mice[97,100,101].

The extra-intestinal microbiota also has mutualistic relationships with the immune system. In the skin, adaptive immunity modulates tissue homeostasis and ensures that microbes do not disseminate into draining LNs[102]. Tolerance to commensal microbes in the skin is modulated in part by a large and diverse population of FoxP3$^+$ Tregs, many of which are specific for microbial-derived antigens[103]. This microbe-specific Treg population in the skin is initially

established during neonatal life when commensals colonizing body surfaces after birth enter developing hair follicles[104]. The presence of microbes on neonatal skin preferentially affects Tregs over other T cell types, as GF neonates generated fewer cutaneous Tregs than SPF mice but showed no differences in $CD4^+$ effector, $CD8^+$, dendritic epidermal, or $\gamma\delta$ T cell counts[104]. This neonatal wave of Tregs appears to be important for maintaining commensal tolerance throughout adult life. For example, mice colonized with the common human skin commensal *Staphylococcus epidermidis* (*S.epi*) as adults and those colonized with *S.epi* from birth both achieved a state of true commensalism characterized by a lack of tissue inflammation and persistence of the microbe on the skin. However, following a minor skin abrasion challenge, adult-colonized mice experienced worse local damage than neonatally colonized animals, exhibiting increased tissue inflammation, a larger *S.epi*-antigen-specific $CD4^+$ Teff:Treg ratio in the skin-draining LNs, and augmented neutrophil infiltration of the damage site[104].

In addition to modulating commensal tolerance, the skin microbiota also modifies tissue-specific responses to injury. Microbial communities on the skin increased accumulation of cutaneous IL-17A-producing $CD8^+$ T cells at steady state through a process that depended on migratory DCs and non-classical H2-M3-mediated antigen presentation[105–107]. Furthermore, tissue-resident memory $CD4^+$ and $CD8^+$ T cells generated by homeostatic encounters with microbes like *S.epi* or *Candida albicans* expressed paradoxical phenotypes characterized by simultaneous expression of Type 2 and Type 17 transcription factor RNA[107]. These programs were differentially activated or suppressed in response to site-specific cues like tissue injury, allowing the organ to rapidly tune local immunity, including T cell recruitment to the wound site[105,107]. Different paradoxical programs were also observed for intra-dermally-administered chitin[107], indicating that the microbiota regulates unique T cell signatures broadly. Importantly, T

cells with these paradoxical programs were localized to the skin; they were not observed in the LNs or spleen[107], suggesting that constant, localized exposure to specific microbial communities modulates these dynamic phenotypes. Similarly, the lung microbiota has been associated with the production of IL-17B and progression to pulmonary fibrosis in a bleomycin-induced fibrosis mouse model. Together, these data suggest that the microbiota in transplanted colonized organs may also affect alloimmunity by interacting with local immune cells.

1.2.2 Impact of the microbiota on alloimmunity and transplant outcome

The microbiota at various body sites changes after transplantation[108], consistent with the use of peri-operative and prophylactic antimicrobials. In addition, taxonomic changes in the microbiome have been associated with acute or chronic rejection[109–113]. As it is difficult to prove causality in humans, we used antibiotic-treated and GF mice to determine whether the microbiota causally modulates alloimmunity and graft outcome.

The gut microbiota impacts both innate inflammatory responses following surgery and adaptive alloimmunity. For example, having taken preoperative oral antibiotics was associated in patients with reduced macrophage and neutrophil infiltration into liver transplants stressed by ischemia/reperfusion injury and with improved hepatic function[114]. In mice, oral antibiotic pretreatment of donors and recipients prior to transplantation, or a GF status, both prolonged survival of minor and major mismatched skin grafts, and of MHC class II-mismatched heart allografts[97], and reduced chronic disease in minor mismatched lung allografts[101]. Conventionalization of GF mice with fecal microbiome transfer (FMT) from control colonized mice but not from antibiotic-treated mice accelerated rejection of minor mismatched skin grafts[97]. This demonstrated the sufficiency of the microbiota in accelerating transplant rejection, and that different microbial community structures can affect transplant outcomes differently.

Prolonged survival of the minor mismatched skin graft in antibiotic-treated and GF mice correlated with reduced licensing of LN DCs that displayed diminished expression of genes involved in NF-κB and type I interferon (IFN) signaling, and had lower ability to prime donor-reactive T cells in vitro and in the graft-draining lymph nodes in vivo[97]. Mice deficient in IFNαR displayed prolonged minor mismatched skin graft survival that was not further extended by antibiotic pretreatment, supporting the importance of the microbiota's tuning of this signaling pathways. The fact that tonic Type I IFN signaling in DCs helps poise these cells for future immune responses was confirmed by Schaupp et al, 2020[115] This effect was dependent on the microbiota acting via the immune adaptors MyD88, TRIF, and CARDIF in plasmacytoid DCs, leading to their secretion of IFNβ.

These results demonstrate that certain community structures can augment alloimmunity and accelerate rejection whereas others are neutral (those remaining after antibiotic treatment). There have been other reports indicating that other communities can dampen transplant rejection, an observation that supports manipulating the microbiota as an adjunct therapy to improve transplant outcomes. For instance, Rey et al, 2018[116] showed that antibiotic treatment early in life prevented normal taxa acquisition, and accelerated the rejection of aortic allografts, suggesting that mice acquire protective bacteria after weaning. Consistent with some microbial communities being protective, we found that mice obtained from Jackson displayed longer survival of minor mismatched skin grafts than genetically similar mice obtained from Taconic Farms that are colonized with different microbiota[117]. Interestingly, co-housing or FMT dominantly converted fast rejectors into slow rejectors, a phenomenon associated with the fecal presence of an *Alistipes* genus in slow rejectors[117]. Guo et al, 2019[118] also implicated the microbiota in the differences in acute and chronic rejection of minor mismatched lung allografts observed in mice purchased

from different vendors. This outcome divergence was associated with different proportions of lung Tregs. Importantly, antibiotic pretreatment of the spontaneously tolerant mice reduced lung Tregs and restored the acute and chronic rejection phenotype, again suggesting a protective microbiota. These two studies also emphasize the importance of the microbiota in determining experimental variability in transplantation, as described in other settings[119].

Microbiota protective for transplantation can also be induced therapeutically or through tolerogenic states like pregnancy. Indeed, Zhang et al, 2018[120] demonstrated that FMT from untransplanted mice that had received high-dose tacrolimus improved fully mismatched skin graft survival in recipients treated with low dose tacrolimus, suggesting the presence of protective microbes in fecal samples from high-dose tacrolimus-treated mice. Bromberg et al, 2018[121] reported that FMT from pregnant mice improved survival of fully mismatched heart allografts in animals treated with low-dose tacrolimus, which correlated with the presence of *Bifidobacterium pseudolongum*. Notably, the administration of this bacterial species to transplant recipients was sufficient to reduce chronic cardiac allograft disease, with correlated with LN structure remodeling[121]. UV-killed *B. pseudolongum* cultured with DCs and macrophage cell lines drove decreased production of the proinflammatory cytokines TNFα and IL-6, and increased synthesis of the immunosuppressive cytokine IL-10[121]. Thus, MAMPs expressed in this commensal may modulate innate immune cells that play a role during graft damage, though whether this occurs in vivo remains to be verified. Thus, there may be a place for oral administration of probiotics to facilitate graft survival.

The impact of extraintestinal microbiota on transplant fate is also emerging. In humans, changes in lung microbiota have been associated with lung allograft outcomes, with restoration of the pre-transplant host lung microbiota in the transplanted lung correlating with better graft

survival[110] and anabolic and catabolic remodeling of the transplanted lung being associated with distinct bacterial strains[122]. To address the impact of the graft microbiota on graft outcome, we used GF mice as hosts of sterile or mono-colonized skin grafts, where the gut was maintained sterile through the oral administration of non-absorbable antibiotics. Donor cutaneous colonization with *S. epi* was sufficient to accelerate skin graft rejection in the absence of intestinal colonization[100], demonstrating a definite causal role for the allograft's microbiota on transplant outcome. Surprisingly, skin *S. epi* did not increase alloreactive T cell priming in the skin graft-dLNs, but instead augmented the effector immune response in the graft itself, as the skin graft but not the LNs expressed higher levels of inflammatory cytokine genes. Although the local impact of extra-intestinal microbiota on alloimmunity has not been investigated in humans, pulmonary infections post-lung transplantation have been shown to promote chemokine production that attracts leukocytes and promotes the development of chronic lung allograft dysfunction[123]. Similarly, observations in patients with pancreatic cancer revealed that a more diverse intra-tumoral microbiota augmented local antitumor immunity, promoting tumor rejection[124]. This points to targeting the allograft's microbiota prior to transplantation as a potential strategy to improve graft survival. Together, these data suggest that both intestinal and graft microbiota may modulate alloreactivity and graft outcome, albeit by different mechanisms.

In addition to calibrating alloimmunity, commensal microbes also drive commensal-specific immune responses. In mice, it has been shown that depending on the age, location, and context in which the host encounters commensals, commensal-reactive T cells might be more regulatory or inflammatory[102–107,125,126]. It should also be noted that many commensal-specific T cells remain in barrier tissues[102,106]. Importantly for transplantation, we have demonstrated that anti-commensal T cells that recognize *S. epi* peptides, play a role in promoting graft damage,

independent from the anti-graft alloreactive immune response[127]. Moreover, previous memory to *S. epi* counteracted immunosuppression, preventing graft prolongation[127]. Anti-commensal T cells also can be cross-reactive with mammalian antigens, and thus, potentially, with donor-specific antigens. For instance, it has been reported that virus-specific T cells cross-react with multiple HLAs[128]. Recent evidence for molecular mimicry has been reported in a mouse model of fibrosarcoma, where T cells reactive to an enterococcal bacteriophage epitope cross-reacted with an MHC class I-presented tumor-specific antigen, correlating with stronger antitumor immune responses driven by $CD8^+$ T cells[129]. Similarly, in a mouse model of spontaneous autoimmune myocarditis, cardiac myosin-specific $CD4^+$ Th17 cells cross-reacted with a Bacteroides-specific antigen[130]. Both studies confirmed that molecular mimicry also occurred in humans. During graft rejection, it is therefore conceivable that cross-reactive commensal-specific T cells may participate in inducing graft damage. Intriguingly, renal transplant recipients who received organs from donors with similar gut microbiota to their own exhibited prolonged graft survival compared to patients who received kidneys from donors with dissimilar microbiota[131].

1.2.3 Influence of microbial metabolites in organ transplantation

MAMPs released by microbes are broadly found in circulation[132], supporting a mechanism by which commensals could fine-tune systemic immunity at steady state and subsequently modulate graft rejection. Additionally, commensal-derived metabolites may also affect immunity and graft outcome[133]. For instance, the metabolite sulfobacin B, which can be produced by the commensal *Alistipes*[134], a genus associated with prolonged skin graft surviva[l117], has been reported to decrease the production of TNFα by macrophages[135], although whether this is the mechanism by which *Alistipes* improves graft survival is not known.

Association studies have determined that during acute graft-vs-host disease, there is a significant variation in metabolites that are end-products of microbes, with a decrease in AhR ligands and differences in bile acids that may impact alloreactive T cell responses[136]. Using unbiased profiling approaches, several groups have discovered microbial-derived metabolites that directly modulate immune cells. For example, using a G protein-coupled receptor (GPCR)-interacting commensal-derived metabolite screening, Chen and colleagues discovered multiple metabolites that can impact local and systemic host physiology[137]. Other studies found that the metabolite inosine, derived from *B. pseudolongum*, enhanced IFNγ^+ T cell immune responses in colorectal cancer mouse models exposed to anti-CTLA4 immune checkpoint blockade. Systemic inosine signaled via the GPCR adenosine A2A receptor on T cells, resulting in enhanced expression of *Il12rb2*, *Tbx21*, and *Ifng*, and augmented antitumor Th1 immune responses[138]. Butyrate, a short-chain fatty acid (SCFA), has the potential to improve transplant outcome[139], due to its Treg-inducing properties. Treg promotion is mediated in part by GPR43, a GPCR[140], and enhanced histone deacetylase inhibition in the FoxP3 locus[141]. Recently, Wu et al. found that the administration of the SCFA acetate, prolonged graft survival in a kidney transplant model, in a Treg- and GPR43-dependent manner[142], confirming a potential therapeutic use in transplantation.

Other studies have determined that commensal-derived bile acid metabolites modulate T cells via non-GPCRs[143,144]. The lithocholic acid (LCA) derivate 3oxoLCA inhibited Th17 polarization by directly binding to the transcription factor RORγT, whereas the LCA derivative isoalloLCA promoted Treg differentiation in a conserved noncoding sequence 3 (CNS3)- and production of mitochondrial reactive oxygen species (mitoROS)-dependent manner[143]. Moreover, IsoDCA was shown to potentiate Treg differentiation by suppressing DC stimulatory

capacity, in a farnesoid X receptor-dependent manner[144]. Understanding the impact of these and other microbiota-derived metabolites on alloimmunity and transplant outcomes might help find new approaches to promote graft acceptance.

The use of specific commensal communities and metabolites to improve allograft outcomes and survival is a great challenge. Rationally designed commensal consortia have been used to potentiate the induction of specific cell types, like Tregs[93]. Utilizing such consortia can potentially facilitate allograft tolerance. Alternatively, the utilization of the metabolite butyrate can lead to similar results. This use of postbiotics[145], direct administration of microbial-derived bioactive molecules, bypasses the microbial communities. Great challenges still remain to identify and understand the signaling pathways and cellular targets of these metabolites. Chronic rejection in solid organ transplant patients and its potential modulation by the microbiota or microbial-derived metabolites has not been addressed.

Unbiased metabolomic profiling of patients with cardiovascular diseases revealed associations between developing diseases and metabolites derived from commensals[146,147]. Because vasculopathy is a common feature of chronic rejection, these metabolites may also be important in the context of transplantation. Trimethylamine N-oxide (TMAO), trimethyllysine (TML), and phenylacetylglutamine (PAGln) are generated from the catabolism of dietary proteins by gut commensals and have been categorized as atherogenic compounds. For example, Nemet and colleagues determined that PAGln affected platelets, via signaling through GPCR α2A, α2B, and β2 adrenergic receptors, rendering them hyperresponsive and prone to forming atherosclerotic plaques[147]. Atherosclerotic-prone, TMAO-producing mouse models transferred the atherogenic susceptibility by FMT, increasing TMAO levels in the recipients, which supports the causality of the microbiome in driving this phenotype[148]. These studies suggest a possible

impact of the microbiota on graft rejection over longer time periods via the metabolomic potential of gut commensals, a possibility that requires further investigation.

Fecal metabolomic data from human heart transplant recipients confirmed that many immunomodulatory metabolites were decreased in transplant versus healthy individuals, including the SCFAs acetate, butyrate, propionate, and the secondary bile acids LCA, isoalloLCA, and 3-oxoLCA[149]. These differences were likely due to disease severity and prior antibiotic exposure. Understanding if these metabolites have a causal role, or can be used as biomarkers of graft outcomes still remains to be validated. Moreover, recent profiling of liver transplant patients, found that low levels of SCFAs, secondary bile acids, and tryptophan metabolites found in patients correlated with an increased risk of postoperative infections[150], confirming interest in using metabolomic profiling in human transplant patients.

1.2.4 The microbiota and immunosuppressive drugs

Although treatment with antibiotics is clearly expected to affect microbiota composition, a recent study that screened over 1000 drugs with mammalian gene product targets reported that 24% of the tested drugs inhibited the growth of at least one bacterial strain[151]. Immunosuppressive drugs themselves have been found to drive some changes in microbial community structures[152,153], whereas cyclosporine A was reported to prevent posttransplant dysbiosis in rats transplanted with allogeneic livers[154]. Conversely, interpersonal microbiome variability has been associated with interpersonal differences in drug metabolism[155], affecting drug dosage. As proof-of-principle outside transplantation, *Eggerthella lenta* strains containing the gene for the reductase Cgr2 were found to inactivate the cardiac medication digoxin[156], such that individuals harboring such strains would need higher drug doses for equal activity. In kidney transplant patients, fecal abundance of *Faecalibacterium prausnitzii* was associated with needing

more tacrolimus within a month post-transplantation[157]. *F. prausnitzii* and other *Clostridiales* bacteria were found to metabolize tacrolimus into a byproduct that was 15-fold less potent than tacrolimus[158]. This metabolite was found to be produced in stool samples from healthy and kidney transplant recipients, confirming that the presence of certain commensals can help predict elimination routes of immunosuppressive drugs and identify optimal dosing[158].

The microbiota may also cause drug side effects. This has been well demonstrated with irinotecan, an anticancer chemotherapy drug. This drug is degraded systemically into inactive metabolites excreted in the gut. People harboring intestinal bacteria expressing β-glucuronidases can reactivate these metabolites that then cause severe toxic diarrhea[159]. Drugs that inhibit bacterial β-glucuronidase prevent gut reactivation of irinotecan metabolites and diarrhea in mice, demonstrating beneficial effects of targeting biochemical pathways in commensal rather than mammalian cells[159]. Mycophenolate mofetil (MMF) is an immunosuppressant commonly prescribed to transplant patients that can also cause diarrhea. In mice, antibiotics treatment or the GF status prevented MMF's gastrointestinal toxicity[153]. Recently, MMF was found to reduce the ratio of secondary to primary bile acids in SPF mice[160]. LCA alleviated MMF-induced colonic inflammation in a vitamin D-dependent manner, and the vitamin D analog paricalcitol could protect MMF side effects, confirming the microbiota-dependent transplant drug side effects[160].

1.2.5 The microbiota as a biomarker of transplant outcome or responsiveness to therapy

Another active area of investigation is whether the microbiota might be used as a biomarker of transplant outcome. In a cross-sectional study, the ratio of firmicutes:proteobacteria was found to be lower in intestinal transplant recipients undergoing acute rejection than in non-rejectors[109], and changes in urinary microbiota correlated with signs of chronic rejection in

kidney transplant recipients[161]. However, inter-personal variations in microbiota composition from either rectal, oral, or urinary samples are so wide[108] that analysis of longitudinal changes in each patient might better predict danger to the allograft or susceptibility to immunosuppression weaning.

Associations have also been made between the microbiota and transplantation tolerance or improved graft survival. Indeed, in a subset of kidney transplant recipients who developed spontaneous transplantation tolerance enabling immunosuppression withdrawal, Colas et al., 2020, described a correlation between tolerance and the presence of urinary *Janthinobacterium*, *Clostridia*, *Bacilli*, and *Lactobacillales* when compared with immunosuppressed patients with stable grafts[162]. Another study found that several beneficial genera in *Lachnospiraceae* in the gut were negatively correlated with serum creatinine and blood urea nitrogen in renal transplant patients[163].

As mentioned above, assessing the relative abundance of *F. prausnitzii* might also help choose the appropriate dose of tacrolimus[157]. Similarly, in the cancer field, the fecal microbiota composition in metastatic cancer patients prior to initiation of checkpoint blockade immunotherapy was recently shown to be predictive of subsequent responsiveness to therapy[164–166]. Importantly, antitumor immunity and susceptibility to anti-PDL1 therapy were transferable into melanoma-bearing GF mice by FMT from responder versus non-responder patient samples[164], showing not only the sufficiency of microbiota from responders to transfer this phenotype but also the conserved immune impact from human to mouse. Similar experiments could be performed in transplantation.

1.2.6 The microbiota as immunomodulating therapy

If shifts in microbiota can cause immune phenotypes, it makes sense to develop strategies to control microbial community structures through dietary interventions, antibiotics, or probiotics. For instance, gut bacteria promoted by a high-fiber diet alleviated type 2 diabetes[167]. In experimental transplantation, diets known to alter the microbiota, such as high-salt and high-fat diets accelerated graft rejection[168–170] and hyperlipidemia prevented tolerance induction[171]. As another lifestyle intervention, exercise, which is also known to alter the microbiota[172], prolonged skin graft survival in mice[173]. The causality of the microbial changes induced by high-fiber or high-salt diet or exercise on allograft outcome has not been established. For obesity, FMT from mice treated with a high-fat diet into GF mice accelerates skin allograft rejection, compared to FMT from mice fed a normal diet, confirming a causal role of the dysbiotic microbiota induced by high-fat diet in transplant outcome[174]. Of note, high-fat diet in GF mice also accelerated skin graft rejection, demonstrating a parallel microbiota-independent pathway for how high-fat diet accelerates graft rejection kinetics[174].

Although the use of antibiotics is probably too crude at the moment to reliably shape the microbiota and also risks promoting antibiotic-resistant bacterial strains, there may be a place for narrow-spectrum antibiotics if specific bacterial strains are proven to be dominantly pro-rejection. Bacterial strain-specific-targeting viral phages can also be developed as a pointed intervention, and commercial phages that target Listeria and Salmonella are already Food and Drug Administration (FDA)-approved. As mentioned above, strategies that target bacterial enzymes can also be considered, as are being tested to eliminate the intestinal toxicity or irinotecan[159].

FMT is now a well-accepted strategy to treat *Clostridium difficile*-driven diarrhea[175], and third-party FMT appears safe following hematopoietic stem cell transplantation (HSCT) to maintain intestinal microbial diversity[176], the loss of which is associated with bacterial domination and sepsis[177]. However, selection criteria for donors of FMT need to be refined as the transfer of pathogens asymptomatically associated with the donor can be life-threatening in the recipient. In solid organ transplantation, one could consider autologous FMT from pre-transplantation banking, as currently tested in clinical trials post-HSCT (ClinicalTrials.gov NCT03061097).

Alternatively, administration of clinical grade probiotics is attractive, but engraftment in recipients can be variable[178]. Interestingly, it might be possible to engineer probiotics to engraft better, as shown in a report in which the transfer of a cluster of genes allowing utilization of porphyrin, a marine polysaccharide not utilized by most bacterial strains, in conjunction with porphyrin dietary supplementation, enabled titrated control of probiotic engraftment across hosts[179]. *B. pseudolongum* and *A. onderdonkii* are the only commensals so far whose administration was sufficient to improve transplant outcome experimentally[121,180], and our new results have added *P. distasonis* to this short list[181]. In animal models, Xie et al., 2014, reported that supplementation with a combination of *Bifidobacterium longum, Lactobacillus acidophilus,* and *Enterococcus faecalis* reduced liver injury through increased Tregs in rats with acute liver transplant rejection. Supplementation with *Bifidobacterium* and *Lactobacillus* promoted partial restoration of gut microbiota and improved intestinal barrier function in malnourished rats after liver transplantation with long-term use of antibiotics[182]. In humans, Rayes et al., 2002[183], reported that patients who received living *Lactobacillus* plantarum plus fiber post-liver transplantation developed significantly fewer bacterial infections than patients with selective

bowel decontamination or than the group treated with inactivated Lactobacilli and fiber. Another randomized, double-blinded trial[184] showed that the incidence of post-operative bacterial infections was significantly reduced in liver transplant patients treated with lactic acid-producing bacteria plus fiber compared to fiber alone. In addition, the duration of antibiotic therapy was significantly shorter in the latter group. More work remains to be done to understand the role of the microbiota and of probiotics in the prevention of post-transplant complications.

In the cancer field, other strains of *Bifidobacterium* improved antitumor immunity and responsiveness to checkpoint blockade therapy in mice[185] and are already in clinical trials in metastatic cancer patients (ClinicalTrials.gov NCT03595683 and NCT03775850), supporting the potential for translation. Two small exploratory clinical trials providing FMT from melanoma patients that respond to anti-PD-1 immune checkpoint blockade into melanoma patients refractory to this treatment have been reported to promote tumor control in a subset of FMT recipients[186,187], confirming immune-dependent human translational benefits of the microbiota.

1.3 Conclusion

The impact of the microbiota in transplantation is only starting to be appreciated. Much more work needs to be done to identify the exact mechanisms by which the microbiota modulates alloimmunity, the specific microbial strains or community structures that participate in this process, the interaction between the microbiota and immunosuppression, and what constitutes a healthy microbiota for transplant patients[188,189]. Additionally, most of the work has focused on the role of bacteria. The study of the effects of resident fungi and viruses that are also part of the microbiota is an entirely open field, and changes post-transplantation are starting to be described in patients[190–193].

Chapter 2: Materials and Methods

2.1 Bacterial cultures

The *P. distasonis* strain DFI.5.70 obtained from the Duchossois Family Institute at the University of Chicago, was cultured in Columbia agar with 5% sheep blood cells (Remel, R01216) in an anaerobic chamber at 37°C for 24h. Bacterial lawns were harvested and resuspended in phosphate-buffered solution (PBS) with 10% glycerol and stored at -80°C. Mice received 200μL of *P. distasonis* (0.2 optical density 600nm) via gavage every two days, beginning 10 days before skin transplantation and continuing until the conclusion of the experiment.

A. onderdonkii DSM19147, DSM108265, and DSM108231 and *A. finegoldii* DSM17242 were obtained from the DSMZ Leibniz Institute (Braunschweig, Germany). *A. onderdonkii* DFI211 was obtained from the University of Chicago Duchossois Family Institute. All strains were cultured in Chopped Meat Medium (Anaerobe System, AS-811) in an anaerobic chamber at 37°C for 24 hours. Bacterial pellets were resuspended in PBS + 10% glycerol and stored at -80°C until used. For heat-killed experiments, *A. onderdonkii* DSM19147 was heated to 95°C for 1 hour immediately before oral gavage. 100 million bacteria or PBS were given every other day starting 7 to 10 days before transplantation and continued in the hosts until graft rejection.

The strains used in this study were *Staphylococcus epidermidis* (*S. epi*) NIHLM087, *Staphylococcus epidermidis* Tü3298, *Staphylococcus aureus* WU1, and *Escherichia coli* DH5α. Glycerol stocks for all strains were kept at –80°C. For culture, stocks were briefly removed from the freezer, poked with a pipette tip, and immediately returned to –80°C. For NIHLM087 and WU1, the pipette tip was deposited into 5 mL sterile Tryptic Soy Broth (TSB; BD Biosciences)

and cultured for 24 hours in a 1g, 37°C shake incubator alongside a negative control. Tü3298 was incubated for 48 hours at 37°C in TSB. DH5α was incubated at 1g at 37°C for 18–24 hours in 5 mL lysogeny broth (LB).

2.2 Mice

Six- to eight-week-old specific pathogen-free (SPF) C57Bl/6 (B6) male and female mice were purchased from Harlan Envigo or Taconic Farms (for *A. onderdonkii* experiments). Mice were mixed randomly to ensure microbiome homogenization. CD45.1^{+} *Rag2*-KO Marilyn B6 mice, used to isolate monoclonal CD4^{+} T cells that recognize a male-specific H-Y antigen presented on I-A$^{b\ 39}$, were obtained from Charles Mainhart via Taconic Biosciences and bred inhouse. TCRαKO mice (B6.129S2-Tcra<tm1Mom>/J, stock 002116) were ordered from The Jackson Laboratory and bred in our mouse facility. Bowie mice containing CD8^{+} TCR-transgenic T cells specific for a formylated peptide of *S. epi*[107] were sent to the University of Chicago from the Belkaid laboratory at the NIH. OT I mice containing CD8^{+} TCR-transgenic T cells specific for ovalbumin[194] on a Rag–/– background were bred at the University of Chicago. CCR2-DTR-CFP mice containing diphtheria toxin receptor (DTR) and cyan fluorescent protein (CFP) BAC construct, were provided by the Pamer laboratory at the University of Chicago. All mice were provided with Harlan Teklad 2018 diet and reverse-osmosis water. All experiments received approval from the University of Chicago Animal Care and Use Committee and were conducted following the National Institutes of Health Guide for the Care and Use of Laboratory Animals.

GF FVB mice (H-2q) were obtained from Tatyana Golovkina (University of Chicago gnotobiotic facility, Chicago, Illinois, USA). GF mice were kept in sterile isolators at the University of Chicago's Gnotobiotic Research Animal Facility and were fed autoclaved food and

water. Fecal aerobic and anaerobic cultures were carried out weekly to verify the status of microbial colonization.

2.3 Antibiotic pre-treatment

B6 male donor and female recipients were divided into 5 groups: control (Ctrl), gentamicin + kanamycin + colistin (GKC), vancomycin (V), vancomycin + metronidazole (VM), and full antibiotic cocktail (VMGKC). The mice received daily gavage with 100μL of the antibiotic combinations for the 10 days preceding skin transplantation. Antibiotic concentrations: 0.35mg/mL for gentamicin (Fresenius Kabi), 5.25mg/mL for kanamycin (Gibco, Thermo), 8500U for colistin (RPI), 0.5mg/mL for vancomycin (Hospira) and 2.15mg/mL for metronidazole (Sigma-Aldrich), all diluted in autoclaved water[17].

2.4 *S. epi* painting

Germ-free mice. NIHLM087 cultures grown as described above were removed from the incubator and immediately delivered to the gnotobiotic facility in a clean, sealable plastic bag. Members of the gnotobiotic facility thoroughly sterilized the tube and introduced it into the flexible firm isolator alongside sterile cotton swabs. Swabs were dipped into the tube carrying *S. epi* and rubbed all over the flank, tail, and ears of the mice. Each mouse was colonized with about 108–109 CFU every 2 or 3 days for a total of 5 applications over 10 days. For their entire time in the isolator, mice received 500 mg/L vancomycin (Hospira) in their drinking water to kill *S. epi* that entered their intestine from grooming. Skin-restricted colonization was verified by placing of skin swabs and fecal samples from colonized mice in 5 mL TSB buffer and incubation of the samples for 24–48 hours in the 1g, 37°C shake incubator. All samples were taken at least 1 day after a painting event to ensure measured bacteria were stably incorporated on the skin and

not recently applied. Mice with cloudy (bacteria-containing) skin sample cultures and clear fecal sample cultures were considered skin-monocolonized.

SPF mice. Chlorhexidine (Mölnlycke Health Care) was painted onto the tails of SPF mice for 5 consecutive days. Then NIHLM087 cultures grown as described previously were centrifuged at 657 g for 5 minutes and resuspended in 1 mL sterile 1× PBS. About 108–109 CFU of *S. epi* were painted on the flank, tail, and ears of conventional (commensal-carrying) mice using sterile cotton swabs. Mice were painted 5 times over the course of 1 week.

2.5 Short-chain fatty acid metabolomic profiling

Samples (200 µL) were extracted with organic solvent (800 µL of 100% methanol spiked with heavy labeled internal standards). Tubes were then centrifuged at -10 °C, 20,000 x *g* for 15 min and supernatant was used for subsequent derivatization and analysis. Metabolites from the spent media were derivatized as described by Haak et al, 2018[195]. Data analysis was performed using MassHunter Quantitative Analysis software (version B.10, Agilent Technologies). All metabolites are confirmed by comparison of retention time and detected *m/z* to authentic standards.

2.6 DNA extraction and quantitative polymerase chain reaction

Bacterial DNA for qPCR. DNA was extracted from fecal samples using QIAamp Fast DNA Stool Mini Kit (Qiagen) according to the manufacturer's protocol. Quantitative polymerase chain reaction (qPCR) was performed using the SYBR Green PCR Master Mix (Applied Biosystems) and QuantStudio3 qPCR thermocycler and software (Applied Biosystems). Primers used to detect *P. distasonis* DFI 5.70 were as follows: forward, TAG TAC CGT CAG GCA ACG TC, and reverse, ACG ACT GGG TTC TAA CAG GG. Primers to detect *B. globosum* were as follows: forward, CAA GGC CAT CAA CTG GTT CA, and reverse, ACG TCG TGC

TGC TCG AAT GT. Primers used to detect 16S ribosomal DNA gene were as follows: forward, AGA GTT TGA TCC TGG CTC AG, and reverse, TGC TGC CTC CCG TAG GAG T. The host housekeeping gene argininosuccinate lyase (ASL) primer sequences were as follows: forward, TCT TCG TTA GCT GGC AAC TCA CCT, and reverse, ATG ACC CAG CAG CTA AGC AGA TCA. Primers used specifically to detect *A. onderdonkii* DSM19147 were as follows: forward, GAG AGC AAT GAA CTG CAC GA, and reverse, GGC ACG ACG GGA TAG TAG AA.

Bacterial DNA for 16S rDNA sequencing. DNA was extracted using the QIAamp PowerFecal Pro DNA kit (Qiagen). Prior to extraction, samples were subjected to mechanical disruption using a bead beating method. Briefly, samples were suspended in a bead tube (Qiagen) along with lysis buffer. Skin swabs were resuspended in lysis buffer for an additional 30 minutes to maximize yield from samples. All samples were homogenized on Qiagen's TissueLyser II. Samples were then centrifuged, and supernatant was resuspended in CD2, that effectively removes inhibitors by precipitating non-DNA organic and inorganic materials including polysaccharides, cell debris and proteins. DNA was purified routinely using a silica spin column filter membrane. By adding solution CD3, a high-concentration salt solution, DNA selectively binds to the membrane which is recovered using elution buffer. DNA is then quantified using Qubit.

S. epi-specific PCR. Tissues painted with S. *epi* were swabbed with a sterile Puritan swab, placed in enzymatic lysis buffer on ice, and frozen at –80°C until DNA extraction. DNA was extracted using reagents from the Master Pure Yeast DNA Purification Kit and the Qiagen QIAmp Fast DNA Stool Mini Kit. *S. epi* DNA was amplified using forward primer 5′-

TTTATCGGAGGTCCAAGCGAA-3′ and reverse primer 5′-ACGGGCAAAAACACTGTCAT-3′ and run on a 1.5% agarose gel. Gels were analyzed using ImageJ software (NIH).

Quantitative real-time PCR for skin and LN cytokine signatures. Skin grafts and graft-draining LNs were isolated and homogenized on ice with TissueRuptor II handheld homogenizer (9002755, Qiagen) in RLT buffer at the volume suggested by the manufacturer's protocol for RNeasy Micro Kit (74004, Qiagen). The supernatant of homogenized skin was then processed with RNeasy Micro Kit for RNA isolation. The resulting RNA was used for cDNA amplification according to the manufacturer's protocol for iScript cDNA Synthesis Kit (1708891, Bio-Rad). The expression level of cytokines was determined by quantitative real-time PCR with primers specific for IFNγ, TNFα, IL-6, IL-12A, and IL-18 genes (Supplemental Table 1) and normalized for expression of β-actin or 18S, using iQ SYBR Green Supermix (Bio-Rad) and 7300 Real Time PCR system (Applied Biosystems).

2.7 16S rDNA sequencing

The V4-V5 region of the 16S rDNA gene was amplified using universal bacterial primers – 563F (5'-nnnnnnnn-NNNNNNNNNNNN-AYTGGGYDTAAA-GNG-3') and 926R (5'-nnnnnnnn-NNNNNNNNNNNN-CCGTCAATTYHT-TTRAGT-3'), where 'N' represents the barcodes, 'n' are additional nucleotides added to offset primer sequencing. The approximately ~412 bp amplicons were then purified using a spin column-based method (Minelute, Qiagen), quantified, and pooled at equimolar concentrations. Illumina sequencing-compatible Combinatorial Dual Index (CDI) adapters were ligated onto the pools using the QIAseq 1-step amplicon library kit (Qiagen). Library QC was performed using Qubit and Tapestation and sequenced on Illumina MiSeq platform to generate 2x250bp paired-end reads.

2.8 Skin transplantation

Skin grafts were harvested from male B6 donors and transplanted onto the flank of female B6 recipients as previously described[40]. Recipients were bandaged and monitored post-surgery. Bandages were removed 7 days after transplantation, and grafts were assessed through visual inspection. Graft rejection was called when what remained of the graft was <20% in size.

Aseptic surgery for SPF mice and sterile surgery for gnotobiotic mice were performed as previously described[196]. Tail skin from male C57BL/6 or FVB donor mice was transplanted onto the flank of female C57BL/6 recipients.

2.9 Recipient bacteria immunizations

NIHLM087, Tü3298, WU1, or DH5α cultures grown and centrifuged as described above were resuspended in 1 mL sterile 1× PBS (NIHLM087, WU1, DH5α) or 600 μL 1× PBS (Tü3298). NIHLM087, WU1, or DH5α cultures were diluted 1:5 in sterile 1× PBS in Eppendorf tubes, mixed thoroughly, and kept on ice. Resuspended solutions of Tü3298 were not diluted further. For experiments with heat-killed bacteria, diluted suspensions were incubated at 95°C for 1 hour. For all strains, 1 × 105 CFU (150 μL) of the bacterial suspensions were injected s.c. into SPF mice above the right hind leg using insulin syringes. Recipients were immunized 2 or 3 times over the course of 1 week and left for 1 month to develop immune memory.

2.10 Butyrate treatment

Butyrate micelle (*ButM*). ButM were prepared at a concentration of 100mg/mL as described in Wang et al, 2023[197]. For gavage experiments, 300ml of ButM were used per mouse, administered twice a day for the duration of the experiment. For intraperitoneal (ip) and

subcutaneous (sc) administration experiments, 200ml were injected per mouse, once a week for the duration of the experiment.

Sodium butyrate (*NaBut*). 100mM of NaBut (Sigma Aldrich) were prepared using purified water. The NaBut was placed in the water bottles and left for mice to drink *ad libitum*.

2.11 Depleting antibody injections

For TNF neutralization experiments, an anti-TNF antibody (BioXcell, clone XT3.11, no. BE0058) was diluted with PBS and injected intraperitoneally starting on the day of transplantation (200 μg per mouse 3 times a week) for 3 to 6 weeks.

Mice were bled to quantify $CD4^+$ and $CD8^+$ T cell populations before treatment. Then they were injected i.p. with 10 mg/kg (250 μg/ mouse) of anti-CD4 (clone GK1.5, Bio X Cell) or anti-CD8 (clone 2.43.1, Bio X Cell) antibody diluted in 200 μL PBS per mouse 3 days before the first *S. epi* immunization. One day later, they were bled, and their circulating lymphocytes were analyzed by flow cytometry alongside the pre-injection blood samples to ensure that the antibodies effectively depleted the targeted cell subset. Mice were injected i.p. with the same concentration of anti-CD4 or anti-CD8 again on the first and third days of s.c. *S. epi* immunization. Mice were left for 6 weeks to recover $CD4^+$ and $CD8^+$ T cell populations before transplantation. This recovery was verified using flow cytometry on longitudinal blood samples.

For $CCR2^+$ cell depletion, mice were injected with 5ng/ml of Diphtheria toxin (DT) on the day of transplantation and 1 and 3 days after.

2.12 Lymphocyte isolation

Spleen and peripheral lymph nodes (LNs, including brachial, axillary, inguinal, cervical, and mesenteric) were collected from $CD45.1^+$ *Rag2*-KO Marilyn B6 mice.

Lymph nodes. LNs were placed in complete DMEM (cDMEM; 1% HEPES, 1% nonessential amino acids, 2μL β-mercaptoethanol, 1% penicillin/streptomycin antibiotic, and 5% fetal bovine serum [FBS]). Samples were homogenized and filtered through 5μm mesh. Cells were centrifuged at 370*g* for 5min and were resuspended in cDMEM.

Spleen. Spleens were placed in cDMEM. Single cells were added to ACK buffer for red blood cell lysis and centrifuged as previously described.

Skin/graft. The flank was shaved before collection of the whole flank (2 × 3 cm) or skin grafts on the back (1 × 1 cm). All specimens were cut into small pieces and placed into digestion buffer: 1:10 DNase, 1:50 Liberase (Roche), and complete RPMI to volume. cRPMI was made by the addition of 2 μL β-mercaptoethanol and 5 mL HEPES solution to 500 mL RPMI stocks. Skin was digested for 2 hours in a 37°C shake incubator at 1g. The digested product was filtered through a 5 μm cell strainer into a Petri dish, and the tissue was smashed with the rubber end of a 1 mL plastic syringe plunger.

Bone marrow. Lymphocytes from femurs and tibia were flushed using a 30-gauge needle and cold 1X PBS into a petri dish and filtered in a 5 μm cell strainer. Single cells were added to ACK buffer for red blood cell lysis and centrifuged as previously described.

2.13 FTY720 injections

FTY720 (Enzo Life Sciences) was resuspended in 100% ethanol and stored in aliquoted stock solutions at –20°C. For injection, stock solutions were diluted in filter-sterilized distilled water and not PBS to improve the drug's solubility. Each recipient mouse was injected i.p. with 20 μg FTY720 in a 60 μL injection volume and monitored carefully to ensure that it did not suffer from alcohol poisoning or osmotic imbalance. Injections were performed 3 days and 1 day before transplantation, and injection success was measured by the absence of circulating

lymphocytes in recipient blood analyzed by flow cytometry. Four and ten days after transplantation, mice were again injected i.p. with the same dose of FTY720.

2.14 CFSE labeling

Lymphocytes from female CD45.1$^+$ *Rag2*-KO Marilyn B6 mice were resuspended in 5% FBS. An equal volume of PBS was mixed with Cell Trace CFSE dye (Thermo Fisher Scientific) diluted 2:1000. The CFSE-containing mixture was slowly added to the cell mixture while vortexing. The mixture was incubated for 5min at room temperature (RT). The reaction was quenched with 3 volumes of cDMEM containing 10% FBS. Stained cells were centrifugated for 5min at 370*g* and resuspended in PBS.

2.15 Adoptive transfer of Marilyn T cells

1×10^6 CFSE-labeled Marilyn T cells in 100μL were injected intravenously (i.v.) into mice 1 day prior to transplantation. On day 4 post-transplantation, skin-draining LN (sdLNs) (brachial, axillary, and inguinal) were harvested, and leukocytes were stained to assess T cell proliferation and stimulated to assess proinflammatory cytokine production.

2.16 Ex vivo stimulation of T cells

Adoptively transferred Marilyn T cells. Marilyn T cells from sdLNs were harvested 4 days post-transplantation. Lymphocytes (2×10^6) were plated in a 96-well plate and were stimulated with 0.5μg/mL anti-CD3 (clone 145-2C11) and 5μg/mL of Brefeldin A. Cells were placed in an incubator at 5% CO_2 and 37°C. After 18h, cells were stained and analyzed using flow cytometry.

In vitro cultured Marilyn T cells. APCs were isolated from skin dLNs of male B6 mice following magnetic enrichment with biotinylated anti-Thy1.2 (53-2.1, eBioscience) and anti-

NK1.1 (Frank W. Fitch Monoclonal Antibody Facility, University of Chicago) antibodies. Marilyn T cells were magnetically enriched from the peripheral LNs and spleens of Marilyn mice using streptavidin magnetic beads (catalog 88817, Pierce), anti–Ter119-biotin (TER-119, eBioscience), anti–CD11b-biotin (M1/70, eBioscience), and anti–NK1.1-biotin (PK136, Frank W. Fitch Monoclonal Antibody Facility at the University of Chicago) prior to CFSE labeling. APCs (2×10^5/well) were cultured with CFSE-labeled Marilyn T cells (1×10^5/well) in cDMEM for 4 days. T cells were restimulated with anti-CD3 (0.5μg/mL) (clone 145-2C11) in the presence of Brefeldin A (5 μg/ml) for 18h at 37°C and analyzed by flow cytometry

Graft-infiltrating/spleen T cells. T cells from grafts were harvested 7 days post-transplantation, or steady stae from the spleen, respectively. Lymphocytes were plated in a 96-well plate and were stimulated with 0.5μg/mL anti-CD3 (clone 145-2C11) in the presence of Brefeldin A (5μg/mL) for 18h at 37°C and analyzed by flow cytometry

2.17 Serum LPS measurement

Mice were bled at day -1, 4, 7 and 13 and serum was collected and stored at -80C. Serum endotoxin levels were measured using the Pierce chromogenic endotoxemia quantification kit (Thermo Scientifics).

2.18 LPS stimulation

Splenocytes were stimulated with lipopolysaccharide (LPS) (10 ng/ mL) and brefeldin A (5 μg/ml) was added into each well. After 18 hours, cells were recovered and stained for flow cytometry analyses.

2.19 Histology

Skin grafts were harvested from recipient mouse flanks. They were trimmed to include minimal tissue on the anterior and posterior edges of the graft and some excess recipient flank skin on the lateral edges. Grafts were cut in half transversely, placed in a tissue cassette, and immediately placed in 15–20 tissue volumes of 10% neutral-buffered formalin for 36–48 hours. Cassettes were rinsed once in 70% ethanol and then kept in 70% ethanol until embedding.

All embedding, sectioning, and staining were performed by the University of Chicago Human Tissue Resource Center. Samples were embedded on-edge, cut-side-down in paraffin. Sections were taken from the cut side, ensuring that analyzed tissue was from the center of the grafts. Slides were stained with H&E and given to a blinded pathologist for analysis.

2.20 Antibody staining and flow cytometry analysis

Cells were stained with a 1:1000 dilution of Live Aqua Live/Dead stain (Life Technologies) for 30min at RT in the dark. Endogenous *S. epi*-specific T cells were stained with H2-H3:fMIIINA tetramer in PE and APC fluorophores. Endogenous alloreactive T cells were stained with HY-IA^{b} tetramer in PE and APC fluorophores. Cells were treated with Fc block (clone 2.4G2, Biolegend) and stained with the following surface panel: anti-CD4 BV605 and BV711 (clone GK1.5, BioLegend), FITC (clone H12-9.19, BioLegend), and PE/Dazzle (clone RM4-5, Biolgened), anti-CD44 Pe-Cy7 and BV421 (clone IM7, BioLegend), anti-B220 V500 (clone RA3-6B2, BD Horizon), anti-CD8 BV711 (clone S3-6.7, BioLegend), TCRβ BV421 (H57597, BioLegend), NK1.1 BV421 (PK136, BioLegend), anti-Ly6C PCPCy5.5 (clone HK1.4, BioLegend), CD11c PE-Cy7 (N418, eBioscience), anti-CD64 APC-eF780 (clone X54-5/7.1, Invitrogen), I-A/I-E FITC (M5/114, BD Horizon), Siglec H PerCP-Cy5.5 (551, BioLegend), CD207 PE (eBioL31, eBioscience), CD103 FITC (2E7, eBioscience), anti-F4/80 BV421 and

FITC (BM8, BioLegend), anti-CD19 FITC (clone eBio103, eBiosciences), anti-Ly6G FITC (clone 1A8, BD Biosciences), anti-CCR2 PE (clone SA203G11, BioLegend), anti-CD11b BV605 (clone M1/70, BioLegend), anti-CD45.1 eF450 (clone A20, Invitrogen) and anti-CD45.2 (clone 104, BioLegend) for 10min at RT in the dark. For intracellular staining, cells were fixed and permeabilized with Foxp3 staining kit (Invitrogen) for 30min at RT in the dark. Cells were then stained with the following proinflammatory cytokine panel: anti-Ki-67 BV711 (clone B56, BD Biosciences), anti-Foxp3 FITC (clone FJK-16S, Invitrogen), anti-IFNγ (clone XMG1.2, BioLegend) and anti-TNFα (clone MP6-XT22, BioLegend) for 30min at RT in the dark, or overnight at 4°C.

Stained samples were analyzed on the LSR Fortessa 4-15 (BD Biosciences) in the University of Chicago Cytometry and Antibody Technology Core Facility.

2.21 Metagenome analysis

MAG were generated using the ATLAS v2.18. MSS reads underwent quality control using BBTools v37.99. The corrected reads were assembled into contigs using metaspades v3.13. The contigs were binned using metaBAT2 v2.14 and Maxbin2 v.2.2.7, resulting in our initial set of MAGs. These then underwent contig refinement using DASTool v1.1.2. MAGs were assessed using CheckM v.2.0. To obtain a unique set of MAGs, dRep was used to cluster genomes and select a representative genome for each cluster.

In order to annotate genomes, coding sequences (CDS) were identified with Prodigal v2.6.3, then annotated using DRAM providing annotations against multiple reference databases. Taxonomy and phylogeny of each MAG was determined using GTDB-Tk.

To extract functional information, contigs were aggregated to obtain a representative set of genes present in samples, resulting in over 300,000 unique genes. These sequences were then

annotated using DRAM and eggnog-mapper. Then mapped onto the resultant gene catalogue to provide gene abundance across samples.

2.22 Alpha Diversity Analysis

Sequencing results from dada2 were stored in phyloseq objects. Taxa with no aligned ASVs were removed from the phyloseq object and ASVs were normalized using edgeR. Alpha diversity (Shannon index) was calculated using phyloseq's estimate_richness function for each sample. Kruskal-Wallis tests were performed to detect differences between the groups.

2.23 Beta Diversity Analysis

Community-level analysis was performed on all samples at the genus level using Bray-Curtis distance metrics in a principal coordinate analysis (PCoA). Permutation analysis of variance (PERMANOVA) with the Bray-Curtis distance matrix was performed to detect global differences between groups using R's vegan package and adonis2 function. Ellipses for groups on the PCoA plot were calculated using a 95% confidence interval. To make pairwise comparisons, the pairwise.adonis function from the pairwiseAdonis package was used with Benjamini-Hochberg p-value adjustments. A Linear Discriminant Analysis (LDA) with Effect Size (LEfSe) differential abundance analysis was also carried out to find differences at the genus level between groups using the run_lefse function from the microbiomeMarker package. Only features (ASVs) with LDA scores > 1 and adjusted p-value < 0.05 were used for analysis.

2.24 Bulk RNA-Seq acquisition and analysis

Using the SMART-Seq mRNA LP kit from Takara Biosciences (cat # 634769), we FACS sorted 2,000 $Ly6C^{hi}CD11b^{+}$ splenic myeloid cells following administration of butyrate micelles or control. Cells were sorted directly into 1x lysis buffer containing RNase inhibitor and 3'

SMART-Seq CDS Primer II A. We followed the manufacturer's instructions, amplifying cDNA for 17 PCR cycles after first-strand synthesis. We then used the same SMART-Seq mRNA LP kit in combination with Takara's Unique Dual Index kit (1-96) (cat # 634752) to create libraries for sequencing per the manufacturer's instructions. The samples were sequenced using the Illumina NovaSeq platform with a 100 bp cassette and SP Flowcell. FAST-QC was performed on the resulting Fastq files to ensure the quality of the samples before moving on to alignment using the STAR splice-aware mapper and the GRCm39 mouse genome from Ensembl. A counts matrix was generated from the resultant BAM files using FeatureCounts. These raw counts were analyzed using the DESeq2 package on R to identify differentially expressed genes and normalized gene counts.

2.25 Statistical analysis

Flow cytometry data were analyzed using FlowJo (BD Biosciences). Analyses were performed in GraphPad Prism. The threshold for significance in all cases was $p<0.05$. Statistical tests used include the Log-rank (Mantel-Cox), the Ordinary one-way ANOVA followed by Šídák's multiple-comparison test, Dunnett's multiple-comparison test, or Kruskal-Wallis test for multiple comparisons, and Unpaired two-tailed t-test. All other MSS tests were performed using Wilcoxon-Rank sum test unless otherwise noted. Results are displayed as mean ± standard error of the mean (SEM). *P* values are as follows: *$p<0.05$; **$p<0.01$; ***$p<0.001$; ****$p<0.0001$.

Chapter 3: Influence of the commensal microbiota on solid organ transplant outcome

3.1 Coordinated elimination of bacterial taxa optimally attenuates alloimmunity and prolongs allograft survival

3.1.1 Abstract

This study aimed to dissect the relationship between specific gut commensal bacterial subgroups, their functional metabolic pathways, and their impact on skin allograft outcome and alloimmunity. Previous research identified that oral broad-spectrum antibiotic pre-treatment in mice delayed skin, heart and lung allograft rejection and dampened alloimmune responses. Rationally designed antibiotic combinations targeting major bacterial groups were used to elucidate their individual contribution in modulating alloimmune responses. Individual antibiotic cocktails targeting intestinal Gram-negative, Gram-positive, or anaerobic/Gram-positive bacteria by oral gavage, all delayed skin allograft rejection and reduced alloreactive T cell priming to different extents. Notably, the most pronounced extension of skin allograft survival and attenuation of alloimmunity were achieved when all gut bacterial groups were simultaneously targeted. These results suggest a model in which the strength of the alloimmune response is additively tuned by gut microbial diversity. Shotgun metagenomic sequencing enabled strain-level resolution and identified a shared commensal, *Parabacteroides distasonis,* as the most enriched following all antibiotic treatments. Oral administration of *P. distasonis* to mice harboring a diverse microbiota significantly prolonged skin allograft survival, identifying a probiotic with therapeutic benefits in transplantation.

3.1.2 Introduction

Solid organ transplantation stands as the best therapeutic option for addressing end-stage organ failure. However, the recipient's immune system detects the transplanted organ as non-self owing to genetic disparities between the donor and host[198]. The alloimmune response that ensues targets donor-derived major and minor histocompatibility antigens and, despite immunosuppression, can culminate in the destruction of the organ by acute or chronic rejection[199].

Exploring environmental factors that modulate immune responses may identify novel strategies to help promote graft survival and enhance a patient's quality of life. In recent years, diet, microbiome, pollutants and exercise, have all been shown to influence alloimmunity and transplant outcomes[200,201], positioning these environmental factors as potential targets of interventions to foster improved graft outcomes.

The microbiota, the complement of commensals that colonize a host, harbors diverse microbial components that can influence the immune system locally as well as systemically[133,202]. At homeostasis, the gut mucosal barrier allows for the translocation of beneficial microbial-associated molecular patterns (MAMPs) and metabolites that are released by microbes and can be found in the systemic circulation[132,203,204]. Using germ-free (GF) mouse models or reducing intestinal bacterial diversity using broad-spectrum antibiotics (Abx) in mice has been reported to result in impaired activation of protective immune responses[96,115,205], decreased severity and pathogenesis in autoimmunity[99,206,207] and resistance to immune checkpoint blockade therapy[138,165,208–211], supporting a mechanism by which commensals can fine-tune systemic immunity at steady-state.

The pre-transplant immune status of the recipient integrates all signals perceived by immune cells, determines how poised immune cells are to respond to activating stimuli, and may theoretically influence the alloimmune response upon transplantation[97,100,117,174,180,212]. Our group has previously shown that pre-treatment of both donor and recipient mice with broad-spectrum Abx before transplantation results in significantly prolonged survival of minor and major mismatched skin, heart and lung allografts[97,212]. The Abx cocktail employed in this study comprised the following components: vancomycin, a glycopeptide that targets Gram-positive bacteria by interfering with synthesis of bacterial cell walls[213]; metronidazole, a nitroimidazole that disrupts DNA structures within anaerobic microorganisms[214]; gentamicin and kanamycin, aminoglycosides that inhibit protein synthesis in Gram-negative bacteria[213]; colistin, a polymyxin that targets Gram-negative bacteria[215]. The alpha- and beta-diversity analysis of the bacterial composition post-cocktail Abx treatment revealed both decreased diversity and altered composition of the bacterial community. Gene expression profiling of skin-draining lymph node (sdLN) dendritic cells (DCs) post-Abx treatment showed decreased type I IFN and NF-κB gene signatures compared to DCs from control mice. Functional analyses exposed an impaired ability of antigen-presenting cells (APCs) from Abx-treated mice to activate alloreactive T cells in vitro and in vivo. These results suggested that Abx-sensitive bacterial taxa poise DCs, via specific signals that may include MAMPS and/or metabolites, to better prime alloreactive T cells, thus revving up the alloimmune response. Conversely, in Abx-treated mice, these signals are depleted resulting in an "un-poised" status of DCs and a weaker alloimmune response. This confirmed that distinct microbial communities can imprint distinct activation states onto DCs.

Transplant patients often develop a dysbiotic state of the microbiome associated with end-stage organ failure[216,217], recurrent viral and *C. difficile* infections[218], colonization with

multi-drug-resistant bacteria[219], co-morbidities that result in exposure to polypharmacy (proton pump-inhibitors, laxatives, immunosuppressive drugs, and antibiotics)[220], which altogether contribute to exacerbated dysbiosis, gut barrier injury, and gut leakiness[221]. The increased level of systemic signals derived from the microbiota can potentially enhance the poising status of immune cells which may put the transplant further at risk. This underscores the importance of understanding the signals provided by specific bacterial communities and the effect they exert on immune cells.

To understand the contribution of each Abx used in the cocktail and their target bacterial taxa to the modulation of graft rejection, we assessed the effects of different Abx combinations on graft outcome and on fecal microbiota composition using metagenome-assembled microbial genomes (MAG) bioinformatics technology. The full Abx cocktail (VMGKC) induced the greatest prolongation of skin graft survival and decrease of fecal bacterial diversity, followed by targeting of Gram-positive and anaerobic bacteria with vancomycin/metronidazole (VM) respectively, whereas the impact of Gram-negative-targeting Abx (GKC) was more modest. We also identified a commensal, *Parabacteroides distasonis* strain, DFI 5.70, that was capable of prolonging graft survival

Rather than identifying a particular grouping of bacteria involved in promoting alloimmunity, these data highlight the contribution of multiple distinct bacterial classes to the strength of the alloimmune response, with additive effects and greatest poising of APCs when the microbiota is most diverse.

3.1.3 Results

3.1.3.1 Targeting of distinct bacterial subgroups with various Abx combinations additively prolongs graft survival

To assess whether the targeting of distinct bacterial subgroups differently impacts graft survival kinetics C57Bl/6 (B6) female mice were gavaged with distinct Abx cocktails for 10 days, prior to transplantation of male B6 skin (Figure 3.1. 1A), as we have demonstrated to optimally modify the microbiota[97]. The combinations employed were: control (C); GKC to target Gram-negative bacteria; V to deplete Gram-positive commensals; VM to reduce both Gram-positive and anaerobic microorganisms; VMGKC to maximally reduce bacterial diversity. Consistent with our previous findings[97], pre-treatment with VMGKC significantly prolonged graft survival (Figure 3.1. 1B). Surprisingly, all Abx combinations significantly prolonged graft survival, although to different extents (Figure 3.1. 1B). These data support the conclusion that the individual targeting of each major bacterial category can improve graft outcome, with additive beneficial effects when the broadest spectrum of commensals is simultaneously targeted.

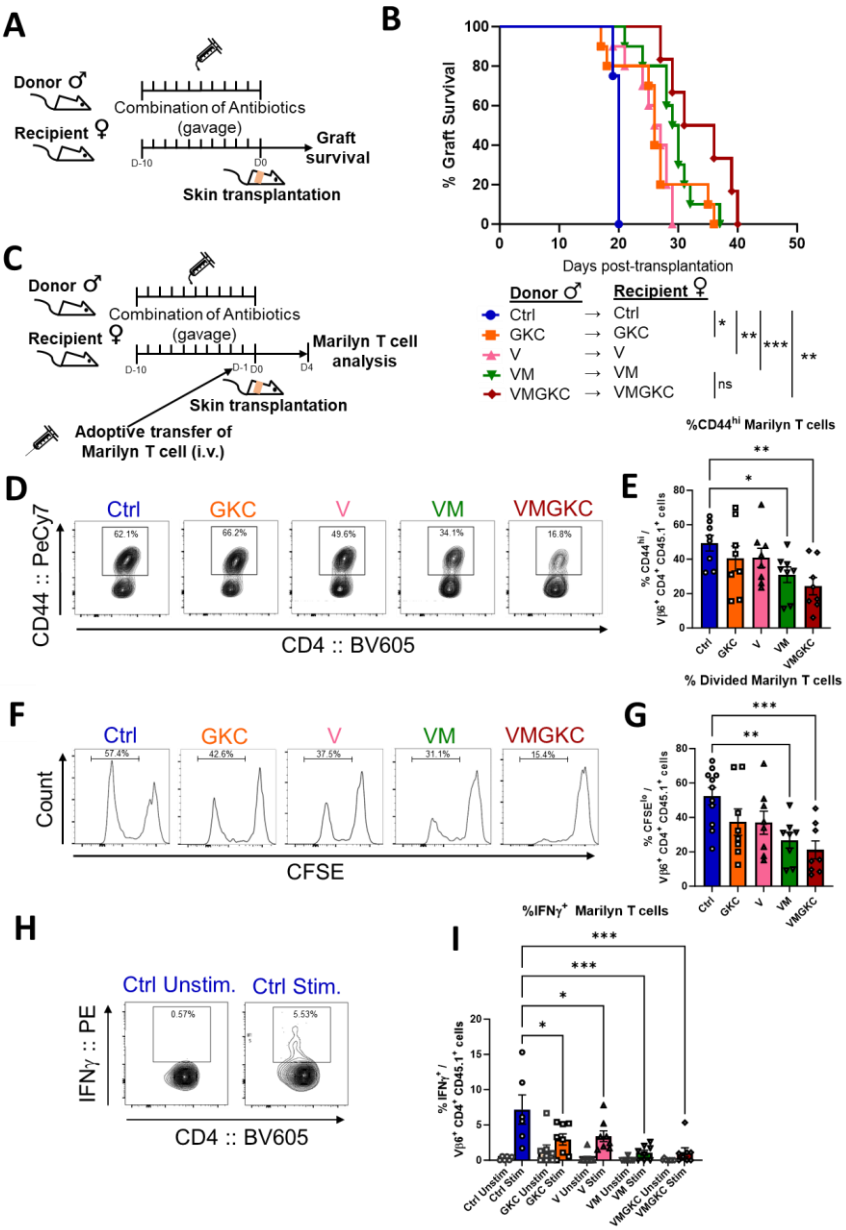

Figure 3.1. 1. Additive prolongation of graft survival and reduction of alloimmunity by cumulative targeting of different bacterial subgroups.

(A) Mice were gavaged for 10 days with different Abx combinations. Male skin was transplanted onto female hosts on d0. (B) Allograft survival curves. (C) CFSE-labeled Marilyn T cells were adoptively transferred into female recipients one day prior to surgery. Four days post-transplantation, sdLNs were harvested, and Marilyn T cell priming was assessed. (D-I) Representative flow cytometry plots and quantification of $CD44^{hi}$ (D, E), CFSE dilution (F, G), and IFNγ production upon anti-CD3 (0.5μg/mL) restimulation (H, I) by Marilyn T cells. Data represent the mean ± SEM. Ctrl, control; V, vancomycin; VM, vancomycin and metronidazole; GKC, gentamicin, kanamycin, and colistin; VMGKV, full antibiotic cocktail, Unstim, unstimulated; Stim, stimulated.

3.1.3.2 Alloimmunity is most decreased by the broadest spectrum Abx cocktail

In previous research, we established that pre-treatment with broad-spectrum Abx attenuated graft rejection by inhibiting alloimmune priming[97]. To investigate the impact of the various Abx combinations, monoclonal H-Y-specific CD45.1$^+$ CD4$^+$ T (Marilyn) T cells were CFSE-labeled and adoptively transferred 1 day prior to transplantation into Abx-pre-treated female B6 recipients (Figure 3.1. 1C). Lymphocytes were isolated 4 days post-transplantation from skin-draining LN (sdLN). Marilyn T cells displayed significantly reduced activation (Figure 3.1. 1D-E) and proliferation (Figure 3.1. 1F-G) in VM- and VMGKC-pre-treated groups, compared to control (Ctrl) recipients. Data from GKC- and V-pre-treated mice did not reach statistical significance. To investigate the effect of depletion of specific bacterial categories on alloreactive T cell differentiation, lymphocytes were re-stimulated overnight with anti-CD3. Marilyn T cells isolated in all Abx displayed a reduced proportion of IFNγ-producing cells (Figure 3.1. 1H-I), with greatest impact by VM- and VMGKC-pre-treatments (6.5-fold). TNFα production was not affected (Figure 3.1. 2A-B). Thus, signals from all major commensal bacteria categories can augment priming of alloreactive T cells and Th1 differentiation, with the greatest contribution coming from Gram-positive and anaerobic commensals.

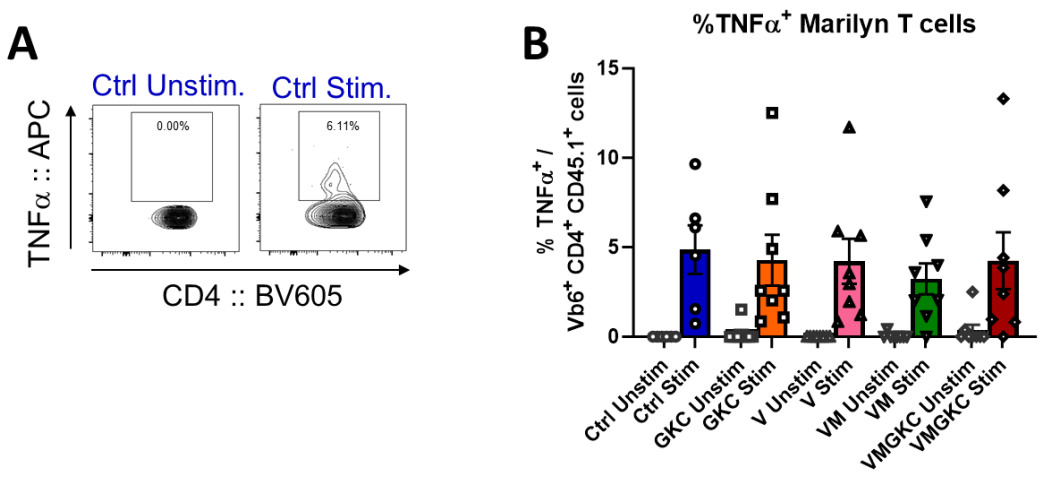

Figure 3.1. 2. Abx cocktails do not reduce TNFα production by Marilyn T cells.
Marylin T cells were transferred one day before transplantation of female recipients that had been pre-treated for 10 days with the Abx regimens as for Figure 1.1.1. Marilyn T cells were harvested from the sdLNs on d4 post-transplantation and stimulated overnight with soluble anti-CD3 (0.5μg/mL). (A, B) Representative flow cytometry plots and quantification of TNFα production. Unstim, unstimulated; Stim, stimulated.

3.1.3.3 Microbial diversity is most reduced by VM and VMGKC

Microbiota composition was analyzed in fecal bacterial DNA extracted before (Pre) and after 10 days of daily Abx gavage. Quantification of the bacterial load using 16S rDNA qPCR revealed that, at the doses used, none of the Abx combinations decreased bacterial burden (Figure 3.1. 3A) (as mice are adults), suggesting that the impact of Abx on alloimmunity and graft survival was due to qualitative rather than quantitative microbiome changes.

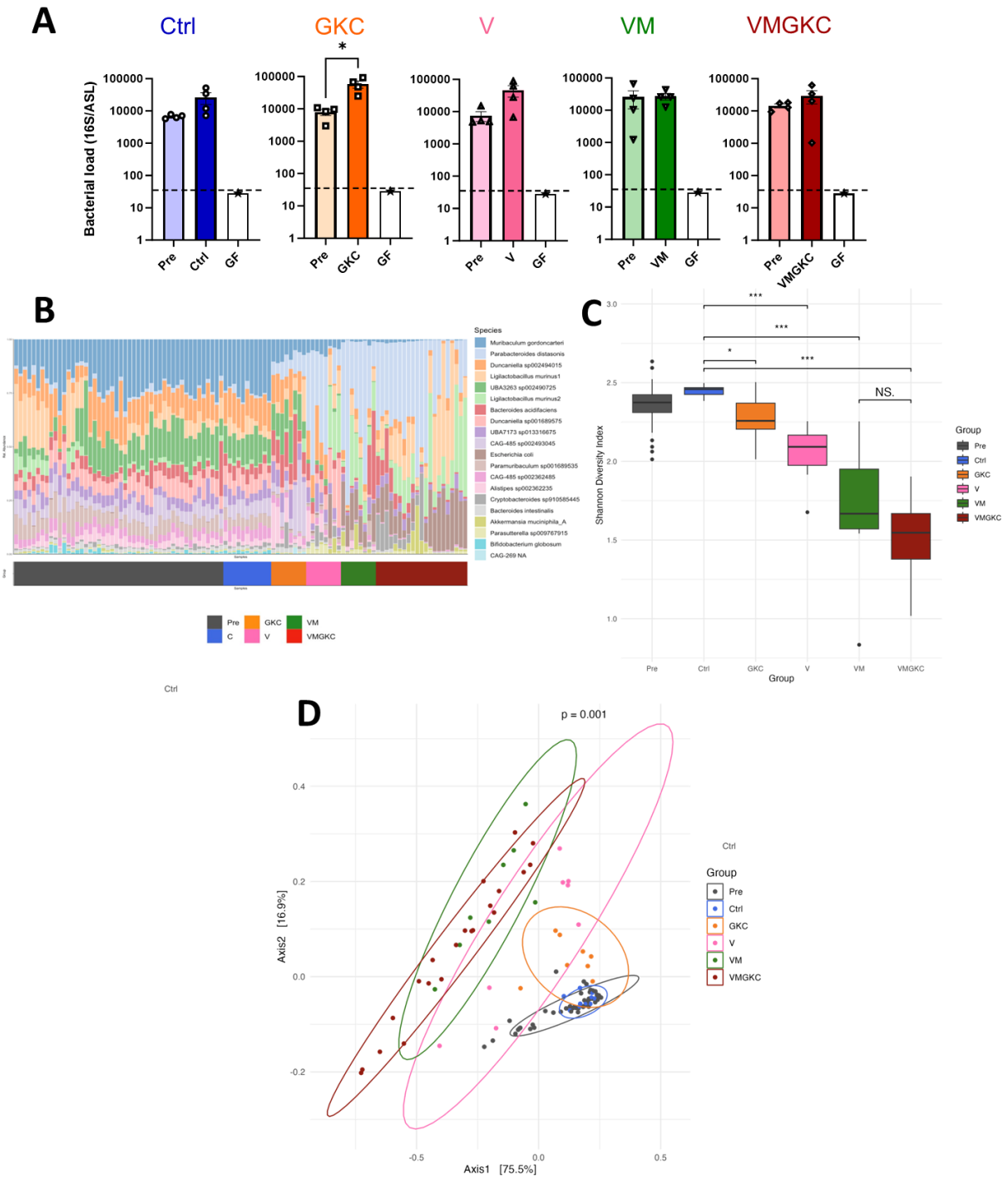

Figure 3.1. 3. *P. distasonis* fecal bloom is common to all Abx cocktails.
Mice received Abx cocktails for 10 days. Fecal samples were collected on d0 and 10 of Abx treatment, and bacterial DNA was isolated for qPCR analysis and MSS. (A) Total bacterial load was measured by qPCR using primers for the bacterial 16S rDNA gene and the host housekeeping gene ASL. (B) Species-level taxonomic relative abundance. (C) Boxplot illustrating the Shannon-diversity index. (D) PCA biplot displaying beta-diversity. GF, germ-free.

We performed metagenomic shotgun sequencing (MSS) with open reading frame (ORF) analysis of the assembled contigs. ORFs were extracted and clustered, revealing around 300,000 unique genes. To parse out the specific bacterial strains enriched/depleted by the different Abx combinations, we generated metagenome-assembled genomes (MAG). We obtained 20 unique complete bacterial genomes (Figure 3.1. 3B). Fecal samples from Pre and Ctrl mice displayed similar microbial composition (Figure 3.1. 3B-C). At the bacterial population level, all Abx cocktails led to significantly reduced richness and diversity (Figure 3.1. 3C-D). Alpha-diversity progressed from most diverse to most reduced following GKC > V > VM > VMGKC Figure 3.1. 3C), which paralleled the progressive decrease in alloimmunity (Figure 3.1. 1). PCA confirmed that the dysbiotic states were qualitatively distinct, with samples clustering separately from both Pre and Ctrl, and VM- and VMGKC-treatments overlapping yet positioned farthest from no treatment (Figure 3.1. 3D). Therefore, greatest variety of commensal elimination achieved by targeting Gram-positive and anaerobic commensals was associated with the greatest beneficial impact on the graft.

3.1.3.4 Targeting different bacterial subgroups with Abx combinations modifies microbial metabolic pathways

MAMPs and metabolites are important regulators of immune responses and are directly associated with the metabolism of commensals[133,202]. In view of our MAG dataset, we identified Kyoto Encyclopedia of Genes and Genomes (KEGG) modules related to metabolic pathways in the different treatments (Figure 3.1. 4A). The clustered heatmap of KEGG modules of Figure 1.1.4A confirms that the Abx combinations impacted metabolic pathways differently. To understand the potential association of the microbiota metabolism with graft outcomes, we searched for two types of correlations: KEGG modules that increased in all combinations of

Abx, as they may be related to protective pathways; and KEGG modules that only decreased in the VMGKC cocktail, which prolonged graft survival the most, as they may be related to pro-rejection pathways.

The amino acid pathways of proline (Figure 3.1. 4B) and lysine (Figure 3.1. 4C) demonstrated a consistent increase across all combinations of Abx. In contrast, the serine module (Figure 3.1. 4D), was depleted in the VMGKC-treated mice. Two vitamin synthesis modules, B2 (Figure 3.1. 4E) and B5 (Figure 3.1. 4F), also exhibited reductions solely in response to the VMGKC cocktail, along with the lipid A module of the lipopolysaccharide (LPS) component (Figure 3.1. 4G). Thus, the analysis of the relative abundance of KEGG modules related to metabolic functions revealed associations with specific graft outcomes.

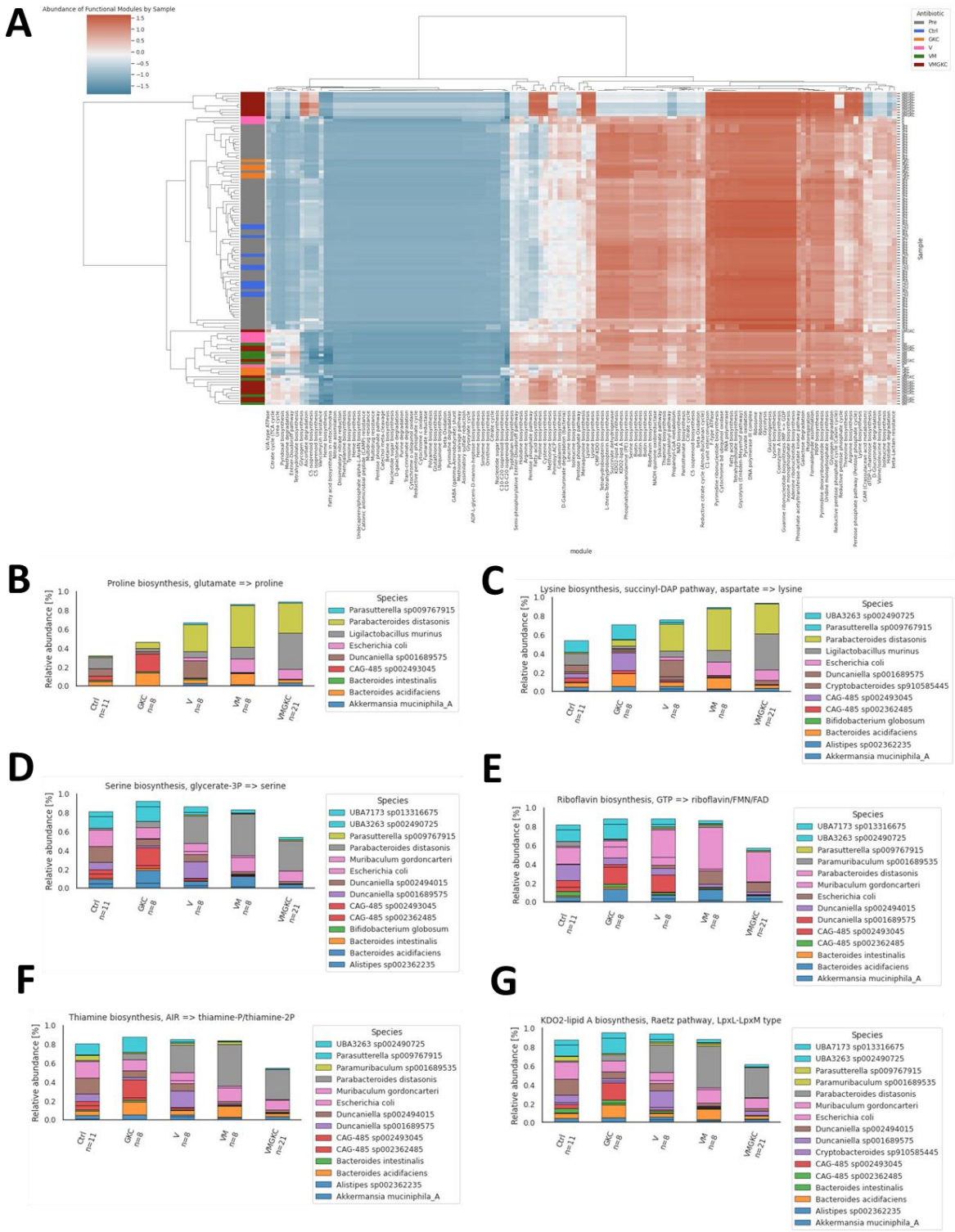

Figure 3.1. 4. Coordinated elimination of major bacterial groups reshapes microbial metabolic pathways.

(A) Clustered heatmap of microbial functions. Functions were annotated using KEGG Modules. (B-G) Key microbial functions as given by the relative abundance of microbial taxa.

3.1.3.5 *P. distasonis* strain DFI 5.70 prolongs graft survival

Because all regimens reduced Th1 differentiation of graft-reactive T cells and prolonged graft survival, we reasoned that bacterial strains that bloomed following all Abx regimens may represent protective strains for alloimmunity, whereas bacterial strains eliminated by all Abx regimens may indicate pro-rejection taxa. Of particular interest were bloomed strains that contained proline and lysine pathway-associated genes identified above. Significant changes common to mice treated with all Abx regimens included a relative expansion of *Parabacteroides distasonis* and a reduction in relative abundance of *Bifidobacterium globosum* (Figure 3.1. 5A).

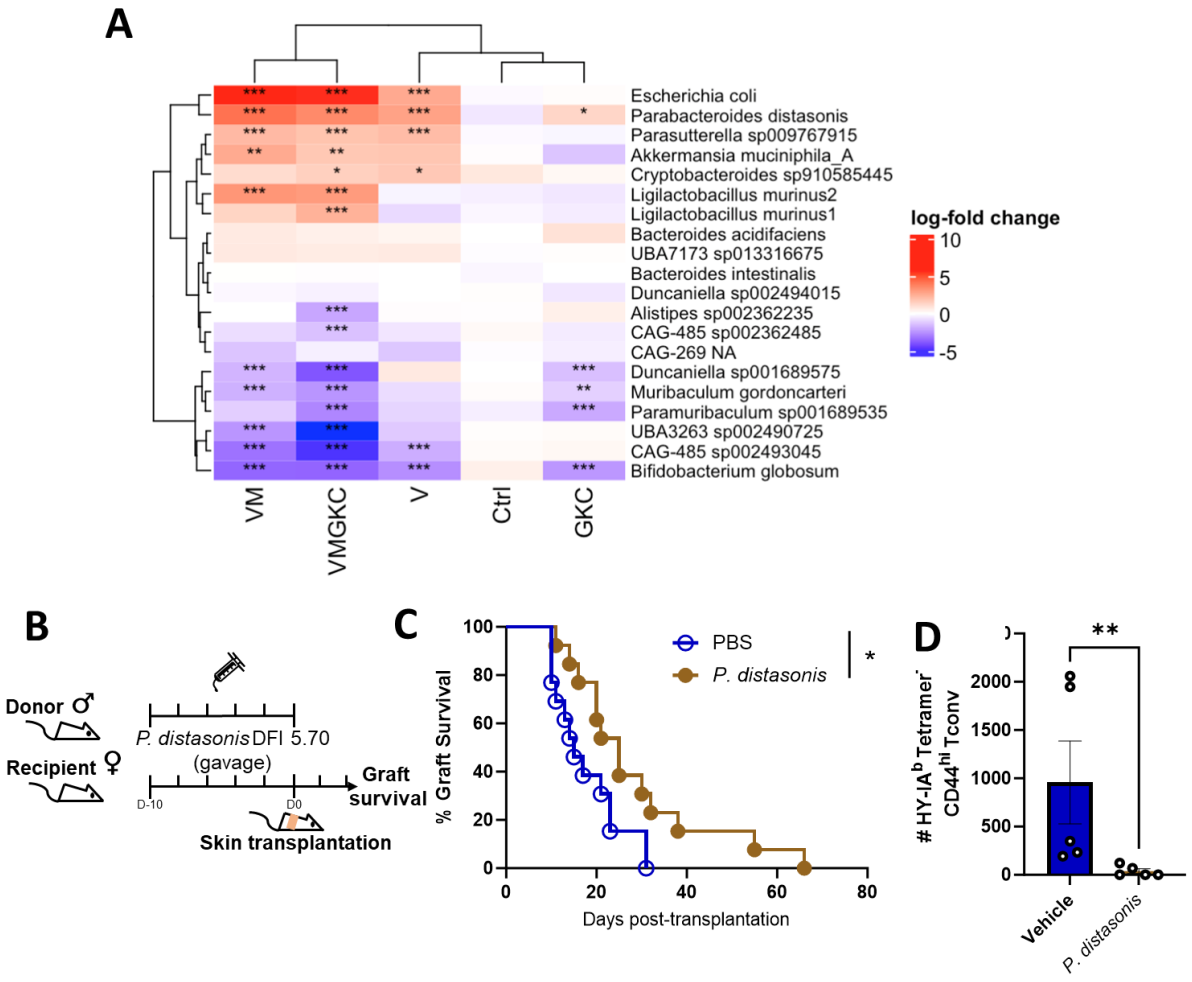

Figure 3.1. 5. Oral administration of *P. distasonis* strain DFI 5.70 prolongs skin allograft survival.
(A) Heatmap displaying differential abundance of microbial taxa calculated by ANCOM-BC. Color gradient represents the log-fold change in abundance. (B) Mice were gavaged with vehicle or *P. distasonis* strain DFI 5.70 every other day starting 10 days before transplantation and continuing until the end of the experiments. (C) Allograft survival curves. (D) Endogenous alloreactive T cells (day 44 post transplantation).

P. distasonis is considered a core member of a healthy microbiota[222] and has recently been identified to be an immunomodulatory commensal, capable of suppressing metabolic dysfunction, fibrosis, and autoimmunity[223–227]. Given the shared elevated abundance in mice treated with all the different Abx regimens and the presence of enriched metabolic pathways (Figure 3.1. 4A-C), we explored whether its administration as a probiotic could improve graft

outcome in mice not treated with Abx (Figure 3.1. 5B). The University of Chicago hosts a biorepository of human commensals. We chose *P. distasonis* DFI 5.70 as the strain that best matched the amplicon sequencing variants observed by MSS in Abx-treated mice. Recipients that received *P. distasonis* strain DFI 5.70 only until the day of transplantation exhibited a significant prolongation of graft survival (Figure 3.1. 5C), and reduced endogenous alloreactive T cells (Figure 3.1. 5D). Despite the improved graft outcome, the treatment did not modify the fecal bacterial load (Figure 3.1. 6A) and did not increase the relative abundance of *P. distasonis* DFI 5.70 (Figure 3.1. 6B), suggesting the probiotic presumably exert its function during its transient passage through the gastrointestinal tract. Of note, *P. distasonis* administration did not reduce the abundance of *B. globosum* (Figure 3.1. 6C), the commensal that was significantly depleted in all Abx combinations (Figure 3.1. 5A), suggesting that *P. distasonis*' effect on graft outcome is not due to elimination of this putatively pro-rejection strain. These data confirm that the commensal *P. distasonis* DFI 5.70 has probiotic potential to help improve graft outcomes.

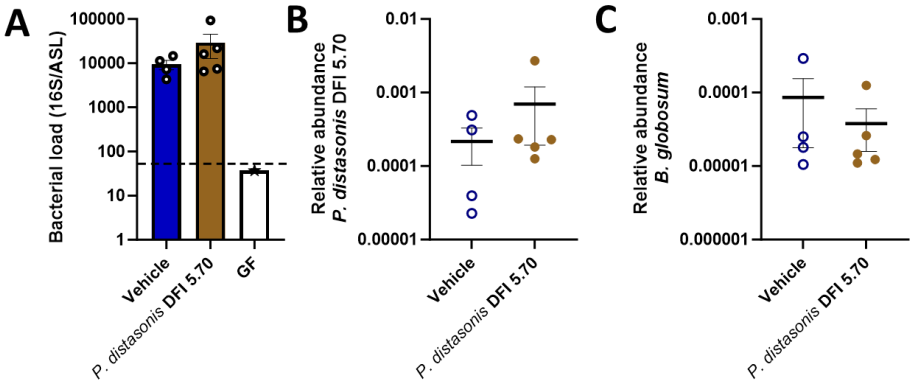

Figure 3.1. 6. Gavage of *P. distasonis* strain DFI 5.70 does not increase fecal bacterial load or *P. distasonis* abundance.
Mice were gavaged every other day with *P. distasonis* strain DFI 5.70 for 10 days. Fecal samples were collected on d0, and bacterial DNA was isolated for qPCR analysis. (A) Total bacterial load was measured by qPCR using primers for the 16S rDNA gene and host housekeeping gene ASL. (B, C) Relative abundance was measured by qPCR using primers for *P. distasonis* strain DFI 5.70 (B) and *B. globosum* (C) and bacterial 16S rDNA gene.

3.1.4 Discussion

In this study, we aimed to identify microbial strains and associated metabolic pathways capable of improving or worsening graft outcomes. Building upon our previous findings that broad-spectrum Abx pre-treatment in mice led to slower graft rejection[97], we used rationally designed Abx combinations to target major bacterial subgroups and investigate their contributions to modulating alloimmune responses. To comprehensively evaluate the impact of Abx combinations on bacterial communities, we complemented our analysis with MSS, enabling us to generate MAG and achieve a strain-level resolution with metabolic functional data.

Our investigations revealed that all major bacterial subgroups, Gram-negative, Gram-positive, anaerobic/Gram-positive, significantly delayed allograft rejection and reduced the priming/differentiation of adoptively transferred and endogenous alloreactive T cells. Moreover, the simultaneously targeting of bacterial subgroups using VMGKC led to the most robust extension of graft survival and attenuation of alloimmunity. These observations point to an additive model in which the strength of an immune response is tuned by the aggregate of microbiota. A diverse microbiome generates a multitude of signals that are recognized by various pattern-recognition receptors (PRRs) and integrated by APCs[228,229].

Depending on the specific bacterial group eliminated, certain MAMPs and metabolites are depleted, extinguishing their respective PRR signaling pathways within APCs[230,231]. This results in differential states of APC poising and variable capacities to elicit immune responses, including reduced alloimmunity and Marilyn T cells activation[97]. For example, targeting bacterial taxa reduces ligands for TLR and NOD receptors, which activate NFκB and IRF3/7[228,229]. Consequently, targeting different bacterial subgroups can impact NFκB and IRF3/7 activation and fine-tuning of the activation potential of APCs[232,233]. These findings underscore

how the greatest positive tuning of APCs is observed when the microbiota exhibits maximal diversity[96,115,205]. Redundant PRR signaling calibrates APCs for context appropriate immune response initiation. The greater prolongation of minor mismatched skin graft survival induced by VMGKC, when compared to the individual effects of VM or GKC, suggests that each combination extends graft survival through distinct mechanisms, potentially by depleting different microbial-derived signals. While VMGKC pretreatment delays rejection more modestly following major than minor mismatched transplantation, there might be synergy with low dose immunosuppression.

Transitioning from correlation to causality, our group[117,174,180] and others[121] have used probiotics to improve graft outcomes. Administration *Alistipes oderdonkii* was sufficient to prolong graft survival through inhibition of TNFα production[117,180]. Administration of *Bifidobacterium pseudolongum*, a commensal that bloomed in pregnant mice, was sufficient to reduce heart transplant chronic rejection and diminish proinflammatory cytokine production in LPS-stimulated myeloid cell lines[121].

Given the reduced Th1 differentiation in graft-reactive T cells and the prolonged graft survival across all Abx regimens, we postulated that bacterial strains flourishing after such treatments could potentially denote transplant protective strains. *P. distasonis* was of interest, as it bloomed under all Abx combination treatments. Remarkably, administration of this commensal to animals with a diverse microbiota significantly prolonged graft survival and reduced priming of endogenous graft-reactive T cells, affirming its causal impact on transplant outcome. *P. distasonis*' effect following daily gavage was apparent despite lack of durable intestinal engraftment. While antibiotic pretreatment may facilitate its engraftment by creating space, it is

unlikely that additional *P. distasonis* administration would prolong graft survival over that achieved with Abx therapy, as Abx already caused bloom of endogenous *P. distasonis*[97].

P. distasonis is present in the gastrointestinal tract of humans and mice[225]. Wei et al, identified the pentadecanoic fatty acid produced by *P. distasonis* as protective in mouse models of non-alcoholic steatohepatitis, via restoring gut barrier and reducing serum LPS[227]. The commensal also alleviated obesity-related dysfunctions in mice by producing succinate and secondary bile acids[224].

In summary, our use of rationally designed Abx cocktails to target bacterial categories, coupled with the assessment of fecal microbiome using MAG technology, has revealed that all bacterial subgroups investigated additively contribute to augmenting alloimmunity and that maximally reducing bacterial diversity correlates with greatest extension of graft survival and suppression of alloimmunity. These findings highlight the importance of microbial diversity in calibrating alloimmunity. Furthermore, our results position *P. distasonis* strain DFI 5.70 as a promising probiotic candidate to facilitate transplant survival.

3.2 Oral administration of the commensal *Alistipes onderdonkii* prolongs allograft survival

3.2.1 Abstract

Intestinal commensals can exert immunomodulatory effects on the host, with beneficial or detrimental consequences depending on underlying diseases. We have previously correlated longer survival of minor mismatched skin grafts in mice with the presence of an intestinal commensal bacterium, *Alistipes onderdonkii*. In this study, we investigated its sufficiency and mechanism of action. Oral administration of *A onderdonkii* strain DSM19147 but not DSM108265 was sufficient to prolong minor mismatched skin graft survival through inhibition of tumor necrosis factor production. Through metabolomic and metagenomic comparisons between DSM19147 and DSM108265, we identified candidate gene products associated with the anti-inflammatory effect of DSM19147. *A onderdonkii* DSM19147 can lower inflammation both at a steady state and after transplantation and may serve as an anti-inflammatory probiotic beneficial for transplant recipients.

3.2.2 Introduction

The gut microbiota plays a fundamental role in the induction, training, and function of its host's immune system. Intestinal commensals can potentially exhibit either immunostimulatory or immunosuppressive effects on the host, with beneficial or detrimental consequences depending on underlying diseases. For example, specific Bifidobacterium strains synergized with immune checkpoint inhibitors to reduce tumor burden in mice[138,234]. Conversely, commensals that suppress the immune system might be of interest in settings of transplantation and

autoimmunity or to reduce chronic systemic inflammation often associated with heart disease, diabetes, obesity, arthritis, and inflammatory bowel disease[235,236].

Previously, we have shown that the gut microbiota composition can causally modify allograft rejection kinetics in mice, with pretreatment antibiotics prolonging skin allograft survival in specific pathogen-free mice, and fecal microbiota transfer (FMT) from conventional but not antibiotic-treated mice, accelerating rejection in germ-free mice[97]. Moreover, the steady-state microbial differences existing between individuals might explain variances in graft rejection kinetics. Indeed, we reported that C57Bl/6 (B6) mice obtained from Jackson Laboratories (JAX) exhibited slower skin graft rejection kinetics than those exhibited by genetically similar B6 mice obtained from Taconic Farms (TAC), which bear intestinal microbiota distinct from those in JAX mice. Importantly, FMT from JAX to TAC and cohousing of TAC and JAX mice both resulted in prolonged graft survival in TAC mice[117] suggesting that an intestinal component from JAX mice could exert a dominant suppressive effect in TAC mice, beneficial to the graft. Analyses of the gut microbiome profile in mice from the different vendors predicted an *Alistipes* spp., most consistent by oligotyping with *Alistipes onderdonkii*, as a candidate for this effect because it was present in the fecal material from JAX mice but not in the fecal material from TAC mice and was one of only 2 species engrafting into TAC mice after both JAX FMT and JAX/TAC cohousing[117]. However, the sufficiency of this taxon or its mechanism of action for improving graft survival remains to be investigated. In this study, we found that oral administration of *A onderdonkii* strain DSM19147 to TAC mice was sufficient to prolong skin graft survival and correlated with reduced production of tumor necrosis factor α (TNFα) by both innate and adaptive immune cells, an immune effect that we show benefited graft survival. Through comparisons between *A onderdonkii* DSM19147 and strains that did not

prolong graft survival, we identified unique genes associated with the beneficial strain. We conclude that select commensals can inhibit TNFα production and be beneficial in the setting of transplantation.

3.2.3 Results

3.2.3.1 Intestinal presence of *A onderdonkii* is associated with prolonged survival of minor mismatched skin grafts

Using a minor mismatch skin graft model in which skin from a male B6 mouse was transplanted onto an otherwise syngeneic female B6 host, we previously found that mice from JAX and TAC, which harbored distinct intestinal microbiota, displayed different rejection kinetics, with JAX mice rejecting skin grafts more slowly than TAC mice[117]. Transfer of JAX mice's gut microbiota into TAC mice dominantly conferred a slow-rejecting phenotype[117]. To identify microbes associated with this prolonged graft survival, we profiled the gut microbiota of JAX and TAC mice using 16S ribosomal RNA gene sequencing and oligotyping analysis for taxonomic assignment. Two taxa present at a significantly lower abundance in TAC mice than in JAX mice, an *Alistipes* spp. and a *Bacteroidales* spp., were significantly enriched in TAC mice after FMT from or cohousing with JAX mice (Figure 3.2. 1). Of these 2 taxa, *A onderdonkii* was identified at the species level and was 20 times more abundant after cohousing than the unspecified *Bacteroidales* spp.

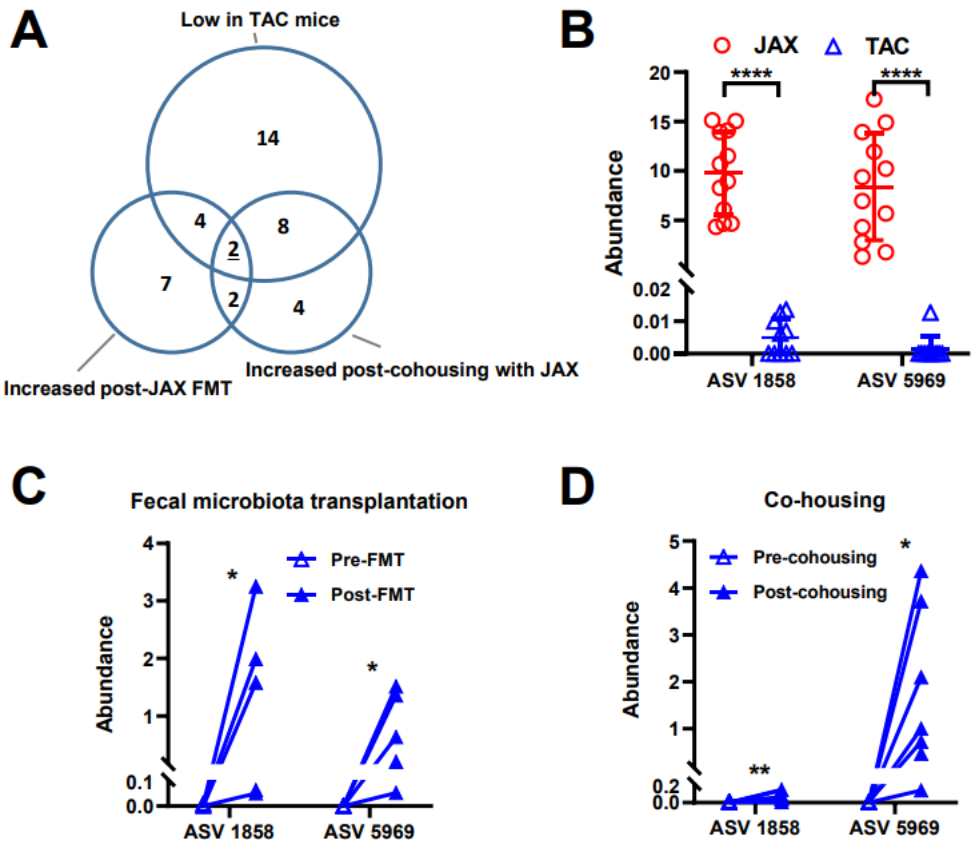

Figure 3.2. 1. Enriched abundance of two taxa correlates with slower skin graft rejection in JAX compared with TAC mice.
(A) Fecal samples from JAX and TAC B6 mice were subjected to 16S rRNA gene sequencing and oligotyping analysis. (B) Amplicon sequence variants (ASV) that were significantly less abundant in TAC mice, (C) significantly enriched after JAX mouse FMT into TAC mice, and (D) significantly enriched after cohousing of JAX mice with TAC mice. The abundance of ASV 1858 (*Bacteroides*) and ASV 5969 (*Alistipes*), the only 2 strains that fulfilled all 3 criteria, is shown.

3.2.3.2 Oral administration of *A onderdonkii* DSM19147 is sufficient to prolong skin allograft survival in conventional mice

To test the impact of *A onderdonkii* on the kinetics of skin graft rejection, we obtained and cultivated 2 available Alistipes spp. These bacteria were then gavaged to donor and recipient mice every other day starting 1 week before transplantation and continuing in host mice until euthanization. Although administration of *A onderdonkii* DSM108265 did not modify skin graft

rejection kinetics, DSM19147 consistently prolonged skin graft survival in independent experiments (Figure 3.2. 2A). To understand the effect of *A onderdonkii* treatment on T cells, the cell type responsible for transplant rejection, we isolated immune cells from spleen and sdLNs after graft rejection, stimulated them overnight with anti-CD3/anti-CD28 antibodies, and measured their ability to produce TNFα and IFNγ. DSM108265 did not alter the cytokine production capacity compared with vehicle-treated mice, whereas DSM19147 modestly but significantly suppressed TNFα production by $CD4^{+}Foxp3^{-}$ conventional T cells Figure 3.2. 2B). To determine whether treatment with DSM19147 affected alloreactivity, another cohort of mice was euthanized 10 days after transplantation, and graft-reactive H-Y–specific $CD4^{+}$ T cells were enumerated in sdLNs using peptide:I-Ab tetramers. The number of graft-reactive $CD4^{+}$ T cells was reduced in the sdLNs of DSM19147-treated mice (Figure 3.2. 2C), supporting the conclusion that administration of *A onderdonkii* DSM19147 resulted in reduced alloreactivity.

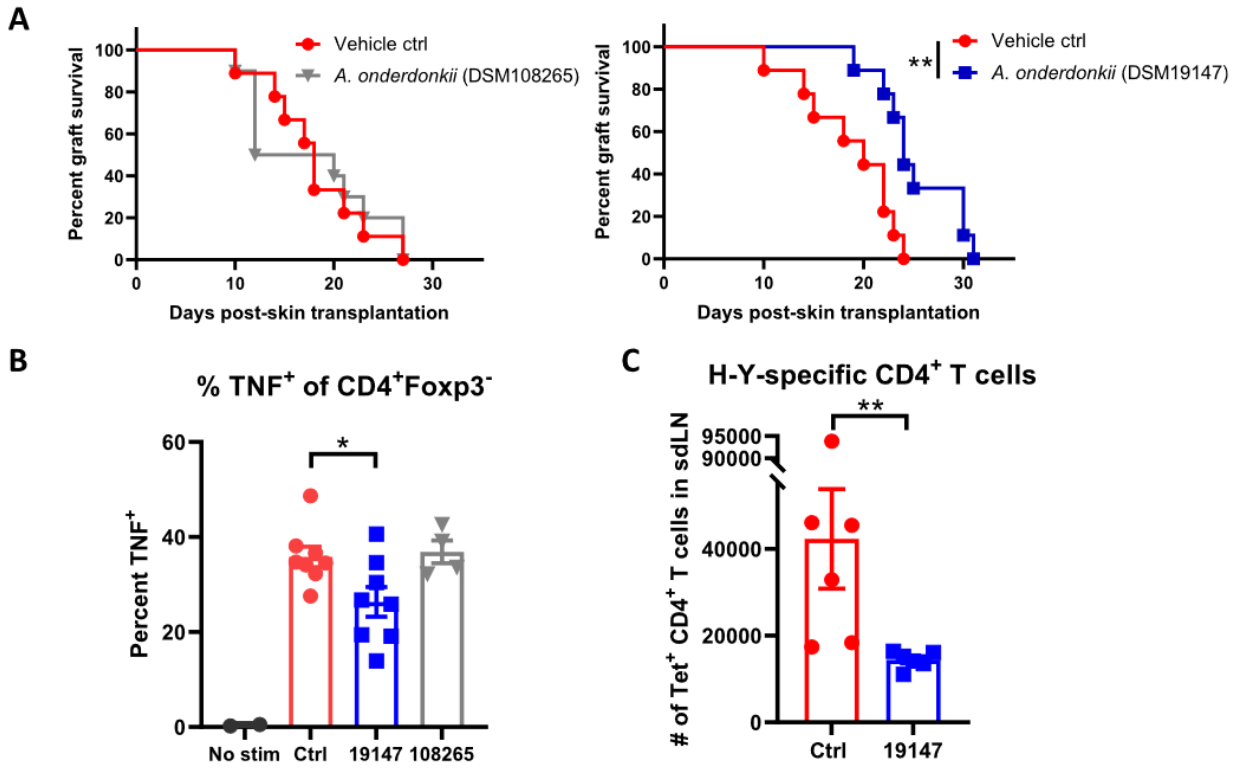

Figure 3.2. 2. Oral administration of *Alistipes onderdonkii* DSM19147 prolongs skin allograft survival and reduces alloimmunity.
Male C57BL/6 skin grafts were transplanted onto female C57BL/6 recipients. Mice received a gavage of either vehicle or *A onderdonkii* DSM108265 or DSM19147 every other day starting 1 week before transplantation and continued until the end of the experiments. (A) Allograft survival curves. (B) Tumor necrosis factor α (TNF α) production in $CD4^+$ T cells after anti-CD3/anti-CD28 stimulation of cells from spleen- and skin-draining lymph nodes (sdLNs) isolated after graft rejection. No stim: no stimulation. (C) Number of Y chromosome (H-Y) peptide:I-Ab–binding alloreactive $CD4^+$ T cells in sdLNs on d10 after transplantation. Ctrl, control.

3.2.3.3 Gavage of *A onderdonkii* DSM19147 reduces TNFα production in T cells, and antigen-presenting cells (APCs) and TNFα neutralization prolongs skin graft survival

To investigate whether the effect of *A onderdonkii* DSM19147 on TNFα production was restricted to mice undergoing an allograft rejection or also occurred at a steady state, we isolated cells from the spleen of untransplanted DSM19147- or vehicle-treated mice. T cells and APCs were stimulated with anti-CD3 or LPSs in vitro, respectively. We found that DSM19147 modestly but significantly decreased the production of TNFα by antigen-experienced

$CD4^+Foxp3^-CD44^{hi}$ and $CD8^+CD44^{hi}$ T cells (Figure 3.2. 3A). Under low-dose LPS stimulation, $CD11c^+$ and $CD11b^+$ cells from DSM19147-treated mice produced less TNFα than that produced by their counterparts from vehicle treated mice (Figure 3.2. 3B), supporting an effect at a steady state. Because *A onderdonkii* DSM19147 prolonged graft survival and suppressed TNFα production, we investigated whether reducing TNFα was sufficient to prolong graft survival. As shown in Fig. 1.2.3C, administration of a neutralizing anti-TNFα antibody after skin transplantation significantly prolonged skin graft survival, similarly to DSM19147 gavage Figure 3.2. 2B). Moreover, gavage of DSM19147 did not improve graft survival in anti TNFα-treated animals (Figure 3.2. 3C), indicating that the beneficial effects of DSM19147 on transplant survival depend on its TNFα-reducing ability.

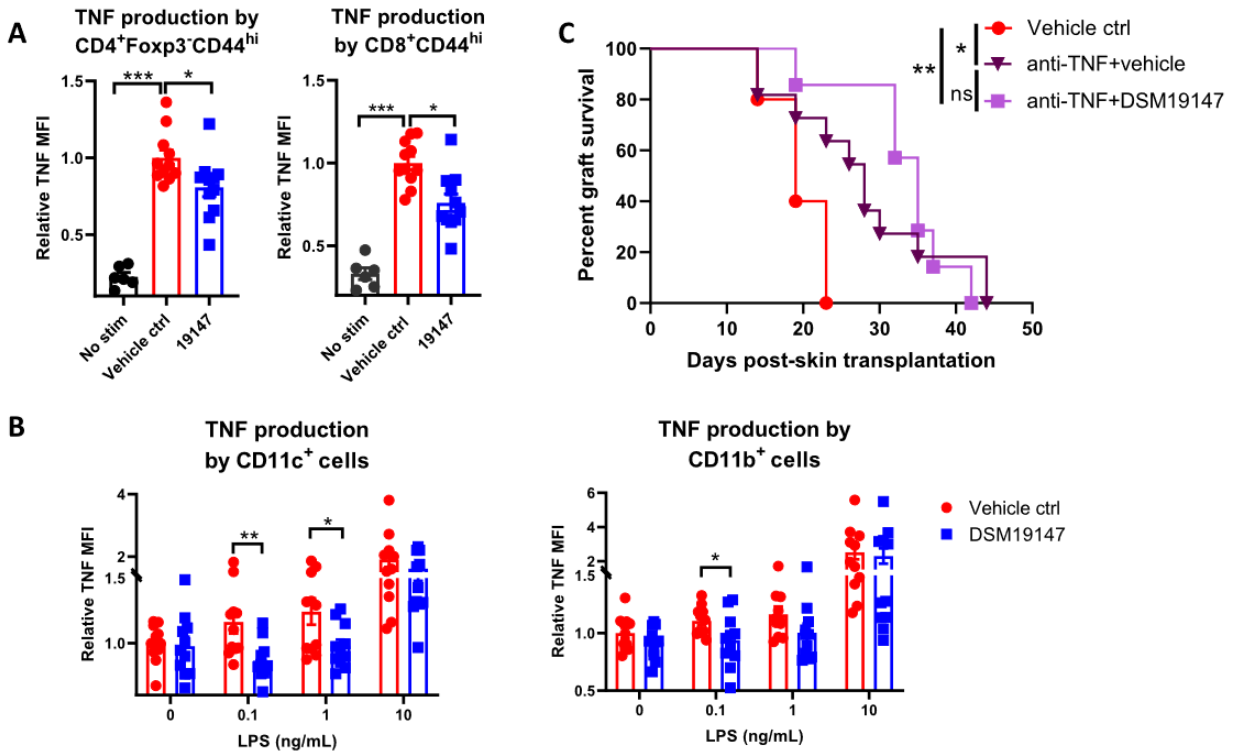

Figure 3.2. 3. Oral administration of *Alistipes onderdonkii* DSM19147 results in reduced tumor necrosis factor a (TNFα) production by immune cells.
(A) Flow cytometry analysis of TNFα production in different populations of T cells after overnight stimulation of splenocytes with soluble anti-CD3 (0.1 μg/mL). MFI: mean fluorescence intensity. (B) Flow cytometry analysis of TNFα production in different populations of myeloid cells ($CD11c^+$ and $Cd11b^+$) after overnight stimulation of splenocytes with lipopolysaccharides (LPS) (0.1, 1 and 10 ng/mL). (C) An anti-TNFα neutralizing antibody was injected intraperitoneally into female hosts of a male skin graft starting on the day of transplantation (200 μg/d, 3 times a week). These mice also received vehicle control (ctrl) or *A onderdonkii* DSM19147. ns, not significant.

3.2.3.4 *A onderdonkii* DSM19147 harbors unique genes

Commensals may mediate their effect by engaging pattern recognition receptors or altering the host's metabolic profile. The administration of heat-killed *A onderdonkii* DSM19147 failed to prolong skin allograft survival (Figure 3.2. 4), suggesting that the active production of metabolites may be responsible for the beneficial effect of live DSM19147 on transplant survival.

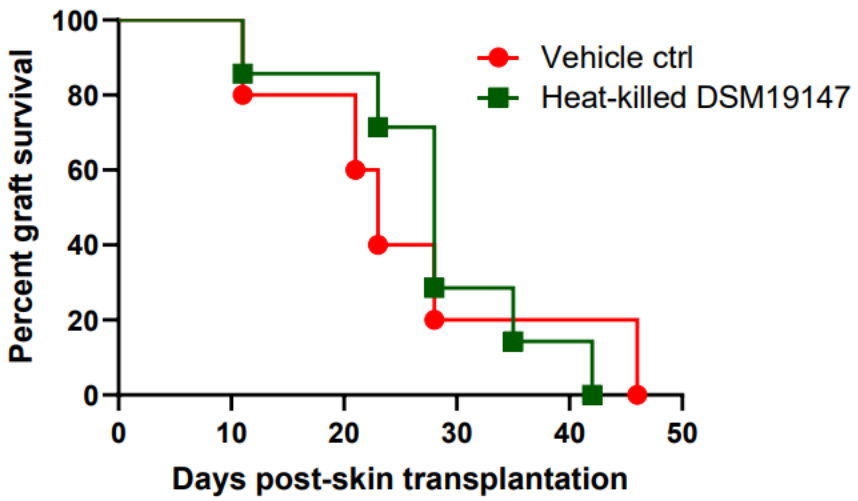

Figure 3.2. 4. Heat-killed *A. oderdonkii* DSM19147 does not prolong skin graft survival. Mice received a gavage of vehicle control or heat-killed *A. oderdonkii* DSM19147 every other day starting 10 days before transplantation of male skin onto female recipients and continued until the end of the experiments. Graft survival was recorded over time. No significant differences between the curves were found.

Measurements of immune modifying metabolites (amino acids, SCFAs, and phenolic metabolites) were similar in the fecal samples isolated after 1 week of gavage with DSM19147 versus DSM108265 (Figure 3.2. 5A); however, in 4 of 5 mice, treatment with DSM19147 was associated with lower levels of valine, leucine, isoleucine, and glycine than those associated with DSM108265 gavage (Figure 3.2. 5B).

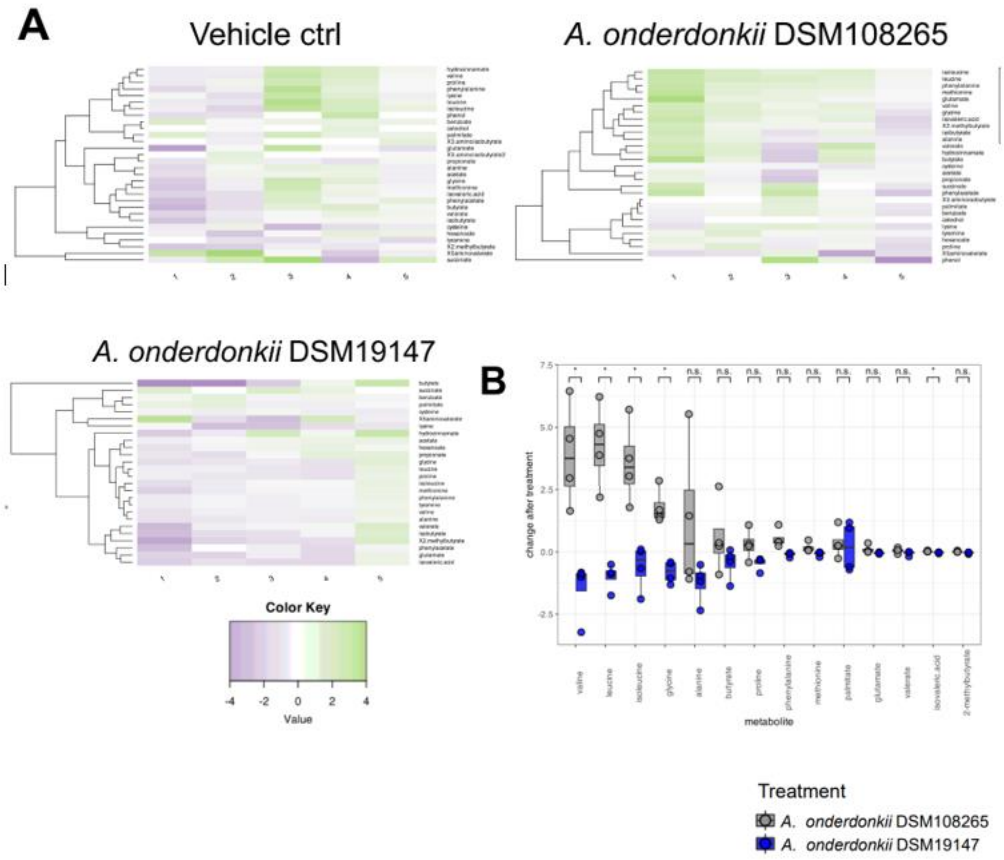

Figure 3.2. 5. Comparison of fecal metabolomics.
(A) Heatmap of differences in normalized relative abundance of analyzed metabolites (Log2 transformed) before and after mice received oral gavage with vehicle control, DSM108265 or DSM19147 every other day for 1 week. (B) The differences of normalized relative abundance for each metabolite before and after 1 week of treatment with DSM19147 or DSM108265 in 4 out of the 5 mice shown in A, with outlier excluded.

To determine whether the DSM19147 genome encoded unique genes absent in DSM188265 and in 2 other *A onderdonkii* and 1 *A finegoldii* control (DSM17242) strains that also failed to prolong graft survival (data not shown), the pangenome of the 5 strains was generated using anvi'o[237,238], revealing a unique set of 234 genes in DSM19147 (Figure 3.2. 6A). To identify potential functional differences between these strains, all genes in the pangenome were annotated using the Kyoto Encyclopedia of Genes and Genomes (KEGG) Orthology database[239] (Figure 3.2. 6B, C) and the Clusters of Orthologous Genes (COG) database (not shown). We found 17 predicted functions within the 234 genes unique to DSM19147. Of these,

11 functions were found to occur in the other 4 strains through a different set of gene clusters, revealing 6 functions only found in DSM19147 (Figure 3.2. 6B). Two of these annotations corresponded to enzymes along a single pathway, 2-keto-3-deoxy-D-glycero-D-galacto-nononate 9-phosphate synthase and 2-keto-3-deoxy-D-glycero-D-galacto-nononate 9-phosphatase, that facilitates the downstream synthesis of the sialic acid N-acetylneuraminic acid[240].

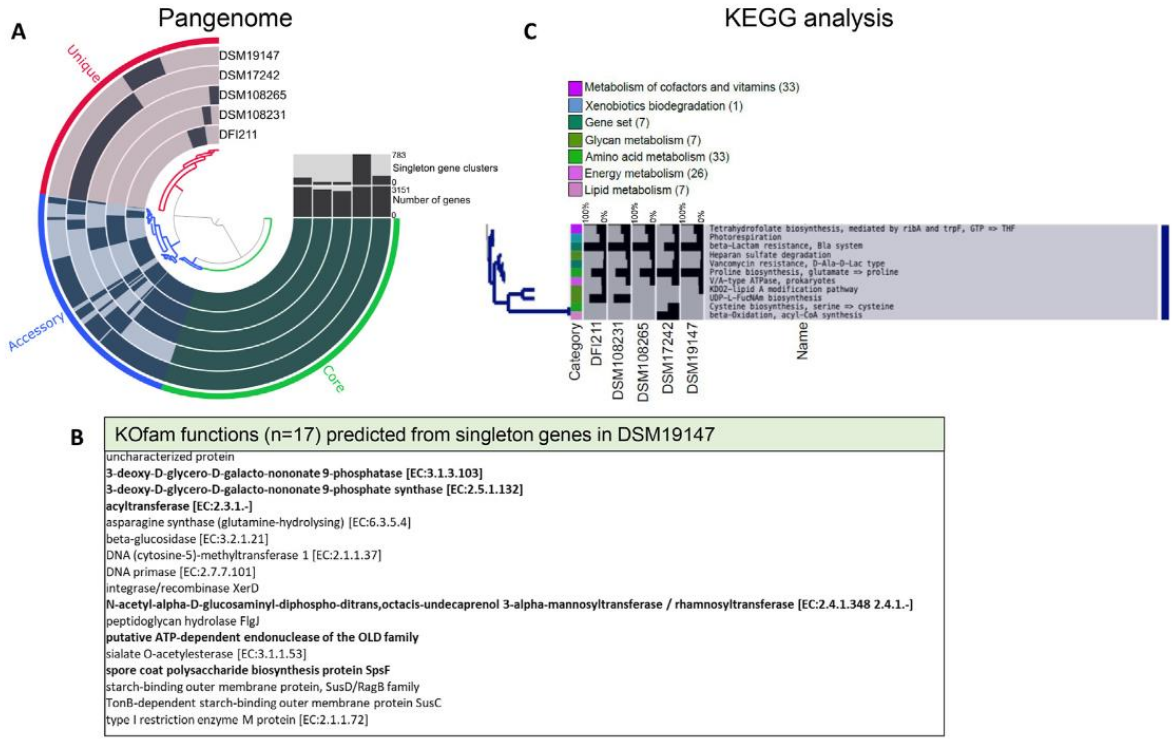

Figure 3.2. 6. *Alistipes onderdonkii* DSM19147 harbors unique genes when compared with strains that do not prolong graft survival.
(A) The generated pangenome for 4 *A onderdonkii* and 1 *A finegoldii* DSM17242 strains identified shared and unique gene clusters. The overall pangenome is organized according to the total number of gene clusters identified across all strains (4410 gene clusters), with each gene cluster marked as a tick (presence/absence) or bar height across multiple measures corresponding to concentric layers as the chart pans from 0 to 270 degrees. The innermost 5 concentric circles display the presence or absence of a given gene cluster for the corresponding strain (labeled after the 270 mark). The outermost ring identifies the sets of genes that are present in all 5 strains (core), more than 1 strain (accessory), or unique to a single strain (singleton). A phylogram within the circle represents clustering of genes on the basis on their presence/absence across strains. The bar plot labeled "Singleton gene clusters" displays the total number of genes unique to each strain (maximum number of unique genes belonging to *A. finegoldii* DSM17242). The bar plot labeled "Number of genes" displays the total gene content number for each strain (values range from 2658 [DSM108625] to 3151 [DSM19147]). (B) The table of Kyoto

Figure 3.2. 6. cont. Encyclopedia of Genes and Genomes (KEGG) functions predicted from the 234 unique genes found in DSM19147. Seventeen genes of the 234 gene clusters unique to DSM19147 were assigned a function. Across these 17 genes, there were 17 unique functions; however, 11 of these were performed by other genes present in the pangenomes of the other 4 strains. A final count of 6 functions unique to DSM19147 (in bold) was determined, of which 2 performed the final 2 steps in N-acetylneuraminic acid synthesis. KOfam: KEGG Orthologs family (C) Metabolic reconstruction map shows differences in *A. onderdonkii* strains' ability to participate across metabolic pathways. A black bar graph represents the percent of functions within the metabolic processes (labeled, right) that is present in a given strain (labeled, below). Metabolic modules are grouped by encompassing category labels (color-coded, left and above).

Metabolic enrichment analysis was then performed on all pangenomes to infer putative strain-level differences in amino acid and glycan metabolism pathways. DSM108625 had partial completion of the proline biosynthesis pathway, whereas DSM19147 had full completion. Additionally, DSM19147 but not DSM108625 had partial functionality in the 3-deoxy-d-manno-octulosonic acid (KDO2)-lipid A modification pathway (Figure 3.2. 6C).

3.2.4 Discussion

In this study, we used data-driven analyses to select *A onderdonkii* as a potential anti-inflammatory gut commensal and showed that a specific *A onderdonkii* strain, DSM19147, could reduce T cell priming and TNFα production in T cells and myeloid cells and prolonged allograft survival. Furthermore, because blocking TNFα using a neutralizing antibody also prolonged skin graft survival and *A onderdonkii* gavage did not have additive effects over this treatment, we conclude that *A onderdonkii* can protect graft survival by reducing TNFα production. *Alistipes* is a relatively newly annotated bacterial genus, isolated primarily from clinical fecal samples, which may play a role in dysbiosis and disease[241]. For instance, *A onderdonkii* was found to be reduced 2.6-fold in patients with nonalcoholic fatty liver disease[242]. Our results indicate that the immunomodulatory effect of *A onderdonkii* is strain-specific, with DSM19147 prolonging allograft survival but DSM108265 being ineffective, thus permitting direct comparison of metagenomics and metabolomics for selection of candidates putatively driving the anti-

inflammatory effect of DSM19147. Previous research has associated *Alistipes* with the production of anti-inflammatory SCFAs and γ-aminobutyric acid[243,244]. Although fecal metabolomic analysis did not reveal differences in SCFA content between mice treated with DSM19147 and mice treated with DSM108265, we cannot exclude that SCFAs induced by DSM19147 are rapidly used by host cells and do not reach the feces. Notably, our data suggest the value of investigating the impact of amino acid levels on transplant outcomes. Indeed, serum levels of phenylalanine, serine, glycine, threonine, and valine were found to be higher in patients rejecting renal transplants than in stable patients with renal transplants; however, whether this is a consequence of rejection or can contribute to it remains to be investigated[245].

A onderdonkii has been reported to produce the sulfonolipid metabolite sulfobacin B[134], and intraperitoneal injection of sulfobacin B led to the suppression of serum TNFα production in an in vivo mouse model of LPS-induced acute inflammation[135]. Our pangenomic comparison between *A onderdonkii* strains identified a bacterial homolog of serine palmitoyl transferase, a key gene involved in the sphingolipid biosynthesis pathway thought to be involved in sulfobacin B biosynthesis[135]. This gene was present in all the strains analyzed; however, it exhibited sequence variations across strains at 18 amino acid residues (data not shown). Whether the transcription or function of sulfobacin B produced by DSM19147 is higher than that produced by other strains needs to be studied.

N-acetylneuraminic acid plays a pivotal role in mammalian immunity, serving as the terminal sugar on glycans on cell surfaces, where it interacts with the immunoinhibitory sialic acid-binding immunoglobulin-like lectins (Siglecs) on immune cells to suppress autoimmunity[246,247]. Our findings suggest that DSM19147 may exhibit immunomodulatory

effects through a sialic acid–mediated mechanism, a hypothesis that can be tested through genetic manipulation of *A onderdonkii* strains in the future. The human gastrointestinal microbiota harbors approximately 1000 distinct bacterial species[248]. Under steady-state conditions, the addition of a single microbial strain to colonized wild-type mice was sufficient to induce a significant change in the global immune response of the host that could slow the kinetics of allograft rejection. However, the persistence of *A onderdonkii* relied on its repeated administration, and it is conceivable that it may fail to become established in some hosts depending on the microbial communities they harbor. Approaches to ensure probiotic engraftment are being developed, such as genetic engineering of probiotic bacteria to depend on unique nutrients that can be co-administered as prebiotics[179].

Another commensal was previously shown to be sufficient as a probiotic to protect allografts in mice. Administration of *Bifidobacterium pseudolongum*, present in greater abundance in the gut of pregnant females, reduced inflammation and the fibrosis of cardiac allografts correlating with laminin lymph node remodeling associated with a more suppressive environment[121]. Whether *A onderdonkii* has similar effects on lymph nodes or whether these commensals' effects could be additive because of their dependence on distinct mechanisms will be of interest to investigate in the future. In summary, our results position *A onderdonkii* DSM19147 as a candidate probiotic agent to facilitate transplant survival.

Chapter 4: Influence of skin-restricted microbiota on solid organ transplant outcome

4.1 Skin-restricted commensal colonization accelerates skin graft rejection

4.1.1 Abstract

Solid organ transplantation can treat end-stage organ failure, but the half-life of transplanted organs colonized with commensals is much shorter than that of sterile organs. Whether organ colonization plays a role in this shorter half-life is not known. We have previously shown that an intact whole-body microbiota can accelerate the kinetics of solid organ allograft rejection in untreated colonized mice, when compared with germ-free (GF) or with antibiotic-pretreated colonized mice, by enhancing the capacity of antigen-presenting cells (APCs) to activate graft-reactive T cells. However, the contribution of intestinal versus skin microbiota to these effects was unknown. Here, we demonstrate that colonizing the skin of GF mice with a single commensal, *Staphylococcus epidermidis* (*S. epi*), while preventing intestinal colonization with oral vancomycin, was sufficient to accelerate skin graft rejection. Notably, unlike the mechanism by which whole-body microbiota accelerates skin graft rejection, cutaneous *S. epi* did not enhance the priming of alloreactive T cells in the skin-draining lymph nodes. Rather, cutaneous *S. epi* augmented the ability of skin APCs to drive the differentiation of alloreactive T cells. This study reveals that the extraintestinal donor microbiota can affect transplant outcome and may contribute to the shorter half-life of colonized organs.

4.1.2 Introduction

Solid organ transplantation is an accepted therapy for end-stage organ failure. Depending on the type and location of the transplanted organ, the level of commensal colonization varies. Sterile organs, such as the heart and kidneys, have a longer half-life following transplantation than barrier organs that are colonized with commensal bacteria, such as intestines and lungs (Organ Procurement and Transplantation Network, https://optn.transplant.hrsa.gov/data/; Scientific Registry of Transplant Recipients, http://www.srtr.org/, December 2012). This clinical observation prompted us to investigate whether the microbiota in barrier organs could promote graft rejection.

Numerous studies have established that the gut microbiota plays a critical role in local immune development and function[202], for instance, inducing lamina propria regulatory T cells[92] and Th17 cells[91]. The gut microbiota can also affect immune responses at distal locations[98,249,250], such that, in theory, the gut microbiota might affect alloimmunity to any transplanted organ, whether sterile or colonized. Indeed, we previously showed that oral administration of broad-spectrum antibiotics that reduced the diversity of gut microbiota resulted in prolonged survival of both skin and heart transplants[97]. However, whether the microbiota within the barrier organ itself can affect alloimmunity or graft outcome after it is transplanted remains to be determined. In fact, our mice gavaged with broad-spectrum antibiotics displayed reduced microbial diversity not only of the intestine but also of the skin[97], making it critical to understand whether graft-restricted microbiota can affect the outcome of that transplanted organ.

Staphylococcus epidermidis, a skin commensal, has been shown to calibrate cutaneous T cell responses and local inflammation, improving local immunity to *Leishmania major* and *Candidia albicans*[105,251]. This tissue-specific barrier immunity was independent of the effect of

the gut microbiota and attributed to interactions between *S. epidermidis* and dermal CD103^{+} and CD11b^{+} dendritic cells (DCs)[105]. Given the influence of a skin commensal to a local infectious immune response, we investigated the impact of skin S. *epidermidis* on skin allograft outcome.

4.1.3 Results

4.1.3.1 Cutaneous *S. epi* colonization is sufficient to accelerate skin allograft rejection.

To investigate the impact on skin graft rejection of a commensal present exclusively on the skin, *S. epi* was painted on the skin of male and female C57BL/6 germ-free (GF) mice, before transplantation of painted or unpainted male skin onto painted or unpainted female recipients (Figure 4.1. 1A).

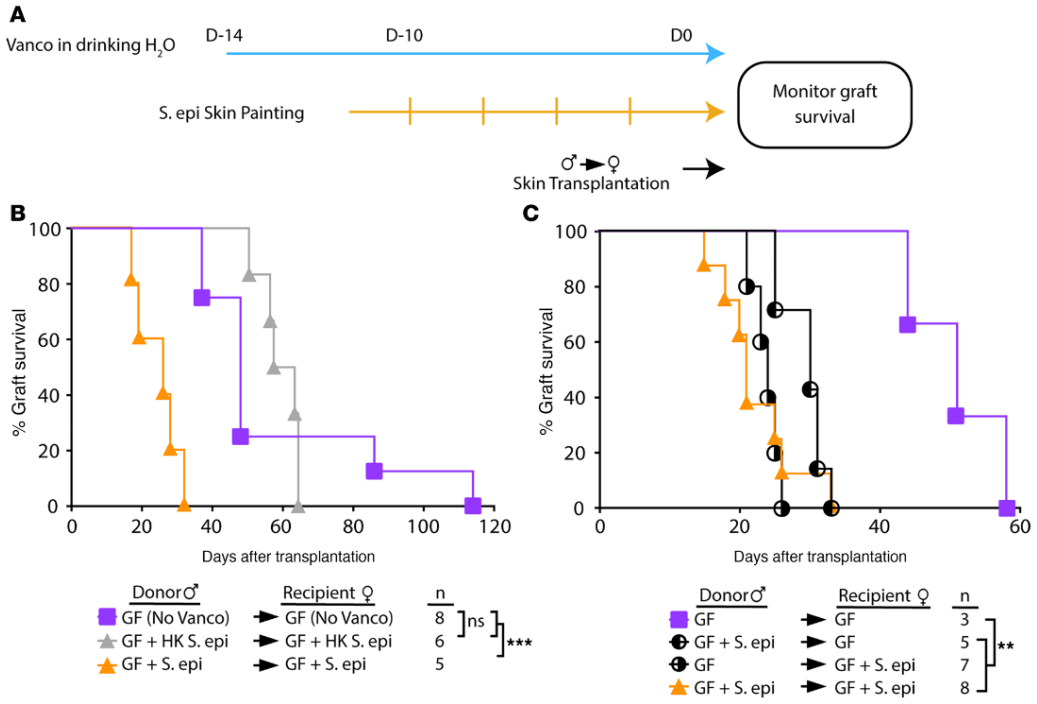

Figure 4.1. 1. Cutaneous *S. epi* colonization is sufficient to accelerate skin allograft rejection.
(A) Schematics of the transplant logistics in the gnotobiotic facility. (B) Both germ-free (GF) male donors and female recipients were colonized with live or heat-killed (HK) *S. epi* for 10 days before male-to-female skin transplantation. (C) GF male donors and/or female recipients were left uncolonized or colonized with *S. epi* for 10 days before skin transplantation. (B and C) All mice received vancomycin-supplemented water except the group labeled “no Vanco.”

To prevent gut colonization from self-grooming, the nonabsorbable antibiotic vancomycin was supplemented in the drinking water, starting before *S. epi* painting and continuing until animal sacrifice. Cultures of skin swabs and fecal samples before transplantation confirmed skin but not gut colonization of the *S. epi*–painted gnotobiotic mice (Figure 4.1. 2).

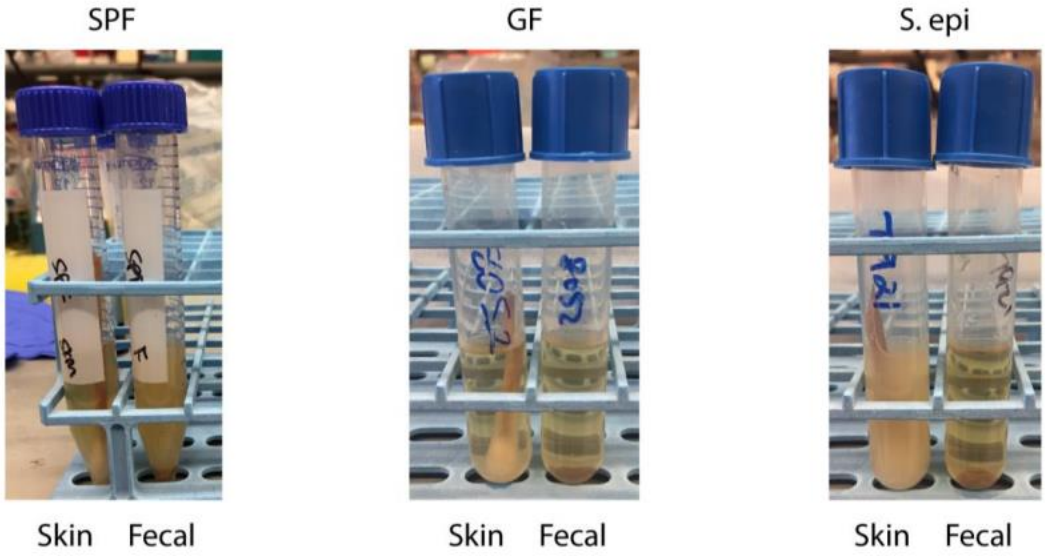

Figure 4.1. 2. *S. epi* colonized the skin but not the gut of oral vancomycin-treated gnotobiotic mice.
GF mice were painted with *S. epi*. After 10 days, skin swabs and fecal samples were cultured in aerobic conditions overnight. Cloudy broths demonstrate bacterial growth whereas clear broths denote the sterility of the culture.

Transplantation of *S. epi*–colonized male skin onto *S. epi*–colonized female gnotobiotic mice resulted in marked acceleration of skin graft rejection over that of GF male skin onto female GF recipients (Figure 4.1. 1B). Skin colonization did not drive local infection because grafts appeared healed and healthy at the time of bandage removal. Importantly, *S. epi* needed to be alive to promote rejection because colonization with heat-killed *S. epi* did not accelerate rejection, suggesting that pattern recognition alone of molecular components in *S. epi* was not sufficient to promote rejection. To determine whether accelerated rejection was driven by donor or recipient skin microbiota, only male donors or female recipients were painted with *S. epi*

before transplantation. Either donor or recipient skin colonization was sufficient to accelerate rejection (Figure 4.1. 1C). We also investigated the impact of donor *skin S. epi* on the outcome of major mismatched skin grafts. Although rejection of fully mismatched skin grafts is extremely rapid, rejection of *S. epi*–painted monocolonized FVB (H-2^q) skin grafts by B6 (H-2^b) hosts trended toward even faster rejection than that of GF FVB grafts (Figure 4.1. 3).

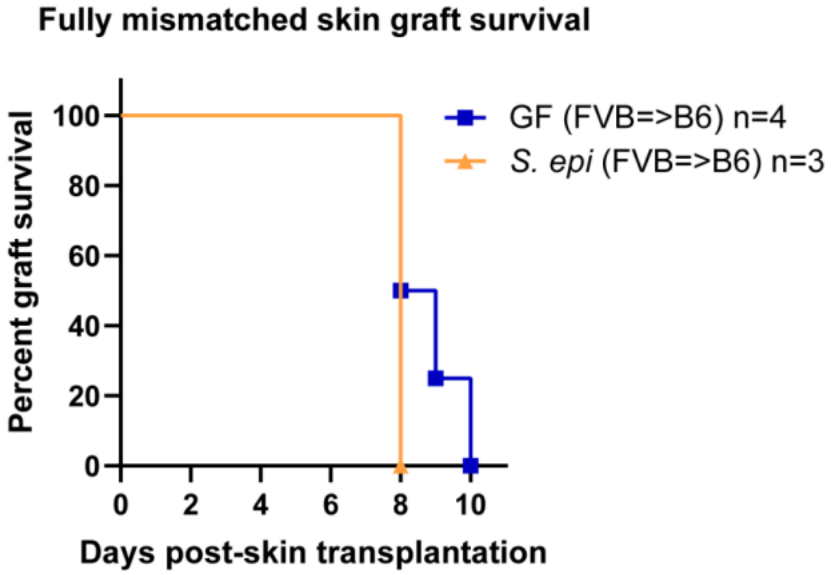

Figure 4.1. 3. Donor skin *S. epi* trends towards accelerating rejection of a fully mismatched skin graft.
Eight GF FVB male mice (H-2^q) were put on vancomycin-supplemented water and 4 mice were painted with *S. epi*. After 10 days, skin from GF FVB or cutaneous *S. epi* monocolonized FVB mice was transplanted onto female C57BL/6 recipients on vancomycin supplemented water. One recipient died during transplantation. Graft survival was evaluated daily after bandage removal on day 7. p=0.1797 by log rank test.

4.1.3.2 *S. epi* colonization does not enhance the priming phase of the alloimmune response in the skin-draining LNs.

Skin colonization–dependent acceleration of skin graft rejection might be due to increased host alloreactivity at the priming phase of the anti–skin graft response. Previously, we found that normal global microbiota enhances the ability of antigen-presenting cells (APCs) in the skin-draining lymph nodes (LNs) to prime alloreactive T cells when compared with APCs

from antibiotic-pretreated or GF mice, without changing the composition or the costimulatory profile of APCs[97]. In keeping with these data, *S. epi* skin colonization did not change either the composition of LN CD8α$^+$CD11b$^+$CD103$^+$ DCs and CD207$^+$ Langerhans cells Figure 4.1. 4A) or their expression of MHC class II, CD80, CD86, or CD40 when compared with GF DCs (Figure 4.1. 4B).

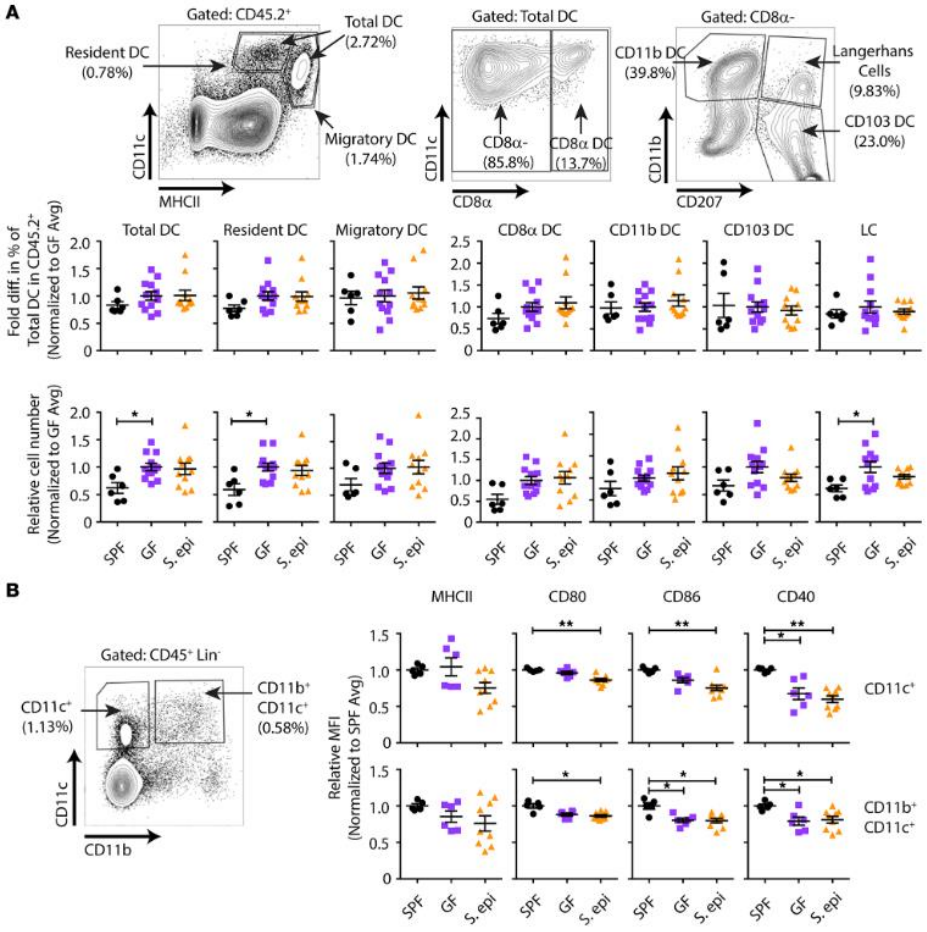

Figure 4.1. 4. *S. epi* skin colonization does not change the composition or costimulatory molecule expression of LN APCs relative to GF APCs.
APCs from the peripheral LNs of specific pathogen–free (SPF), GF, and 10-day-painted *S. epi*–monocolonized GF mice were analyzed by flow cytometry. (A) Gating strategy for different dendritic cell (DC) populations and fold change relative to the average in the percentage of DC subsets observed in GF controls within each experiment. LC, Langerhans cell. (B) Fold change in mean fluorescence intensity (MFI) relative to that in GF mice for costimulatory molecules on CD11c$^+$-gated cells.

To determine whether LN APCs from *S. epi*–skin-colonized mice acquire better T cell priming capacity, we cultured CFSE-labeled, male-specific, $CD4^+$ TCR-transgenic T cells (Marilyn T cells) with LN APCs from *S. epi*–painted GF male mice in vitro. Unlike LN APCs from globally colonized SPF mice, which induced greater Marilyn T cell proliferation than APCs from GF mice, LN APCs from *S. epi*–painted monocolonized mice failed to significantly enhance Marilyn T cell division relative to that induced by APCs from GF mice (Figure 4.1. 5A-B). This was likely not due to a fixed immaturity of the innate immune system in GF mice because we have previously reported that fecal transfer from colonized mice rapidly restores, in less than a week, the ability of peripheral LN APCs from ex-GF mice to activate Marilyn T cells in vitro and in vivo[97]; in contrast, skin *S. epi* monocolonization did not increase the stimulatory capacity of LN APCs. To investigate the impact of skin *S. epi* painting on the priming of T cells in vivo, CFSE-labeled Marilyn T cells were transferred into uncolonized *or S. epi*–colonized female GF mice on the day of transplantation with skin from uncolonized or *S. epi*–colonized male GF mice, and T cells were harvested from skin-draining LNs on day 4 or 6 after transplantation. Surprisingly, but consistent with the in vitro priming data, Marilyn T cell proliferation was not enhanced in *S. epi*–colonized mice, suggesting that *S. epi* skin colonization does not accelerate rejection by increasing the priming phase of the alloresponse (Figure 4.1. 5C-D).

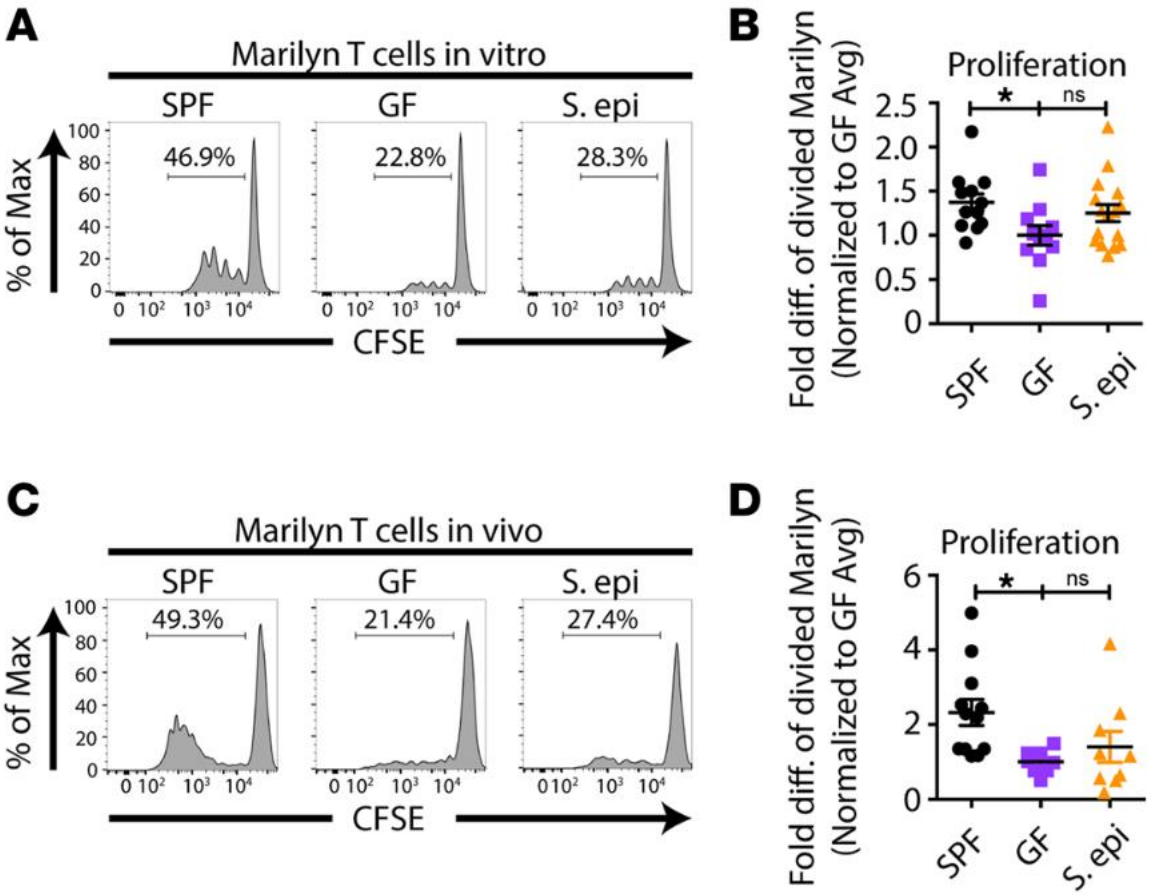

Figure 4.1. 5. Skin *S. epi* colonization does not enhance the proliferation of alloreactive T cells in the skin-draining LNs.
(A and B) APCs from skin-draining LNs were isolated from male SPF, GF, or *S. epi*–painted GF mice 10 days after initial painting and cultured with CFSE-labeled T cells from Marilyn females for 3 days, followed by flow cytometric analysis. (C and D) Congenic Marilyn T cells were labeled with CFSE and transferred into GF and *S. epi*–painted GF recipients on the day of transplantation with male GF or GF plus *S. epi* skin grafts. Mice were sacrificed 4 or 6 days after transplantation, and cells were isolated from the graft draining LNs for analysis of CFSE dilution. Representative plots (A and C) and quantitation of CFSE dilution (B and D) of divided Marilyn T cells. (B and D) Quantitation represents normalized data with normalization to the average of percentage of divided Marilyn T cells in GF mice

4.1.3.3 *S. epi* colonization enhances the effector phase of the alloimmune response in the allograft.

S. epi colonization can modulate local cutaneous immune responses[105,251]. Although the proportion of skin DCs and their expression of costimulatory molecules were unchanged in *S.*

epi–colonized mice compared with uncolonized GF mice (Figure 4.1. 6), it was possible that skin *S. epi* affected their function.

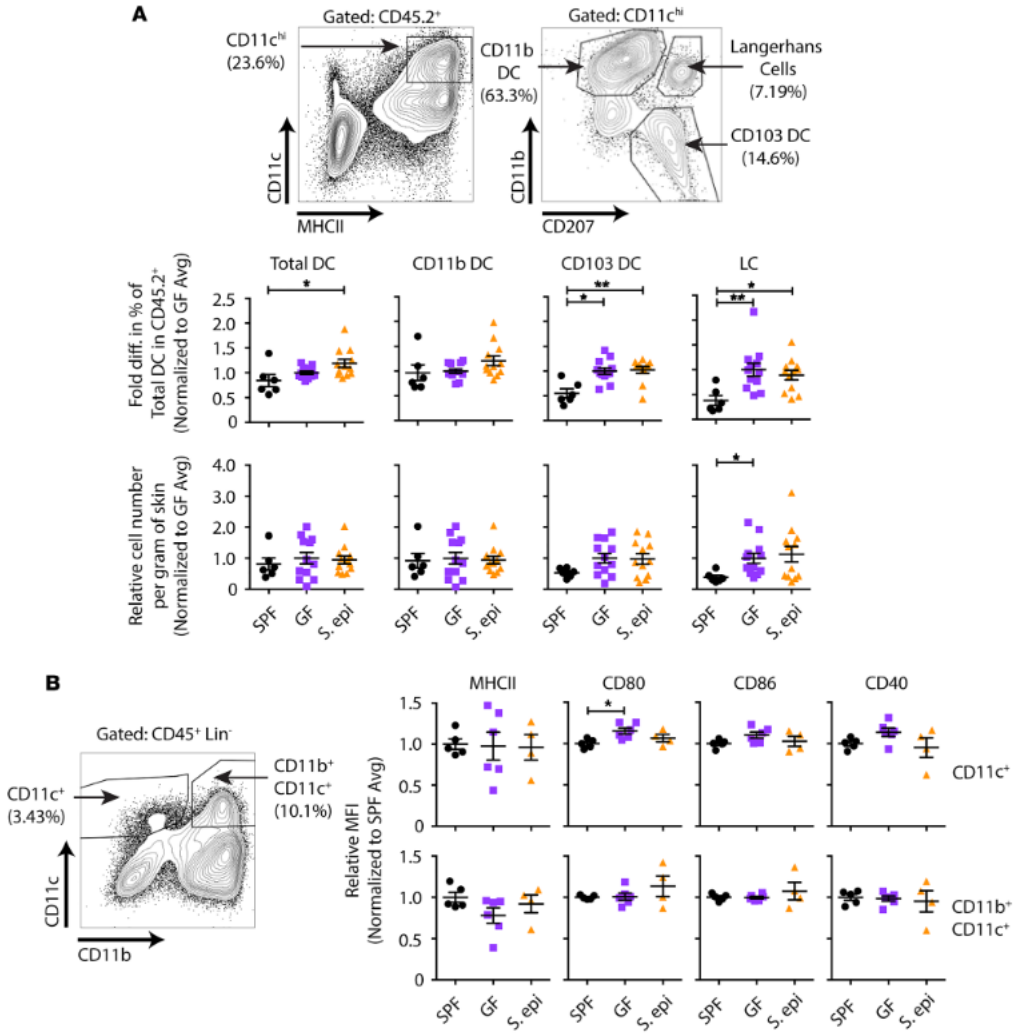

Figure 4.1. 6. *S. epi* skin colonization does not change the composition or costimulatory molecule expression of skin APCs relative to GF APCs.
APCs from the flank skin of SPF, GF, and 10 day–painted *S. epi*–monocolonized GF mice were analyzed by flow cytometry. (A) Gating strategy for different DC populations and fold change relative to the average percentage of DC subsets within GF controls in each experiment. (B) Fold change in MFI relative to that in GF mice for costimulatory molecules on $CD11c^+$-gated cells.

To determine whether skin *S. epi* accelerates skin graft rejection by driving a stronger effector rather than priming phase of the alloresponse, we harvested skin-draining LNs and skin grafts from GF or *S. epi*–colonized animals on day 10 after transplantation, a time point before

any evidence of skin graft rejection. cDNA was prepared from the homogenized LNs and skin grafts, and real-time quantitative PCR for inflammatory cytokines was performed. Whereas cytokine expression was similar in the LNs of recipients of GF and *S. epi*–monocolonized skin grafts (Figure 4.1. 7A), TNFα, IL-12A, and IL-18 were significantly elevated in the colonized versus GF skin grafts (Figure 4.1. 7B), suggesting a local skin environment favorable to Th1 differentiation, which often correlates with graft rejection[252].

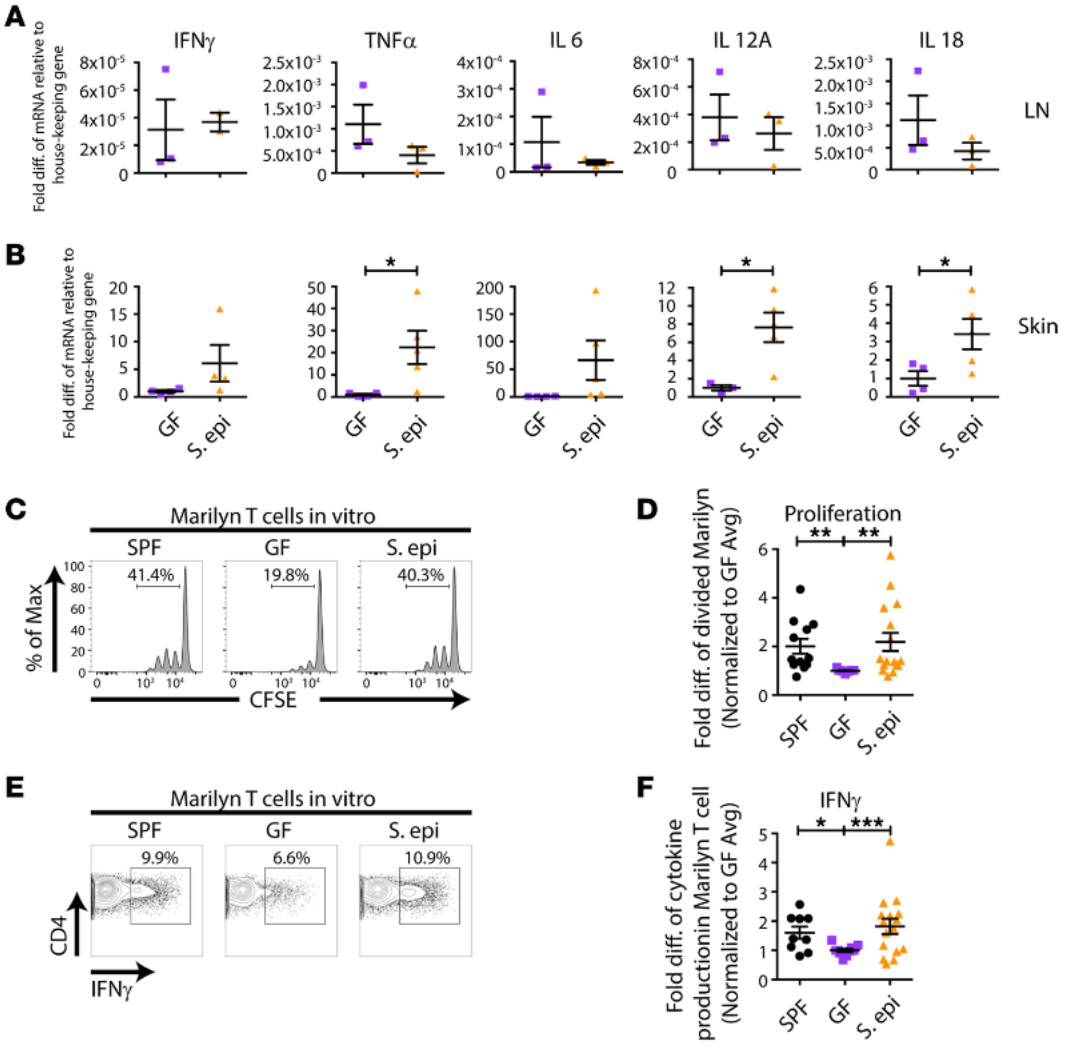

Figure 4.1. 7. Skin *S. epi* colonization enhances skin APC activation of alloreactive T cells. (A and B) GF or *S. epi*–colonized skin-draining LNs
(A) and skin grafts (B) were isolated on day 10 after transplantation of male skin onto female recipients, cDNA was prepared, and qPCR for cytokines was performed. Pooled results from 2 independent experiments are shown for the skin graft, normalized to GF average values. (C–F) Skin APCs were isolated from male SPF, GF, or *S. epi*–painted GF mice and cultured with CFSE-labeled T cells from Marilyn females for 3 days, followed by flow cytometric analysis. (E and F) For IFNγ detection, cells were stimulated with PMA and ionomycin before staining. Representative plots (C and E) and quantitation of CFSE dilution of Marilyn T cells (D) and IFNγ production by Marilyn T cells (F). Quantitation represents data normalized to the average of the percentage of divided Marilyn T cells (D) or IFNγ production (F) in GF mice

To investigate the impact of this microenvironment on the ability of local APCs to activate graft-reactive T cells, we isolated APCs from the skin of GF and *S. epi*–painted

monocolonized male mice. Upon culture with CFSE-labeled Marilyn T cells, skin APCs from *S. epi*–colonized mice induced T cell proliferation (Figure 4.1. 7C-D) and IFNγ production upon PMA and ionomycin restimulation (Figure 4.1. 7E-F) that was as robust as skin APCs from SPF mice and greater than skin APCs from GF mice. Moreover, supporting a functional role for the inflammatory cytokines found in the day 10 *S. epi*–colonized skin graft, exogenous addition of IL-6 and IL-12 enhanced the ability of both skin and LN APCs to induce IFNγ production by Marilyn T cells (Figure 4.1. 8).

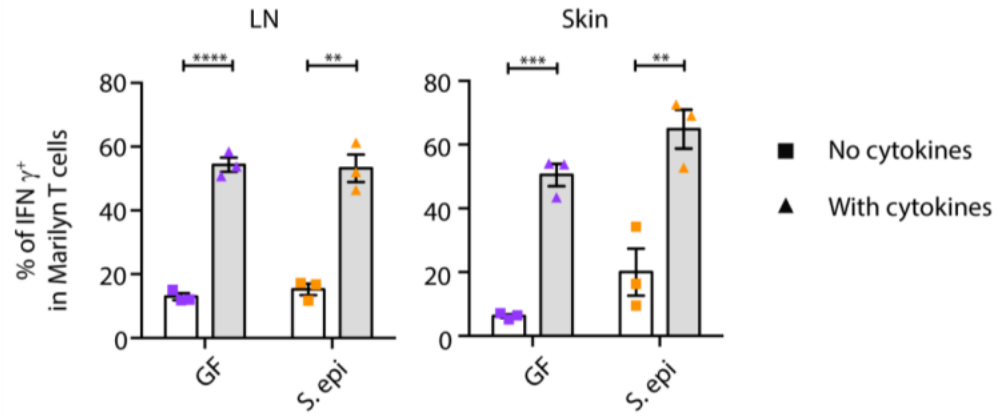

Figure 4.1. 8. Exogenous addition of inflammatory cytokines results in augmented effector function by donor-reactive T cells.
APCs ($2x10^5$) from the LNs or flank skin of GF and 10 day-painted *S. epi*-monocolonized mice were incubated with Marilyn T cells ($5x10^4$) in the presence or absence of exogenous IL-6+IL-12 for 3 days. Cells were then restimulated with PMA + ionomycin for 4h and analyzed by flow cytometry for IFNγ expression by Marilyn T cells

In vivo, approximately 7-fold more Marilyn T cells were retrieved from *S. epi*–colonized than GF skin grafts on day 10 after transplantation (Figure 4.1. 9). Together, these results suggest that the skin graft *S. epi* acts locally in the skin, at the target site rather than at the priming site of the alloimmune response, by augmenting the effector function of the alloreactive T cells.

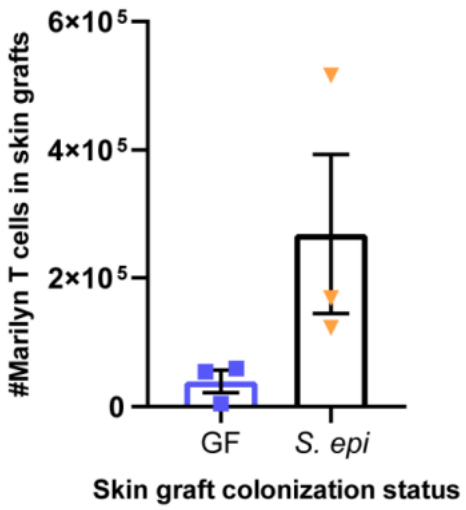

Figure 4.1. 9. Trend toward increased numbers of donor-reactive T cells in *S. epi* colonized skin grafts.
Spleen and LNs from CD45.1^{+} Marilyn TCR-Tg x RAG-KO mice were CFSE-labeled and transferred (10^{6}) into GF female C57BL/6 mice 4 days after transplantation with male GF or *S. epi*-monocolonized skin grafts. Animals were sacrificed on day 10, hematopoietic cells extracted from the skin grafts and CD45.1^{+}TCRβ^{+} cells enumerated by flow cytometry.

4.1.4 Discussion

Our results demonstrate that monocolonization with *S. epi*, restricted to the donor skin, causes accelerated rejection following transplantation of this skin onto GF recipients. This supports the sufficiency of the transplanted organ's microbiota for the tuning up of host alloreactivity. Moreover, our data support the conclusion that cutaneous *S. epi* modulates alloimmunity in the skin graft itself, at the effector, rather than during the priming phase of the alloresponse, and therefore by a different mechanism than the enhanced priming observed in mice also harboring intestinal colonization[97]. These results provide a possible explanation for why colonized organs have a shorter half-life than sterile organs following transplantation in the clinic.

The kinetics of skin graft rejection in skin only–colonized GF mice were similar to those of globally colonized SPF mice or of GF mice that were conventionalized and became globally

colonized, in the gut and skin, following SPF fecal transfer by gavage[97]. However, it is important to note that not all skin microbiota accelerates skin graft rejection. Indeed, we previously showed that fecal transfer from antibiotic-pretreated mice into GF mice by oral gavage, which resulted in both gut and skin colonization, did not hasten skin graft rejection[97], suggesting that different skin microbiota communities have different consequences on alloimmunity. Indeed, association of mice with a defined clade of *S. epi*, but not *S. xylosus* or *S. aureus*, enhanced IFNγ and IL-17A production by dermal $CD8^+$ T cells[105,106], indicating that even single commensals of the same genus can have different immune impacts. Whether skin commensals other than *S. epi* can accelerate skin allograft rejection, and if so whether their mechanism of action is the same, remains to be investigated.

The fact that donor microbiota is sufficient to accelerate skin graft rejection is consistent with our previous findings[97] that global colonization of either the donor or the recipient was sufficient to drive fast skin graft rejection, although those experiments did not distinguish which microbial compartment (intestine or skin) affected graft outcome. Our current results demonstrate that skin microbiota in either the donor or the recipient is sufficient to accelerate skin graft rejection. We acknowledge that a GF graft will be rapidly colonized when transplanted onto an *S. epi*–colonized host, and vice versa, that a host GF skin will be rapidly colonized following transplantation of an *S. epi*–painted skin graft, but such cross-colonization will occur after transplantation. Thus, if donor colonization requires the donor commensals to colonize the host skin to accelerate graft rejection, our results still suggest an extremely rapid impact of the donor microbiota on the host alloimmune response.

4.2 Host-versus-commensal immune responses participate in the rejection of colonized solid organ transplants

4.2.1 Abstract

Solid organ transplantation is the preferred treatment for end-stage organ failure. Although transplant recipients take life-long immunosuppressive drugs, a substantial percentage of them still reject their allografts. Strikingly, barrier organs colonized with microbiota have significantly shorter half-lives than non-barrier transplanted organs, even in immunosuppressed hosts. We previously demonstrated that skin allografts monocolonized with the common human commensal *Staphylococcus epidermidis* (*S. epi*) are rejected faster than germ-free (GF) allografts in mice because the presence of *S. epi* augments the effector alloimmune response locally in the graft. Here, we tested whether host immune responses against graft-resident commensal microbes, including *S. epi*, can damage colonized grafts independently from the alloresponse. Naive hosts mounted an anti-commensal T cell response to colonized, but not GF, syngeneic skin grafts. Whereas naive antigraft commensal T cells modestly damaged colonized syngeneic skin grafts, hosts with prior anti-commensal T cell memory mounted a post-transplant immune response against graft-resident commensals that significantly damaged colonized, syngeneic skin grafts. Importantly, allograft recipients harboring this host-versus-commensal immune response resisted immunosuppression. The dual effects of host-versus-commensal and host-versus-allograft responses may partially explain why colonized organs have poorer outcomes than sterile organs in the clinic.

4.2.2 Introduction

Solid organ transplantation is the preferred treatment for end stage organ failure. Recipients of allogeneic grafts mount immune responses that can lead to transplant rejection,

even when hosts are treated with immunosuppressive drugs. Importantly, the survival of grafts depends on the type of organ transplanted; within 5 years of surgery, 41% of lung and 54% of intestinal transplant recipients were reported to have rejected their grafts. In that same time frame, only 27% rejected a kidney and 23% a heart[253,254]. Several factors distinguish these tissue types. One critical differentiator is the presence of donor microbiota on organs with the shortest half-lives and the absence of donor microbiota on organs that survive longer. The microbiota is vastly different between distinct individuals[125], raising the possibility that hosts of colonized organ allografts mount an immune response not only to mammalian cells within the graft, but also to donor commensals that accompany the tissue.

In previous work, we demonstrated that the presence of a single commensal organism, *S. epi*, on a skin allograft was sufficient to accelerate allograft rejection in comparison with germ-free (GF) transplants. *S. epi* augmented the expression of inflammatory cytokines in the skin allograft and enhanced the effector phase of the host's alloresponse locally in the graft[100]. This published study investigated *S. epi*'s impact on the alloresponse but did not address whether a concurrent immune response to *S. epi* was elicited and, if so, whether it contributed to transplant rejection.

Patients, like conventional mice housed in specific pathogen free (SPF) conditions, harbor a complex microbiota that generates a diverse repertoire of commensal-specific lymphocytes[125,255,256]. Many of these lymphocytes are tissue-resident memory T cells induced upon colonization with specific commensals[105,257,258]. These cells are poised to recognize commensal organisms at steady state and respond in a proinflammatory manner following tissue injury[104,106,107]. Our results show that commensal-specific host naive and memory T cells mount an anti-commensal immune response following transplantation with colonized organs. This host-

versus-commensal immune response acts in parallel to the host-versus-graft alloresponse and causes hosts to resist immunosuppression, thus providing a mechanistic explanation for why colonized organs have a shorter half-life than sterile organs following transplantation.

4.2.3 Results

4.2.3.1 Skin graft recipients mount a T cell response to commensals on donor organs that is independent from the alloresponse.

Organs colonized with commensal microbiota have a shorter half-life following transplantation than sterile organs. Using a mouse model of allogeneic skin transplantation, we previously demonstrated that one mechanism explaining why rejection of a skin allograft colonized with *S. epi* is faster than rejection of a GF skin allograft is that cutaneous *S. epi* augments the effector phase of the alloresponse, locally, when alloreactive T cells enter the skin allograft[100]. We reasoned that another way donor skin colonization might accelerate graft loss is by prompting the host to mount a specific immune response to the donor commensals present in the graft. This response would accelerate graft loss if it contributed to post-transplant graft damage. We adopted the skin colonization regimen used previously[100] in which GF donor mice were painted with the common human skin commensal *S. epi* (strain NIHLM087), every other day for 10 days. To ensure that colonization was restricted to the skin, animals received vancomycin in their drinking water to eliminate *S. epi* that may have entered their intestinal tract during grooming (Figure 4.2. 1A). This protocol resulted in colonization of the donor's skin, and not the intestine, for at least 2 weeks after the last painting (Figure 4.2. 2A–C).

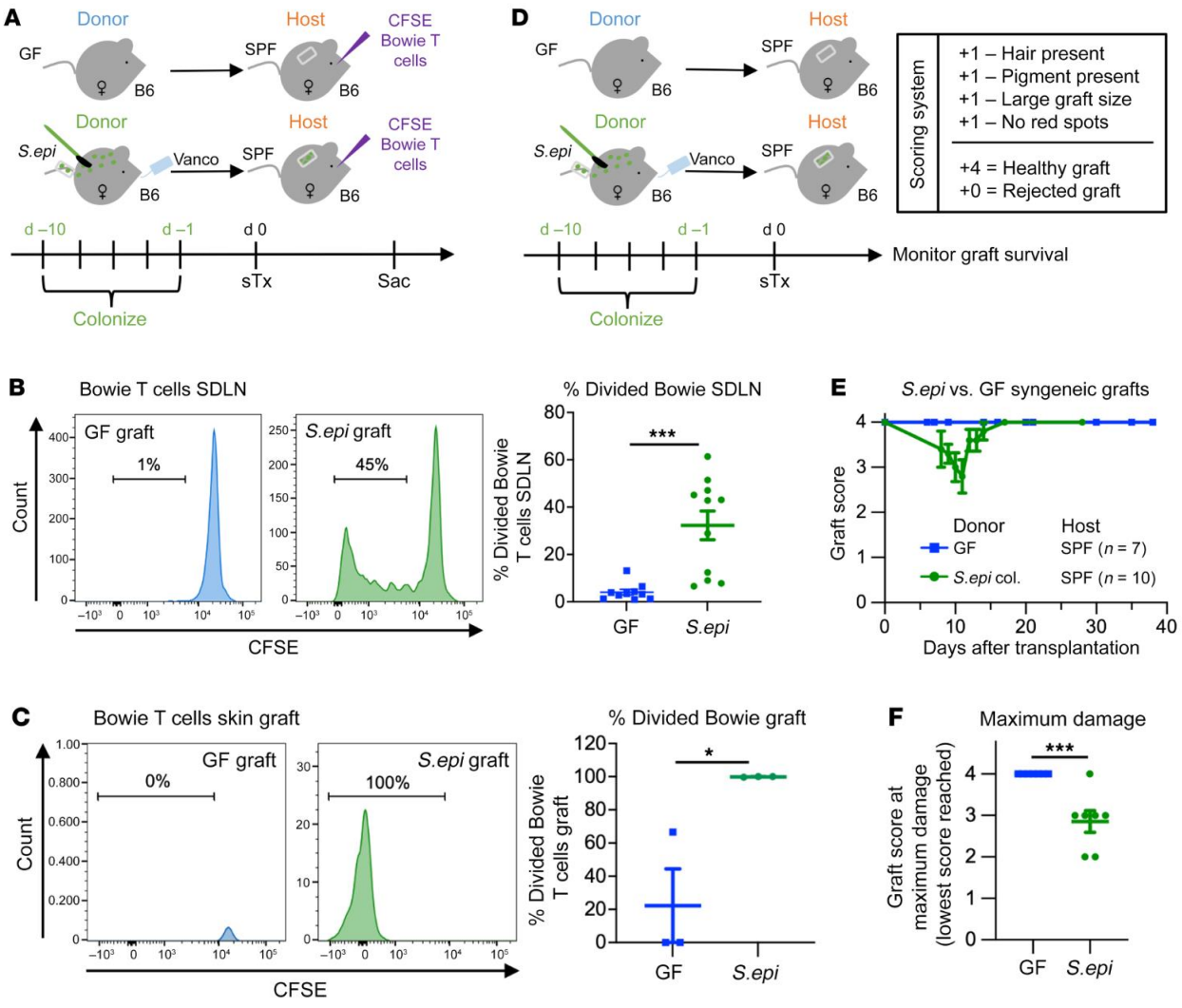

Figure 4.2. 1. Skin graft recipients mount a T cell response to commensals on syngeneic donor organs.

(A) Skin graft recipients were seeded with CFSE-labeled *S. epi*-specific $CD8^+$ TCR-transgenic Bowie T cells (1×10^6 cells) and then given a GF or *S. epi*-monocolonized syngeneic skin graft. B6, C57BL/6. (B and C) CFSE dilution of Bowie cells was examined 6 days (B) and 10 days (C) after transplantation in the SDLNs (B) and skin graft (C). Plots represent mean ± SEM and were analyzed by Welch's unpaired, 2-tailed t test. Results were pooled from three (B) independent experiments. (D and E) *S. epi*-monocolonized or GF skin grafts were transplanted onto syngeneic SPF mice. Grafts were scored on a 4-point scale, gaining 1 point each for the presence of hair, the presence of pigment, a large graft size, and the absence of red spots. (E) These scores were plotted over time. (F) The lowest graft score each individual graft reached was plotted. col., colonized; d, day.

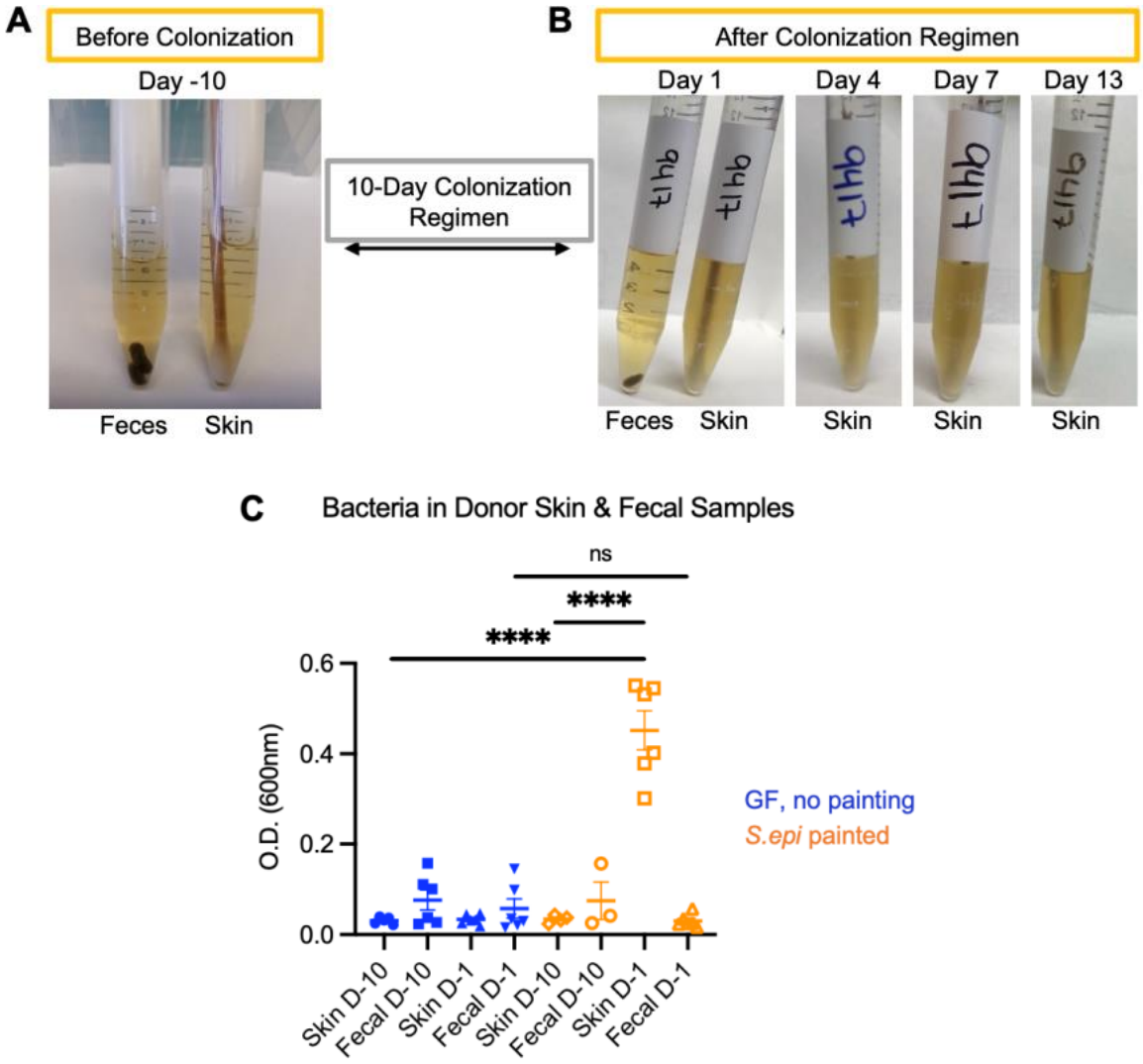

Figure 4.2. 2. The protocol for *S. epi* painting of GF mice induces selective colonization of mouse skin that is stable for at least two weeks.
(A) Skin swab and fecal sample cultures from a skin graft donor before colonization. (B) Fecal sample (day 1, left) and skin swabs (days 1, 4, 7, and 13) from mice painted following the protocol outlined in Figure 1A. Cloudy media indicates bacterial growth, clear media indicates a sterile sample. Day 0 is the last day of the 10-day colonization regimen. No additional painting occurred after that time. (C) Quantified bacterial growth in skin and fecal swabs from donor mice painted (*S. epi*) or not (GF) with S. epi following the protocol described in Figure 1A. Swabs and fecal pellets were cultured for 24h prior to measurement. D-10: samples were taken before painting the mice on this day. D1: second-to-last day of colonization protocol.

To investigate whether the host mounted an anti–donor commensal immune response following skin transplantation in the absence of a concurrent alloresponse, we used syngeneic transplants, and *S. epi*-specific $CD8^+$ TCR-transgenic T cells (Bowie T cells) to track anti-*S. epi*

T cell responses. Skin grafts from female GF or *S. epi*-colonized mice were placed onto SPF syngeneic female hosts that had been seeded with CFSE-labeled Bowie T cells 1 day before transplantation. Hosts were sacrificed 6 days after transplantation (Figure 4.2. 1A). Bowie T cells in the host's skin graft–draining lymph nodes (SDLNs) proliferated (Figure 4.2. 1B). By 10 days after transplantation, divided $CD44^{hi}$ Bowie T cells in recipients of colonized but not GF syngeneic grafts were detected in the graft itself (Figure 4.2. 1C). We confirmed by PCR that hosts housed in our SPF mouse facilities were not colonized with *S. epi* before transplantation, consistent with the fact that *S. epi* is not a native mouse commensal (Figure 4.2. 3A)[259]. Notably, the surgical trauma of skin transplantation was not necessary to elicit an anti-commensal response in the host, as Bowie T cells proliferated significantly, albeit modestly, in SPF mice without transplants following painting with *S. epi* (Figure 4.2. 3B, C).

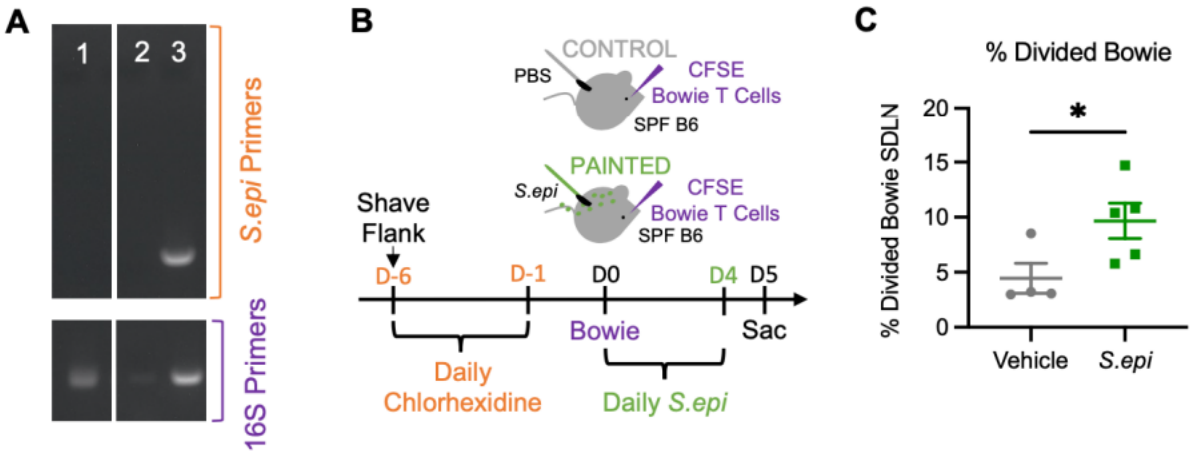

Figure 4.2. 3. *S. epi* does not colonize skin of SPF mice housed in our mouse facility. (A) *S. epi*-specific (top row) and 16S (bottom row) PCR of DNA isolated from swabbing the skin of a mouse housed under SPF conditions (lane 1), from the materials and buffer used for isolation (lane 2), or from the tail swab of a *S. epi*-mono-colonized gnotobiotic positive control mouse (lane 3). (B) SPF mice were shaved, painted with chlorhexidine for 5 consecutive days to open a niche for *S. epi*, and then seeded with $1x10^6$ CFSE-labeled Bowie T cells. One group then was painted with PBS (vehicle control) and the other with *S. epi* for 5 consecutive days. All mice were sacrificed 1 day after the last painting. (C) Bowie T cell proliferation in mice painted or not with *S. epi*.

We next asked whether an endogenous T cell response against graft-resident commensals was sufficient to damage or reject syngeneic organs. To this end, we transplanted skin from GF or *S. epi*-colonized female mice into SPF syngeneic female hosts and monitored graft survival. We scored skin grafts on a 4-point scale for signs of chronic rejection. Grafts received 1 point each for the presence of hair, the presence of pigment, a large graft size, and an absence of red inflamed spots (Figure 4.2. 1D). Brief and modest damage was observed on *S. epi*-colonized but not GF syngeneic grafts (Figure 4.2. 1E, F), with *S. epi*-colonized grafts displaying significantly more damage at their worst scoring point than GF grafts (Figure 4.2. 1F).

To address whether a higher frequency of *S. epi*-reactive naive T cells would heighten the damage to *S. epi*-colonized skin grafts, hosts received Bowie T cells (1.5×10^6) 1 day before transplantation with a *S. epi*-colonized syngeneic skin graft (Figure 4.2. 4). Increasing the precursor frequency of *S. epi*-reactive naive T cells to supraphysiological levels did not worsen the damage in colonized syngeneic skin grafts. This could be because the endogenous response was already maximal or because Bowie T cells cannot cause skin graft damage. Nonetheless, the data indicate that a primary endogenous immune response against *S. epi* only modestly damages *S. epi*-colonized skin grafts.

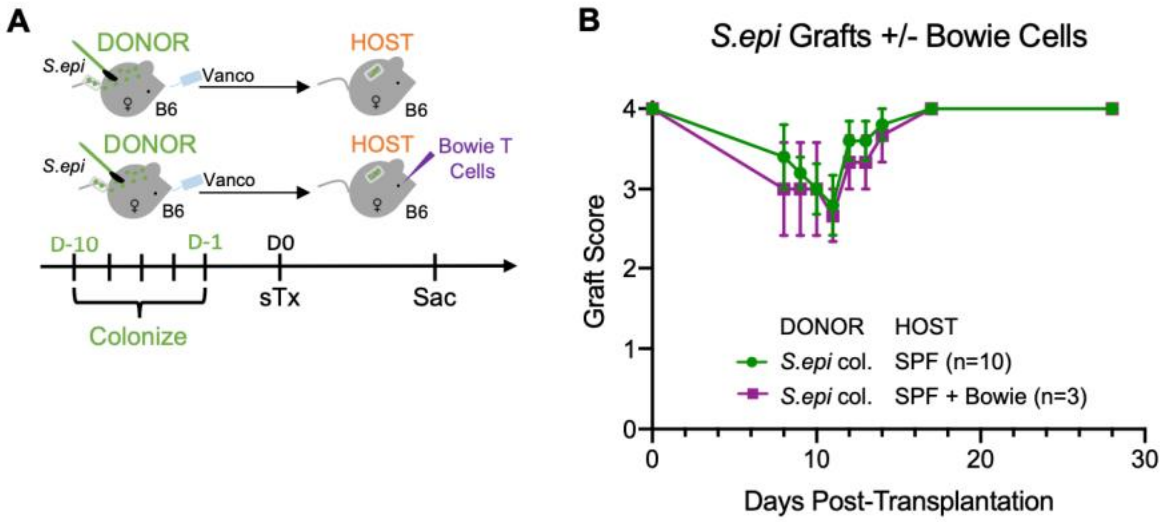

Figure 4.2. 4. Addition of naïve CD8+ graft-commensal-reactive T cells does not perpetuate major damage to colonized, syngeneic skin grafts.
(A) *S. epi*-mono-colonized skin graft recipients that were seeded (purple line) or not seeded (green line) with $1.5x10^6$ enriched Bowie T cells one day before transplantation. (B) Four-point graft scores over time. Curves are not significantly different

4.2.3.2 Hosts with memory against commensals present on donated organs display strong damage of syngeneic skin grafts.

In contrast to laboratory mice in controlled animal facilities, barrier tissues in humans and wild mice have many commensal-specific memory T cells, reflecting exposure to a variety of microbes and environmental antigens over time[125,255,260,261]. We therefore asked whether hosts with memory against *S. epi* would damage syngeneic, *S. epi*-colonized skin grafts more than hosts naive to *S. epi*. Because *S. epi* is not a native mouse commensal, we generated anti-commensal memory using s.c. immunizations with *S. epi*, as this approach is known to induce local immune responses in the skin[262,263]. SPF mice were immunized s.c. with *S. epi* or not, 1 month before receiving a *S. epi*-monocolonized or GF syngeneic skin graft (Figure 4.2. 5A). For all 3 transplantation conditions, we tested syngeneic grafts from male donors into male hosts and from female donors into female hosts. In a group of mice without transplants sacrificed 1 month after s.c. *S. epi* immunization, we confirmed that s.c. immunization expanded endogenous *S. epi*-

reactive $CD8^+$ $CD44^+$ T cells in the SDLNs and skin, using a tetramer of the nonclassical MHC H2-M3 presenting a formylated peptide of *S. epi* to identify *S. epi*-reactive $CD8^+$ T cells (Figure 4.2. 5B).

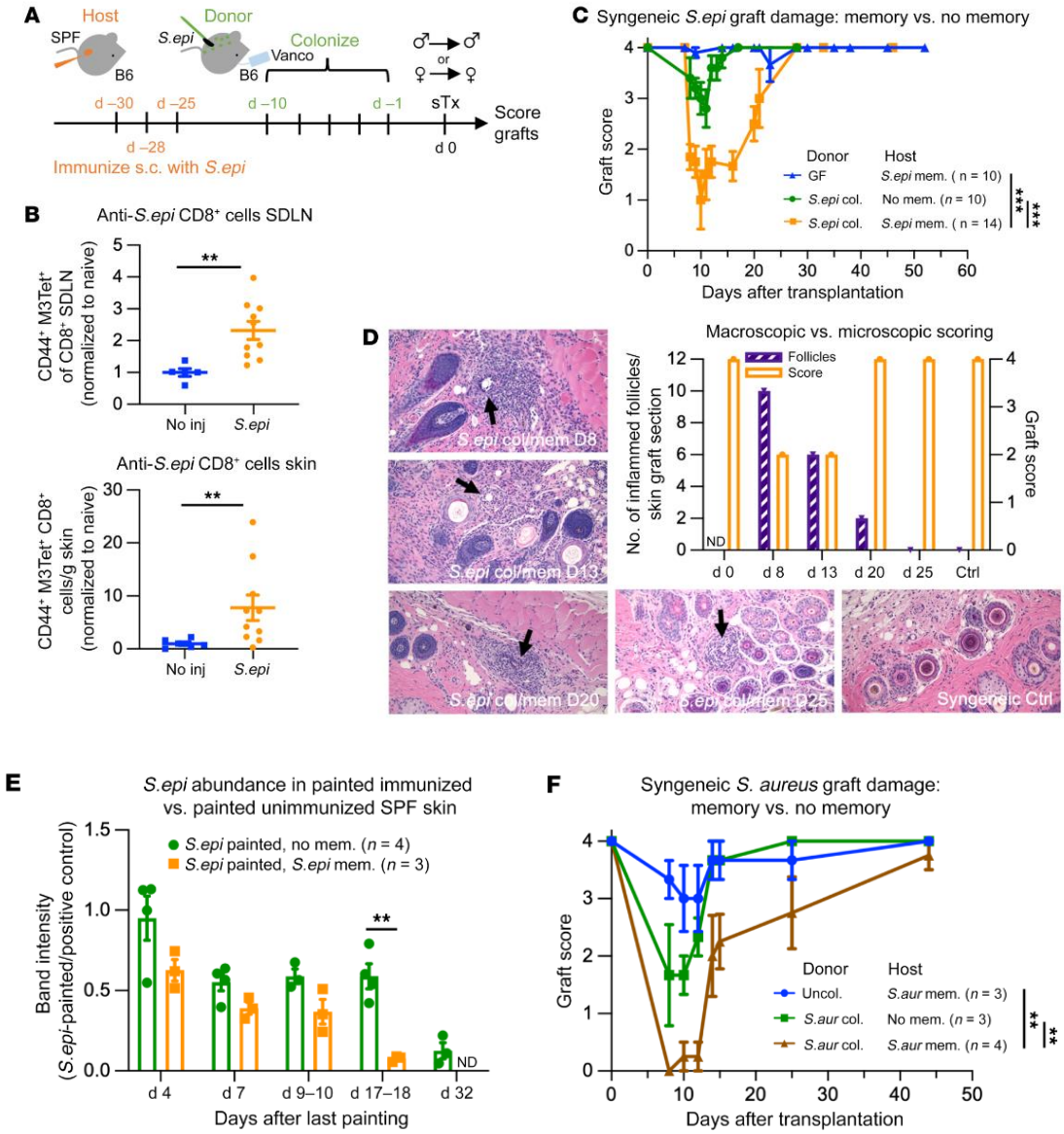

Figure 4.2. 5. Hosts with memory against commensals present on donated organs damage colonized syngeneic skin grafts.

(A) Hosts were injected with *S. epi* (1×10^5 CFU s.c.) 30, 28, and 25 days before receiving *S. epi*-monocolonized syngeneic skin grafts. Grafts were scored on a 4-point scale. (B) Endogenous *S. epi*-specific T cells in the skin and SDLNs 1 month after *S. epi* immunization. Gated on $CD45.2^+TCR\beta^+CD8^+CD4^-CD44^+$ H2-M3:fMIIINA–PE^+ (tetramer against *S. epi*-reactive T cells) events. Plots show fold change relative to unimmunized mice (mean ± SEM) analyzed by Wilcoxon's log-rank test. (C) Graft scores of syngeneic hosts with or without anti-*S. epi* memory that received GF or S. *epi*-monocolonized skin grafts. (D) H&E-stained sections from *S. epi*-monocolonized syngeneic grafts in hosts with anti-*S. epi* memory or a syngeneic, uncolonized graft in a naive host. A blinded pathologist identified (black arrows) and quantified (purple bars) abnormal mixed lymphocytic/neutrophilic infiltrates around hair follicles. Quantifications are plotted with the macroscopic 4-point score of the graft at sacrifice (orange bars). Original

Figure 4.2. 5. cont. magnification ×20. (E) PCR band intensities of *S. epi* DNA isolated from skin swabs of *S. epi*-painted SPF hosts naive to (green) or with memory against (orange) *S. epi*. Intensities are normalized to a *S. epi*-positive control. An unpaired, 2-tailed t test was performed at each time point. (F) Graft scores of syngeneic hosts with or without anti–S. aureus memory that received skin grafts from SPF donors with or without S. aureus colonization. (C, E, and F) The area under the graft score curves was calculated for each mouse, and ANOVA with multiple comparisons was performed. Plots show 1 (F), 2 (E), 3 (B and C, green and blue lines), or 4 (C, orange line) independent experiments. mem., memory; col., colonized; d, day; ND, no data.

Strikingly, mice with anti-*S. epi* memory damaged *S. epi*-colonized syngeneic skin grafts significantly more than hosts lacking anti-*S. epi* memory (Figure 4.2. 5C). Because the extent of damage was equal in male and female hosts of syngeneic grafts under all transplantation conditions, the data were aggregated for male and female mice in the same experimental groups. The damage was not due to infection caused by the *S. epi* immunization protocol, since GF skin grafts in hosts harboring anti-*S. epi* memory did not develop any graft damage (Figure 4.2. 5C). Thus, the damage to *S. epi*-colonized skin grafts observed in SPF hosts with memory to *S. epi* was extensive enough to occur in a syngeneic setting, thus independently from an alloresponse.

Microscopically, colonized grafts in hosts with anti-*S. epi* memory had abnormal lymphocytic and neutrophilic infiltration around hair follicles (Figure 4.2. 5D). *S. epi* is known to associate with keratinocytes at the base of hair follicles[103]. Therefore, the graft pathology was consistent with a host immune response against graft-resident *S. epi*.

Notably, over time, the syngeneic colonized grafts in hosts with anti-*S. epi* memory recovered (Figure 4.2. 5C). This correlated with a resolution of the cellular infiltrates in hair follicles in histological sections (Figure 4.2. 5D). We hypothesized that this was due to progressive disappearance of *S. epi* colonization, either because the graft-resident *S. epi* was outcompeted by the native mouse microbiota or because it was eliminated by the host's immune system. To determine the longevity of *S. epi* colonization, mice harboring or lacking anti-*S. epi* memory were painted with *S. epi*. After the last painting, tail skin was swabbed every few days.

DNA was isolated from these samples, and putative *S. epi* DNA was amplified by PCR. The presence of anti-*S. epi* memory accelerated *S. epi* elimination from the skin; *S. epi* DNA abundance in tail swabs from mice harboring anti-*S. epi* memory became almost undetectable 18 days after the last painting, while *S. epi* DNA from mice without memory was still abundant at that time (Figure 4.2. 5E). In mice lacking memory, *S. epi* DNA was significantly reduced 32 days after the last painting (Figure 4.2. 5E). These time frames correlated with how long it took for syngeneic, colonized grafts to start improving (around 20 days after transplantation) in hosts with anti-commensal memory (Figure 4.2. 5C). We hypothesize that graft recovery can occur in syngeneic grafts because there are no alloantigens present to perpetuate the immune response against the transplanted organ. In allograft recipients, however, we propose that this host-versus-commensal immune response would work in parallel to the host-versus-graft immune response to heighten graft damage and accelerate rejection.

To determine whether commensal memory–associated graft damage was unique to *S. epi* or whether it extended to other commensals, we colonized SPF donor mice with a strain of *S. aureus* adapted to mouse colonization[264]. To improve *S. aureus* establishment, the skin of SPF female donor mice was first topically treated with the antiseptic chlorhexidine, and then painted for 5 consecutive days with *S. aureus*. Skin colonized with *S. aureus* or not was transplanted onto syngeneic hosts that had been immunized or not with *S. aureus* a month earlier. A similar pattern was observed to that seen with *S. epi*: some syngeneic skin graft damage occurred in naive hosts that received S. aureus–colonized syngeneic grafts when compared with grafts without *S. aureus*, and this damage was significantly heightened in hosts with preexisting memory to *S. aureus* (Figure 4.2. 5F). Together, these results support the notion that host-versus-commensal immune memory participates in damage to colonized solid organ transplants.

4.2.3.3 Anti-commensal memory T cells are required to damage colonized syngeneic skin grafts.

Given the T cell response to *S. epi* following transplantation (Figure 4.2. 1B, C) and the fact that *S. epi* is known to generate a wide array of T cell responses in mouse skin[106,255], we hypothesized that memory T cells were responsible for the damage observed in hosts with anti-*S. epi* memory. To test this hypothesis, we transplanted *S. epi*-monocolonized skin into syngeneic T cell receptor α–knockout (TCRαKO) hosts immunized a month earlier with *S. epi* (Figure 4.2. 6A). Compared with the severe graft damage observed in T cell–replete mice, TCRαKO hosts displayed either no damage to their syngeneic skin grafts, or mild damage that resolved quickly (Figure 4.2. 6B). Further, colonized skin graft sections taken from *S. epi*-sensitized TCRαKO hosts 12 days after transplantation (the peak of damage in WT mice with anti-commensal memory) revealed none of the abnormal infiltrates around hair follicles that were present in WT hosts with anti-*S. epi* memory (Figure 4.2. 6C; controls in Figure 4.2. 5D). The lack of macro- or microscopic damage to colonized skin grafts in sensitized TCRαKO hosts suggests that T cells are required to damage colonized, syngeneic grafts.

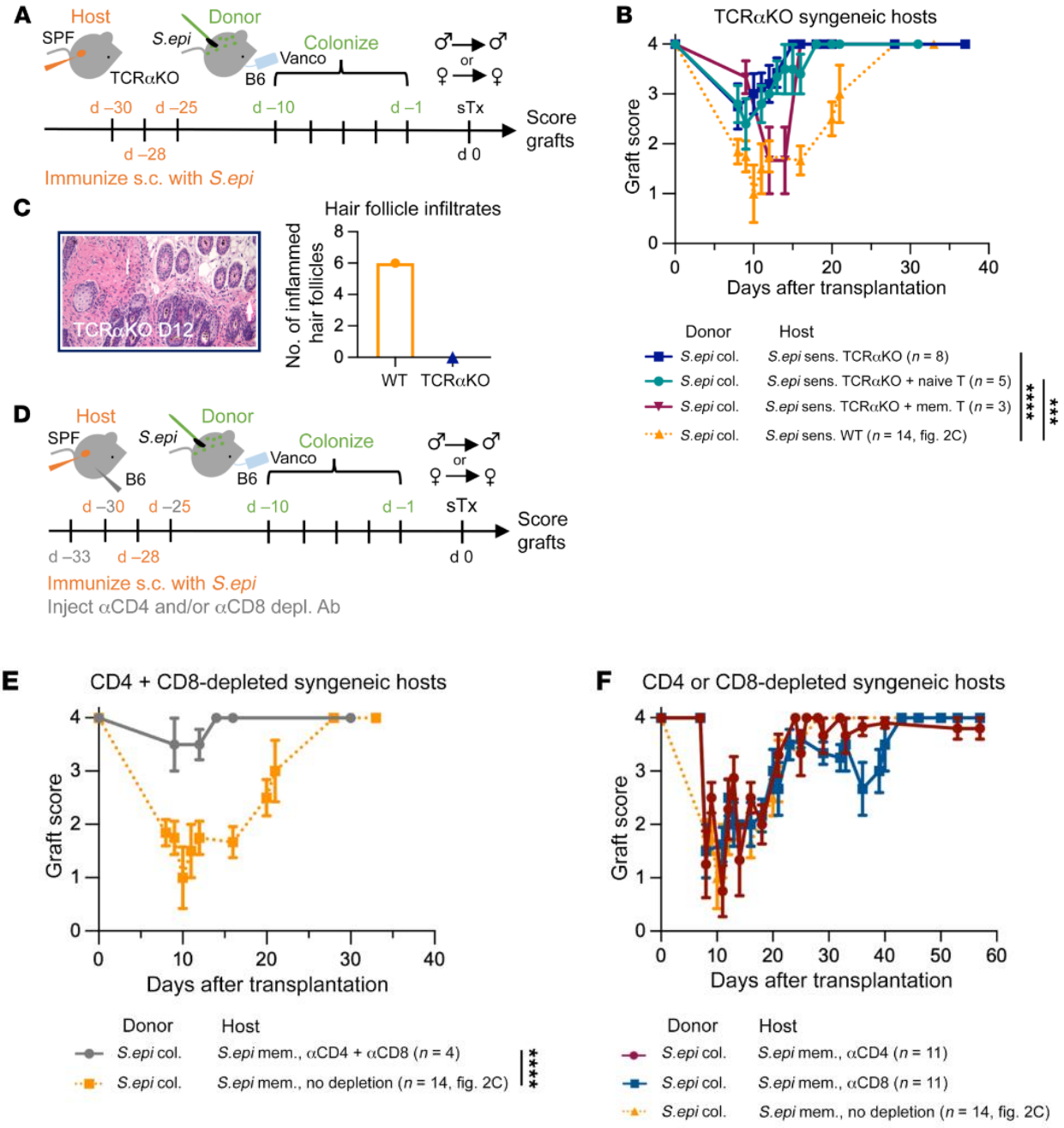

Figure 4.2. 6. Both CD4$^+$ and CD8$^+$ host memory T cells are required to damage colonized, syngeneic skin grafts.

(A) TCRαKO hosts were immunized 3 times s.c. with *S. epi* to induce anti-*S. epi* memory. One month later, they received syngeneic skin grafts from *S. epi*-monocolonized hosts. (B and C) Graft scores (B) and H&E-stained skin graft sections (C) from memory-harboring TCRαKO hosts of *S. epi*-monocolonized skin grafts (B and C, dark blue) compared with curves and images of WT hosts with anti-*S. epi* memory that received *S. epi*-monocolonized, syngeneic skin grafts (B and C, orange, dotted; same cumulative data shown in Figure 2C). Original magnification ×20. (B) Graft scores of TCRαKO mice with anti-*S.epi* memory seeded with T cells from the

Figure 4.2. 6. cont. lymph nodes and spleen of C57BL/6 mice naive to *S. epi* (teal) or T cells from the lymph nodes, spleen, and skin of C57BL/6 mice sensitized s.c. with *S. epi* (maroon) before transplantation with a *S. epi*-monocolonized syngeneic skin graft. Plots show 1 (maroon), 2 (teal), or 3 (dark blue) independent experiments. (C) Number of inflamed hair follicles in H&E-stained skin grafts counted by a blinded pathologist. (D) Hosts received anti-CD4 (GK1.5) and/or anti-CD8 (2.43.1) i.p. on days –2, 0, and 5 relative to s.c. injection with *S. epi*. $CD4^+$ and/or $CD8^+$ populations recovered before skin transplantation with a *S. epi*-monocolonized skin graft. (E) Anti-CD4 and anti-CD8 co-depletion plotted against relevant data from Figure 2C. (F) Anti-CD4 (maroon) or anti-CD8 (blue) depletion alone plotted against cumulative data from Figure 2C. Plots combine 3 independent experiments. (B, E, and F). mem., memory; col., colonized; d, day; sens., sensitized.

TCRαKO hosts are genetically devoid of αβ T cells, such that they lack both anti-commensal memory T cells and all other αβ T cells at transplantation. To ensure that the protective phenotype we observed was from the lack of anti-*S. epi* memory and not the global lack of T cells, we adoptively transferred T cells from naive or *S. epi*-sensitized WT mice into previously *S. epi*-sensitized TCRαKO mice, 1 day before transplantation with a syngeneic *S. epi*-colonized skin graft. Transfer of T cells from *S. epi*-sensitized but not naive WT mice resulted in graft damage (Figure 4.2. 6B). The damage in memory T cell–seeded TCRαKO mice did not persist as long as the damage in sensitized WT mice, perhaps because of more rapid clearance of graft-resident *S. epi* due to the high number of adoptively transferred memory T cells.

As an alternative approach to TCRαKO hosts, we used antibodies to deplete $CD4^+$ and/or $CD8^+$ T cells 1 day before immunizing mice for the generation of anti-*S. epi* memory. We depleted $CD4^+$ and/or $CD8^+$ T cells again before the second and third *S. epi* immunizations and then allowed the $CD4^+$ and $CD8^+$ T cell populations to recover before skin transplantation Figure 4.2. 6D). We reasoned that this approach would allow us to selectively prevent anti-*S. epi* T cell memory without compromising T cell immunity at the time of syngeneic skin transplantation. In keeping with results observed in TCRαKO mice, hosts lacking $CD4^+$ and $CD8^+$ T cells during *S. epi* immunization minimally damaged subsequent *S. epi*-colonized syngeneic skin grafts (Figure 4.2. 6E). Conversely, hosts that received only the anti-CD4 or the anti-CD8 depleting antibody

throughout the *S. epi* immunization displayed graft damage similar to that seen in their un-depleted counterparts (Figure 4.2. 6F). Together, these results indicate that damage to colonized, syngeneic skin grafts in hosts harboring anti-commensal memory is dependent on αβ T cells. Neither $CD4^+$ nor $CD8^+$ T cell memory was required for graft damage to occur, suggesting that one memory subset is sufficient for, and both subsets can contribute to, the graft damage.

4.2.3.4 Host tissue-resident memory cells are sufficient to damage colonized syngeneic skin grafts.

S. epi is known to generate tissue-resident memory T cells (Trm cells) in the skin[105,106]. In our model, the s.c. immunizations that generated anti-*S. epi* memory established a robust population of $CD4^+$ and $CD8^+$ Trm cells in mouse skin (Figure 4.2. 7A).

To determine whether Trm cells were sufficient to damage colonized syngeneic skin grafts in hosts with anti-*S. epi* memory, we treated hosts with the sphingosine-1-phosphate receptor (S1PR) agonist FTY720 on days –2, 0, 4, and 10 relative to transplantation of *S. epi*-colonized skin grafts (Figure 4.2. 7B). FTY720 downregulates S1PR and traps naive and central memory lymphocytes in the lymph nodes, thus revealing the impact of effector memory and Trm cells[265]. Preventing recruitment of new naive and central memory T cells into the skin graft using FTY720 did not reduce damage to colonized syngeneic skin grafts compared with damage in untreated hosts (Figure 4.2. 7C). Skin grafts from FTY720-treated mice had the same hair follicle pathology as those from untreated mice, even 20 days after transplantation, a time point slightly past the peak of graft damage (Figure 4.2. 7D). These data support the conclusion that Trm and/or effector memory cells are sufficient to potentiate damage against colonized, syngeneic skin grafts.

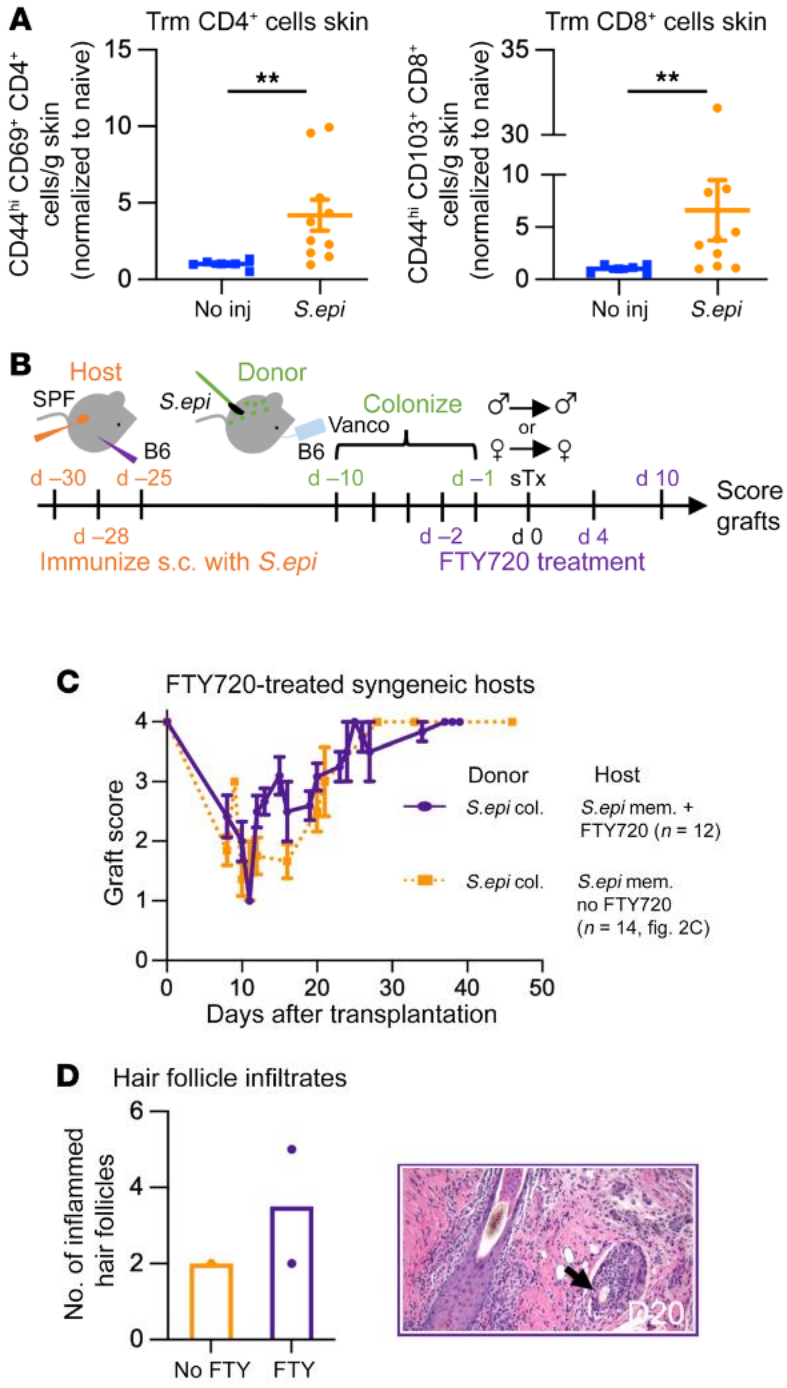

Figure 4.2. 7. Host tissue-resident memory cells are sufficient to damage colonized, syngeneic skin grafts.

(A) Trm cells isolated from the skin of mice that were immunized s.c. with *S. epi* one month earlier. Cells gated on CD45.2$^+$CD8$^-$CD4$^+$CD44$^+$CD69$^+$ (CD4$^+$, left) or CD45.2$^+$CD8$^+$CD4$^-$ CD44$^+$CD103$^+$ (CD8$^+$, right) populations. Plots show fold change relative to naive mice (mean ± SEM) and include 3 independent experiments analyzed using Wilcoxon's log-rank test. **P < 0.005. (B) Mice harboring anti-*S. epi* memory were injected i.p. with FTY720 on days –2, 0, 4,

Figure 4.2. 7. cont. and 10 relative to transplantation with *S. epi*-monocolonized skin grafts. (C and D) Graft scores (C) and H&E-stained graft sections (D) from mice treated with FTY720 (purple line) compared with untreated controls shown in Figure 2C (dotted orange line). Black arrow denotes abnormal immune infiltrates around hair follicles, which were quantified by a blinded pathologist. Original magnification ×20. mem., memory; col., colonized; d, day.

4.2.4 Discussion

Organs harboring their own tissue-specific microbiome are rejected faster than sterile organs after transplantation. Here we show that this accelerated rejection occurs at least in part because of host immune responses against the commensal microbes present on the donated organ. Naive commensal-specific T cells in graft-recipient mice expanded in response to commensals present on transplanted organs and inflicted modest transient damage to the colonized graft. More significantly, memory commensal-specific T cells caused substantial and more durable damage to colonized organs. Trm and/or effector memory T cells in the host were sufficient to drive this damage. This host-versus-commensal immune response was distinct from the alloresponse and resulted in resistance to immunosuppression.

Many prior studies implicate the microbiome in altering transplant outcomes. For example, our group showed that mice pretreated with antibiotics before skin transplantation exhibited delayed rejection compared with untreated mice[97], and that the presence of intestinal communities such as *Alistipes* spp. correlated with longer skin graft survival[117]. These studies highlighted the importance of the gut microbiota in skin graft outcomes, but did not address whether the organ-specific microbiome alone was sufficient to impact allograft rejection. To that end, we previously showed that graft *S. epi* can accelerate skin transplant rejection by augmenting the effector phase of the alloresponse in the graft[100]. In addition to that mechanism, we show here that anti-commensal immune responses contribute to damage of colonized organs. To our knowledge, this is the first study demonstrating that host T cell–mediated immune

responses to commensal bacteria on the transplanted organ reduce survival of a colonized transplant. Thus, importantly, our results show that adaptive immune responses beyond the alloresponse can contribute to organ damage.

Our results also demonstrate that host-versus-commensal memory immune responses resist immunosuppression with rapamycin and tacrolimus. This is not entirely surprising because we implicate Trm and/or effector memory T cells in potentiating damage against colonized grafts. Owing to their largely tissue resident status and their memory phenotype, these cells are harder to suppress with immunosuppressive drugs, which are better at inhibiting newly dividing, naive lymphocytes[266].

In our experiments, colonized syngeneic skin grafts that were damaged by anti-commensal memory recovered. We hypothesize that this is because the damaging anti-commensal immune response, which localizes around hair follicles, a known *S. epi* niche, successfully eliminates the bacteria and then abates. Given that memory against bacteria closely related to the strain on the skin graft, but not memory against distant bacterial taxa, can perpetuate graft damage, we hypothesize that these immune responses are specific for *S. epi* antigens. However, Gram-negative E. coli and Gram-positive *S. epi* may train different innate immune programs, and these differences may also account for the findings. Future studies should assess the degree of antigen specificity and characterize (a) which commensal peptides are immunogenic, (b) the pathways through which they signal, and (c) which are the deleterious T cell profiles. Importantly, in this study, the damage we observe cannot be caused by anti-commensal memory cross-reacting to alloantigen, because the damage occurs in syngeneic grafts in which no alloantigen is present. It also is not mediated by postsurgical infection caused by *S.*

epi colonization on the skin graft, because graft damage is much more severe in colonized graft recipients harboring anti-commensal memory than in recipients naive to *S. epi*.

In our model, we establish anti-*S. epi* memory through subcutaneous injections. In human transplant recipients, we hypothesize that Trm cells naturally accumulate against many commensals and can perpetuate chronic damage to colonized organs. In fact, mouse studies show that steady-state microbial colonization in adult life and minor barrier damage that exposes the hosts to commensals in pathogenic contexts establish a cohort of Trm cells poised to attack microbes in colonized organs[104,107]. Indeed, when *S. epi* is painted on adult mouse skin at steady state, it generates Trm $CD4^+$ and $CD8^+$ cells that preferentially adopt type 17 and type 1 programs[106]. Some of these IL-17A–producing $CD8^+$ T cells harbor mRNA for the type 2 transcription factor GATA3. They aid in wound repair after tissue injury[107]. However, when mice colonized with *S. epi* as adults receive punch wounds or minor skin abrasions and then are repainted with *S. epi,* they mount proinflammatory responses against *S. epi* that seem to outweigh wound-healing benefits[104]. Therefore, the type 1 and type 17 cells induced by steady-state colonization do attack *S. epi* in pathogenic contexts. Whether these are the T cell profiles involved in damaging colonized skin grafts remains to be determined.

Additionally, how commensal-specific Trm cells in the host's skin migrate into colonized skin grafts, or whether only effector memory T cells recruited into the graft mediate damage of colonized skin grafts, needs to be investigated. In the skin, Trm cells localize most strongly to the site where antigen was first encountered and provide the strongest protective immunity in that region[267]. However, $CD8^+$ Trm cells induced in one part of the skin can confer protective immunity to the same bacterial infection at other skin sites[267]. Indeed, a small proportion of $CD8^+$ Trm cells migrate away from the initial infection site and randomly disperse throughout

the epidermis, where they defend the host at distal locations[268,269]. Additionally, in a cancer setting, activated tumor antigen–specific $CD8^+$ Trm cells in the skin caused cross-presenting dermal dendritic cells to mature and migrate to the lymph nodes, where they activated additional T cells that attacked tumor antigen–expressing cells both in, and far from, the initial Trm-rich region[270]. $CD4^+$ Trm cells are less migratory than $CD8^+$ Trm cells. Nonetheless, a proportion of them transiently downregulate CD69, exit the dermis, and recirculate[271]. These $CD4^+$ ex-tissue-resident memory T cells can activate additional immune responses in the lymph node or reenter the tissue from which they exited at the same or a different site[272,273]. These migratory capacities of both $CD4^+$ and $CD8^+$ memory T cells indicate that host Trm cells induced upon s.c. *S. epi* immunization may migrate laterally or through circulation into the graft, which is adjacent to the injection site, and damage it. It is possible that lateral migration and/or recirculation could be upregulated in response to the tissue injury conferred by surgery. Exactly how and where graft-derived *S. epi* antigens are presented to memory T cells, and to what extent surgical trauma or reperfusion injury is required to initiate the memory-dependent damage, remain to be determined.

In our experiments, we observe minimal and early damage to *S. epi*-colonized grafts even in immunized hosts that lack T cells. This damage could be mediated by T cell–independent antibody responses or, given its rapid onset and recovery, driven by trained innate memory. Invertebrates that lack adaptive immunity develop allospecific responses[274–276]. Similar innate mechanisms exist in vertebrates and contribute to organ rejection. Rag–/– mice that lack B and T cells can reject allografts when they have been preimmunized with donor antigens[277,278]. Further, for at least 1 month after sensitization, macrophages retain “trained” responses that are sufficient to reject allografts in an antigen-specific manner[279]. Therefore, trained innate memory against

microbial antigens that accompany transplanted organs might also contribute to colonized organ rejection[280]. The mechanisms through which macrophages transmit this memory beyond their possibly short lifespan, and whether trained innate memory is relevant for transplant outcomes if established more than 1 month before transplantation, remain to be fully determined.

Our results suggest that graft sterilization prior to transplantation might result in better outcomes for barrier organ allografts. Perfusing the organs with antibiotics shortly before transplantation may reduce donor commensal load and enable colonization of the graft by host commensals. However, antibiotics may also eliminate pro-tolerogenic donor commensals, as some bacteria are known to promote Treg expansion[281]. We conclude that memory T cells specific for select bacterial commensals can significantly damage colonized skin grafts independently from an alloresponse and render hosts more resistant to immunosuppression.

Chapter 5: Influence of microbial-derived metabolites on solid organ transplant outcome

5.1 Oral butyrate prolongs survival of distal skin allografts

5.1.1 Abstract

The microbiota composition is now known to influence the kinetics of graft rejection, but many questions remain as to whether/how microbiota-derived metabolites affect graft outcome. This study investigated the effects of the short-chain fatty acid butyrate, a product of dietary fiber fermentation. Sustained oral butyrate (ButM) administration significantly prolonged minor- and major-mismatched skin allograft survival in mice. ButM treatment elevated cecal butyrate content and altered the gut and skin microbiota. While ButM did not influence regulatory T cells or adaptive alloimmune responses, it modulated the myeloid cell compartment. At steady-state, it reduced the number of circulating $Ly6C^{hi}CD11b^{+}$ monocytes and other myeloid cells in secondary lymphoid organs and skin, altered their expression of genes involved in mitochondrial metabolism and key inflammatory processes, and reduced their ability to produce TNFα. Consistent with its critical effect on myeloid cells, the prolongation of graft survival induced by ButM depended on the presence of $CCR2^{+}$ cells. These findings imply that ButM enhances distal allograft outcomes by quantitatively and qualitatively modulating myeloid cells, thereby inhibiting the innate immune cell-mediated effector phase of the alloimmune response.

5.1.2 Introduction

The principal drivers of the alloimmune response against transplanted solid organs are peptide disparities between the donor and the recipient in major and minor histocompatibility

antigens. Some of those polymorphisms are detected by the recipient's adaptive immune compartment, triggering allograft rejection[198,199]. The steady-state immune status of the recipient before receiving a transplant; i.e, the poising level of myeloid cells that results from the sum of all signals these cells receive, can influence the alloimmune response and allograft rejection kinetics[97,100,117,174,180,181,212]. Our group has previously demonstrated that altering the whole-body microbial composition in mice following treatment with oral antibiotics results in significantly prolonged allograft survival in skin, heart, and lung transplant models[97,212]. Mechanistic studies showed that a diverse microbiota structure poises systemic antigen-presenting cells (APCs) that then prime alloreactive T cell responses more effectively than APCs in hosts with less diverse or absent microbial communities. These findings underscore the capacity of the microbiota to calibrate the host's immune system and modulate allograft outcomes.

The microbiota, encompassing the complete set of commensals that reside on mucosal and epithelial surfaces, can influence the immune system by expression or generation of bioactive molecules. Among these are microbial-associated molecular patterns (MAMPS) and microbial-derived metabolites[133,202], which serve as key immunomodulatory agents. For the intestinal microbiota, the impact of these molecules extends both locally within the gut, where they interact with gut epithelial or immune cells, and systemically, through the circulation of metabolites, communication relay between diverse cell types, or migration of cells from the gut to distal locations[133,202]. Microbial communities at other body sites can theoretically have similar local and distal effects. We have shown that skin commensals can enable skin graft APCs to better re-activate T cells at the effector phase of the alloresponse. Understanding how the microbiota and their derived molecules fine-tune immunity can be used to leverage their use in therapeutic settings and to improve current immunosuppressive regimens for allograft recipients.

Transplant patients have a compromised gut barrier integrity, characterized by the dysbiotic state of the microbiome of patients at end-stage organ failure[216,217], recurrent viral and *C. difficile* infections[218], colonization with multi-drug-resistant bacteria[219], co-morbidities that result in exposure to polypharmacy (proton pump-inhibitors, laxatives, immunosuppressive drugs, and antibiotics)[220]. Collectively, these factors contribute to exacerbated microbiota dysbiosis, gut barrier injury, gut leakiness[221], and worse clinical outcomes[217]. Fecal metabolomic profiling from human heart transplant recipients confirmed that many immunomodulatory metabolites were decreased in transplant vs healthy individuals including the short-chain fatty acids (SCFA) acetate, propionate and butyrate, and secondary bile acids[149]. Association studies have determined that during acute graft-vs-host disease, there is a significant variation in metabolites that are end-products of microbes, with a decrease in AhR ligands and differences in bile acid levels[136]. Moreover, recent profiling of liver transplant patients, found that low levels of SCFA, secondary bile acids, and tryptophan metabolites correlated with an increased risk of postoperative infections[150]. Understanding if these perturbed microbial and metabolic profiles are causal factors for graft damage or are a consequence of rejection can potentially lead to therapeutic strategies to improve allograft survival. Alternatively, relative abundance of select microbes or metabolites may serve as biomarkers to help predict clinical outcomes.

Strategically designed commensal consortia have demonstrated efficacy in targeting specific cell populations, such as Th1 and IFNγ-producing $CD8^+$ T cells for cancer immunotherapy[138,282], intestinal epithelial cells to mitigate food allergen sensitization[283], or Tregs for experimental colitis treatments[281]. Exploiting such consortia holds promise for improving allograft outcomes. In animal models, the supplementation with a combination of *Bifidobacterium longum*, *Lactobacillus acidophilus*, and *Enterococcus faecalis* attenuated liver

injury in rats experiencing acute liver transplant rejection[284]. Notably, *Bifidobacterium pseudolongum*, *Alistipes oderdonkii*, and *Parabacteroides distasonis* stand out as single-strain probiotics capable of individually improving transplant outcome when supplemented to microbiota-replete conventional mice[121,180,181]. However, challenges persist in achieving sustained engraftment of transferred bacteria following fecal microbiota transfer (FMT) or oral delivery[285,286]. Consequently, we explored the use of microbial-derived metabolites themselves, known as postbiotics[287], as drug agents that bypass the microbial communities, to attempt to ameliorate graft survival directly.

Gut barrier integrity maintenance is mediated in part by the microbe-derived group of metabolites SCFA[133]. These compounds are end-products of the fermentation of non-digestible polysaccharide[288] and have pivotal functions in promoting barrier function by modifying intestinal epithelial and immune cell function[133]. Among the SCFA, butyrate stands out as therapeutically promising, due to its dual action as a histone deacetylase (HDAC) inhibitor and its ability to signal via different G protein-coupled receptors (GPCRs)[139,289]. Butyrate is important for fostering gut homeostasis and tolerogenic responses, by influencing intestinal epithelial cell metabolism[290], differentiation of colonic regulatory T cells (Tregs)[140,141,291], and imprinting anti-inflammatory properties to colonic macrophages and dendritic cells[292,293]. Decreased relative abundance of butyrate-producing commensals has been found in patients with food allergy[294,295] and inflammatory bowel disease[296,297], providing evidence for associations between low levels of butyrate and disease.

In the context of transplantation, lower levels of butyrate-producing commensals and of systemic butyrate correlated with worse outcomes in allogeneic hematopoietic stem cell transplantation[12,13]. Similarly, lower levels of microbial metagenomic pathways for butyrate

production were found in stool samples of liver and kidney transplant patients[4]. Furthermore, decreased levels of fecal butyrate were reported in human heart[149] and liver[150] transplant patients, supporting their importance in transplantation.

The enhanced capability of butyrate to regulate immunity makes it an ideal postbiotic to treat inflammatory conditions such as alloimmune responses. Nevertheless, therapeutic delivery of butyrate has proven challenging. Experimental models have utilized supra-physiological concentrations of butyrate, typically administered in the form of sodium butyrate (NaBut) or butyrylated starches[140,141,291]. In human clinical trials targeting colitis, intrarectal administration of butyrate has yielded only moderate success[298]. Developing targeted delivery of butyrate into the lower gastrointestinal (GI) tract, where it can exert its bioactive properties, has been challenging. Recently, a butyrate delivery platform encapsulated with protective micelles (ButM) has been developed with the capacity to increase the accumulation and retention of butyrate in the ileum and colon of mice, enhance gut barrier function, and treat mice in models of colitis and peanut allergy[197].

To study if the SCFA butyrate could improve allograft outcomes with this rationally designed delivery platform, we assessed the effects of oral delivery of ButM in murine skin allograft rejection models. We identified that sustained oral administration of ButM, both before and after transplantation, and not NaBut, optimally prolonged minor- and major-mismatched skin allograft survival. ButM significantly increased the cecal content of butyrate and modified the gut and skin microbiota of mice and reduced the numbers and function myeloid cells and their presence was necessary for the beneficial effect of butyrate on graft outcome. These data suggest that ButM improves distal allograft outcomes by quantitatively and qualitatively

modulating the myeloid cell compartment, thereby inhibiting the innate immune cell execution of the effector phase of rejection.

5.1.3 Results

5.1.3.1 Oral ButM administration prolongs the survival of a distal skin allograft and modifies the microbiota composition

To assess whether oral butyrate treatment could impact the rejection kinetics of a distal skin allograft, C57Bl/6 (B6) female recipient mice were gavaged with butyrate micelles (ButM) or given oral sodium butyrate (NaBut) starting 3 weeks prior to transplantation of male B6 skin and continued until graft rejection (Figure 5.1. 1A). Notably, only ButM treatment resulted in significant prolongation of allograft survival (Figure 5.1. 1B). While treating recipients with ButM only until surgery significantly slowed down rejection kinetics, prolongation of graft survival did not reach statistical significance when the treatment was started post-transplantation (Figure 5.1. 2A-D). Other routes of administration, e.i. intraperitoneally (ip) (Figure 5.1. 2E, F), for systemic delivery, or subcutaneously (sc) (Figure 5.1. 2E, G), for a localized effect to where the priming of T cells occurs post-skin transplantation, did not result in improved allograft outcomes, implying that only oral delivery has graft-promoting effects. Importantly, oral ButM in the absence of other immunosuppressants also prolonged survival of a BALB/c (B/c) to B6 major-mismatched skin allograft (Figure 5.1. 1A, C). These data collectively support that oral delivery of ButM elicits distal effects beyond the gut, prolonging survival of a distal skin allograft.

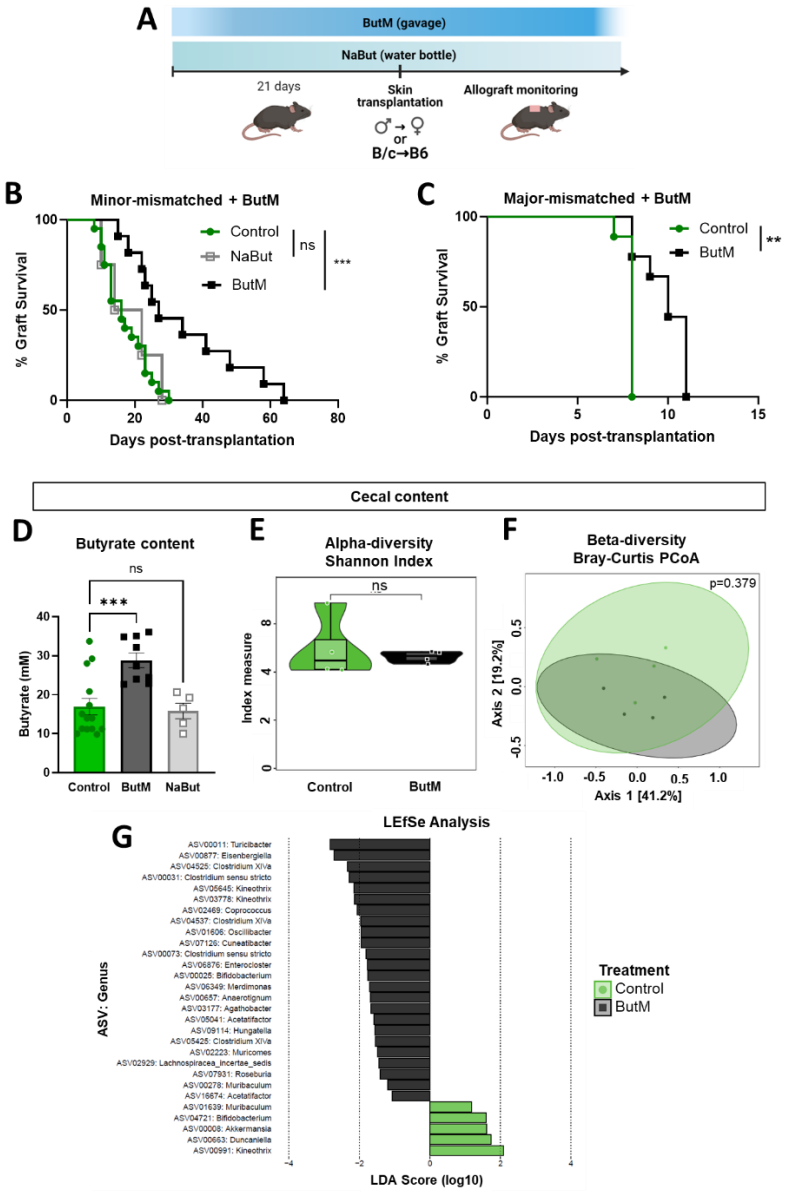

Figure 5.1. 1. Butyrate micelles treatment prolongs allograft survival, increases cecal butyrate levels, and modifies the intestinal microbiota.
(A) Mice were given butyrate micelles (ButM) or sodium butyrate (NaBut) starting 21 days before skin transplantation and treatment was continued until allograft rejection. C57Bl/6 (B6) male (minor-antigen mismatched) or BALB/c (B/c) (major-antigen mismatched) skin was transplanted onto female hosts on d0. (B) Minor-antigen mismatched skin allograft survival curves of ButM- or NaBut-treated mice (n=4-20). (C) Major-antigen mismatched skin allograft survival curves of ButM-treated mice (n= 9). (D-G) Mice were treated with ButM or NaBut for 21 days and their cecal content was extracted for metabolomic analysis and 16S rDNA sequencing. (D) Butyrate cecal content of ButM- or NaBut-treated mice (n=5-14). (E) Cecal microbiota alpha-diversity measure by Shannon-diversity index (n=4). (F) Cecal microbiota beta-diversity measure by Bray-Curtis Principal Coordinate Analysis (PCoA) (n=4). (G) Cecal microbiota LEfSe analysis.

As we and others have established that the microbiota can modulate solid organ transplantation[97,100,117,121,127,180], we investigated whether ButM administration modified microbiota composition or microbiota-derived metabolites, using metagenomic and metabolomic profiling. Cecal content of ButM-treated mice exhibited increased levels of butyrate compared to control and NaBut-treated mice, confirming that only the micelle-base delivery platform can augment the concentration of the SCFA in the distal portion of the GI tract (Figure 5.1. 1D). Although 16S rDNA sequencing of cecal content did not reveal major variation in the intra- and inter-individual microbiota composition between control and ButM treatment (Figure 5.1. 1E, F), amplicon sequence variant (ASV) technology confirmed that some commensals bloomed under the treatment (Figure 5.1. 1G). Bacteria that were enriched in the ButM treatment included *Turicibacter*, *Eisenbergiella*, and several ASVs of the *Clostridium* cluster XIVa (ASV04525, ASV04537, and ASV05425), whereas control mice had higher levels of *Kineothrix*, *Duncaniella*, and *Akkermansia* (Figure 5.1. 1G).

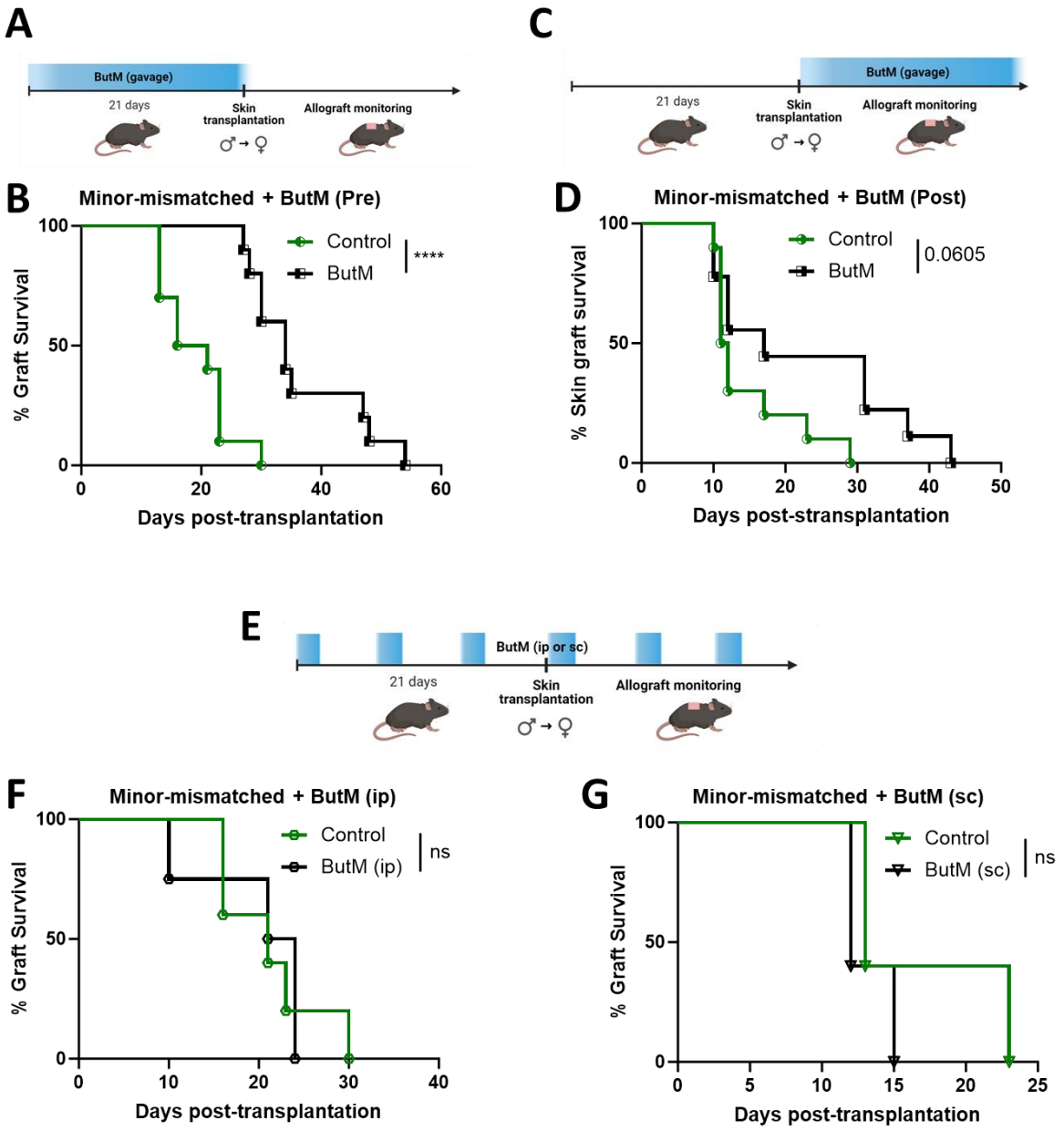

Figure 5.1. 2. Different butyrate micelle regimens of administration result in suboptimal allograft prolongation.

(A) Mice were only given butyrate micelles (ButM) for 21 days prior to skin transplantation. C57Bl/6 (B6) male (minor-antigen mismatched skin was transplanted onto female hosts on d0. (B) Minor-antigen mismatched skin allograft survival curves of ButM-pretreated mice (n=10). (C) Mice received skin transplantation and started the ButM treatment. (B) Minor-antigen mismatched skin allograft survival curves of post-skin transplant ButM-treated mice (n=9-10). (E) Mice were injected intraperitoneally (ip) or subcutaneously (sc) with ButM once a week starting 21 days prior to skin transplantation and treatment was continued until allograft rejection. (F) Minor-antigen mismatched skin allograft survival curves of ButM (ip) mice (n=4-5). (G) Minor-antigen mismatched skin allograft survival curves of ButM (sc) mice (n=5).

Interestingly, ButM treatment promoted major changes in the skin microbiota composition (Figure 5.1. 3A-C). Thus, oral administration of ButM promotes increased intestinal butyrate levels and modifies the local (gut) as well as distal (skin) microbiota.

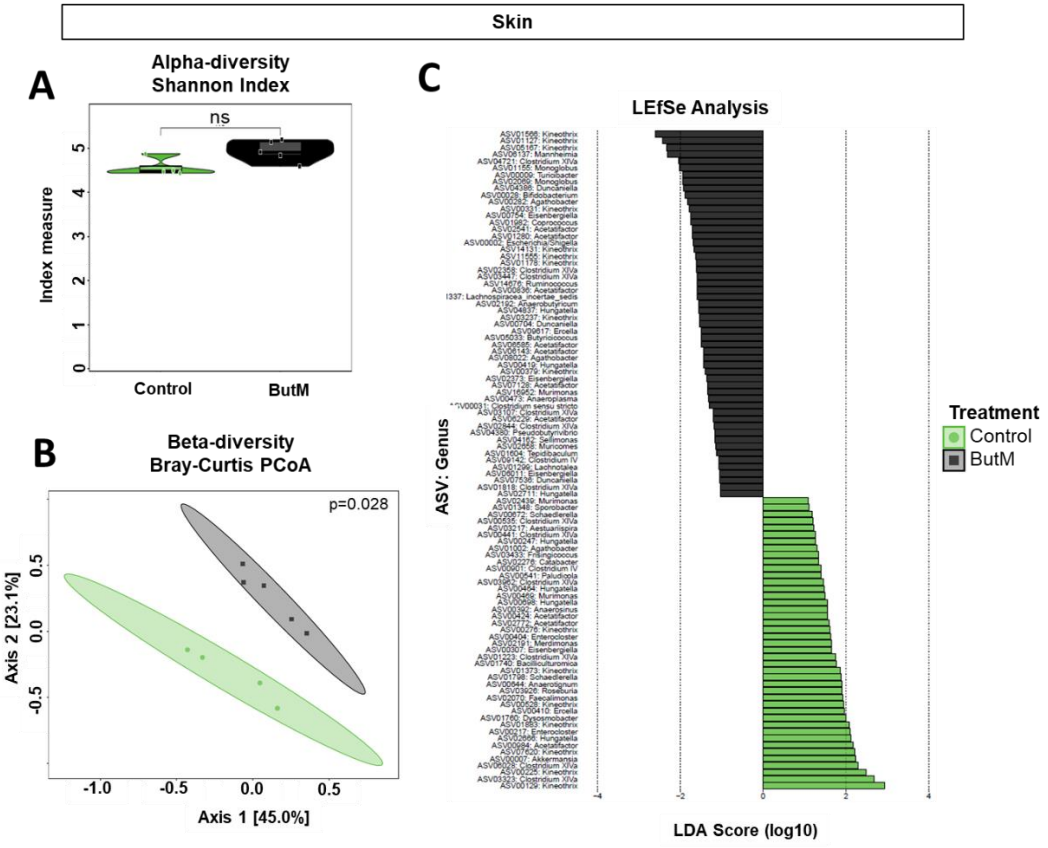

Figure 5.1. 3. Butyrate micelle treatment alters the skin microbiota.
Mice were given butyrate micelles (ButM) for 21 days and then cecal content and skin swabs were isolated for 16S rDNA sequencing. (A) Normalized relative frequency of cecal microbiota (n=4). (B) Normalized relative frequency of skin microbiota (n=4-5). (C) Skin microbiota alpha-diversity measure by Shannon-diversity index (n=4-5). (D) Skin microbiota beta-diversity measure by Bray-Curtis Principal Coordinate Analysis (PCoA) (n=4-5). (E) Skin microbiota LEfSe analysis.

5.1.3.2 Butyrate micelle treatment results in a quantitative impact on the myeloid cell compartment at steady-state

As butyrate has been described to promote Treg cells[140,141,291], we first performed immunophenotyping for Tregs located in different organs, including mesenteric lymph nodes

(mLN), spleen, skin-draining LN (dLN) and skin (Figure 5.1. 4). We did not find significant alterations in Tregs percentages or their capacity to proliferate as determined by Ki67 staining (Figure 5.1. 4), confirming that ButM was not impacting steady-state Tregs.

In previous research, we established that pre-treatment with broad-spectrum Abx attenuated graft rejection by inhibiting alloimmune T cell priming[97,181]. To investigate if ButM was prolonging allograft outcomes by modulating T cell alloimmunity we measured different phases of the anti-graft immune response, including the priming and differentiation (Figure 5.1. 5), migration (Figure 5.1. 6), and effector function of graft-infiltrating T cells upon ex vivo restimulation with 0. 5µg/mL anti-CD3 (0.5µg/mL) (Figure 5.1. 7). Surprisingly, we did not find any differences induced by ButM treatment in any of these T cell phases. These findings suggest that ButM is not prolonging allograft survival by modulating the T cell-mediated alloimmune response.

As butyrate is a strong enhancer of gut barrier function[133,202], we hypothesized that ButM treatment could reinforce the intestinal lining at steady state, or after transplantation. Serum LPS of ButM-treated mice was not lower than control mice (Figure 5.1. 8), demonstrating that the butyrate treatment does not decrease endotoxemia at homeostasis. Furthermore, after transplantation, both control and ButM had elevated serum LPS levels and decreased with similar kinetics (Figure 5.1. 8), supporting that ButM treatment does not improve intestinal barrier function after transplantation as well.

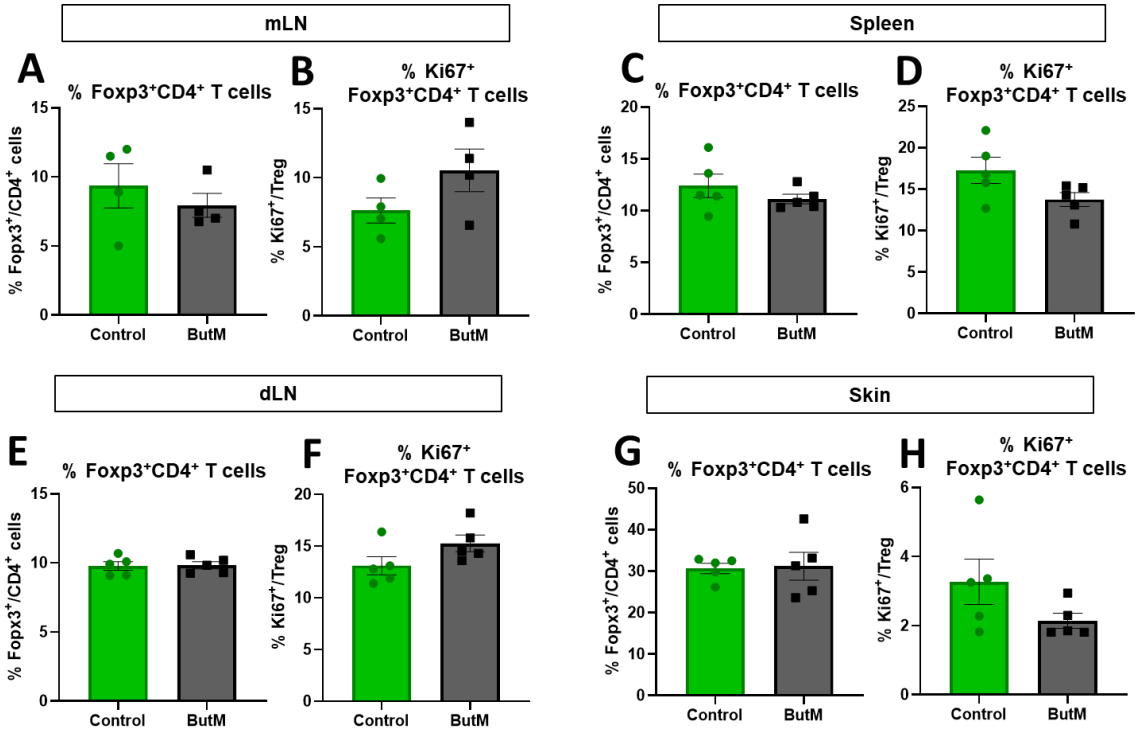

Figure 5.1. 4. Butyrate micelle treatment does not modify systemic levels of Tregs.
Mice were given butyrate micelles (ButM) for 21 days and then mesenteric lymph node (mLN), spleen, skin-draining LN (dLN), and skin were harvested to measure Treg cells. (A-H) $Foxp3^+$ $CD4^+$ Treg and $Ki67^+$ Treg cells from the (A, B) mLN, (C, D) spleen, (E, F) dLN and (G, H) skin. (n=5)

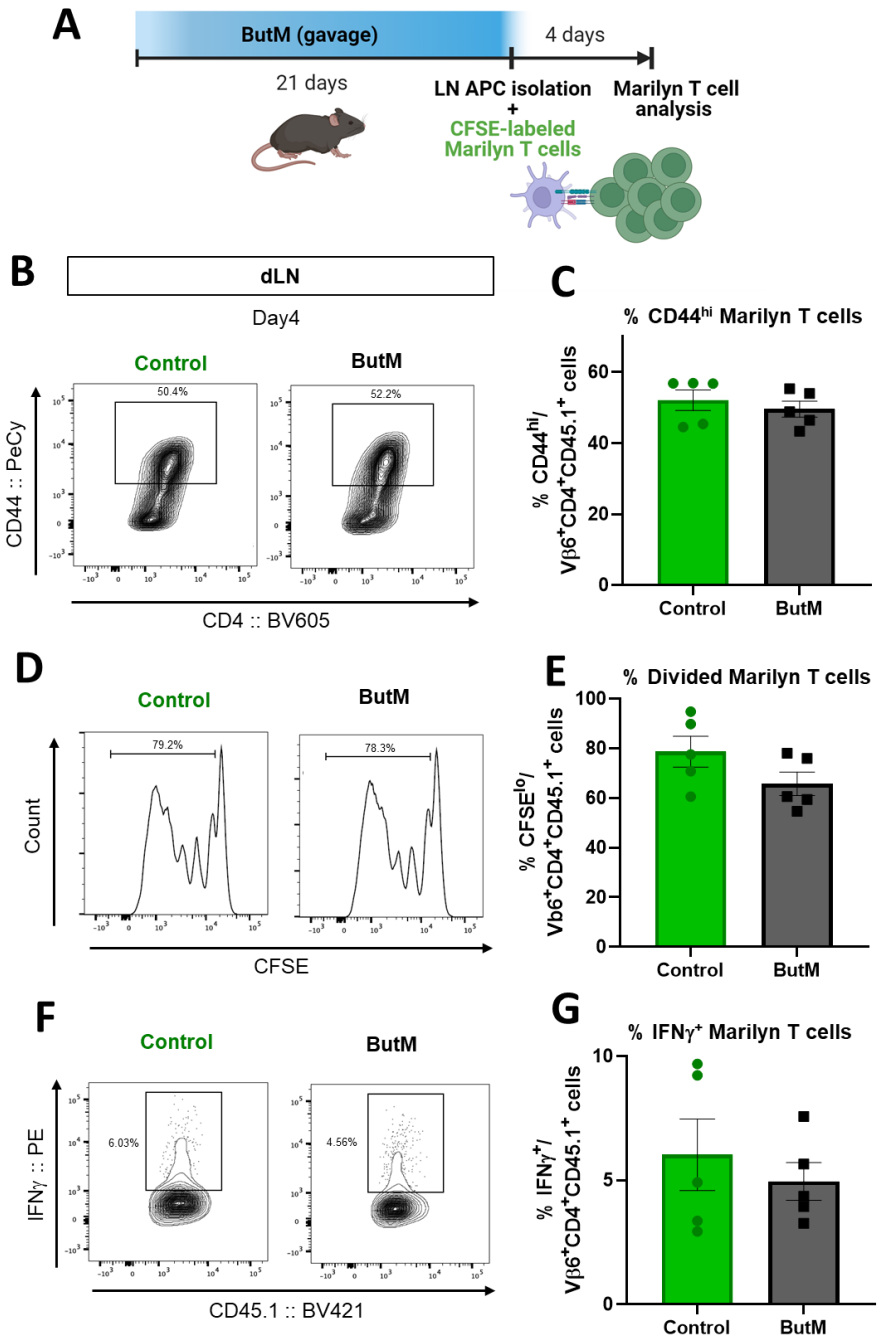

Figure 5.1. 5. Butyrate micelle treatment does not modify the priming phase of the alloimmune response.

(A) Male B6 mice were gavaged with butyrate micelles (ButM) for 21 days and then splenic antigen presenting cells (APC) were harvested and co-cultured with CFSE-labeled Marilyn T cells for 4 days and their priming was assessed. (B-G) Representative flow cytometry plots and quantification of (B, C) $CD44^{hi}$, (D, F) CFSE dilution, and (F, G) IFNγ production upon restimulation by Marilyn T cells (n=5)

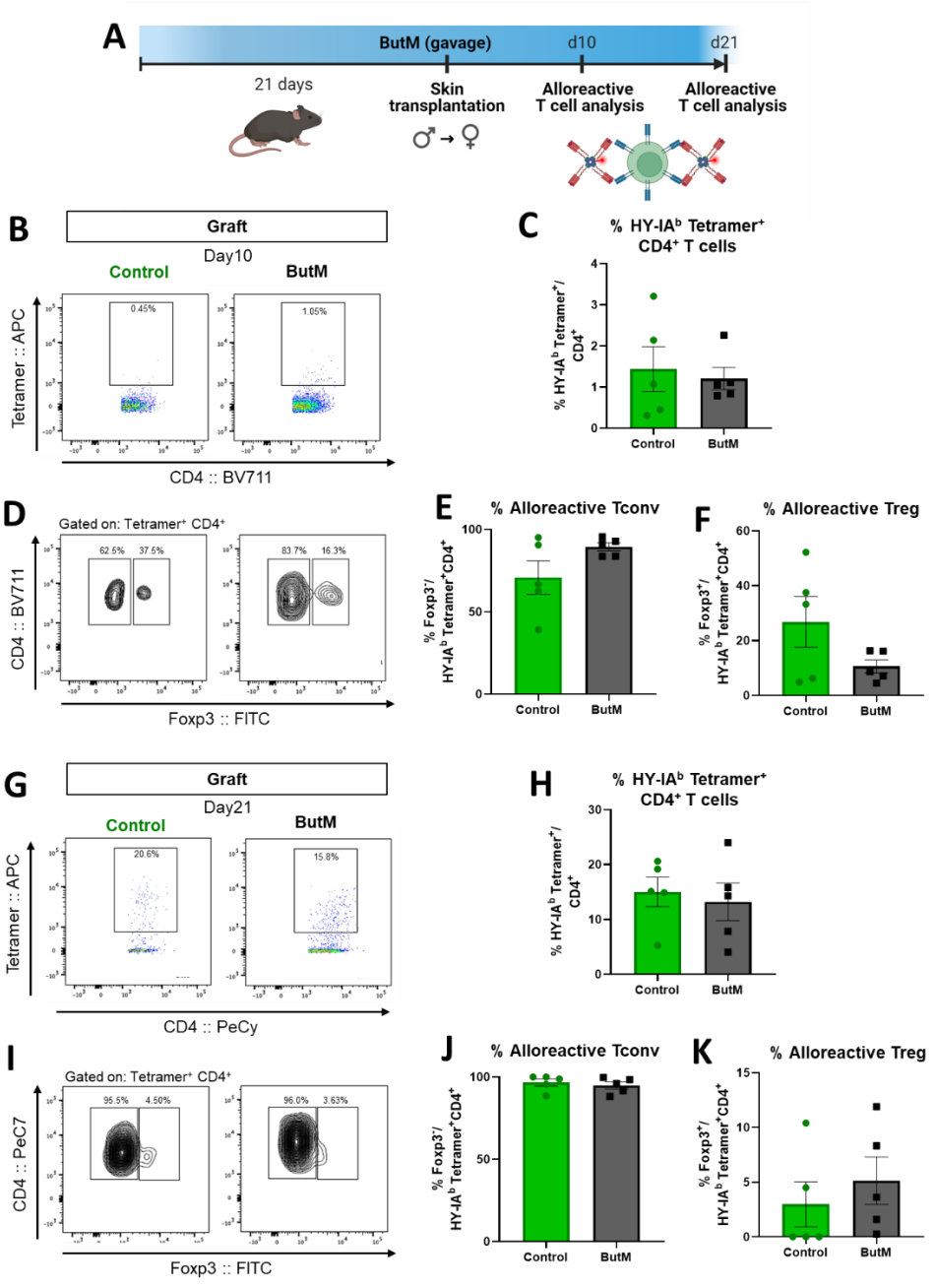

Figure 5.1. 6. Butyrate micelle treatment does not modify the migration and accumulation of endogenous alloreactive T cells into the graft.

(A) Mice were given butyrate micelles (ButM) starting 21 days before skin transplantation and treatment was continued until the day of analysis. C57Bl/6 (B6) male skin was transplanted onto female hosts on d0, and skin allografts were harvested on days 10 and 21 for endogenous alloreactive T cell assessment. (B-K) Representative flow cytometry plots and quantification of day 10 graft-infiltrating (B, C) HY-IA^{b} tetramer^{+} T cells, (D-F) alloreactive Tconv (HY-IA^{b} tetramer^{+} Foxp3^{-}) and a Treg (HY-IA^{b} tetramer^{+} Foxp3^{+}) cells, day 21 graft-infiltrating (G, H) HY-IA^{b} tetramer^{+} T cells, and (I-K) alloreactive Tconv (HY-IA^{b} tetramer^{+} Foxp3^{-}) and Treg (HY-IA^{b} tetramer^{+} Foxp3^{+}) cells. (n=5)

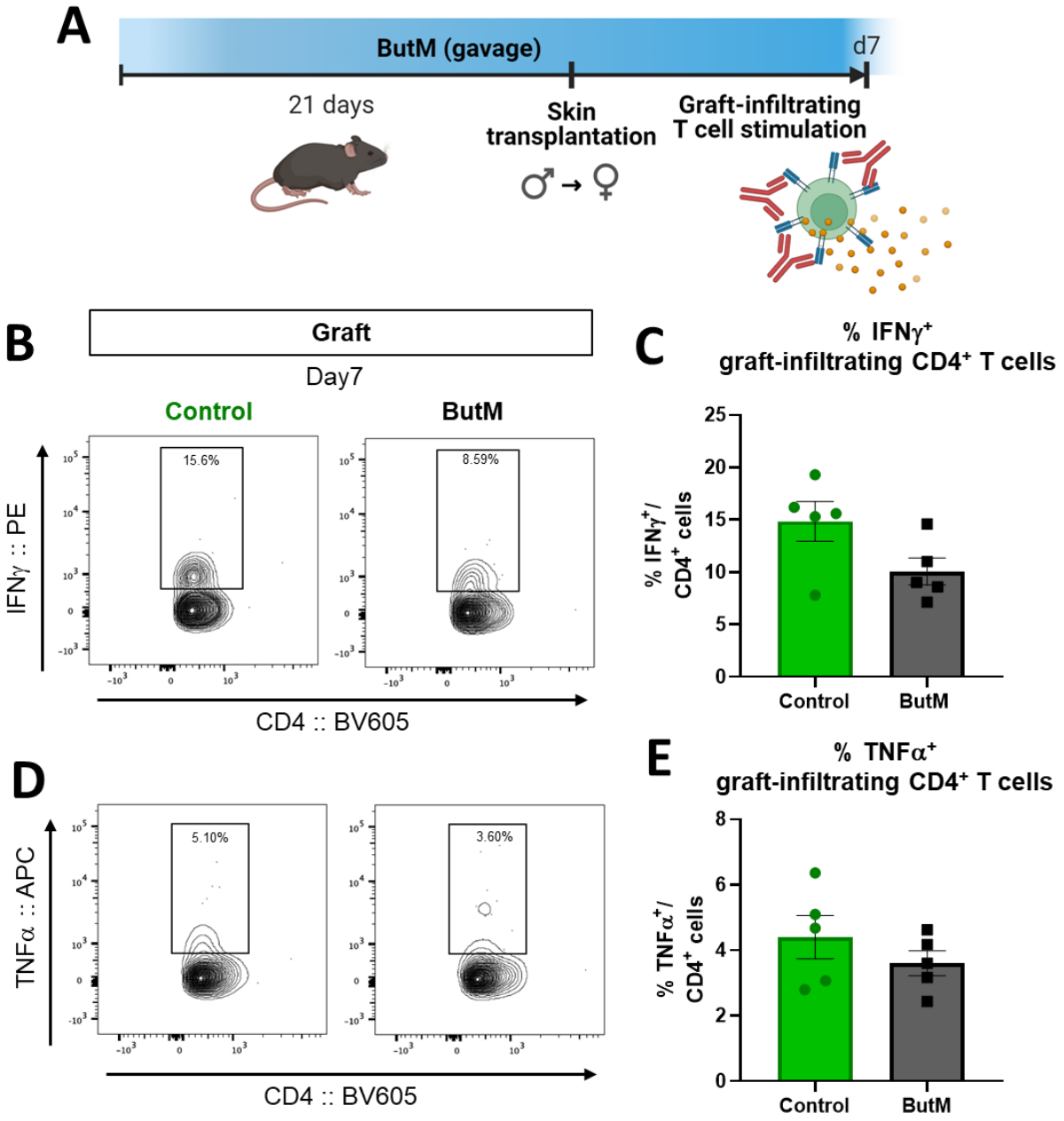

Figure 5.1. 7. Butyrate micelle treatment does not modify the capacity of graft-infiltrating T cells to produce Th1 pro-inflammatory.
(A) Mice were given butyrate micelles (ButM) starting 21 days before skin transplantation and treatment was continued until the day of analysis. C57Bl/6 (B6) male skin was transplanted onto female hosts on d0, and skin allografts were harvested on day 7 to assess pro-inflammatory cytokine production by graft-infiltrating $CD4^+$ T cells upon anti-CD3 restimulation. (B-E) Representative flow cytometry plots and quantification of graft-infiltrating $CD4^+$ T cells (B, C) IFNγ and (D, E) TNFα production. (n=5)

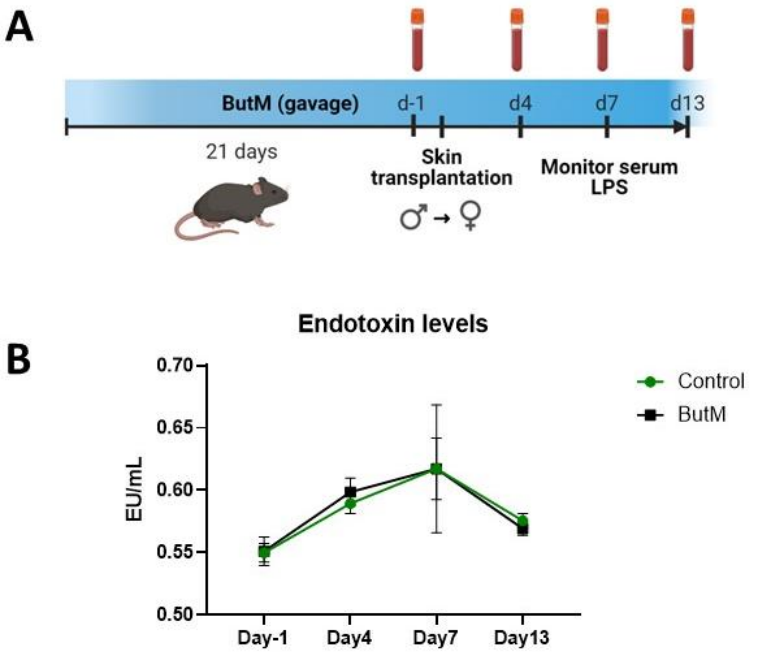

Figure 5.1. 8. ButM does not decrease the levels of serum LPS at steady state and after transplantation.
(A) Mice were given butyrate micelles (ButM) starting 21 days before skin transplantation and treatment was continued until 2 weeks after surgery. Mice were bled one day before (Day-1) and 4 (Day4), 7 (Day7), and 13 (Day13) days after transplantation for serum LPS analysis. (B) Kinetics of endotoxin units (EU)/mL levels before and after transplantation.

To parse out the mechanism by which ButM prolongs allograft survival, we focused on a potential impact of ButM on the myeloid cell compartment, as it has been previously described that butyrate can impact macrophage and dendritic cells[292,293]. At steady state, we found that BuM treatment resulted in a decreased frequency of blood Ly6C^{hi}CD11b^{+} monocytes (Figure 5.1. 9A-C). These monocytes, which serve as circulating precursors of various myeloid cells, play important roles during inflammation[299,300], including transplant rejection[78]. The effect of ButM on myeloid cells was confirmed in spleen and skin as ButM-treated mice displayed reduced numbers of splenic and skin Ly6C^{hi}CD11b^{+} monocytes (Figure 5.1. 9D, E). A time course experiment revealed that the frequency of circulating Ly6C^{hi}CD11b^{+} monocytes started to decrease after 2 weeks of ButM treatment (Figure 5.1. 10). These cells retained normal levels of

CCR2, a chemokine receptor important for monocyte migration out of the bone marrow and to sites of inflammation (Figure 5.1. 11A-C). Of note, ButM treatment did not decrease the percentage of bone marrow Ly6C^{hi}CD11b^{+} monocytes or their level of CCR2 expression (Figure 5.1. 11E, F), suggesting that ButM was not reducing the development of these cells or ability to exit the bone marrow.

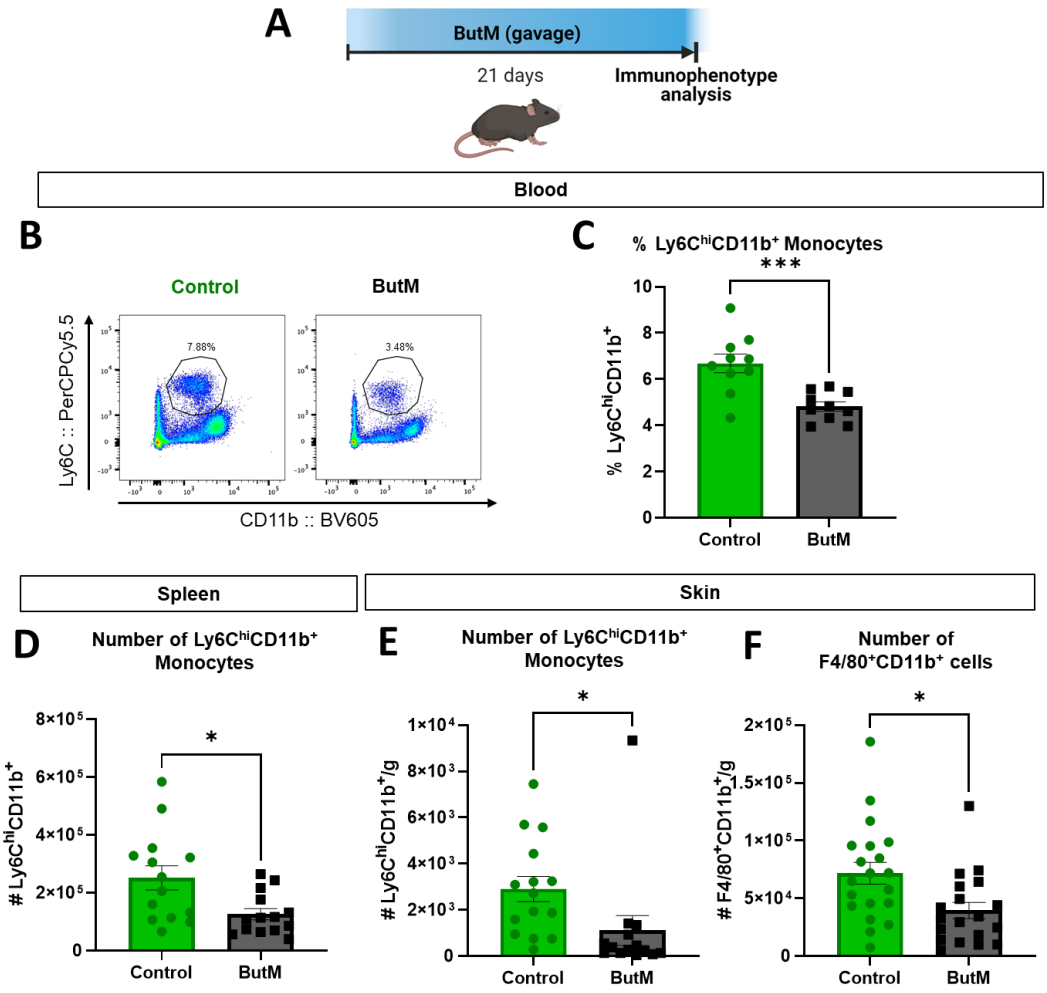

Figure 5.1. 9. Butyrate micelles decrease the myeloid cell compartment at steady-state. (A) Mice were given butyrate micelles (ButM) for 21 days and then blood, spleen, and skin were harvested to identify different myeloid cells. (B, C) Representative flow cytometry plots and quantification of circulating blood Ly6C^{hi}CD11b^{+} monocytes (n=10). (D, E) Number of splenic and skin Ly6C^{hi}CD11b^{+} monocytes. (F) Number of skin F4/80^{+}CD11b^{+} myeloid cells. (n=14-20).

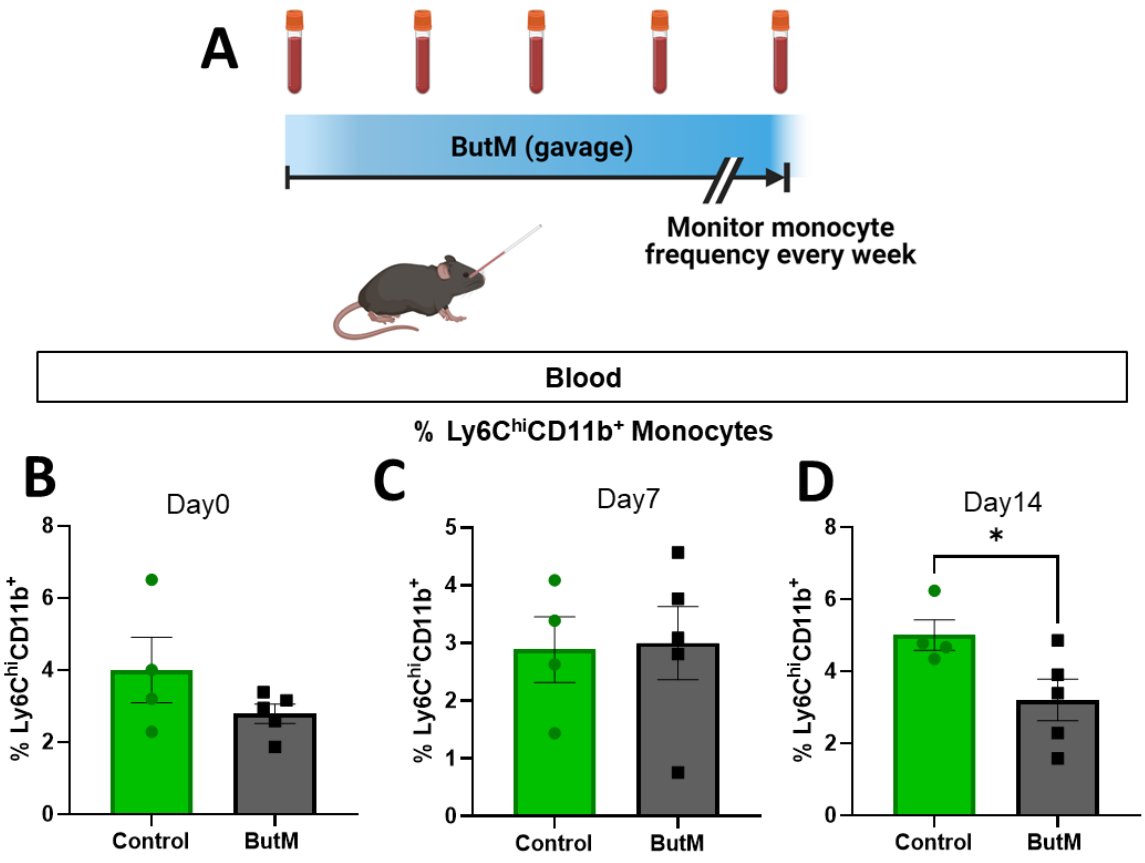

Figure 5.1. 10. Tracking of monocyte frequency during butyrate micelle treatment. (A) Mice were given butyrate micelles (ButM) and bled every other week to measure the frequency of circulating Ly6C^{hi}CD11b^{+} monocytes. (B-D) Percent of circulating Ly6C^{hi}CD11b^{+} monocytes at (B) steady state, (C) after 1 week, (D) and 2 weeks of ButM treatment. (n=4-5)

Additionally, ButM-treated mice exhibited a lower number of F4/80^{+}CD11b^{+} macrophages in the skin (Figure 5.1. 9F) at steady-state, without any alterations in CCR2 surface levels (Figure 5.1. 11D). Together, these data indicate that oral ButM triggers a systemic decrease in myeloid cell numbers.

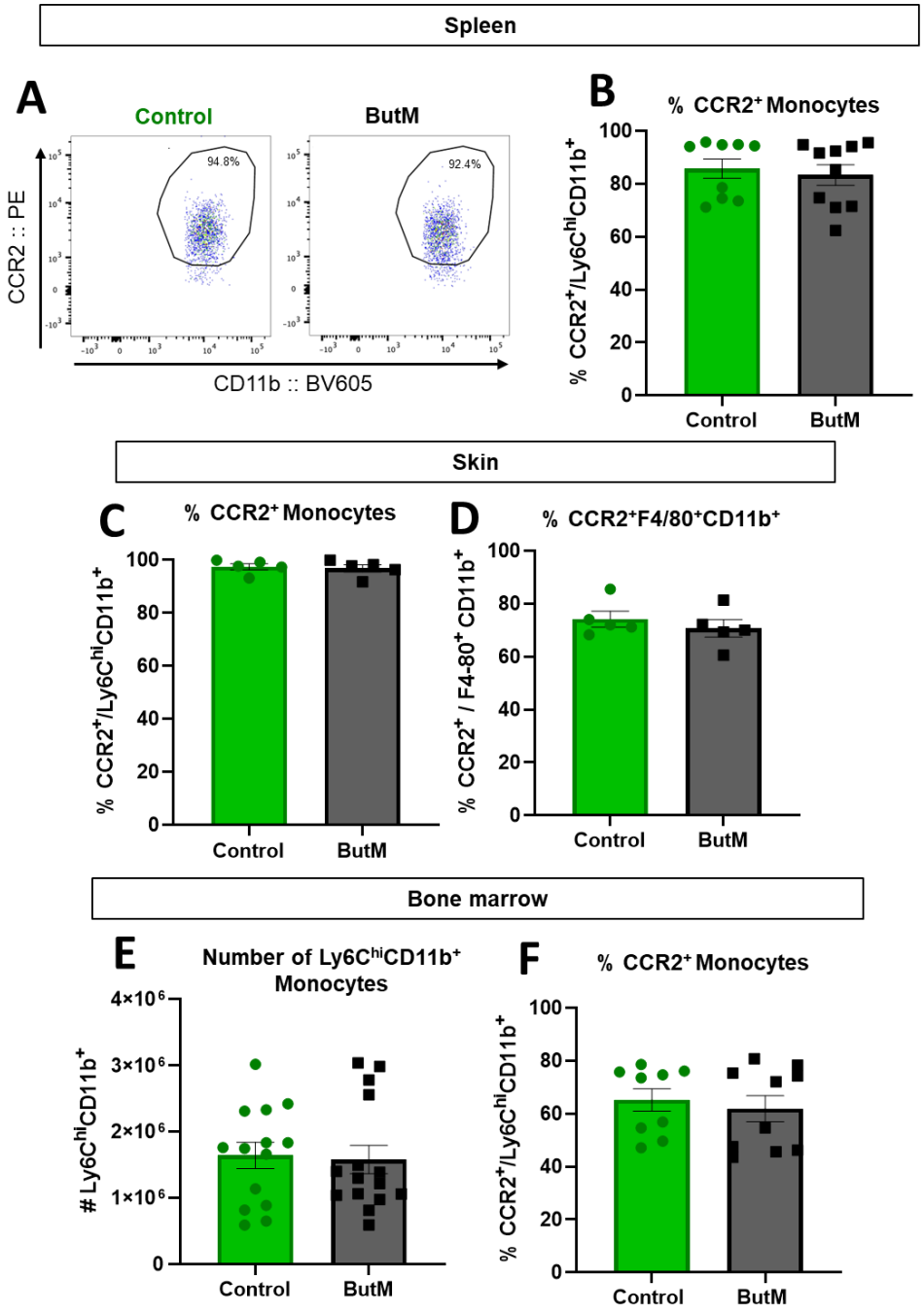

Figure 5.1. 11. Butyrate micelles treatment does not impact bone marrow monocytes and expression of CCR2.

Mice were given butyrate micelles (ButM) for 21 days and then spleen, skin, and bone marrow were harvested to measure $Ly6C^{hi}CD11b^{+}$ monocytes and the CCR2 expression. (A, B) Representative flow cytometry plots and quantification of spleen $CCR2^{+}Ly6C^{hi}CD11b^{+}$ monocytes (n=9-10). CCR2 expression on (C) skin $Ly6C^{hi}CD11b^{+}$ monocytes and (D) $F4/80^{+}CD11b^{+}$ myeloid cells (n=5). (E, F) Number of bone marrow (E) $Ly6C^{hi}CD11b^{+}$ and (F) percent $CCR2^{+}Ly6C^{hi}CD11b^{+}$ monocytes (n=9-15)

5.1.3.3 ButM treatment reduces graft-infiltrating myeloid cells

As monocytes are important mediators of graft damage, we next tested if the quantitative impact induced by ButM at steady-state was also apparent during the alloimmune response. To this end, we examined graft-infiltrating myeloid cells at day 13 post-transplantation of ButM-treated mice (Figure 5.1. 12A). Our analysis revealed a reduction in graft-infiltrating myeloid cells in ButM-treated mice, with significantly fewer $Ly6C^{hi}CD11b^{+}$ monocytes (Figure 5.1. 12B) and $F4/80^{+}CD11b^{+}$ macrophages (Figure 5.1. 12C). $Ly6C^{hi}CD11b^{+}$ monocytes were also decreased in numbers in the host skin of the ButM-treated transplanted mice, albeit numbers of myeloid cells in normal skin were 10-fold lower than in the skin graft (Figure 5.1. 12D). These data demonstrate that the quantitative impact induced by ButM extends to myeloid cells that are recruited to the graft during the alloimmune response and correlates the prolonged graft survival induced by ButM with reduced graft infiltration by myeloid cells.

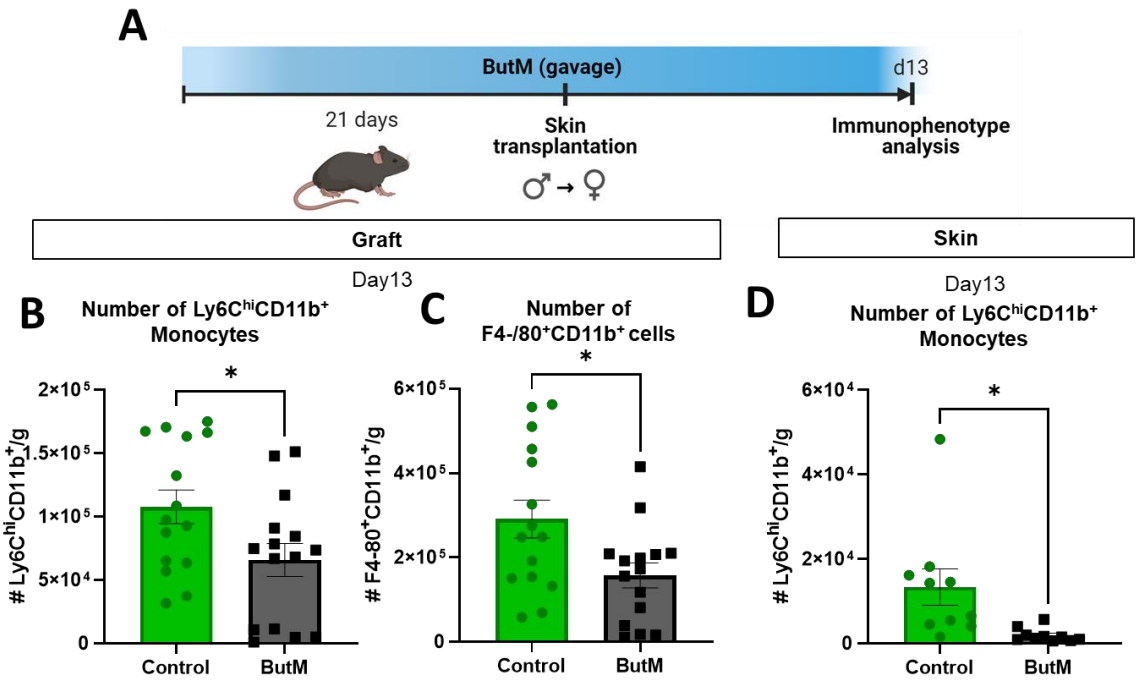

Figure 5.1. 12. Butyrate micelle treatment results in decreased graft-infiltrating myeloid cells.
(A) Mice were given butyrate micelles (ButM) starting 21 days before skin transplantation and treatment was continued the until day of analysis. C57Bl/6 (B6) male skin was transplanted onto female hosts on d0, and skin allografts were harvested on day 13 for graft- and naïve skin-infiltrating myeloid cell analysis. (B, C) Numbers of graft-infiltrating Ly6C^{hi}CD11b^{+} monocytes and F4/80^{+}CD11b^{+} myeloid cells. (D) Number of naïve skin-infiltrating Ly6C^{hi}CD11b^{+} monocytes. (n=10-15)

5.1.3.4 Butyrate treatments results in a qualitative impact of the myeloid cell compartment at steady-state

In view of myeloid cells being important mediators of graft damage via the production of pro-inflammatory cytokines and reactive oxygen species (ROS)[299,300], we reasoned that the graft-prolonging capacity of ButM treatment might also entail qualitative alterations in these cells. For an unbiased analysis, we isolated control and ButM-treated splenic Ly6C^{hi}CD11b^{+} monocytes and conducted bulk RNA sequencing to probe changes at the transcriptional level (Figure 5.1. 13A). Principal component analysis (PCA) revealed a large variance in transcriptional profiles of

Ly6C^{hi}CD11b^{+} monocytes from different control mice, whereas monocytes from ButM-treated mice were more tightly clustered with reduced sample-to-sample distances (Figure 5.1. 13B and Figure 5.1. 14A, B). The second axis of the PCA plot effectively distinguished Ly6C^{hi}CD11b^{+} monocytes clusters from control and ButM-treated mice, underscoring the difference in RNA expression levels between them (Figure 5.1. 13B).

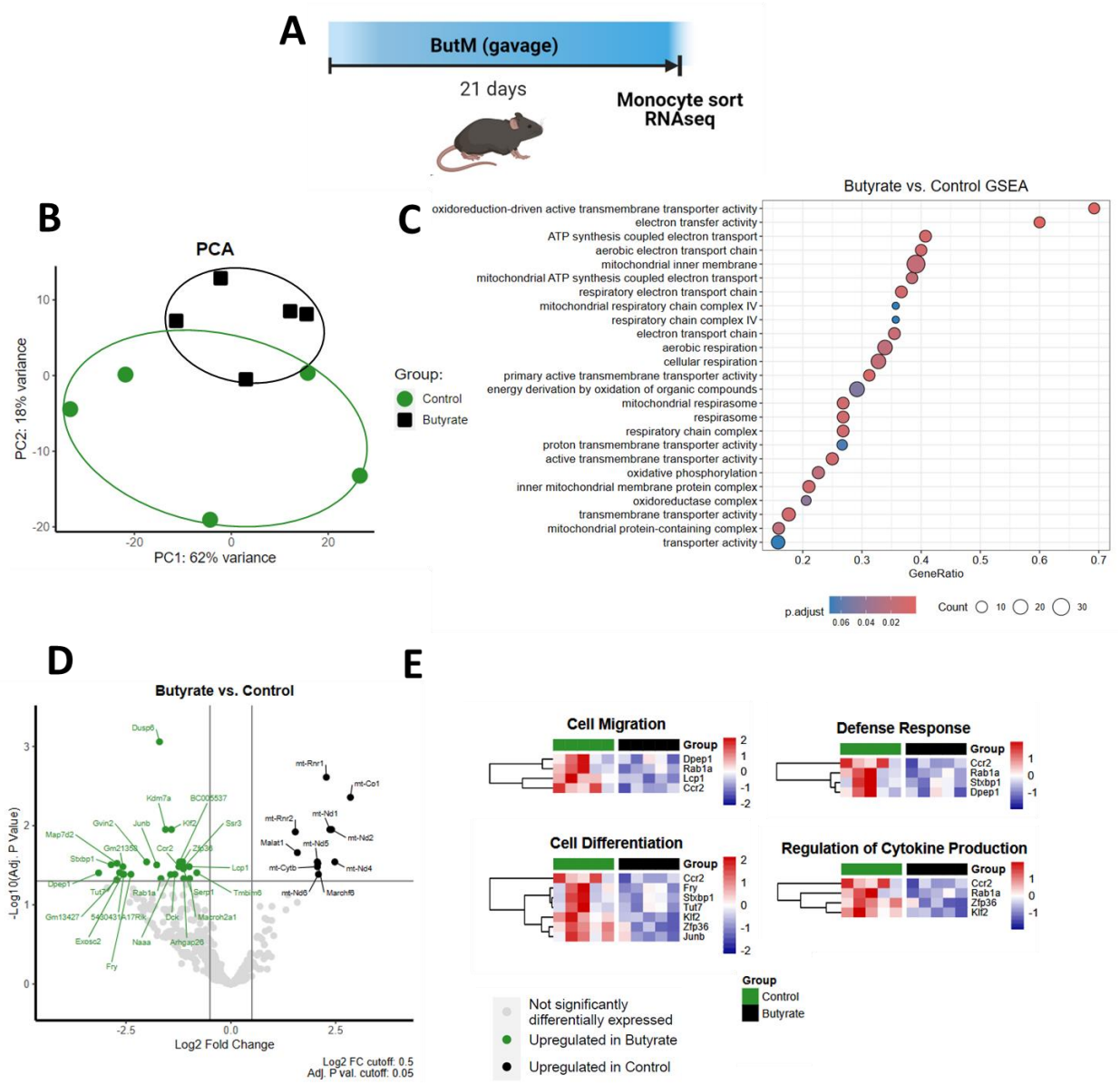

Figure 5.1. 13. Butyrate micelle treatment enhances monocyte mitochondrial metabolism at the transcriptional level.
(A) Mice were given butyrate micelles (ButM) for 21 days and then spleen Ly6C^{hi}CD11b^{+} monocytes were sorted and used for RNA sequencing. (B) Principal component analysis (PCA), (C) Gene-set enrichment analysis (GSEA), (D) Volcano plot, and (E) heatmap of deferentially expressed genes in control and ButM-treated mice.

To elucidate the alterations in Ly6C^{hi}CD11b^{+} monocyte transcriptional profile induced by ButM, we conducted Gene Set Enrichment Analysis (GSEA) with the differentially expressed genes (DEGs) (Figure 5.1. 13C). Notably, genes associated with electron transport chain,

mitochondrial respiration, and oxidative phosphorylation (OXPHOS) were upregulated in Ly6C^{hi}CD11b^{+} monocytes from ButM-treated mice (Figure 5.1. 13C), indicating that ButM-treatment enhances the steady-state mitochondrial metabolism potential of these cells. Furthermore, the volcano plot of Figure 5.1. 13D illustrates that most of the overexpressed genes in the ButM group are mitochondrial genes, except for *Malat1* and *Marchf6*. Conversely, genes downregulated by ButM treatment include *Dusp6*, *Kdm7a*, and *Dpep1*. To analyze the genes that were reduced by ButM treatment, we identified Gene Ontology (GO) modules related to them (Figure 5.1. 13E). The lists of genes reduced after ButM treatment are associated with key inflammatory pathways, including cell migration, defense response, cell differentiation and regulation of cytokine production (Figure 5.1. 13E). These findings suggest that ButM induces profound transcriptional changes in Ly6C^{hi}CD11b^{+} monocytes, potentially decreasing their ability to mount an inflammatory response.

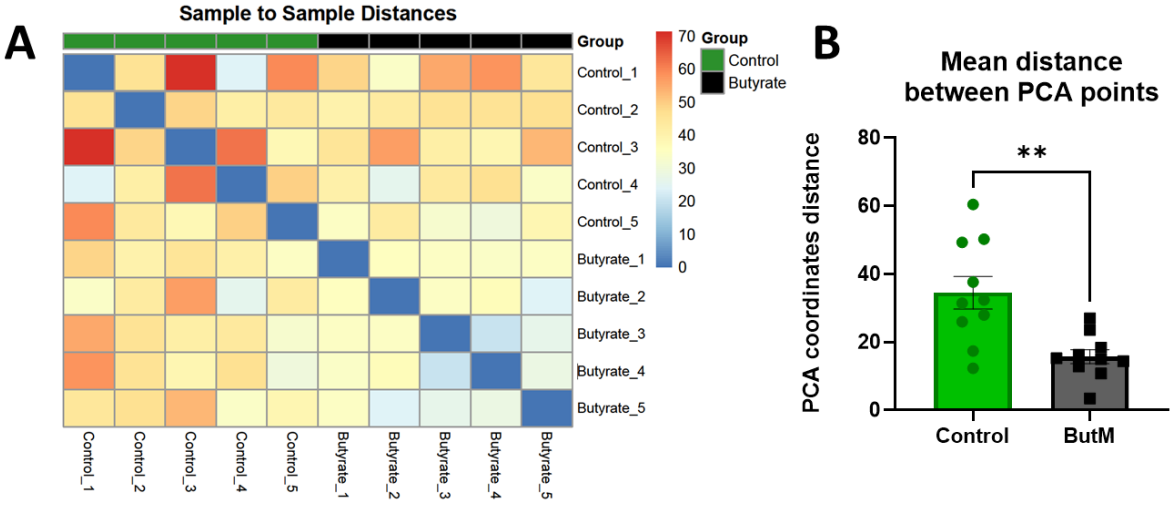

Figure 5.1. 14. Butyrate micelle treatment homogenizes monocyte transcriptional profile and upregulates genes related to aerobic cellular respiration.
Butyrate treated splenic Ly6C^{hi}CD11b^{+} monocytes were sorted and their RNA was sequenced. (A) Sample distance. (B) Distance between PCA coordinates (sqrt((x2-x1)2+(y2-y1)2))

Because the Ly6C^{hi}CD11b^{+} monocytes from ButM-treated mice exhibited a downregulation of genes related to defense response and regulation of cytokine production (Figure 5.1. 13E), we hypothesized that these myeloid cells would exhibit impaired pro-inflammatory effector functions. Indeed, stimulation with LPS (Figure 5.1. 15A) confirmed that splenic F4/80^{+}CD11b^{+} (Figure 5.1. 15B, C) and F4/80^{+}CD64^{+} (Figure 5.1. 15D, E) myeloid cells from ButM-treated mice produced less TNFα compared to those from control mice. Collectively, these data support a model where oral ButM reduces not only the numbers of myeloid cells systemically, but also their effector function, rendering them less responsive to inflammatory stimuli.

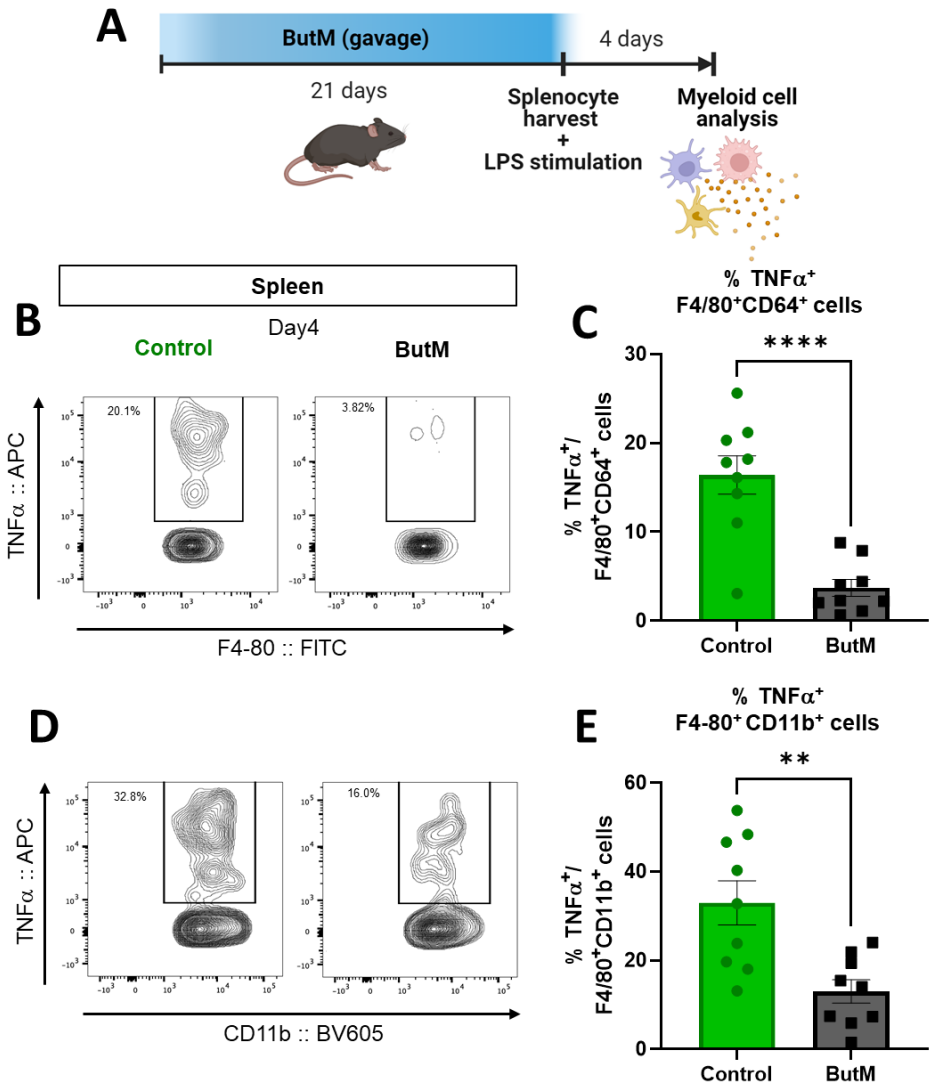

Figure 5.1. 15. Butyrate micelle treatment impairs myeloid cell function.
(A) Mice were given butyrate micelles (ButM) for 21 days and then splenic myeloid cells were stimulated with LPS overnight. (B-E) Representative flow cytometry plots and quantification of (B, C) TNFα$^+$ F4/80$^+$CD64$^+$ and (D, E) TNFα$^+$ F4/80$^+$CD11b$^+$ myeloid cells. (n=9)

5.1.3.5 CCR2 depletion protects allograft survival similar to ButM treatment

Finally, to ascertain whether the reduction in myeloid cells induced by ButM treatment causally influences its graft-prolonging capacity, we sought to deplete circulating monocytes and evaluate the impact of an impaired myeloid cell compartment on allograft outcomes, both independently and in combination with ButM (Figure 5.1. 16A).

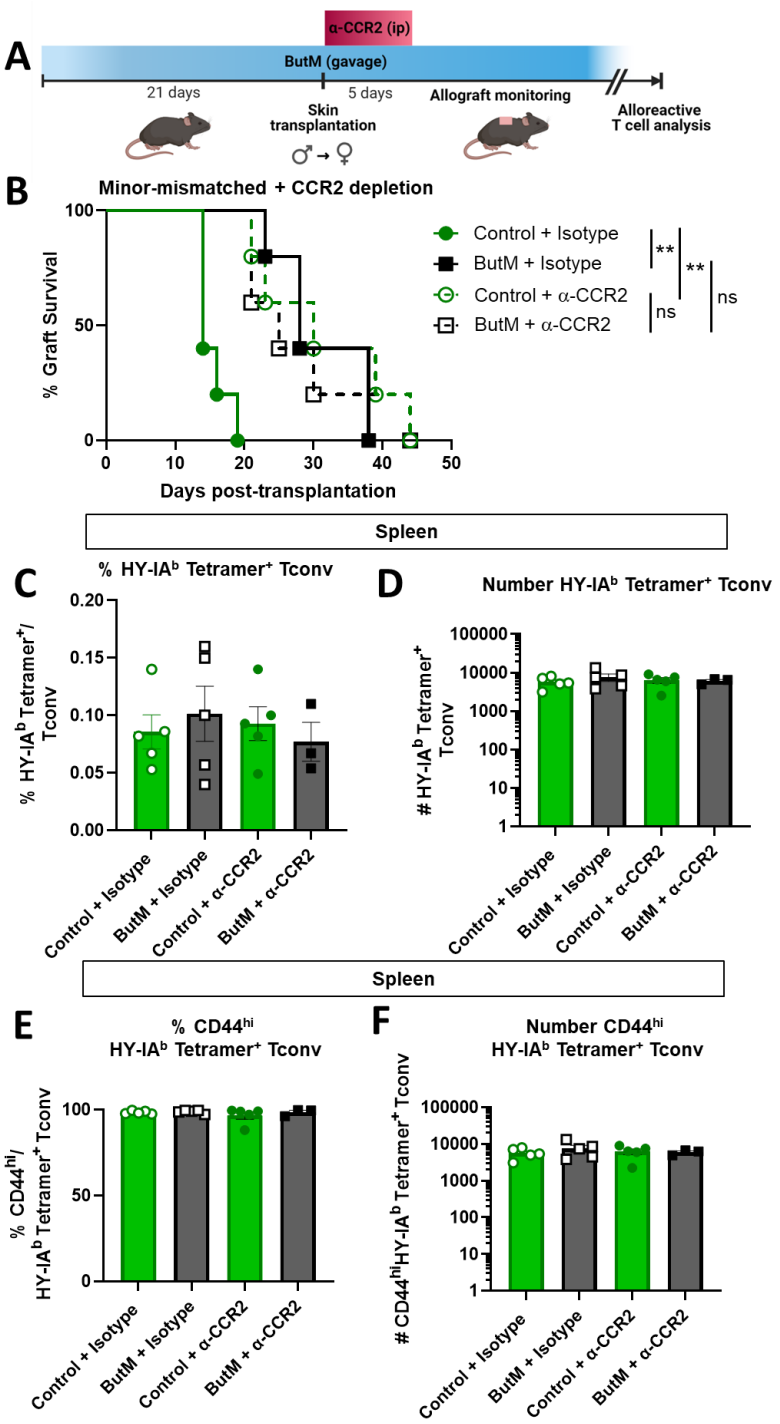

Figure 5.1. 16. CCR2 depletion prolongs allograft survival similar to butyrate micelle treatment.

(A) Mice were given butyrate micelles (ButM) starting 21 days before skin transplantation and treatment was continued until allograft rejection. C57Bl/6 (B6) male (minor-antigen mismatched) skin was transplanted onto female hosts on d0. aCCR2 depleting antibodies were injected intraperitoneally (ip) every day for 5 days starting on the day of skin transplantation.

Figure 5.1. 16. cont. Post-rejection splenic endogenous alloreactive T cells were analyzed. (B) Minor-antigen mismatched skin allograft survival curves of ButM- and aCCR2-treated mice (n=5). Quantification of (C, D) HY-IA^{b} tetramer^{+} Tconv and (E, F) CD44^{hi} HY-IA^{b} tetramer^{+} Tconv cells. (n=3-5)

We depleted monocytes systemically using the αCCR2 antibody MC-21[301], which transiently eliminated Ly6C^{hi}CD11b^{+} monocytes (Figure 5.1. 17A, B) while leaving circulating CD4^{+} (Figure 5.1. 17C, D) and CD8^{+} (Figure 5.1. 17C, E) T cells unaffected. To assess the impact of Ly6C^{hi}CD11b^{+} monocyte depletion on allograft survival, mice received either isotype control or αCCR2 depleting antibodies starting from the day of surgery for a total of 5 days (Figure 5.1. 16A, B). αCCR2 prolonged graft survival similarly to ButM treatment, confirming that a reduction in Ly6C^{hi}CD11b^{+} monocytes improves graft survival (Figure 5.1. 16B). Similar results were found using CCR2-DTR mice and diphtheria toxin (DT) treatment (Figure 5.1. 18A). Most importantly, co-administration of ButM and αCCR2 did not prolong allograft survival beyond that observed in ButM alone-treated mice (Figure 5.1. 16B), suggesting that ButM's ability to prolong graft survival is via its ability to reduce myeloid cell number and function. Additionally, αCCR2 or combination treatments did not prevent the expansion of graft-reactive Tconv cells as determined by pMHC tetramer analysis (Figure 5.1. 16C-F), consistent with our previous observations that ButM did not reduce alloreactive T cell priming, expansion or differentiation (Figure 5.1. 6). These findings support the conclusion that ButM improves allograft survival by reducing myeloid cell function and number rather than by affecting alloreactive T cell function.

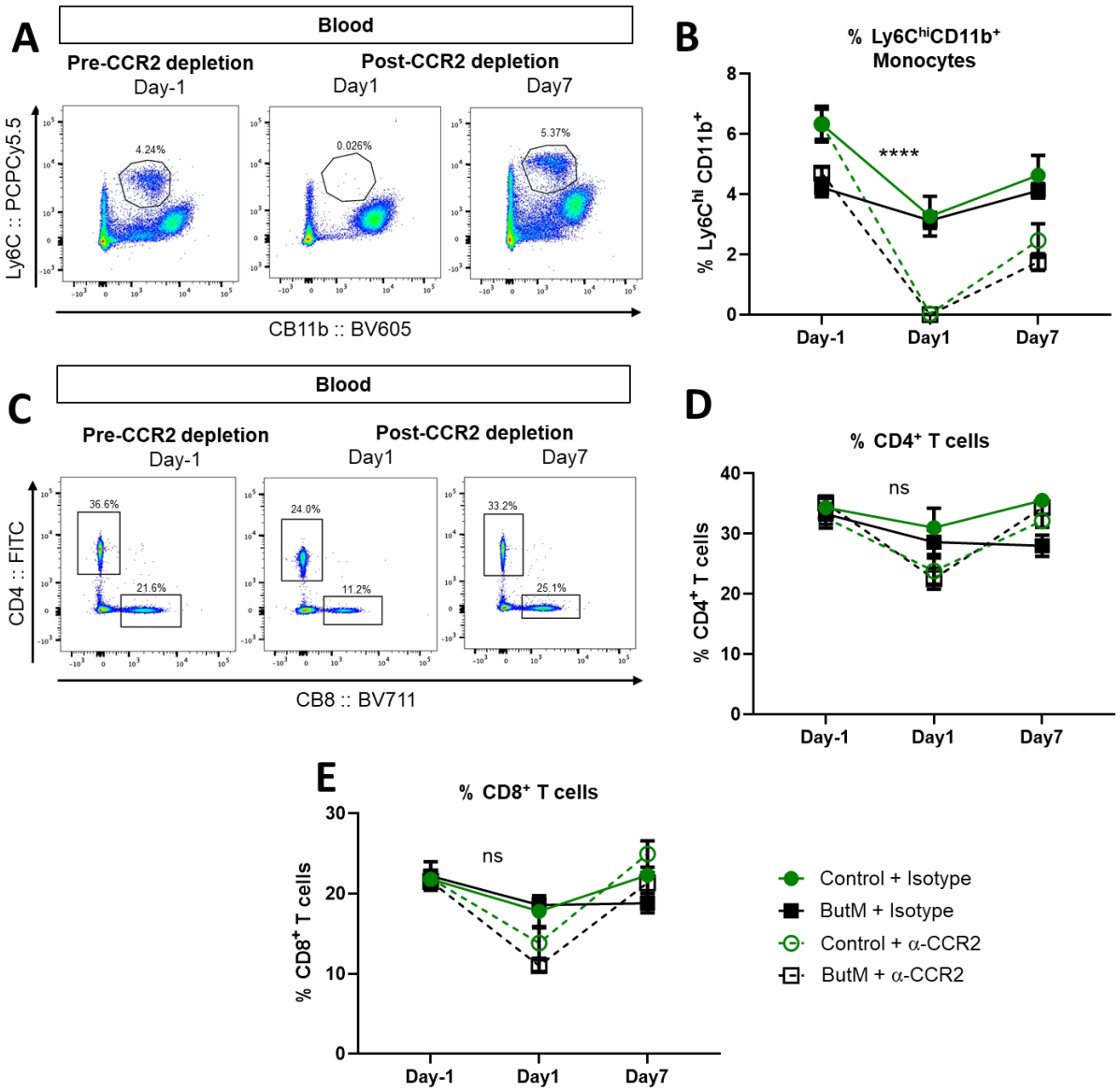

Figure 5.1. 17. CCR2 depletion impact on monocytes and T cells.
Mice were given butyrate micelles (ButM) starting 21 days before skin transplantation. C57Bl/6 (B6) male skin was transplanted onto female hosts on d0. αCCR2 depleting antibodies were injected intraperitoneally (ip) every day for 5 days starting on the day of skin transplantation. To track $CCR2^+$ cells, mice were bled on days -1, 1 and 7. (A-E) Representative flow cytometry plots and quantification of circulating (A, B) $Ly6C^{hi}CD11b^+$ monocytes and (C, D) $CD4^+$ and (C, E) $CD8^+$ T cells. (n=5, Statistic analysis between Control/ButM + aCCR2 day -1 and day 1)

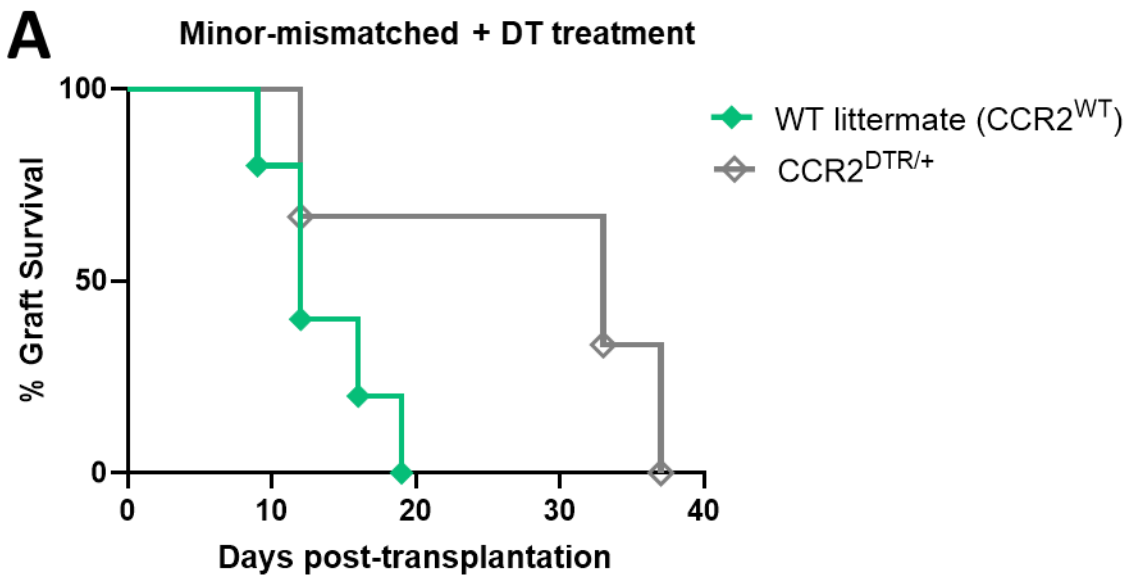

Figure 5.1. 18. DT treatment in CCR2-DTR mice prolongs graft survival.
Female WT littermate controls and CCR2$^{DTR/+}$ mice were injected with 5ng/ml of Diphtheria toxin (DT) on the day of transplantation and 1 and 3 days after. Donor skin used for transplantation was from male WT littermate controls.

5.1.4 Discussion

Identifying environmental factors capable of calibrating the strength of the alloimmune response and amenable to therapeutic targeting represents a promising strategy to complement current immunosuppressive regimens. One of these factors is the family of metabolites called SCFA, which are derived from commensal-dependent fermentation of dietary fibers and play pivotal roles in maintaining gut and immune homeostasis[302]. In this study, we investigated the effect of the SCFA butyrate on organ transplant outcomes and alloimmunity. Employing a rationally designed delivery micelle-based platform (ButM) to safeguard the butyrate payload, we achieved accurate targeting of butyrate to the lower GI tract, where its biological properties are more pronounced.

Our investigations revealed that oral delivery of ButM was sufficient to significantly prolong the survival of both minor- and major-mismatched skin allografts, without the use of

immunosuppression. Moreover, using NaBut[140,141] failed to delay skin rejection kinetics, confirming that the micelle-based delivery of butyrate was superior in our model. The augmented concentration of butyrate in the lower GI tract could explain why ButM, but not NaBut, could prolong allograft survival, owing to the increased biological impact of butyrate on gut colonocytes and/or immune cells[140,141,290–293].

Our group and others have outlined the causative roles of the microbiota in modulating distal allograft rejection and alloimmunity[97,100,117,121,127,174,180,181,200,201]. Upon administration of ButM, mice exhibited a bloom several ASVs of the *Clostridium* cluster XIVa. We hypothesize that the proliferation of butyrate-producing commensals upon ButM treatment forms a feedforward loop, where ButM promotes an anaerobic niche in the gut lumen that fosters the expansion of anaerobic *Clostridia* species[303]. Because of the immunomodulatory capacities of these expanded commensals, they may contribute directly or indirectly to the prolongation of allograft survival induced by ButM treatment.

ButM treatment did not alter the Treg profile locally or systemically, consistent with the findings reported by Wang et al. 2023[197]. Employing graft-reactive TCR-Tg T cells and analyzing endogenous alloreactive T cells during the various phases of the alloimmune response in ButM-treated mice failed to detect changes in the priming, migration, or adaptive immune cell-mediated effector phases. This suggests that the ButM-mediated modulation of other cell types is likely a direct effect of butyrate rather than indirect from modified T cells affecting other immune cell types.

We observed that at homeostasis, ButM significantly decreased $Ly6C^{hi}CD11b^{+}$ monocyte percentage and numbers systemically. This quantitative impact extended to skin $F4/80^{+}CD11b^{+}$ macrophages, suggesting a broad systemic impact of ButM on the myeloid compartment.

However, Ly6C^{hi}CD11b^{+} monocytes remained unaltered in the bone marrow, indicating that the systemic decrease of myeloid cells is not due to impaired hematopoiesis. Continued administration of ButM before and after skin transplantation was associated with lower numbers of graft-infiltrating myeloid cells. This suggests a model where ButM systemically and quantitatively impacts the myeloid cell compartment at steady-state and the impact is maintained upon alloimmune responses.

RNA sequencing analysis of these cells revealed that ButM treatment upregulated genes associated with mitochondrial aerobic metabolism, OXPHOS, and respiration. Similarly, butyrate has been shown to drive mitochondrial respiration and fatty-acid oxidation in intestinal epithelial cells[290], confirming its capacity to drive metabolic changes in other cell types. Conversely, inflammatory macrophages primarily rely on glycolysis for their inflammatory phenotypes[76,304]. Hence, the observed alterations in steady-state Ly6C^{hi}CD11b^{+} monocyte metabolic potential induced by ButM treatment may render them less capable of mounting robust pro-inflammatory responses.

Various myeloid cell populations produced lower levels of TNFα, upon LPS stimulation, confirming a qualitative impact of ButM treatment. Butyrate has been reported to reduce pro-inflammatory activities in colonic mononuclear phagocytes in a GPR109a-dependent manner[292], in bone marrow-derived macrophages (BMDM) in an HDAC inhibition-dependent manner[293], and facilitate M2-like polarization of BMDMs[305]. Altogether, these data suggest that ButM is not only impacting the number of myeloid cells but also their quality, i.e, their capacity to generate inflammatory cytokines once recruited into the allograft.

Lastly, we established that the reduction in myeloid cells induced by ButM treatment played a causal role in promoting slower allograft rejection kinetics as depleting Ly6C^{hi}CD11b^{+}

monocytes using the αCCR2 antibody was sufficient to prolong graft survival. To determine if ButM prolonged allograft survival via its ability to decrease myeloid cell numbers and function, we co-treated mice with ButM and CCR2-depleting antibodies. No additive effects resulted from this co-administration, suggesting that the mechanism by which ButM slows allograft rejection kinetics is by its quantitative impact on $CCR2^{+}$ myeloid cells.

In summary, our use of a delivery system that effectively increases cecal butyrate levels enabled significant prolongation of minor- and major-mismatched skin allograft survival. At steady-state, ButM treatment mediated a decrease in circulating $Ly6C^{hi}CD11b^{+}$ monocytes and other myeloid cells, changed the mitochondrial metabolism and key inflammatory processes. Furthermore, ButM's prolongation of allograft survival was dependent on the presence of $CCR2^{+}$ cells. These findings suggest that ButM enhances distal allograft outcomes by quantitatively and qualitatively modulating myeloid cells, thereby inhibiting the innate immune cell-mediated effector phase of the alloimmune response.

Chapter 6: Discussion & Future Directions

6.1 Influence of the commensal microbiota on solid organ transplant outcome

In this study, our objective was to pinpoint microbial strains and their respective metabolic pathways that could either enhance or hinder graft outcomes. Leveraging our prior discovery that administering broad-spectrum Abx to mice resulted in delayed graft rejection[97], we employed rationally designed Abx combinations to specifically target key bacterial groups.

Our investigations revealed that all major bacterial groups, Gram-negative, Gram-positive, anaerobic/Gram-positive, individually targeted using GKC, V, and VM, respectively, significantly delayed allograft rejection, accompanied by a reduction in the priming and differentiation of alloreactive T cells. Furthermore, simultaneous targeting of all these bacterial taxa using VMGKC yielded the most pronounced extension of graft survival and dampening of alloimmunity. These observations suggest an additive model in which the intensity of an immune response is finely tuned by the collective influence of the microbiota (Figure 6. 1). A diverse microbiome generates a multitude of signals that are recognized by various pattern-recognition receptors (PRR) and integrated by APCs[228,229]. This integration culminates in a poised state in which APCs are calibrated for robust T cell priming and differentiation[115]. Conversely, when Abx treatments reduce microbial diversity, the variety of microbial-derived molecules diminishes, resulting in a reduced level of tonic signaling to PRRs and metabolite receptors. This subsequently leads to APCs that are less effective at initiating immune responses, including alloimmunity[96,115,205].

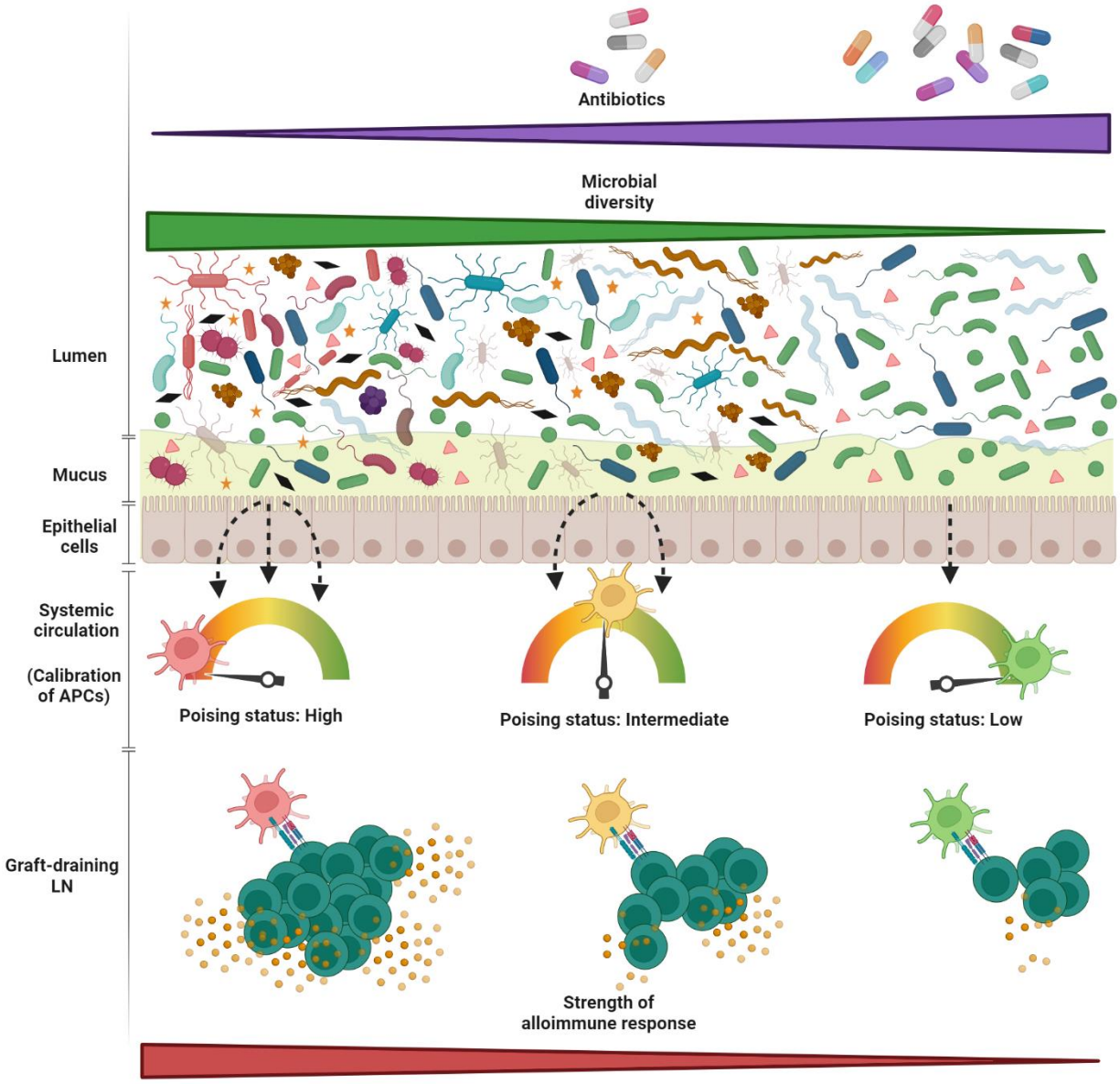

Figure 6. 1. Working model on how the microbiota diversity calibrates alloimmune responses.
In an unperturbed state with maximal microbiota diversity, multiple microbial-produced signals are sensed by systemic APCs and tonic signaling results in strong poising status. These APCs can mount robust alloimmune responses by priming alloreactive T cells and promoting their differentiation, which contributes to fast graft rejection. With the addition of Abx that target specific bacterial groups, specific microbial-derived signals are depleted, resulting in decreased poising status, and intermediate potential to trigger alloimmune responses. Finally, targeting all bacterial groups results in lower diversity, APC poising status, and the weakest alloimmune response, correlating with long allograft survival.

Depending on the specific bacterial group targeted, certain MAMPs and metabolites are depleted, consequently extinguishing their respective PRR and metabolite receptor signaling pathways within APCs[230,231]. This results in differential states of APC poising and variable capacities to elicit immune responses. For example, targeting bacterial taxa reduces ligands for TLR5, TLR1/2, TLR2/6, TLR9, and TLR4[228,229]. Consequently, targeting different bacterial subgroups can distinctly impact NFκB and IRF3/7 activation, fine-tuning the activation potential of APCs[232,233]. These findings underscore how the greatest positive revving of APCs is observed when the microbiota exhibits maximal diversity. Redundant and overlapping PRR/metabolite receptor signaling helps calibrate APCs for context appropriate immune response initiation. Moreover, survival of a minor-mismatched skin graft was significantly prolonged when both donor and recipient were MyD88-deficient, suggesting a role of TLR signaling in transplant rejection[306]. However, MyD88 is an adaptor not only for microbial sensing but also for damage-associated molecular pattern sensing, such that it is not clear if prolonged graft survival in the absence of MyD88 is due to reduced microbial sensing or more limited IRI. The greater prolongation of graft survival induced by VMGKC, when compared to the individual effects of VM or GKC, suggests that each combination extends graft survival through distinct mechanisms, potentially by depleting different microbial-derived signals. Only when these combinations are used together does the collective removal of stimuli maximally reduces the APC poising state. RNAseq of APCs from the different Abx combinations may help understand whether different bacterial groups drive qualitatively distinct poising status.

Our group and others have delineated the causative roles of the microbiota in orchestrating graft rejection and alloimmunity[97,100,117,121,127,174,180,200,201], and these effects can be strain-specific[180]. To correlate microbiome composition with graft outcome, we employed

metagenomic technology, allowing us to achieve bacterial strain resolution and infer functional metabolic pathways. As previously documented[97], at Abx doses used, VMGKC did not reduce fecal bacterial burden in adult mice, nor did the other different Abx combinations used. This is in contrast to the reduced bacterial load that VMGKC maintains when initiated in neonate mice, which leads to heightened susceptibility to food allergen sensitization[283].

These data support a qualitatively rather than quantitative influence of microbial diversity on graft outcome. Both GKC and V intermediately reduced alloimmunity, possibly due to the redundancy in PRR signaling in response to MAMPs[228,229]. Moreover, VM frequently mirrored the effects of VMGKC, indicating a predominant impact exerted by the strains targeted by these taxa. In fact, intestinal bacterial load and oxygen levels are inversely correlated, reaching the highest burden and anaerobic environment in the distal large intestine[307]. Under anaerobic conditions, M is metabolically reduced, generating toxic intermediates that inhibit nucleic acid synthesis[214], potentially impacting a broad-spectrum of anaerobic Gram-positive and Gram-negative commensals. To understand how the different signals cooperate in systemic APC poising, using combination of gnotobiotic mice and colonization with specific bacteria, future studies should investigate gene expression differences performing RNAseq on APCs of mono-associated or poly-associated ex-GF mice. This will shed light onto what pathways are upregulated upon colonization, if there is overlap when mice are mono-colonized with different commensals, and, when poly-associated with more species, how the different signals added are sensed by APCs.

Given the consistent observation of reduced IFNγ production in graft-reactive T cells and the prolonged graft survival across all Abx regimens, we postulated that bacterial strains flourishing after such treatments may potentially denote transplant-protective strains.

Commensals that bloomed under both VM and VMGKC treatments were of interest, as they seem protective in various mouse models. For example, *E. coli* can be pathogenic[308], but the probiotic strain Nissle 1917 enhanced host immune responses to pathogens[309] and strengthened the intestinal barrier[310]. *Parasutterela* spp are core members of the human microbiota[311], can deconjugate primary bile acids[311], and their abundance in mice negatively correlated with high-fat diet-associated metabolic disease[312]. *A. muciniphila* ameliorated multiple metabolic and autoimmune disorders in mice[313] by increasing gut barrier integrity[314,315] and decreasing inflammation[316,317]. Similarly, *L. murinus* exerted antibacterial activity against pathogens[318] and lowered blood pressure and intestinal permeability in rat models[319]. Lastly, *P. distasonis* is also considered a member of the healthy microbiome[222], has been reported to modulate metabolic disfunction[224], fibrosis[226,227] and autoimmunity[223]. The various features exhibited by these commensals may contribute directly or indirectly to reducing alloimmunity.

Conversely, the bacterial strains that were consistently eradicated by all Abx regimens have the potential to be taxa associated with pro-rejection tendencies. VM and VMGKC treatments reduced strains that were of interest, as members of their species have been associated with pro-inflammatory immune responses. For instance, the presence of *Duncaniella murocolitica* (strain DSM 112986) was correlated with disease heterogeneity in mouse models of dextran sulfate sodium (DSS) colitis[320]. A cardiolipin produced by *Muribaculum intestinale* (strain S24-7) stimulated the production of the pro-inflammatory cytokines TNFα, interleukin (IL)-6 and IL-23 by bone marrow-derived DCs (BMDCs) via TLR1/2[321]. Furthermore, *Bifidobacterium globosum*, also known as *Bifidobacterium pseudolongum* subsp. *globosum*[322], could potentiate immune-checkpoint blockade (ICB) therapy by producing the metabolite inosine, which signals via the adenosine A2A receptor in T cells[138]. Similarly, *Bifidobacterium*

spp. (strains ATCC 15700 and ATCC BAA-999) improved ICB therapy by augmenting DC function leading to enhanced antigen-specific $CD8^+$ T cell responses in the tumor[185]. It is important to consider the specific strain utilized, as administration of *B. pseudolongum* (strain ATCC 25526) was shown to reduce inflammation and the fibrosis of cardiac allografts[121]. Additional research, particularly using bacteriophage therapy[323] to target the specific strains, may help understand if they have direct or indirect roles in promoting graft rejection.

Alternatively, proliferation of commensals post-Abx treatments may be facilitated by antibiotic resistance mechanisms. Indeed, our MAG data uncovered the presence of multidrug efflux transporters, biofilm/acid-resistance regulators, virulence factors (VF), and antimicrobial resistance genes (AMR) in many surviving commensals, supporting a basis for their resilience. Of note, the gut microbiome of transplant recipients is enriched with AMR genes and VF[217], and Abx treatments can lead to opportunistic infections in these recipients[324], emphasizing the limitations of widespread antibiotic use. Additionally, manipulating the microbiome could be a safe strategy to overcome these risks. For instance, a 4-commensal strain consortium reversed vancomycin-resistant enterococcal (VRE) infections in GF mice conventionalized with feces from VRE-infected patients[325]. Moreover, fecal-microbiome transfer (FMT) in human kidney transplant recipients reduced antimicrobial resistance by strain replacement[326].

The microbiome plays a crucial role in modulating immune responses through the generation of MAMPs and metabolites, which are direct byproducts of their microbial metabolism[133,202]. To explore metabolic pathways that could serve as biomarkers or potentially influence graft outcome and alloimmunity, we conducted an assessment of KEGG modules using our post-Abx MAG dataset. We concentrated on pathways enriched post-Abx, as these pathways might have potential as therapeutic targets to mitigate alloimmune responses. Notably, these

pathways exhibited a stepwise increase, escalating through GKC, V, VM, and reaching peak abundance in the VMGKC group. This pattern is likely due to the proliferation of specific commensals that encode genes in these metabolic pathways. Directly measuring the metabolomic profiles of Abx-treated mice, rather than inferring putative metabolic pathways from the bacterial genes present, will help elucidate if the presence/absence of KEGG modules is conserved at the metabolite level.

Proline and lysine were found to be depleted in the serum and colon of mice treated with DSS colitis, indicating the association of inflammation with their lower levels[327]. Furthermore, proline levels were reported to be lower in the serum of inflammatory bowel disease (IBD) patients compared to healthy people[328], and lysine was reduced in the serum of rejecting renal transplant patients compared to stable recipients[245]. A study by Swarte et al. (2022), surveyed fecal samples from patients with end-stage liver disease (ESLD), end-stage renal disease (ESRD), liver transplant recipients (LTR) and renal transplant recipients (RTR), and compared their microbiome using MSS to that in healthy individuals[217]. Proline and lysine metabolic pathways were significantly reduced in multiple biosynthetic modules in ESLD, ESRD, and RTR[217]. Whether this is a consequence or cause of inflammation and/or rejection remains to be investigated.

Recent studies have explored the physiological significance of diets rich in these amino acids using in vivo mouse models. In a mouse DSS colitis model, disruption of exogenous proline uptake through dietary restriction in mice with conditional knock-out (cKO) of the proline transporter *Slc6a7* in lymphoid tissue inducer (LTi) cells impaired their IL-22 response, exacerbating DSS pathogenicity[329]. Low proline levels compromised IL-22 production by LTi cells and affected gut tissue repair, whereas therapeutic diet supplementation with proline

protected mice by regulating gut homeostasis[329]. Additionally, in a rat model of hypertension and kidney damage, lysine administration protected against kidney dysfunction by inducing heightened kidney metabolic function, promoting metabolite excretion, and inhibiting tubular albumin uptake, offering potential therapeutic benefits for patients at risk of hypertension and kidney disease[330]. These findings suggest that these metabolites may have a therapeutic benefit in promoting mucosal barrier integrity and improving kidney function for favorable transplant outcomes.

Other KEGG modules of particular interest included pathways exclusively depleted in the VMCKG-treated mice, as this combination consistently resulted in the most robust suppression of alloimmunity. The modules that followed this correlation encompassed the amino acid serine, water-soluble vitamins B2 and B5, and LPS biosynthetic pathways. Serum serine levels were found to be lower in stable renal transplant patients compared to rejecting recipients[245]. Additionally, serine is considered a key immune metabolite that directly facilitates T cell proliferation, by promoting de novo nucleotide biosynthesis[331]. Vitamins B2 and B5 were significantly enriched in the ileostomy fluid of rejecting human intestinal transplant patients, compared to non-rejecting conterparts[332]. Vitamin B2 metabolites are recognized by mucosal-associated invariant T (MAIT) cells[333], and their presence in BM grafts could predict the occurrence of acute graft-vs-host disease (GVHD)[334]. Moreover, vitamin B5 and its by-product coenzyme A, enhanced the differentiation of cytotoxic $CD8^+$ T cells that produced IL-22[335]. In mouse cancer models, vitamin B5 diet supplementation augmented anti-tumor immune responses, and in human melanoma patients, plasma levels were positively correlated with ICB therapy efficacy[335]. Lastly, LPS levels were increased in the serum of end-stage heart disease and heart transplants recipients[336]. LPS administration in a mouse lung transplant model enhanced

alloimmunity, triggering chronic rejection and fibrosis[337]. Further investigation is required to assess if low levels of these metabolites could serve as biomarkers of better graft outcomes by metabolomic profiling of the serum, colonic content and feces of Abx-treated mice. Conversely depleting these metabolites therapeutically by diet interventions might improve the graft quality in transplant recipients by suppressing immune responses.

Transitioning from correlation to causality, our group[18,21,22] and others[38] have used probiotics to try and improve graft outcomes. Administration *Alistipes oderdonkii* to SPF mice was sufficient to prolong graft survival through inhibition of TNFα production by hematopoietic cells[18,21]. Administration to SPF mice of *Bifidobacterium pseudolongum*, a commensal that bloomed in pregnant mice, was sufficient to reduce heart transplant chronic rejection and diminish proinflammatory cytokine production in LPS-stimulated myeloid cell lines[38].

P. distasonis is a member of the *Parabacteroides* genus, recently separated from the *Bacteroides* genus[338], and is a Gram-negative, non-spore-forming, strict anaerobe present in the gastrointestinal tract of humans and mice[225]. Recognized as one of the 18 core members of the healthy microbiome of humans[222], *P. distasonis* prevailed in a population of Japanese centenarians, who had decreased susceptibility to aging-associated illnesses, chronic inflammation, and infectious diseases[339]. Notably, its abundance was lower in inflammatory conditions like obesity[340], non-alcoholic liver disease[341], and multiple sclerosis[342]. Mechanistic studies have underscored the commensal's capacity to produce microbial-derived molecules that modulate gut health and immune responses. Oral gavage of membranous fractions of *P. distasonis* protected mice in a DSS colitis model, by reducing the level of pro-inflammatory cytokines in various gut regions[223]. Wei et al. (2023), identified the fatty acid pentadecanoic acid as a bioactive lipid produced by *P. distasonis* that protected mouse models of non-alcoholic

steatohepatitis (NASH), via restoring gut barrier function, reducing serum LPS levels and liver pro-inflammatory cytokine expression[227]. The commensal also alleviated obesity and obesity-related dysfunctions in mice by producing the metabolite succinate and secondary bile acids in the gut[224]. Succinate induced intestinal gluconeogenesis, promoting insulin sensitivity and preventing obesity, while the bile acids lithocholic acid (LCA) and ursodeoxycholic acid (UDCA) promoted gut barrier integrity via the farnesoid X receptor (FXR)[224]. Lastly, *P. distasonis* inhibited disease in a mouse model of methionine and choline-deficient diet-induced hepatic fibrosis by promoting bile acid excretion, decreasing the levels of taurochenodeoxycholic acid (TCDCA), and reducing hepatic toxicity[226]. We confirmed that gavaging *P. distasonis* DFI 5.70 to SPF mice was sufficient to prolong allograft survival and result in decreased numbers of graft-reactive T cells after rejection. Further studies will query if the mechanisms of graft prolongation are dependent on its capacity to improve gut barrier function or produce succinate and modify bile acids, and what phase of the alloimmune response it is regulating.

To initiate our exploration of the signals necessary for APC poising, we propose adopting a similar in vitro approach as outlined in Lei et al, (2016)[97]. In this approach, male APCs will be co-cultured with CFSE-labeled Marilyn T cells, with the proliferation and differentiation of these cells serving as indicators of the APC posing status. We have identified that APCs exhibiting the highest capacity to activate Marilyn T cells can be obtained from SPF LNs, ex-GF mice conventionalized with SPF feces LNs, and skin APCs from *S. epi*-colonized mice. Conversely, APCs with the lowest poising status are LN APCs derived from GF, Abx-treated, and ex-GF mice conventionalized with Abs-treated feces. To elucidate the specific molecules sensed by APCs, we propose incorporating into our experimental setup lysates from intestinal content, or serum, from various settings. The murine source for the serum or intestinal content can be SPF,

GF, or mono-colonized animals, or mice treated with different Abx combinations. It is important to use both serum and intestinal content, as certain metabolites are formed via combined metabolism from host cells and the microbiota. For instance, secondary bile acids, generated from host-dependent metabolism of cholesterol and subsequent microbiota-mediated conjugation of primary bile acids are only detected in the intestinal content or portal vein blood, but not systemically in the host[343]. Moreover, immunomodulatory metabolites like TMAO require a two-step process, where dietary choline is converted into TMA by the gut enzyme choline-TMA lyase, and then, once it enters the portal circulation, into TMAO by host-derived liver enzymes[211]. Obtaining blood from the portal vein could serve as an alternative, as it has a higher concentration of microbial-derived molecules.

To investigate molecules responsible for increasing the poised status, unpoised APCs will be cultured with serum/intestinal lysate content. If this leads to re-poising of the cells, a combination of centrifugation and fractionation can be employed to narrow down the size of the molecule of interest. Subsequently, the molecule can be identified by performing un-targeted mass-spec profiling at the DFI metabolomics core for characterization. Another potential mediator of poising could be MAMPs. Although we did not observe re-poising of skin APCs upon heat-killed *S. epi* colonization, or graft prolongation when gavaging heat-killed *Alistipes*[180], which suggests the requirement for active biological activity, we cannot eliminate this possibility, as MAMPs are diverse and have distinct immunoregulatory properties[344]. Performing RNAseq in these APCs may help understand the signaling pathways promoted by poising molecules. We and others have shown that Type I IFN and activated NFκB pathways are important for APC posing[97,115]. Finding if these are the main mediators of calibration of APCs, or if there are others will help understand how metabolites modulate alloimmunity.

Another interesting avenue is to test whether the gut barrier function is important during the alloimmune response. To test this, we could try decreasing or increasing it during skin transplantation. To decrease intestinal barrier integrity, we could treat mice with low-dose DSS, to promote intestinal epithelium damage[345]. If a breach in the gut epithelium has a causal impact on allograft survival, we would expect to have accelerated allograft rejection kinetics. Likewise, to promote barrier integrity, we could use recombinant IL-22-Fc[283] in our transplant model, to see if it improves allograft outcomes. Understanding the importance of gut integrity and how it impacts systemic immunity could lead to therapeutic targeting of barrier function to reduce complications and improve clinical outcomes in transplant patients.

A largely unaddressed question is whether microbiota-specific heterologous immunity plays a role in the anti-graft immune response. Cross-reactivity has been widely reported in the context of transplantation[128]. Up to 45% of virus-specific T cells against Epstein-Barr virus, cytomegalovirus, varicella zoster, and influenza virus have been shown to cross-react with allogeneic HLA molecules[128]. Evidence for molecular mimicry has been reported in a mouse model of fibrosarcoma, where T cells reactive to an enterococcal bacteriophage epitope cross-reacted with an MHC class I-presented tumor-specific antigen, correlating with stronger antitumor immune responses driven by $CD8^+$ T cells[129]. Similarly, in a mouse model of spontaneous autoimmune myocarditis, cardiac myosin-specific $CD4^+$ Th17 cells cross-reacted with a *Bacteroides*-specific antigen[130]. Both studies confirmed that molecular mimicry also occurred in humans. During graft rejection, it is therefore conceivable that cross-reactive commensal-specific T cells may participate in inducing graft damage. Intriguingly, renal transplant recipients who received organs from donors with more similar gut microbiota to their

own exhibited prolonged graft survival compared to patients who received kidneys from donors with dissimilar microbiota[131].

The first approach to test if microbiota-specific commensal heterologous immunity plays a role in allograft rejection is to determine if T cells that are localized in the gut are found systemically, and more specifically in the allograft. The Kaede and Kikume green-red (KikGR) mouse can be used to identify if T cells that have been in the gut can circulate to distal locations. Upon exposure to 405nm light, the KikGR protein is photoconverted and can be detected via flow cytometry. Lefferts et al, (2022)[346] found that by exposing the colon to light via colonoscopy, photoconverted KikGR$^+$ T cells from the gut were found in joints in a rheumatoid arthritis model[346]. This mouse model can be used to see if photoconverted T cells reach the allograft (comparing to syngeneic and GF settings). If this happens, sorting KikGR$^+$ T cells and sequencing their TCR can help start understanding if they have microbiota specificity. To study if these T cells do cross-react with alloantigen, culturing them with donor APCs or with host APCs pulsed with alloantigen (or APCs from an F1 mouse that shares host and donor genotypes) or with host APCs pulsed with microbial-derived lysates, will help identify what their cognate antigens are, and if there is structural similarity between alloantigens and commensal-derived antigens.

In summary, our use of rationally designed Abx cocktails to target bacterial taxa, coupled with the assessment of fecal microbiome using MAG technology, has revealed that all bacterial subgroups investigated additively contribute to augmenting alloimmunity, and that maximally reducing bacterial diversity correlates with optimal extension of graft survival and suppression of alloimmunity. These findings highlight the importance of microbial diversity in calibrating

alloimmunity (Figure 6. 2, lower right and left quadrant). Furthermore, our results position *P. distasonis* strain DFI 5.70 as a promising probiotic candidate to facilitate transplant survival.

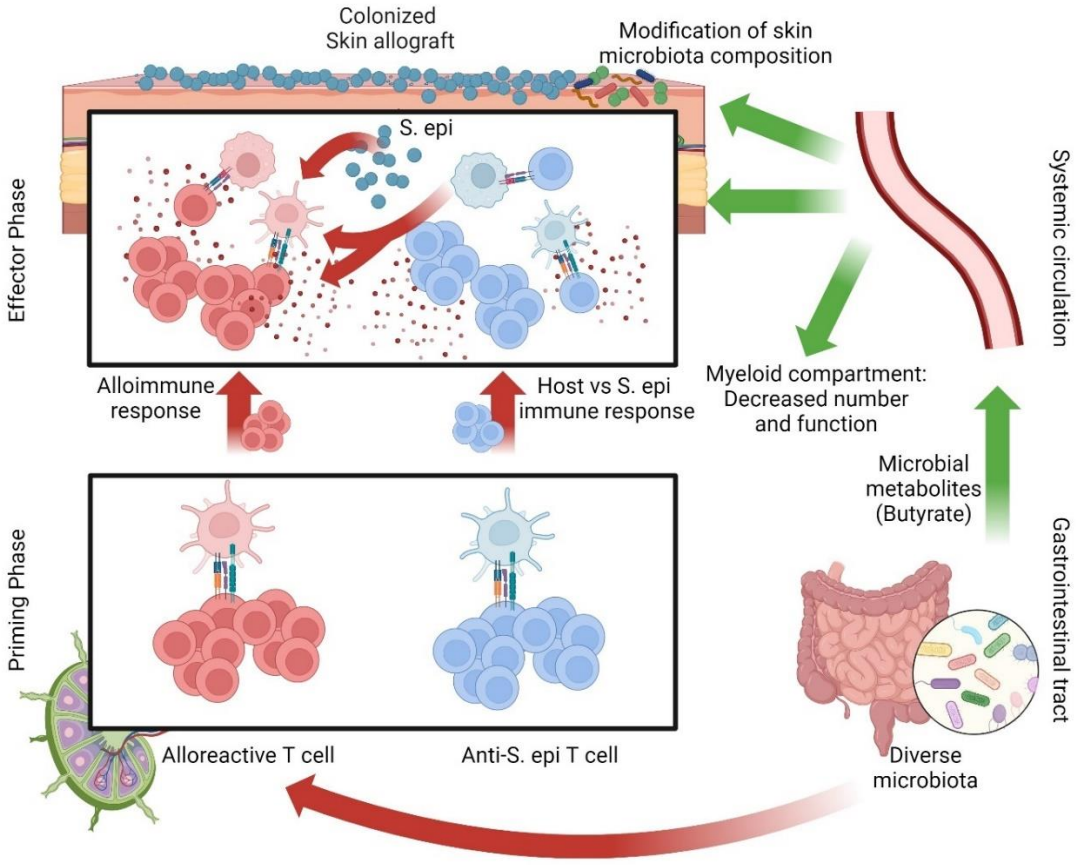

Figure 6. 2. Working model for how the microbiota and derived metabolites can impact alloimmune responses.
(Lower right and left quadrant) Highly diverse microbiota provides microbial-derived signals that poise APCs to enhance the T cell priming phase of alloimmune responses. (Upper left quadrant) *S. epi* colonization accelerates colonized allograft rejection by providing signals to skin APCs that augment their capacity to activate alloreactive T cells once they infiltrate the allografts and via generation of a host-vs-commensal T cell response, which contributes to damaging the colonized allograft. Likewise, a potential bystander impact from the anti-*S. epi* immune response could enhance the host-vs-graft immune response. (Upper right quadrant) High levels of cecal butyrate inhibit the myeloid compartment systemically both quantitatively and qualitatively, which result in less damage once they infiltrate allografts. Butyrate treatment changes the microbial composition of the skin. Red arrows: Impact that results in stronger alloimmune responses, and thus more damage to the allograft. Green arrows: Impact that results in weaker alloimmune responses, and thus more protection to the allograft. Red cells: APCs presenting alloantigen and driving alloreactive T cell responses. Blue cells: APCs presenting commensal-antigen and driving anti-commensal T cell responses.

6.2 Influence of skin-restricted microbiota on solid organ transplant outcome

Our results demonstrate that cutaneous colonization with *S. epi* can act locally to enhance the effector phase of alloimmunity via two distinct mechanisms: providing signals to skin APCs to augment their capacity to activate alloreactive T cells once they infiltrate the allografts, and via induction of a host-vs-commensal T cell response, that contributes to damaging the colonized allograft (Figure 6. 2, upper left quadrant). This enhanced immune response in the inflamed allograft might also explain why colonized organs have shorter half-life than sterile organs and suggests that modulation of the graft microbiota before transplantation may improve graft outcomes.

To our knowledge, this is the first time an extraintestinal commensal is shown to accelerate graft rejection. The mechanism also appears novel as skin *S. epi* modulated the effector rather than priming phase of the adaptive cell-mediated alloimmune response[97].

The kinetics of skin graft rejection in mice transplanted with skin-restricted *S. epi* were similar to those of globally colonized SPF mice or of GF mice that were conventionalized with SPF FMT gavage and became globally colonized, in the gut and skin[97]. However, it is important to note that not all skin microbiota accelerates skin graft rejection, as we previously showed that FMT from antibiotic-pretreated mice into GF mice by oral gavage, which resulted in both gut and skin colonization, did not hasten skin graft rejection[97], suggesting that different skin microbiota communities have different consequences on alloimmunity. Indeed, association of mice with a defined clade of *S. epi*, but not *S. xylosus* or *S. aureus*, enhanced IFNγ and IL-17A production by dermal $CD8^+$ T cells[105,106], indicating that even single commensals of the same genus can have different immune impacts.

Of note, Chen et al. (2023)[347] engineered *S. epi* to express the model antigen ovalbumin (OVA), and demonstrated that cutaneous colonization of OVA-*S. epi* was sufficient to drive an OVA-specific T cell response, capable of mounting a systemic anti-cancer immune response in to and OVA-expressing tumor. This demonstrates that the anti-commensal immune response generated locally at the level of the skin could not only attack the *S. epi*-colonized skin grafts, but also travel systemically. Nevertheless, we hypothesize that T cell activation requires a second inflammatory stimulus to occur, as colonization with *S. epi* of intact normal skin in adult mice did not result in activation of T cells at steady-state. In our model, mounting an anti-*S. epi* T cell response requires tissue damage from surgery. In the cancer model, it requires the damage generated by a growing tumor. Heterologous immunity to *S. epi* could theoretically also promote graft rejection via cross-reactivity of anti-*S. epi* T cells with an alloantigen.

The exact signal skin *S. epi* provides to skin APCs to accelerate allograft rejection is not fully elucidated. The observation that painting with heat-killed *S. epi* did not result in accelerated graft rejection suggests that PRR signaling from *S. epi* MAMPs is not sufficient. In addition to engaging PRRs, live *S. epi* may produce metabolites that enable local cutaneous APCs to better reactivate alloreactive T cells when they reach the skin, either because of closer proximity of the skin APCs to the cutaneous *S. epi* or because the APC subset composition in the skin is more susceptible to modulation by *S. epi* metabolites. Skin *S. epi* has also been linked to faster skin wound closure[106], which might allow faster infiltration of alloreactive T cells following skin transplantation. Alternatively, *S. epi* can form biofilms, which have high oxygen consumption rates, creating hypoxic microenvironments[348]. Under low-oxygen levels, myeloid cells express the hypoxia-inducible factor 1α (HIF-1α), which imprints an inflammatory polarization, characterized by iNOS expression[349]. Macrophages can also act as APCs in the allograft,

amplifying T cell responses via expression of MHC II and co-stimulatory molecules, which in turn, further activate macrophages. It is conceivable that *S. epi* induces a hypoxic environment in the allograft that promotes inflammatory myeloid cells to promote enhanced damage directly of via increased T cell responses. Moreover, *S. epi* resulted in higher mRNA expression levels of inflammatory cytokines in the skin graft 10 days after transplantation, supporting the augmented effector phase of the alloimmune response.

S. epi itself was also responsible for promoting graft damage via a host-vs-commensal immune response. naïve commensal-specific T cells in graft-recipient mice expanded in response to commensals present on transplanted organs and inflicted modest transient damage to the colonized graft. More significantly, memory commensal-specific T cells caused substantial and more durable damage to colonized organs. Trm and/or effector memory T cells in the host were sufficient to drive this damage. This host-versus-commensal immune response was distinct from the alloresponse and resulted in resistance to immunosuppression.

In our model, it is conceivable that the APCs that present commensal-specific and allo-specific peptides are the same or are in close proximity (Figure 6. 2, upper left quadrant). We envision a scenario where first, memory anti-commensal T cell responses are generated upon skin colonization with a new bacterium. Trm cells then colonize the skin and may be ready to respond to a skin graft colonized with their cognate microbe, as upon stimulus with a commensal-colonized allograft, these Trm cells can interact with APCs presenting *S. epi* peptides. This interaction can directly modulate the APC, potentially via a costimulatory or cytokine-mediated effect. This APC could then have a better ability to present alloantigen during the effector phase of the anti-graft immune response. This would result in the modulated APC driving enhanced alloreactive T cell activation. The effect could also be mediated by bystander

activation, where anti-commensal Trm cells can interact with *S. epi*-presenting APCs and during this immune activation, a secreted inflammatory cue could enhance a set of allo-antigen-presenting APCs, thus improving the alloreactive T cell response. Intriguingly, the signal we hypothesize could be accelerating allograft rejection may involve an intricate interaction of commensals with the innate and adaptive immune compartments.

To tease this out, we could use P14/RAG-KO mice as recipients and adoptively transfer TCR transgenic T cells with distinct specificities. P14/RAG-KO mice are TCR transgenic mice that only have $CD8^+$ T cells that recognize a peptide from LCMV, so they cannot recognize male grafts. Our group has used these mice as hosts before because the presence of endogenous monoclonal T cells prevents homeostatic proliferation of the transferred T cells[350]. To study the interaction between T cells that recognize male antigens and T cells that recognize *S. epi*-specific antigens, we will use Marilyn T cells and Bowie T cells. By transferring either or both tracer populations to *S. epi*-colonized allograft-bearing P14/RAG-KO recipients, we can analyze the survival of the graft over time and analyze their impact of each set of T cells on skin APCs, in a model where graft rejection is only mediated by the transferred T cells. If the anti-commensal immune response plays a role in augmenting the anti-graft immune response, we expect to see a stronger immune response in the Marilyn T cell compartment, when we co-transferred with Bowie T cells. RNAseq of skin APCs in the different experimental setups can start elucidating regulated gene pathways when the system has one or both T cell clones, and help understand how *S. epi* enhances the effector phase of the alloimmune response.

Our results suggest that graft sterilization prior to transplantation might result in better outcomes for barrier organ allografts. Perfusing the organs with antibiotics shortly before transplantation may reduce donor commensal load and enable colonization of the graft by host

commensals. However, antibiotics may also eliminate pro-tolerogenic donor commensals, as some bacteria are known to promote Treg expansion[281]. Conversely, matching the commensal microbiota could also be beneficial for transplant recipients[131], decreasing the probability of anti-commensal immune responses against the different commensals that are passengers in the allograft. We conclude that memory T cells specific for select bacterial commensals can significantly damage colonized skin grafts independently from an alloresponse and render hosts more resistant to immunosuppression.

6.3 Influence of the SCFA butyrate on solid organ transplant outcome

Despite the use of immunosuppressive therapies, transplant patients frequently experience acute rejection episodes, with many eventually developing chronic allograft rejection. Consequently, identifying environmental factors capable of calibrating the strength of the alloimmune response and amenable to therapeutic targeting represents a promising strategy to complement current immunosuppressive regimens. One of these factors is the family of metabolites called SCFAs, which are derived from commensal-dependent fermentation of dietary fibers and play pivotal roles in maintaining gut and immune homeostasis[302]. In this study, we aimed to investigate the effect of the SCFA butyrate on organ transplant outcomes and alloimmunity. Employing a rationally designed delivery micelle-based platform (ButM) to safeguard the butyrate payload, we achieved accurate targeting of butyrate to the lower GI tract, where its biological properties are more pronounced.

Our investigations revealed that oral delivery of ButM was sufficient to significantly prolong the survival of both minor- and major-mismatched skin allografts, without the use of immunosuppression. Moreover, using previously described concentrations of NaBut[140,141] in the

drinking water failed to delay skin rejection kinetics, confirming that the micelle-based delivery of butyrate was superior in our model. This is likely due to the ButM having better accumulation and retention in the ileum and cecum, yielding elevated concentrations for up to 8 hours post-administration[197]. In contrast, NaBut undergoes rapid metabolism in the acidic gastric environment in the first 4 hours, becoming undetectable in the ileum and cecum afterwards[197]. The augmented concentration of butyrate in the lower GI tract could explain why ButM, but not NaBut, could prolong allograft survival, owing to the increased biological impact of butyrate on gut colonocytes and/or immune cells[140,141,290–293].

Colonic butyrate serves as an energy source for intestinal epithelial cells, supplying up to 70% of their metabolic needs[290]. The remaining butyrate is absorbed into the bloodstream via the portal vein and subsequently reaches the liver, where hepatocytes predominantly metabolize it from the portal circulation[351]. As we demonstrated that ButM had the capacity to impact distal immune responses to the allograft, we hypothesized that butyrate was modulating systemic immunity. The delivery mechanism of ButM involves the release of butyrate through esterases in the GI tract, indicating that its graft-prolonging capacity is likely exclusive to oral administration. Consistent with this, systemic administration of ButM via ip injections, or sc administration, to compartmentalize its effect in the vicinity of the allograft, was incapable of promoting better graft outcomes, as free butyrate may not reach the desired target sites. These observations support a model where ButM delivers sufficient amounts of butyrate, even after undergoing consumption by colonocytes and metabolism in the liver to exert systemic effects at extra-intestinal sites. Alternatively, consumption by these intestinal epithelial cells or hepatocytes results in the production of a metabolite that is systemically distributed.

Our group and others have outlined the causative roles of the microbiota in modulating allograft rejection and alloimmunity[97,100,117,121,127,174,180,181,200,201]. As it is well-established that butyrate induces the expression of antimicrobial peptides (AMP)[139], as does ButM[197], we analyzed if ButM treatment elicited alterations in the diversity of the commensal microbiota, which may be associated with slower rejection kinetics. Upon administration of ButM, mice exhibited a bloom of *Turicibacter, Eisenbergiella,* and several ASVs of the *Clostridium* cluster XIVa, all of which correlate positively with improved allograft outcomes. *Turicibacter* is a prevalent gut commensal of humans and mice and has been described to modify host lipid levels, including reducing serum cholesterol, triglycerides, and adipose tissue mass, while also impacting secondary bile acid profiles in mice[352]. Similarly, *Clostridium* cluster XIVa, along with related obligate anaerobe species like *Eisenbergiella*[353], are known for their ability to produce butyrate, modulate systemic immunity, and induce Tregs[139]. We hypothesize that the proliferation of butyrate-producing commensals upon ButM treatment enables a feedforward loop, where ButM enhances β-oxidation of colonocytes, creating an anaerobic niche in the gut lumen that fosters the expansion of anaerobic *Clostridia* species[303]. This could also explain why there are several ASVs enriched in ButM-treated mice, compared to control mice. Because of the immunomodulatory capacity of these expanded commensals, they may contribute directly or indirectly to the prolongation of allograft survival induced by ButM treatment.

Given the importance of skin commensals in modulating local immunity[102,125], and considering the impact that they have in modulating colonized allograft rejection kinetics[100,127], we investigated whether ButM treatment impacted the skin microbiota. ButM-treated mice had profound differences in skin microbial composition compared to control mice. These alterations may stem from dysbiotic fecal pellets being in contact with the skin, immune-mediated

mechanisms, or direct effects of butyrate, or of metabolites produced downstream of its administration by enterocytes or hepatocytes, on skin physiology. Notably, gut-derived SCFAs, including butyrate, have been implicated in modulating skin barrier integrity by promoting keratinocyte metabolism and differentiation[354]. Additionally, the gut microbiota of patients with atopic dermatitis is characterized by a reduced capacity to produce SCFAs, particularly butyrate[295], suggesting a strong association between butyrate skin health. However, whether these shifts in skin bacterial diversity are causal in promoting better allograft outcomes remains to be studied. Painting Abx-treated or GF mice with skin microbiota from ButM-treated mice under sterile conditions can help elucidate the impact it has on skin immunity. Notably, applying a mannose-decorated co-polymer with butyrate into a skin wound healing model, significantly improved the inflammatory microenvironment and accelerated skin wound recovery, confirming a potential role of butyrate in accelerating tissue healing[355]. If ButM treatment helps with wound healing, it could help the transplant engraft and heal faster from IRI, and result in prolongation of survival.

Experiments utilizing *ad libitum* NaBut have elucidated butyrate's robust promotion of colonic Tregs[140,141,291]. In specific pathogen-free (SPF) mice, NaBut induces the differentiation of peripheral Tregs within the colonic lamina propria, while in GF or antibiotic-treated mice, these Tregs are also detectable in the spleen[140,141,291]. ButM treatment did not alter the Treg profile locally (mLN) or systemically (spleen, dLN, or skin), consistent with the findings reported by Wang et al (2023)[197]. This is in contrast to what Wu et al, (2020)[356] reported, where NaBut was found to improve kidney allograft survival and correlated with intra-graft increase of polyclonal Treg populations. We hypothesize that this might be due to the B/c into B6 kidney transplant model being less immunogenic than our skin transplant model, in which 50% of

recipients do not reject their allografts[356]. Additionally, employing graft-reactive TCR-Tg T cells and analyzing endogenous alloreactive T cells during the various phases of the T cell alloimmune response in ButM-treated mice failed to induce detectable changes in the T cell priming, migration, or adaptive immune cell-mediated effector phases. This suggests that the ButM-mediated modulation of other cell types not indirect from modified T cells affecting other immune cell types.

Both NaBut[140,141] and ButM[197] protected mice in T cell transfer models of colitis, which are characterized by bowel infiltration by not only lymphocytes but also monocytes, macrophages, and polymorphonuclear leukocytes (PMNs)[345]. This implies that myeloid cells could be modulated by ButM for its effect on colitis and, by extension, for its graft-prolonging effect. Indeed, SCFA could imprint anti-inflammatory phenotypes in colonic macrophages and dendritic cells[292,293], supporting a model where ButM treatment is modulating myeloid cells, leading to slower allograft rejection kinetics.

Circulating $Ly6C^{hi}CD11b^{+}$ monocytes serve as precursor cells that undergo differentiation into distinct myeloid cell types upon tissue infiltration. During solid organ transplantation, allografts are damaged as they are cut from their blood supply, suffering a loss of oxygenation (ischemia phase). When the allograft is transplanted in the recipients, perfusion and oxygenation are restored, leading to ischemia and reperfusion injury (IRI) which is characterized by inflammation, oxidative damage, and the release of damage-associated molecular patterns (DAMPs) in the organ, leading to the activation of the recipient's immune system[57]. Early after IRI, graft endothelial and parenchymal cells express TNFα and IL-1β, promoting the expression of the monocyte chemoattractant MCP-1. High levels of MCP-1 mediate the egress of monocytes from the bone marrow and their infiltration to inflamed allografts, in a CCR2-dependent

manner[58–60]. As monocytes infiltrate the allografts, they are exposed to an inflamed microenvironment, which mediates their differentiation into inflammatory macrophages[62], and their accumulation is associated with worse clinical outcomes for kidney and heart transplant patients[63,64]. These macrophages secrete a wide variety of pro-inflammatory cytokines, including IL-1, IL-6, IL-12, TNFα, and IFNγ, which damage the allograft by different mechanisms[73]. As $Ly6C^{hi}CD11b^{+}$ monocytes play an important role in the innate immune cell-mediated effector phase of the anti-graft response, we focused on how they, and other myeloid cells, were impacted by ButM.

We observed that at homeostasis, ButM significantly decreased $Ly6C^{hi}CD11b^{+}$ monocyte percentage and numbers systemically, including in the blood, spleen, and intact skin. This quantitative impact extended to skin $F4/80^{+}CD11b^{+}$ macrophages, suggesting a broad systemic impact of ButM on the myeloid compartment (Figure 6. 2, upper right quadrant). Taking into consideration that the SCFA propionate has been reported to alter bone marrow hematopoiesis by enhancing the generation of macrophage/dendritic cell precursors (MDPs)[354], we assessed if ButM reduced generation of $Ly6C^{hi}CD11b^{+}$ monocytes in the bone marrow. However, $Ly6C^{hi}CD11b^{+}$ monocytes remained unaltered in the bone marrow, indicating that the systemic decrease of myeloid cells is not due to impaired hematopoiesis. Moreover, CCR2 expression at the protein levels was also similar between control and ButM-treated mice, in bone marrow, spleen, and skin myeloid cells, suggesting that lack of CCR2-dependent recruitment may not explain the lower number of these cells systemically in ButM-treated mice.

Continued administration of ButM before and after skin transplantation was associated with lower numbers of graft-infiltrating myeloid cells. Myeloid cell recruitment to the graft is attributed to the surgery-related tissue damage, IRI happening in the allograft, and the

alloimmune response cooperating to further attract myeloid cells[67]. In ButM-treated mice, fewer $Ly6C^{hi}CD11b^{+}$ monocytes are available in the circulation or neighboring tissues to be recruited into the graft. This suggests a model where ButM systemically and quantitatively impacts the myeloid cell compartment at steady-state and the impact is maintained upon alloimmune responses (Figure 6. 2, upper right quadrant).

The decreased frequency of circulating $Ly6C^{hi}CD11b^{+}$ monocytes required 2 weeks of continued exposure to ButM, indicating that sustained administration is necessary for this phenotype. This may explain why initiating ButM administration after transplantation failed to significantly prolong allograft survival.

As transplant patients have poor gut barrier integrity[216,217], and ButM has the capacity to protect the gut in colitis models[197], we analyzed serum LPS levels in our model, a measure of tissue barrier function. Interestingly, serum endotoxin levels were not different between control and ButM-treated mice, both at homeostasis and after transplantation. The increase in LPS levels seen in both groups after transplantation is likely due to surgery. These data suggest that ButM is not prolonging allograft survival via an impact on tissue barrier integrity (whether skin or gut tissue), but this does not mean its oral administration is not impacting an intestinal cell or an immune cell type located in the gut.

The pre-transplant immune status of the recipient integrates all signals perceived by immune cells, which determine how poised immune cells are to respond to activating stimuli, and to influence the alloimmune response upon transplantation[97,100,117,174,180,212]. Considering that butyrate can modulate the inflammatory and antimicrobial properties of colonic macrophages and dendritic cells[293,357], we examined whether ButM was providing a signal to $Ly6C^{hi}CD11b^{+}$ monocytes and exerting a qualitative impact. RNAseq analysis of these cells revealed that ButM

treatment upregulated genes associated with mitochondrial aerobic metabolism, OXPHOS, and respiration. This suggests that butyrate can influence Ly6C^{hi}CD11b^{+} monocyte mitochondrial function. Similarly, butyrate has been shown to drive mitochondrial respiration and fatty-acid oxidation in intestinal epithelial cells[290], confirming its capacity to drive metabolic changes in other cell types. Conversely, inflammatory macrophages primarily rely on glycolysis for their inflammatory phenotypes, including processes such as phagocytosis, ROS production, and secretion of pro-inflammatory cytokines[76,304]. Hence, the observed alterations in steady-state Ly6C^{hi}CD11b^{+} monocyte metabolic potential induced by ButM treatment may render them less capable of mounting robust pro-inflammatory responses. Measuring mitochondrial respiration after ButM treatment will help verify if the changes seen at the transcriptional level do have a functional correlation in monocytes.

Notably, alternatively activated macrophages, also defined as M2-like macrophages[72], exhibit metabolic profiles more dependent on OXPHOS, Krebs cycle, and elevated levels of mitochondrial electron transport chain (ETC) respiration[76]. Likewise, Vitamin D3-induced tolerogenic, anti-inflammatory DCs prioritize fatty-acid oxidation and OXPHOS[358], and low dose LPS pretreatment-induced tolerant states in monocytes and macrophages promoted the production of the anti-inflammatory cytokine IL-10, inhibited glycolysis and enforced OXPHOS metabolism[359]. Collectively these data support that ButM treatment induces metabolism alterations in Ly6C^{hi}CD11b^{+} monocytes that resemble myeloid cells with suboptimal inflammatory phenotypes and suggest a qualitative effect within the myeloid cell compartment. To test if ButM is mediating the effects on Ly6C^{hi}CD11b^{+} monocytes via an impact on their OXPHOS capacity, we could use an ETC cKO on myeloid cells. Using LyzM-Cre x Complex

III$^{fl/fl}$ we can determine if ButM fails to prolong allograft survival when it is incapable of potentiating mitochondrial respiration.

In addition to the upregulation of mitochondrial metabolism genes, ButM treatment resulted in higher expression of two other genes in Ly6C^{hi}CD11b^{+} monocytes: *Malat1* and *Marchf6*. *Malat1* is a long noncoding RNA (lncRNA) that undergoes distinct regulation during macrophage polarization[360]. Knockdown of this lncRNA attenuated LPS-induced M1-like activation and enhanced IL-4-activated M2-like differentiation, while also promoting OXPHOS and pro-fibrotic phenotypes[360]. Notably, lncRNAs have been identified to inhibit Ly6C^{hi}CD11b^{+} monocyte differentiation into pro-inflammatory macrophages in a butyrate-dependent manner, highlighting the importance of microbiota-dependent transcriptional regulation of myeloid cells[361]. Conditional knockout of *Malat1* in myeloid cells led to more severe bleomycin-induced lung fibrosis with alveolar macrophages displaying augmented M2-like and profibrotic phenotypes[360]. On the other hand, *Marchf6* is an E3 ubiquitin ligase that acts as an NADPH sensor and regulates ferroptosis. Knockdown of this gene in HeLa cells resulted in increased lipid peroxidation, ROS production, and suppression of feroptosis[362]. Ferroptosis and iron metabolism are critical mediators of macrophage polarization, where intracellular iron overload fosters M1-like macrophage activation and secretion of TNFα, while diminished iron levels promote M2-like polarization[363]. The upregulation of these genes suggests that ButM also modifies the inflammatory polarization potential and iron metabolism of Ly6C^{hi}CD11b^{+}, both of which play important roles in transplant rejection[72,364]. Studying the expression of these genes under in vitro stimulation and throughout the alloimmune response can help us understand their impact in monocytes.

Conversely, downregulated genes in Ly6C^{hi}CD11b^{+} monocytes from ButM-treated mice may be associated with pro-rejection phenotypes. *Dusp6*, was the most significantly downregulated gene. *Dusp6*-KO mice had improved cardiac repair and function in a myocardial infarction (MI) model, by predominantly attenuating activity of neutrophils[365], which are important mediators of the innate immune cell execution of graft rejection[366]. In addition, *Dusp6* acts as a rheostat of the p38 MAPK activity by inhibiting pERK in neutrophils[365]. Neutrophil-specific *Dusp6*-conditional KO mouse models confirmed its cell-intrinsic capacity to decrease ROS production and degranulation at the acute inflammatory phase of post-myocardial infarction[365]. *Dpep1*, another downregulated gene after ButM treatment, is a major neutrophil adhesion receptor that helps the recruitment of neutrophils and monocytes into kidneys undergoing IRI[367]. Renal inflammation and acute kidney injury (AKI) were attenuated in *Dpep1*-KO mice or mice pretreated with DPEP1 antagonists, by blocking neutrophil adhesion to peritubular capillaries and reduced inflammatory monocyte recruitment to the kidney after IRI[367]. These two genes are important mediators of tissue damage under IRI, but their impact on transplant outcome has not been studied. We hypothesize that the downregulation of these genes in Ly6C^{hi}CD11b^{+} monocytes after ButM treatment might be protective during the myeloid cell execution of the effector phase of the alloresponse in the graft.

Kdm7a was also significantly repressed in ButM-treated mice. *Kdm7a* is a member of the histone demethylases, which are important regulators of immunity and inflammation[368]. During inflammatory responses, TNFα-responsive genes are activated upon rapid demethylation of H3K9 and H3K27 histone markers which is in part mediated by Kdm7a[369]. Histone methylation has been described as an important mediator of myeloid cell activation. Butyrate promotes the expression of the ultra-conserved lncRNA *lncLy6C,* which promotes

Ly6C^{hi}CD11b^{+} monocyte differentiation into Ly6C^{lo} monocytes, in part by binding to the transcription factor C/EBPb and multiple lysine methyltransferases in a butyrate-dependent manner[361]. This molecular complex bound to the promoter region of Nr4A1, which supports the downregulation of Ly6C^{hi} into Ly6C^{lo} monocytes[361]. Exposure to butyrate also promoted the suppression of TNFα, IL-6, iNOS, IL-1β and promoted Arg-1[361]. This confirms an important mechanism by which gut commensal metabolites regulate myeloid cell gene expression. This suggests that ButM treatment is also impacting the function of myeloid cells, as they may be less capable of activating inflammatory responses during immune activation.

Given that the downregulated genes in ButM-treated Ly6C^{hi}CD11b^{+} monocytes were related to cell migration and differentiation, defense response, and cytokine production, we assessed if ButM could impact their pro-inflammatory potential upon LPS stimulation. Indeed, various myeloid cell populations produced lower levels of TNFα, confirming a qualitative impact of ButM treatment. Butyrate has been reported to reduce pro-inflammatory activities in colonic mononuclear phagocytes in a GPR109a-dependent manner[292], inhibit NO, IL-6, and IL12 (but not TNFα) in bone marrow-derived macrophages (BMDMs) in an HDAC inhibition-dependent manner[293], and facilitate M2-like polarization of BMDMs[305]. Altogether, these data suggest that ButM is not only impacting the number of myeloid cells but also their quality, i.e, their capacity to generate inflammatory cytokines once recruited into the allograft. This supports a model where ButM modulates allograft rejection by exerting a dual quantitative and qualitative impact on myeloid cells, potentially reducing their execution of the effector phase of the anti-graft immune response (Figure 6. 2, upper right quadrant).

Mechanisms by which ButM treatment could affect monocytes include direct pathways, via their expression of the GPCRs: GPR41, GPR43, or GPR109a[139]. SCFA signaling via these

GPCRs has been reported to be an important regulator of immunity. GPR41 was shown to be necessary for allergy model protection, mediated by the SCFA propionate[354]. GPCR43-deficient mice displayed heightened susceptibility to experimental models of colitis, asthma, and arthritis[370]. Meanwhile, expression of GPR109a on APCs induced a repressed inflammatory niche in the colonic mucosa and promoted IL-10-producing Tregs[292]. These GPCRs are also important dietary metabolite sensors that regulate host metabolism in enteroendocrine, pancreatic, and adipose cells[139], suggesting an additional possible impact on myeloid cell metabolism.

Another direct impact can be the inhibition of HDAC activity. Butyrate can induce acetylation of histones in the *Foxp3* locus to help polarize Tregs[371], and HDAC inhibition improved Tregs suppression in autoimmunity and transplantation[371,372]. Similarly, myeloid cells also are modulated via butyrate-mediated HDAC inhibition[291,293], and using an HDAC inhibitor was sufficient to phenocopy butyrate treatment, suggesting a beneficial impact of studying these inhibitors in the context of myeloid cells in transplantation. Moreover, propionate can decrease the expression of HDAC6 and HDAC9, in a GPR43-dependent manner, promoting Treg expansion and suppressive properties[140], showing a potential dual impact via both GPCR signaling and HDAC inhibition in the same cell. As we do not find ButM modulating Tregs, understanding whether ButM treatment is impacting myeloid cells via a direct effect on GPCRs or HDACs can help understand if these are the mechanism by which butyrate is exerting its quantitative and qualitative modulation.

Nonetheless, indirect pathways of modulating circulating $Ly6C^{hi}CD11b^{+}$ monocytes are also possible. Butyrate has been shown to drive mitochondrial respiration, fatty-acid oxidation, and autophagy in intestinal epithelial cells[290], as well as induction of AMPs[373]. Likewise,

butyrate inhibits Tuft cell hyperplasia via modulating intestinal stem cells in an HDAC3-dependent manner, decreasing anti-helminth and type 2 immunity in the gut[374] and suppresses proliferation by inhibiting the transcription factor FoxO3[375]. It is conceivable that butyrate impacts other cell types in the intestine, which in turn may produce signals or influence the niche that can modulate myeloid cells. Circulating $Ly6C^{hi}CD11b^{+}$ monocytes in the gut, portal vein, or liver may perceive these signals and undergo systemic modulation upon recirculation.

Lastly, we established that the reduction in myeloid cells induced by ButM treatment played a causal role in promoting slower allograft rejection kinetics as depleting $Ly6C^{hi}CD11b^{+}$ monocytes using the αCCR2 antibody or DT treatment of CCR2-DTR mice was sufficient to prolong graft survival. This is in line with the experimental depletion of macrophages in transplantation, which has proven to attenuate graft injury. For instance, in a rat renal allograft model[68] and a heart-lung transplant model[69], the use of liposomal-clodronate was effective at depleting infiltrating macrophages and resulted in less acute rejection[68]. Similarly, the depletion of $CD11b^{+}$ myeloid cells in CD11b-DTR mice resulted in less kidney damage to the microvasculature in a mouse renal transplant model[70]. Moreover, depletion of monocytes/macrophages with a c-Fms kinase inhibitor resulted in less renal allograft dysfunction and structural damage[71] and depletion of donor-derived $CCR2^{+}$ myeloid cells in a heart transplant model prolonged allograft survival[376]. Notably, the prolongation of graft survival induced by depletion of $CCR2^{+}$ cells was similar to that triggered by ButM treatment. To determine if ButM prolonged allograft survival via its ability to decrease myeloid cell numbers and function, we co-treated mice with ButM and CCR2-depleting antibodies. No additive effects resulted from this co-administration, suggesting that the mechanism by which ButM slows allograft rejection kinetics is by its quantitative reduction of $CCR2^{+}$ myeloid cells. These

findings reinforce the notion that ButM likely improves allograft outcomes by systemically attenuating myeloid cells, which when recruited into the inflamed allograft are then less capable of executing the effector phase of alloimmunity.

Having recognized the advantageous role of butyrate in mitigating graft rejection prompts exploration into the potential of other microbial-derived metabolites to influence alloimmune responses. Beyond butyrate, numerous metabolites exhibit immunomodulatory properties, including the SCFAs acetate and propionate, along with secondary bile acids, long-chain fatty acids (LCFAs)[377], polysaccharides, and amino acids[289]. Exploring if these metabolites impact graft acceptance or rejection could yield valuable insights for refining current immunosuppressive protocols by fine-tuning alloimmune responses. Using rationally designed delivery platforms can be an efficient way to target these molecules to the correct location in the GI tract[197] or directly in the skin[355].

In summary, our use of a delivery system that effectively increases cecal butyrate levels enabled significant prolongation of minor- and major-mismatched skin allograft survival. The delivery of ButM did not influence Tregs or alloreactive conventional T cells but had a profound impact on the myeloid cell compartment. At steady-state, ButM treatment mediated a decrease in circulating $Ly6C^{hi}CD11b^{+}$ monocytes and other myeloid cells, changed the mitochondrial metabolism and key inflammatory processes, and reduced TNFα production upon LPS stimulation of myeloid cells. Furthermore, ButM's prolongation of allograft survival was dependent on the presence of $CCR2^{+}$ cells. These findings suggest that ButM enhances distal allograft outcomes by quantitatively and qualitatively modulating myeloid cells, thereby inhibiting the innate immune cell-mediated effector phase of the alloimmune response (Figure 6. 2, upper right quadrant).

References

1. Sherman, L. A. & Chattopadhyay, S. The Molecular Basis of Allorecognition. *Annu. Rev. Immunol.* **11**, 385–402 (1993).
2. Lakkis, F. G. Where Is the Alloimmune Response Initiated? *Am. J. Transplant.* **3**, 241–242 (2003).
3. Liu, Q. *et al.* Donor dendritic cell–derived exosomes promote allograft-targeting immune response. *J. Clin. Invest.* **126**, 2805–2820 (2016).
4. Barker, C. F. & Billingham, R. E. THE ROLE OF AFFERENT LYMPHATICS IN THE REJECTION OF SKIN HOMOGRAFTS. *J. Exp. Med.* **128**, 197–221 (1968).
5. Vetto, M. & Lawson, R. THE ROLE OF VASCULAR ENDOTHELIUM IN THE AFFERENT PATHWAY AS SUGGESTED BY THE ALYMPHATIC RENAL HOMOTRANS-PLANT. *Transplantation* **5**, 1537–1539 (1967).
6. Brent, L. & Medawar, P. B. CELLULAR IMMUNITY AND THE HOMOGRAFT REACTION. *Br. Med. Bull.* **23**, 55–59 (1967).
7. Snell, G. D. The Homograft Reaction. *Annu. Rev. Microbiol.* **11**, 439–458 (1957).
8. Collins, T. *et al.* Immune interferon activates multiple class II major histocompatibility complex genes and the associated invariant chain gene in human endothelial cells and dermal fibroblasts. *Proc. Natl. Acad. Sci.* **81**, 4917–4921 (1984).
9. Milton, A. D. & Fabre, J. W. Massive induction of donor-type class I and class II major histocompatibility complex antigens in rejecting cardiac allografts in the rat. *J. Exp. Med.* **161**, 98–112 (1985).
10. Kreisel, D. *et al.* Non-hematopoietic allograft cells directly activate CD8+ T cells and trigger acute rejection: An alternative mechanism of allorecognition. *Nat. Med.* **8**, 233–239 (2002).
11. Miyawaki, S. *et al.* A new mutation, aly, that induces a generalized lack of lymph nodes accompanied by immunodeficiency in mice. *Eur. J. Immunol.* **24**, 429–434 (1994).
12. Lakkis, F. G., Arakelov, A., Konieczny, B. T. & Inoue, Y. Immunologic 'ignorance' of vascularized organ transplants in the absence of secondary lymphoid tissue. *Nat. Med.* **6**, 686–688 (2000).
13. Zhou, P. *et al.* Secondary lymphoid organs are important but not absolutely required for allograft responses. *Am. J. Transplant. Off. J. Am. Soc. Transplant. Am. Soc. Transpl. Surg.* **3**, 259–266 (2003).
14. Fütterer, A., Mink, K., Luz, A., Kosco-Vilbois, M. H. & Pfeffer, K. The lymphotoxin beta receptor controls organogenesis and affinity maturation in peripheral lymphoid tissues. *Immunity* **9**, 59–70 (1998).
15. Chalasani, G., Dai, Z., Konieczny, B. T., Baddoura, F. K. & Lakkis, F. G. Recall and propagation of allospecific memory T cells independent of secondary lymphoid organs. *Proc. Natl. Acad. Sci.* **99**, 6175–6180 (2002).
16. Wang, J. *et al.* Donor Lymphoid Organs Are a Major Site of Alloreactive T-Cell Priming Following Intestinal Transplantation. *Am. J. Transplant.* **6**, 2563–2571 (2006).
17. Gould, D. S. & Auchincloss, H. Direct and indirect recognition: the role of MHC antigens in graft rejection. *Immunol. Today* **20**, 77–82 (1999).
18. Lafferty, K. J., Bootes, A., Dart, G. & Talmage, D. W. EFFECT OF ORGAN CULTURE ON THE SURVIVAL OF THYROID ALLOGRAFTS IN MICE. *Transplantation* **22**, 138–149 (1976).
19. Pietra, B. A., Wiseman, A., Bolwerk, A., Rizeq, M. & Gill, R. G. CD4 T cell–mediated cardiac allograft rejection requires donor but not host MHC class II. *J. Clin. Invest.* **106**, 1003–1010 (2000).
20. Brennan, T. V. *et al.* Preferential Priming of Alloreactive T Cells with Indirect Reactivity. *Am. J. Transplant.* **9**, 709–718 (2009).
21. Garrod, K. R. *et al.* NK Cell Patrolling and Elimination of Donor-Derived Dendritic Cells Favor Indirect Alloreactivity. *J. Immunol.* **184**, 2329–2336 (2010).

22. Auchincloss, H. *et al.* The role of 'indirect' recognition in initiating rejection of skin grafts from major histocompatibility complex class II-deficient mice. *Proc. Natl. Acad. Sci. U. S. A.* **90**, 3373–3377 (1993).
23. He, C. & Heeger, P. S. CD8 T cells can reject major histocompatibility complex class I-deficient skin allografts. *Am. J. Transplant. Off. J. Am. Soc. Transplant. Am. Soc. Transpl. Surg.* **4**, 698–704 (2004).
24. Valujskikh, A. & Heeger, P. S. CD4+ T cells responsive through the indirect pathway can mediate skin graft rejection in the absence of interferon-gamma. *Transplantation* **69**, 1016–1019 (2000).
25. Wise, M. *et al.* CD4 T cells can reject major histocompatibility complex class I-incompatible skin grafts. *Eur. J. Immunol.* **29**, 156–167 (1999).
26. Herrera, O. B. *et al.* A Novel Pathway of Alloantigen Presentation by Dendritic Cells. *J. Immunol.* **173**, 4828–4837 (2004).
27. Zeng, F. & Morelli, A. E. Extracellular vesicle-mediated MHC cross-dressing in immune homeostasis, transplantation, infectious diseases, and cancer. *Semin. Immunopathol.* **40**, 477–490 (2018).
28. Rocha, P. N., Plumb, T. J., Crowley, S. D. & Coffman, T. M. Effector mechanisms in transplant rejection. *Immunol. Rev.* **196**, 51–64 (2003).
29. Steiger, J., Nickerson, P. W., Steurer, W., Moscovitch-Lopatin, M. & Strom, T. B. IL-2 knockout recipient mice reject islet cell allografts. *J. Immunol. Baltim. Md 1950* **155**, 489–498 (1995).
30. Kishimoto, K. *et al.* Th1 cytokines, programmed cell death, and alloreactive T cell clone size in transplant tolerance. *J. Clin. Invest.* **109**, 1471–1479 (2002).
31. Piccotti, J. R. *et al.* Alloantigen-reactive Th1 development in IL-12-deficient mice. *J. Immunol. Baltim. Md 1950* **160**, 1132–1138 (1998).
32. Konieczny, B. T. *et al.* IFN-gamma is critical for long-term allograft survival induced by blocking the CD28 and CD40 ligand T cell costimulation pathways. *J. Immunol. Baltim. Md 1950* **160**, 2059–2064 (1998).
33. Dalloul, A. H., Chmouzis, E., Ngo, K. & Fung-Leung, W. P. Adoptively transferred CD4+ lymphocytes from CD8 -/- mice are sufficient to mediate the rejection of MHC class II or class I disparate skin grafts. *J. Immunol.* 7 (1996).
34. Valujskikh, A. *et al.* T cells reactive to a single immunodominant self-restricted allopeptide induce skin graft rejection in mice. *J. Clin. Invest.* **101**, 1398–1407 (1998).
35. Honjo, K., Xu, X. yan & Bucy, R. P. HETEROGENEITY OF T CELL CLONES SPECIFIC FOR A SINGLE INDIRECT ALLOANTIGENIC EPITOPE (I-Ab/H-2Kd54???68) THAT MEDIATE TRANSPLANT REJECTION1: *Transplantation* **70**, 1516–1524 (2000).
36. Honjo, K., Xu, X. yan & Bucy, R. P. CD4+ T-cell receptor transgenic T cells alone can reject vascularized heart transplants through the indirect pathway of alloantigen recognition: *Transplantation* **77**, 452–455 (2004).
37. Grazia, T. J. *et al.* A Two-Step Model of Acute CD4 T-Cell Mediated Cardiac Allograft Rejection. *J. Immunol.* **172**, 7451–7458 (2004).
38. Geppert, T. D. & Lipsky, P. E. Antigen presentation by interferon-gamma-treated endothelial cells and fibroblasts: differential ability to function as antigen-presenting cells despite comparable Ia expression. 14 (2004).
39. Hughes, A. D. *et al.* Cross-dressed dendritic cells sustain effector T cell responses in islet and kidney allografts. *J. Clin. Invest.* **130**, 287–294 (2019).
40. Baker, R. J. *et al.* Loss of Direct and Maintenance of Indirect Alloresponses in Renal Allograft Recipients: Implications for the Pathogenesis of Chronic Allograft Nephropathy. *J. Immunol.* **167**, 7199–7206 (2001).
41. Ali, J. M. *et al.* Diversity of the CD4 T Cell Alloresponse: The Short and the Long of It. *Cell Rep.* **14**, 1232–1245 (2016).
42. Koglin, J., Glysing-Jensen, T. & Russell, M. E. Th1 responses control development of graft vasculopathy: Insights from studies in STAT4-knock out mice. *Transplantation* **65**, 239 (1998).

43. Zhou, P. *et al.* Role of STAT4 and STAT6 signaling in allograft rejection and CTLA4-Ig-mediated tolerance. *J. Immunol. Baltim. Md 1950* **165**, 5580–5587 (2000).
44. Kishimoto, K. *et al.* The role of CD154-CD40 versus CD28-B7 costimulatory pathways in regulating allogeneic Th1 and Th2 responses in vivo. *J. Clin. Invest.* **106**, 63–72 (2000).
45. Taniuchi, I. CD4 Helper and CD8 Cytotoxic T Cell Differentiation. *Annu. Rev. Immunol.* **36**, 579–601 (2018).
46. Rosenberg, A. S., Mizuochi, T., Sharrow, S. O. & Singer, A. Phenotype, specificity, and function of T cell subsets and T cell interactions involved in skin allograft rejection. *J. Exp. Med.* **165**, 1296–1315 (1987).
47. Sutton, V. R. *et al.* Initiation of Apoptosis by Granzyme B Requires Direct Cleavage of Bid, but Not Direct Granzyme B–Mediated Caspase Activation. *J. Exp. Med.* **192**, 1403 (2000).
48. Russell, J. H. & Ley, T. J. Lymphocyte-Mediated Cytotoxicity. *Annu. Rev. Immunol.* **20**, 323–370 (2002).
49. de Saint Basile, G. & Fischer, A. The role of cytotoxicity in lymphocyte homeostasis. *Curr. Opin. Immunol.* **13**, 549–554 (2001).
50. Narula, J. *et al.* Annexin-V imaging for noninvasive detection of cardiac allograft rejection. *Nat. Med.* **7**, 1347–1352 (2001).
51. Kown, M. H. *et al.* Zinc-mediated reduction of apoptosis in cardiac allografts. *Circulation* **102**, III228-232 (2000).
52. Kägi, D. *et al.* Cytotoxicity mediated by T cells and natural killer cells is greatly impaired in perforin-deficient mice. *Nature* **369**, 31–37 (1994).
53. Kägi, D. *et al.* Fas and perforin pathways as major mechanisms of T cell-mediated cytotoxicity. *Science* **265**, 528–530 (1994).
54. Wever, P. C. *et al.* Mechanisms of lymphocyte-mediated cytotoxicity in acute renal allograft rejection. *Transplantation* **66**, 259–264 (1998).
55. Sleater, M., Diamond, A. S. & Gill, R. G. Islet Allograft Rejection by Contact-Dependent CD8+ T cells: Perforin and FasL Play Alternate but Obligatory Roles1. *Am. J. Transplant.* **7**, 1927–1933 (2007).
56. Diamond, A. S. & Gill, R. G. An essential contribution by IFN-gamma to CD8+ T cell-mediated rejection of pancreatic islet allografts. *J. Immunol. Baltim. Md 1950* **165**, 247–255 (2000).
57. Salvadori, M., Rosso, G. & Bertoni, E. Update on ischemia-reperfusion injury in kidney transplantation: Pathogenesis and treatment. **5**, 17 (2015).
58. El-Sawy, T., Fahmy, N. M. & Fairchild, R. L. Chemokines: directing leukocyte infiltration into allografts. *Curr. Opin. Immunol.* **14**, 562–568 (2002).
59. Gelman, A. E. *et al.* CCR2 Regulates Monocyte Recruitment As Well As $CD4^+$ T_h1 Allorecognition After Lung Transplantation. *Am. J. Transplant.* **10**, 1189–1199 (2010).
60. Li, L. *et al.* The chemokine receptors CCR2 and CX3CR1 mediate monocyte/macrophage trafficking in kidney ischemia–reperfusion injury. *Kidney Int.* **74**, 1526–1537 (2008).
61. Li, J. *et al.* The Evolving Roles of Macrophages in Organ Transplantation. *J. Immunol. Res.* **2019**, 1–11 (2019).
62. Geissmann, F. *et al.* Development of Monocytes, Macrophages, and Dendritic Cells. *Science* **327**, 656–661 (2010).
63. Tinckam, K. J., Djurdjev, O. & Magil, A. B. Glomerular monocytes predict worse outcomes after acute renal allograft rejection independent of C4d status. *Kidney Int.* **68**, 1866–1874 (2005).
64. Hoshinaga, K. *et al.* CLINICAL SIGNIFICANCE OF IN SITU DETECTION OF T LYMPHOCYTE SUBSETS AND MONOCYTE/MACROPHAGE LINEAGES IN HEART ALLOGRAFTS. *Transplantation* **38**, 634 (1984).
65. Hancock, W. W., Thomson, N. M. & Atkins, R. C. COMPOSITION OF INTERSTITIAL CELLULAR INFILTRATE IDENTIFIED BY MONOCLONAL ANTIBODIES IN RENAL BIOPSIES OF REJECTING HUMAN RENAL ALLOGRAFTS. *Transplantation* **35**, 458 (1983).

66. McLean, A. G. *et al.* PATTERNS OF GRAFT INFILTRATION AND CYTOKINE GENE EXPRESSION DURING THE FIRST 10 DAYS OF KIDNEY TRANSPLANTATION1. *Transplantation* **63**, 374 (1997).
67. Schreiner, G. F., Kamei, T., Lefkowith, J. & Flye, M. W. Modulation of the kinetics of the initial leukocyte migration into renal allografts by 16,16-dimethyl PGE2. *Transplantation* **56**, 417–422 (1993).
68. Jose, M. D., Ikezumi, Y., van Rooijen, N., Atkins, R. C. & Chadban, S. J. Macrophages act as effectors of tissue damage in acute renal allograft rejection: *Transplantation* **76**, 1015–1022 (2003).
69. Wu, Y. L. *et al.* Magnetic Resonance Imaging Investigation of Macrophages in Acute Cardiac Allograft Rejection After Heart Transplantation. *Circ. Cardiovasc. Imaging* **6**, 965–973 (2013).
70. Qi, F. *et al.* Depletion of Cells of Monocyte Lineage Prevents Loss of Renal Microvasculature in Murine Kidney Transplantation. *Transplantation* **86**, 1267 (2008).
71. Ma, F. Y., Woodman, N., Mulley, W. R., Kanellis, J. & Nikolic-Paterson, D. J. Macrophages Contribute to Cellular But Not Humoral Mechanisms of Acute Rejection in Rat Renal Allografts. *Transplantation* **96**, 949 (2013).
72. Ordikhani, F., Pothula, V., Sanchez-Tarjuelo, R., Jordan, S. & Ochando, J. Macrophages in Organ Transplantation. *Front. Immunol.* **11**, (2020).
73. Rowshani, A. T. & Vereyken, E. J. F. The Role of Macrophage Lineage Cells in Kidney Graft Rejection and Survival: *Transplant. J.* **94**, 309–318 (2012).
74. Zuckerbraun, B. S. *et al.* Carbon Monoxide Protects against Liver Failure through Nitric Oxide–induced Heme Oxygenase 1. *J. Exp. Med.* **198**, 1707–1716 (2003).
75. Vos, I. H. C. *et al.* Inhibition of inducible nitric oxide synthase improves graft function and reduces tubulointerstitial injury in renal allograft rejection. *Eur. J. Pharmacol.* **391**, 31–38 (2000).
76. Viola, A., Munari, F., Sánchez-Rodríguez, R., Scolaro, T. & Castegna, A. The Metabolic Signature of Macrophage Responses. *Front. Immunol.* **10**, (2019).
77. Garcia, M. R. *et al.* Monocytic suppressive cells mediate cardiovascular transplantation tolerance in mice. *J. Clin. Invest.* **120**, 2486–2496 (2010).
78. Conde, P. *et al.* DC-SIGN+ Macrophages Control the Induction of Transplantation Tolerance. *Immunity* **42**, 1143–1158 (2015).
79. Thaunat, O. & Nicoletti, A. Lymphoid neogenesis in chronic rejection: *Curr. Opin. Organ Transplant.* **13**, 16–19 (2008).
80. Ikezumi, Y. *et al.* Alternatively activated macrophages in the pathogenesis of chronic kidney allograft injury. *Pediatr. Nephrol.* **30**, 1007–1017 (2015).
81. Bergler, T. *et al.* Infiltration of Macrophages Correlates with Severity of Allograft Rejection and Outcome in Human Kidney Transplantation. *PLOS ONE* **11**, e0156900 (2016).
82. Dai, H. *et al.* Donor SIRP□ polymorphism modulates the innate immune response to allogeneic grafts. *Sci. Immunol.* 10 (2017).
83. Dai, H. *et al.* PIRs mediate innate myeloid cell memory to nonself MHC molecules. *Science* **368**, 1122–1127 (2020).
84. Stewart, C. J. *et al.* Temporal development of the gut microbiome in early childhood from the TEDDY study. *Nature* **562**, 583–588 (2018).
85. Rothschild, D. *et al.* Environment dominates over host genetics in shaping human gut microbiota. *Nature* **555**, 210–215 (2018).
86. Mazmanian, S. K., Liu, C. H., Tzianabos, A. O. & Kasper, D. L. An Immunomodulatory Molecule of Symbiotic Bacteria Directs Maturation of the Host Immune System. *Cell* **122**, 107–118 (2005).
87. Suh, S. H. *et al.* Gut microbiota regulates lacteal integrity by inducing VEGF-C in intestinal villus macrophages. *EMBO Rep.* **20**, e46927 (2019).
88. Nagashima, K. *et al.* Mapping the T cell repertoire to a complex gut bacterial community. *Nature* **621**, 162–170 (2023).
89. Bunker, J. J. *et al.* Innate and Adaptive Humoral Responses Coat Distinct Commensal Bacteria with Immunoglobulin A. *Immunity* **43**, 541–553 (2015).

90. Gaboriau-Routhiau, V. *et al.* The Key Role of Segmented Filamentous Bacteria in the Coordinated Maturation of Gut Helper T Cell Responses. *Immunity* **31**, 677–689 (2009).
91. Ivanov, I. I. *et al.* Induction of Intestinal Th17 Cells by Segmented Filamentous Bacteria. *Cell* **139**, 485–498 (2009).
92. Atarashi, K. *et al.* Induction of Colonic Regulatory T Cells by Indigenous Clostridium Species. *Science* **331**, 337–341 (2011).
93. Atarashi, K. *et al.* Treg induction by a rationally selected mixture of Clostridia strains from the human microbiota. *Nature* **500**, 232–236 (2013).
94. Shen, Y. *et al.* Outer Membrane Vesicles of a Human Commensal Mediate Immune Regulation and Disease Protection. *Cell Host Microbe* **12**, 509–520 (2012).
95. Wegorzewska, M. M. *et al.* Diet modulates colonic T cell responses by regulating the expression of a Bacteroides thetaiotaomicron antigen. *Sci. Immunol.* **4**, eaau9079 (2019).
96. Abt, M. C. *et al.* Commensal Bacteria Calibrate the Activation Threshold of Innate Antiviral Immunity. *Immunity* **37**, 158–170 (2012).
97. Lei, Y. M. *et al.* The composition of the microbiota modulates allograft rejection. *J. Clin. Invest.* **126**, 2736–2744 (2016).
98. Lee, Y. K., Menezes, J. S., Umesaki, Y. & Mazmanian, S. K. Proinflammatory T-cell responses to gut microbiota promote experimental autoimmune encephalomyelitis. *Proc. Natl. Acad. Sci. U. S. A.* **108 Suppl 1**, 4615–4622 (2011).
99. Wu, H.-J. *et al.* Gut-Residing Segmented Filamentous Bacteria Drive Autoimmune Arthritis via T Helper 17 Cells. *Immunity* **32**, 815–827 (2010).
100. Lei, Y. M. *et al.* Skin-restricted commensal colonization accelerates skin graft rejection. *JCI Insight* **4**, (2019).
101. Wu, Q. *et al.* Gut Microbiota Can Impact Chronic Murine Lung Allograft Rejection. *Am. J. Respir. Cell Mol. Biol.* **60**, 131–134 (2019).
102. Belkaid, Y. & Tamoutounour, S. The influence of skin microorganisms on cutaneous immunity. *Nat. Rev. Immunol.* **16**, 353–366 (2016).
103. Scharschmidt, T. C. *et al.* Commensal Microbes and Hair Follicle Morphogenesis Coordinately Drive Treg Migration into Neonatal Skin. *Cell Host Microbe* **21**, 467-477.e5 (2017).
104. Scharschmidt, T. C. *et al.* A Wave of Regulatory T Cells into Neonatal Skin Mediates Tolerance to Commensal Microbes. *Immunity* **43**, 1011–1021 (2015).
105. Naik, S. *et al.* Commensal–dendritic-cell interaction specifies a unique protective skin immune signature. *Nature* **520**, 104–108 (2015).
106. Linehan, J. L. *et al.* Non-classical Immunity Controls Microbiota Impact on Skin Immunity and Tissue Repair. *Cell* **172**, 784-796.e18 (2018).
107. Harrison, O. J. *et al.* Commensal-specific T cell plasticity promotes rapid tissue adaptation to injury. *Science* **363**, eaat6280 (2019).
108. Fricke, W. F., Maddox, C., Song, Y. & Bromberg, J. S. Human microbiota characterization in the course of renal transplantation. *Am. J. Transplant. Off. J. Am. Soc. Transplant. Am. Soc. Transpl. Surg.* **14**, 416–427 (2014).
109. Oh, P. L. *et al.* Characterization of the Ileal Microbiota in Rejecting and Nonrejecting Recipients of Small Bowel Transplants: Microbiota Changes Associated with Intestinal Allograft Rejection. *Am. J. Transplant.* **12**, 753–762 (2012).
110. Willner, D. L. *et al.* Reestablishment of recipient-associated microbiota in the lung allograft is linked to reduced risk of bronchiolitis obliterans syndrome. *Am. J. Respir. Crit. Care Med.* **187**, 640–647 (2013).
111. Weigt, S. S. *et al.* Colonization with small conidia Aspergillus species is associated with bronchiolitis obliterans syndrome: a two-center validation study. *Am. J. Transplant. Off. J. Am. Soc. Transplant. Am. Soc. Transpl. Surg.* **13**, 919–927 (2013).
112. Wu, J. F. *et al.* Urinary microbiome associated with chronic allograft dysfunction in kidney transplant recipients. *Clin. Transplant.* **32**, e13436 (2018).

113. Kato, K. *et al.* Longitudinal Analysis of the Intestinal Microbiota in Liver Transplantation. *Transplant. Direct* **3**, e144 (2017).
114. Nakamura, K. *et al.* Antibiotic pretreatment alleviates liver transplant damage in mice and humans. *J. Clin. Invest.* **129**, 3420–3434 (2019).
115. Schaupp, L. *et al.* Microbiota-Induced Type I Interferons Instruct a Poised Basal State of Dendritic Cells. *Cell* **181**, 1080-1096.e19 (2020).
116. Rey, K. *et al.* Disruption of the Gut Microbiota With Antibiotics Exacerbates Acute Vascular Rejection. *Transplantation* **102**, 1085–1095 (2018).
117. McIntosh, C. M., Chen, L., Shaiber, A., Eren, A. M. & Alegre, M.-L. Gut microbes contribute to variation in solid organ transplant outcomes in mice. *Microbiome* **6**, 96 (2018).
118. Guo, Y. *et al.* Vendor-specific microbiome controls both acute and chronic murine lung allograft rejection by altering CD4+ Foxp3+ regulatory T cell levels. *Am. J. Transplant. Off. J. Am. Soc. Transplant. Am. Soc. Transpl. Surg.* **19**, 2705–2718 (2019).
119. Alegre, M.-L. Mouse microbiomes: overlooked culprits of experimental variability. *Genome Biol.* **20**, 108 (2019).
120. Zhang, Z. *et al.* Immunosuppressive effect of the gut microbiome altered by high-dose tacrolimus in mice. *Am. J. Transplant.* **18**, 1646–1656 (2018).
121. Bromberg, J. S. *et al.* Gut microbiota-dependent modulation of innate immunity and lymph node remodeling affects cardiac allograft outcomes. *JCI Insight* **3**, (2018).
122. Mouraux, S. *et al.* Airway microbiota signals anabolic and catabolic remodeling in the transplanted lung. *J. Allergy Clin. Immunol.* **141**, 718-729.e7 (2018).
123. Belperio, J., Palmer, S. M. & Weigt, S. S. Host–Pathogen Interactions and Chronic Lung Allograft Dysfunction. *Ann. Am. Thorac. Soc.* **14**, S242–S246 (2017).
124. Riquelme, E. *et al.* Tumor Microbiome Diversity and Composition Influence Pancreatic Cancer Outcomes. *Cell* **178**, 795-806.e12 (2019).
125. Byrd, A. L., Belkaid, Y. & Segre, J. A. The human skin microbiome. *Nat. Rev. Microbiol.* **16**, 143–155 (2018).
126. Gensollen, T., Iyer, S. S., Kasper, D. L. & Blumberg, R. S. How colonization by microbiota in early life shapes the immune system. *Science* **352**, 539–544 (2016).
127. Pirozzolo, I. *et al.* Host-versus-commensal immune responses participate in the rejection of colonized solid organ transplants. https://www.jci.org/articles/view/153403/pdf (2022) doi:10.1172/JCI153403.
128. Amir, A. L. *et al.* Allo-HLA reactivity of virus-specific memory T cells is common. *Blood* **115**, 3146–3157 (2010).
129. Fluckiger, A. *et al.* Cross-reactivity between tumor MHC class I–restricted antigens and an enterococcal bacteriophage. *Science* **369**, 936–942 (2020).
130. Gil-Cruz, C. *et al.* Microbiota-derived peptide mimics drive lethal inflammatory cardiomyopathy. *Science* **366**, 881–886 (2019).
131. Kim, J. E. *et al.* Effect of the similarity of gut microbiota composition between donor and recipient on graft function after living donor kidney transplantation. *Sci. Rep.* **10**, 18881 (2020).
132. Thaiss, C. A. *et al.* Hyperglycemia drives intestinal barrier dysfunction and risk for enteric infection. 9 (2018).
133. Rooks, M. G. & Garrett, W. S. Gut microbiota, metabolites and host immunity. *Nat. Rev. Immunol.* **16**, 341–352 (2016).
134. Walker, A. *et al.* Sulfonolipids as novel metabolite markers of Alistipes and Odoribacter affected by high-fat diets. *Sci. Rep.* **7**, 11047 (2017).
135. Maeda et al. Inhibitory effects of sulfobacin B on DNA polymerase and inflammation. *Int. J. Mol. Med.* **26**, (2010).
136. Michonneau, D. *et al.* Metabolomics analysis of human acute graft-versus-host disease reveals changes in host and microbiota-derived metabolites. *Nat. Commun.* **10**, 5695 (2019).

137. Chen, H. *et al.* A Forward Chemical Genetic Screen Reveals Gut Microbiota Metabolites That Modulate Host Physiology. *Cell* **177**, 1217-1231.e18 (2019).
138. Mager, L. F. *et al.* Microbiome-derived inosine modulates response to checkpoint inhibitor immunotherapy. *Science* **369**, 1481–1489 (2020).
139. van der Hee, B. & Wells, J. M. Microbial Regulation of Host Physiology by Short-chain Fatty Acids. *Trends Microbiol.* **29**, 700–712 (2021).
140. Smith, P. M. *et al.* The Microbial Metabolites, Short-Chain Fatty Acids, Regulate Colonic Treg Cell Homeostasis. *Science* **341**, 569–573 (2013).
141. Furusawa, Y. *et al.* Commensal microbe-derived butyrate induces the differentiation of colonic regulatory T cells. *Nature* **504**, 446–450 (2013).
142. Wu, H. *et al.* Absence of MyD88 Signaling Induces Donor-Specific Kidney Allograft Tolerance. *J. Am. Soc. Nephrol. JASN* **23**, 1701–1716 (2012).
143. Hang, S. *et al.* Bile acid metabolites control TH17 and Treg cell differentiation. *Nature* **576**, 143–148 (2019).
144. Campbell, C. *et al.* Bacterial metabolism of bile acids promotes generation of peripheral regulatory T cells. *Nature* **581**, 475–479 (2020).
145. Aguilar-Toalá, J. E. *et al.* Postbiotics: An evolving term within the functional foods field. *Trends Food Sci. Technol.* **75**, 105–114 (2018).
146. Li, X. S. *et al.* Untargeted metabolomics identifies trimethyllysine, a TMAO-producing nutrient precursor, as a predictor of incident cardiovascular disease risk. *JCI Insight* **3**, e99096 (2018).
147. Nemet, I. *et al.* A Cardiovascular Disease-Linked Gut Microbial Metabolite Acts via Adrenergic Receptors. *Cell* **180**, 862-877.e22 (2020).
148. Gregory, J. C. *et al.* Transmission of Atherosclerosis Susceptibility with Gut Microbial Transplantation. *J. Biol. Chem.* **290**, 5647–5660 (2015).
149. Dela Cruz, M. *et al.* Reduced immunomodulatory metabolite concentrations in peri-transplant fecal samples from heart allograft recipients. *Front. Transplant.* **2**, (2023).
150. Lehmann, C. J. *et al.* Fecal metabolite profiling identifies liver transplant recipients at risk for postoperative infection. *Cell Host Microbe* **32**, 117-130.e4 (2024).
151. Maier, L. *et al.* Extensive impact of non-antibiotic drugs on human gut bacteria. *Nature* **555**, 623–628 (2018).
152. Tourret, J. *et al.* Immunosuppressive Treatment Alters Secretion of Ileal Antimicrobial Peptides and Gut Microbiota, and Favors Subsequent Colonization by Uropathogenic Escherichia coli: *Transplantation* **101**, 74–82 (2017).
153. Flannigan, K. L. *et al.* An intact microbiota is required for the gastrointestinal toxicity of the immunosuppressant mycophenolate mofetil. *J. Heart Lung Transplant.* **37**, 1047–1059 (2018).
154. Jia, J. *et al.* Structural shifts in the intestinal microbiota of rats treated with cyclosporine A after orthotropic liver transplantation. *Front. Med.* **13**, 451–460 (2019).
155. Zimmermann, M., Zimmermann-Kogadeeva, M., Wegmann, R. & Goodman, A. L. Mapping human microbiome drug metabolism by gut bacteria and their genes. *Nature* **570**, 462–467 (2019).
156. Koppel, N., Bisanz, J. E., Pandelia, M.-E., Turnbaugh, P. J. & Balskus, E. P. Discovery and characterization of a prevalent human gut bacterial enzyme sufficient for the inactivation of a family of plant toxins. *eLife* **7**, e33953 (2018).
157. Lee, J. R. *et al.* Gut Microbiota and Tacrolimus Dosing in Kidney Transplantation. *PLOS ONE* **10**, e0122399 (2015).
158. Guo, Y. *et al.* Commensal Gut Bacteria Convert the Immunosuppressant Tacrolimus to Less Potent Metabolites. *Drug Metab. Dispos.* **47**, 194–202 (2019).
159. Chamseddine, A. N. *et al.* Intestinal bacterial β-glucuronidase as a possible predictive biomarker of irinotecan-induced diarrhea severity. *Pharmacol. Ther.* **199**, 1–15 (2019).
160. Zhang, D. *et al.* Microbial bile acid metabolite ameliorates mycophenolate mofetil-induced gastrointestinal toxicity through vitamin D3 receptor. *Am. J. Transplant. Off. J. Am. Soc. Transplant. Am. Soc. Transpl. Surg.* S1600-6135(24)00171–0 (2024) doi:10.1016/j.ajt.2024.02.029.

161. Modena, B. D. *et al.* Changes in Urinary Microbiome Populations Correlate in Kidney Transplants With Interstitial Fibrosis and Tubular Atrophy Documented in Early Surveillance Biopsies. *Am. J. Transplant.* **17**, 712–723 (2017).
162. Colas, L. *et al.* Unique and specific *Proteobacteria* diversity in urinary microbiota of tolerant kidney transplanted recipients. *Am. J. Transplant.* **20**, 145–158 (2020).
163. Gut microbiota in renal transplant recipients, patients with chronic kidney disease and healthy subjects. *J. South. Med. Univ.* **38**, 1401–1408 (2018).
164. Matson, V. *et al.* The commensal microbiome is associated with anti–PD-1 efficacy in metastatic melanoma patients. *Science* **359**, 104–108 (2018).
165. Routy, B. *et al.* Gut microbiome influences efficacy of PD-1–based immunotherapy against epithelial tumors. *Science* **359**, 91–97 (2018).
166. Gopalakrishnan, V. *et al.* Gut microbiome modulates response to anti-PD-1 immunotherapy in melanoma patients. *Science* **359**, 97–103 (2018).
167. Zhao, L. *et al.* Gut bacteria selectively promoted by dietary fibers alleviate type 2 diabetes. *Science* **359**, 1151–1156 (2018).
168. Yuan, J., Bagley, J. & Iacomini, J. Hyperlipidemia Promotes Anti-Donor Th17 Responses That Accelerate Allograft Rejection. *Am. J. Transplant. Off. J. Am. Soc. Transplant. Am. Soc. Transpl. Surg.* **15**, 2336–2345 (2015).
169. Safa, K. *et al.* Salt Accelerates Allograft Rejection through Serum- and Glucocorticoid-Regulated Kinase-1–Dependent Inhibition of Regulatory T Cells. *J. Am. Soc. Nephrol. JASN* **26**, 2341–2347 (2015).
170. Molinero, L. High Fat Diet-induced Obesity Enhances Allograft Rejection - PMC. https://www.ncbi.nlm.nih.gov/pmc/articles/PMC4846555/.
171. Bagley, J., Yuan, J., Chandrakar, A. & Iacomini, J. Hyperlipidemia Alters Regulatory T Cell Function and Promotes Resistance to Tolerance Induction Through Costimulatory Molecule Blockade. *Am. J. Transplant. Off. J. Am. Soc. Transplant. Am. Soc. Transpl. Surg.* **15**, 2324–2335 (2015).
172. Scheiman, J. *et al.* Meta-omics analysis of elite athletes identifies a performance-enhancing microbe that functions via lactate metabolism. *Nat. Med.* **25**, 1104–1109 (2019).
173. Rael, V. E., Chen, L., McIntosh, C. M. & Alegre, M. Exercise increases skin graft resistance to rejection. *Am. J. Transplant.* **19**, 1560–1567 (2019).
174. Li, Z. *et al.* Microbiota-dependent and -independent effects of obesity on transplant rejection and hyperglycemia. *Am. J. Transplant.* (2023) doi:10.1016/j.ajt.2023.06.011.
175. van Nood, E. *et al.* Duodenal infusion of donor feces for recurrent Clostridium difficile. *N. Engl. J. Med.* **368**, 407–415 (2013).
176. DeFilipp, Z. *et al.* Third-party fecal microbiota transplantation following allo-HCT reconstitutes microbiome diversity. *Blood Adv.* **2**, 745–753 (2018).
177. Taur, Y. *et al.* Intestinal domination and the risk of bacteremia in patients undergoing allogeneic hematopoietic stem cell transplantation. *Clin. Infect. Dis. Off. Publ. Infect. Dis. Soc. Am.* **55**, 905–914 (2012).
178. Zmora, N. *et al.* Personalized Gut Mucosal Colonization Resistance to Empiric Probiotics Is Associated with Unique Host and Microbiome Features. *Cell* **174**, 1388-1405.e21 (2018).
179. Shepherd, E. S., DeLoache, W. C., Pruss, K. M., Whitaker, W. R. & Sonnenburg, J. L. An exclusive metabolic niche enables strain engraftment in the gut microbiota. *Nature* **557**, 434–438 (2018).
180. Li, Z. *et al.* Oral administration of the commensal Alistipes onderdonkii prolongs allograft survival. *Am. J. Transplant.* **23**, 272–277 (2023).
181. Sepulveda, M. *et al.* Coordinated elimination of bacterial taxa optimally attenuates alloimmunity and prolongs allograft survival. *Am. J. Transplant.* (2024) doi:10.1016/j.ajt.2024.03.020.
182. Ren, Z.-G. *et al.* Protective effect of probiotics on intestinal barrier function in malnourished rats after liver transplantation. *Hepatobiliary Pancreat. Dis. Int.* **10**, 489–496 (2011).

183. Rayes, N. *et al.* Early enteral supply of lactobacillus and fiber versus selective bowel decontamination: a controlled trial in liver transplant recipients. *Transplantation* **74**, 123 (2002).
184. Rayes, N. *et al.* Supply of pre- and probiotics reduces bacterial infection rates after liver transplantation--a randomized, double-blind trial. *Am. J. Transplant. Off. J. Am. Soc. Transplant. Am. Soc. Transpl. Surg.* **5**, 125–130 (2005).
185. Sivan, A. *et al.* Commensal Bifidobacterium promotes antitumor immunity and facilitates anti–PD-L1 efficacy. *Science* **350**, 1084–1089 (2015).
186. Baruch, E. N. *et al.* Fecal microbiota transplant promotes response in immunotherapy-refractory melanoma patients. *Science* **371**, 602–609 (2021).
187. Davar, D. *et al.* Fecal microbiota transplant overcomes resistance to anti–PD-1 therapy in melanoma patients. *Science* **371**, 595–602 (2021).
188. Sorbara, M. T. & Pamer, E. G. Microbiome-based therapeutics. *Nat. Rev. Microbiol.* **20**, 365–380 (2022).
189. Ratiner, K., Ciocan, D., Abdeen, S. K. & Elinav, E. Utilization of the microbiome in personalized medicine. *Nat. Rev. Microbiol.* 1–18 (2023) doi:10.1038/s41579-023-00998-9.
190. Abbas, A. A. *et al.* The Perioperative Lung Transplant Virome: Torque Teno Viruses Are Elevated in Donor Lungs and Show Divergent Dynamics in Primary Graft Dysfunction. *Am. J. Transplant. Off. J. Am. Soc. Transplant. Am. Soc. Transpl. Surg.* **17**, 1313–1324 (2017).
191. Young, J. C. *et al.* Viral metagenomics reveal blooms of anelloviruses in the respiratory tract of lung transplant recipients. *Am. J. Transplant. Off. J. Am. Soc. Transplant. Am. Soc. Transpl. Surg.* **15**, 200–209 (2015).
192. Sigdel, T. K. *et al.* Urinary Virome Perturbations in Kidney Transplantation. *Front. Med.* **5**, 72 (2018).
193. Rani, A. *et al.* A diverse virome in kidney transplant patients contains multiple viral subtypes with distinct polymorphisms. *Sci. Rep.* **6**, 33327 (2016).
194. Kelly, J. M. *et al.* Identification of conserved T cell receptor CDR3 residues contacting known exposed peptide side chains from a major histocompatibility complex class I-bound determinant. *Eur. J. Immunol.* **23**, 3318–3326 (1993).
195. Haak, B. W. *et al.* Impact of gut colonization with butyrate-producing microbiota on respiratory viral infection following allo-HCT. *Blood* **131**, 2978–2986 (2018).
196. Theriault, B. *et al.* Long-term Maintenance of Sterility Following Skin Transplantation in Germ-free Mice. *Transplant. Direct* **1**, e28 (2015).
197. Wang, R. *et al.* Treatment of peanut allergy and colitis in mice via the intestinal release of butyrate from polymeric micelles. *Nat. Biomed. Eng.* **7**, 38–55 (2023).
198. Vanholder, R. *et al.* Organ donation and transplantation: a multi-stakeholder call to action. *Nat. Rev. Nephrol.* **17**, 554–568 (2021).
199. Moreau, A., Varey, E., Anegon, I. & Cuturi, M.-C. Effector Mechanisms of Rejection. *Cold Spring Harb. Perspect. Med.* **3**, a015461 (2013).
200. Pirozzolo, I., Li, Z., Sepulveda, M. & Alegre, M.-L. Influence of the microbiome on solid organ transplant survival. *J. Heart Lung Transplant.* **40**, 745–753 (2021).
201. Sepulveda, M., Pirozzolo, I. & Alegre, M.-L. Impact of the microbiota on solid organ transplant rejection: *Curr. Opin. Organ Transplant.* **24**, 679–686 (2019).
202. Belkaid, Y. & Hand, T. W. Role of the Microbiota in Immunity and Inflammation. *Cell* **157**, 121–141 (2014).
203. Chen, L. *et al.* Influence of the microbiome, diet and genetics on inter-individual variation in the human plasma metabolome. *Nat. Med.* **28**, 2333–2343 (2022).
204. Bar, N. *et al.* A reference map of potential determinants for the human serum metabolome. *Nature* **588**, 135–140 (2020).
205. Ganal, S. C. *et al.* Priming of Natural Killer Cells by Nonmucosal Mononuclear Phagocytes Requires Instructive Signals from Commensal Microbiota. *Immunity* **37**, 171–186 (2012).

206. Berer, K. *et al.* Commensal microbiota and myelin autoantigen cooperate to trigger autoimmune demyelination. *Nature* **479**, 538–541 (2011).
207. Horai, R. *et al.* Microbiota-Dependent Activation of an Autoreactive T Cell Receptor Provokes Autoimmunity in an Immunologically Privileged Site. *Immunity* **43**, 343–353 (2015).
208. Vétizou, M. *et al.* Anticancer immunotherapy by CTLA-4 blockade relies on the gut microbiota. *Science* **350**, 1079–1084 (2015).
209. Griffin, M. E. *et al.* Enterococcus peptidoglycan remodeling promotes checkpoint inhibitor cancer immunotherapy. *Science* **373**, 1040–1046 (2021).
210. Lam, K. C. *et al.* Microbiota triggers STING-type I IFN-dependent monocyte reprogramming of the tumor microenvironment. *Cell* **184**, 5338-5356.e21 (2021).
211. Mirji, G. *et al.* The microbiome-derived metabolite TMAO drives immune activation and boosts responses to immune checkpoint blockade in pancreatic cancer. *Sci. Immunol.* **7**, eabn0704 (2022).
212. Wu, Q. *et al.* Gut Microbiota Can Impact Chronic Murine Lung Allograft Rejection. *Am. J. Respir. Cell Mol. Biol.* **60**, 131–134 (2018).
213. Kohanski, M. A., Dwyer, D. J. & Collins, J. J. How antibiotics kill bacteria: from targets to networks. *Nat. Rev. Microbiol.* **8**, 423–435 (2010).
214. Freeman, C. D., Klutman, N. E. & Lamp, K. C. Metronidazole. *Drugs* **54**, 679–708 (1997).
215. El-Sayed Ahmed, M. A. E.-G. *et al.* Colistin and its role in the Era of antibiotic resistance: an extended review (2000–2019). *Emerg. Microbes Infect.* **9**, 868–885 (2020).
216. Swarte, J. C. *et al.* Characteristics and Dysbiosis of the Gut Microbiome in Renal Transplant Recipients. *J. Clin. Med.* **9**, 386 (2020).
217. Swarte, J. C. *et al.* Gut microbiome dysbiosis is associated with increased mortality after solid organ transplantation. *Sci. Transl. Med.* **14**, eabn7566 (2022).
218. Baghai Arassi, M., Zeller, G., Karcher, N., Zimmermann, M. & Toenshoff, B. The gut microbiome in solid organ transplantation. *Pediatr. Transplant.* **24**, e13866 (2020).
219. Annavajhala, M. K. *et al.* Colonizing multidrug-resistant bacteria and the longitudinal evolution of the intestinal microbiome after liver transplantation. *Nat. Commun.* **10**, 4715 (2019).
220. Vich Vila, A. *et al.* Impact of commonly used drugs on the composition and metabolic function of the gut microbiota. *Nat. Commun.* **11**, 362 (2020).
221. Thoo, L., Noti, M. & Krebs, P. Keep calm: the intestinal barrier at the interface of peace and war. *Cell Death Dis.* **10**, 849 (2019).
222. Falony, G. *et al.* Population-level analysis of gut microbiome variation. *Science* **352**, 560–564 (2016).
223. Kverka, M. *et al.* Oral administration of Parabacteroides distasonis antigens attenuates experimental murine colitis through modulation of immunity and microbiota composition. *Clin. Exp. Immunol.* **163**, 250–259 (2011).
224. Wang, K. *et al.* Parabacteroides distasonis Alleviates Obesity and Metabolic Dysfunctions via Production of Succinate and Secondary Bile Acids. *Cell Rep.* **26**, 222-235.e5 (2019).
225. Ezeji, J. C. *et al.* Parabacteroides distasonis: intriguing aerotolerant gut anaerobe with emerging antimicrobial resistance and pathogenic and probiotic roles in human health. *Gut Microbes* **13**, 1922241 (2021).
226. Zhao, Q. *et al.* Parabacteroides distasonis ameliorates hepatic fibrosis potentially via modulating intestinal bile acid metabolism and hepatocyte pyroptosis in male mice. *Nat. Commun.* **14**, 1829 (2023).
227. Wei, W. *et al.* Parabacteroides distasonis uses dietary inulin to suppress NASH via its metabolite pentadecanoic acid. *Nat. Microbiol.* **8**, 1534–1548 (2023).
228. Brubaker, S. W., Bonham, K. S., Zanoni, I. & Kagan, J. C. Innate Immune Pattern Recognition: A Cell Biological Perspective. *Annu. Rev. Immunol.* **33**, 257–290 (2015).
229. Li, D. & Wu, M. Pattern recognition receptors in health and diseases. *Signal Transduct. Target. Ther.* **6**, 1–24 (2021).

230. Paul-Clark, M. J., Sorrentino, R., Bailey, L. K., Sriskandan, S. & Mitchell, J. A. Gram-positive and Gram-negative bacteria synergize with oxidants to release CXCL8 from innate immune cells. *Mol. Med. Camb. Mass* **14**, 238–246 (2008).
231. Elson, G., Dunn-Siegrist, I., Daubeuf, B. & Pugin, J. Contribution of Toll-like receptors to the innate immune response to Gram-negative and Gram-positive bacteria. *Blood* **109**, 1574–1583 (2007).
232. Liu, T., Zhang, L., Joo, D. & Sun, S.-C. NF-κB signaling in inflammation. *Signal Transduct. Target. Ther.* **2**, 1–9 (2017).
233. McNab, F., Mayer-Barber, K., Sher, A., Wack, A. & O'Garra, A. Type I interferons in infectious disease. *Nat. Rev. Immunol.* **15**, 87–103 (2015).
234. Lee, S.-H. *et al.* Bifidobacterium bifidum strains synergize with immune checkpoint inhibitors to reduce tumour burden in mice. *Nat. Microbiol.* **6**, 277–288 (2021).
235. Lontchi-Yimagou, E., Sobngwi, E., Matsha, T. E. & Kengne, A. P. Diabetes Mellitus and Inflammation. *Curr. Diab. Rep.* **13**, 435–444 (2013).
236. Singh, N. *et al.* Inflammation and cancer. *Ann. Afr. Med.* **18**, 121–126 (2019).
237. Eren, A. M. *et al.* Community-led, integrated, reproducible multi-omics with anvi'o. *Nat. Microbiol.* **6**, 3–6 (2021).
238. Eren, A. M. *et al.* Anvi'o: an advanced analysis and visualization platform for 'omics data. *PeerJ* **3**, e1319 (2015).
239. Kanehisa, M. & Goto, S. KEGG: Kyoto Encyclopedia of Genes and Genomes. *Nucleic Acids Res.* **28**, 27–30 (2000).
240. Cao, H. & Chen, X. General Consideration on Sialic Acid Chemistry. in *Carbohydrate Microarrays: Methods and Protocols* (ed. Chevolot, Y.) 31–56 (Humana Press, Totowa, NJ, 2012). doi:10.1007/978-1-61779-373-8_3.
241. Parker, B. J., Wearsch, P. A., Veloo, A. C. M. & Rodriguez-Palacios, A. The Genus Alistipes: Gut Bacteria With Emerging Implications to Inflammation, Cancer, and Mental Health. *Front. Immunol.* **11**, (2020).
242. Rau, M. *et al.* Fecal SCFAs and SCFA-producing bacteria in gut microbiome of human NAFLD as a putative link to systemic T-cell activation and advanced disease. *United Eur. Gastroenterol. J.* **6**, 1496–1507 (2018).
243. Oliphant, K. & Allen-Vercoe, E. Macronutrient metabolism by the human gut microbiome: Major fermentation by-products and their impact on host health. *Microbiome* **7**, (2019).
244. Polansky, O. *et al.* Important Metabolic Pathways and Biological Processes Expressed by Chicken Cecal Microbiota. *Appl. Environ. Microbiol.* **82**, 1569–1576 (2016).
245. Mao, Y. *et al.* A pilot study of GC/MS-based serum metabolic profiling of acute rejection in renal transplantation. *Transpl. Immunol.* **19**, 74–80 (2008).
246. Macauley, M. S., Crocker, P. R. & Paulson, J. C. Siglec-mediated regulation of immune cell function in disease. *Nat. Rev. Immunol.* **14**, 653–666 (2014).
247. Han, Z. *et al.* Identification of an N-acetylneuraminic acid-presenting bacteria isolated from a human microbiome. *Sci. Rep.* **11**, 4763 (2021).
248. Guarner, F. & Malagelada, J.-R. Gut flora in health and disease. *The Lancet* **361**, 512–519 (2003).
249. Wilmore, J. R. *et al.* Commensal Microbes Induce Serum IgA Responses that Protect against Polymicrobial Sepsis. *Cell Host Microbe* **23**, 302-311.e3 (2018).
250. Teng, F. *et al.* Gut Microbiota Drive Autoimmune Arthritis by Promoting Differentiation and Migration of Peyer's Patch T Follicular Helper Cells. *Immunity* **44**, 875–888 (2016).
251. Naik, S. *et al.* Compartmentalized control of skin immunity by resident commensals. *Science* **337**, 1115–1119 (2012).
252. Atalar, K., Afzali, B., Lord, G. & Lombardi, G. Relative roles of Th1 and Th17 effector cells in allograft rejection. *Curr. Opin. Organ Transplant.* **14**, 23 (2009).
253. Wang, J. H., Skeans, M. A. & Israni, A. K. Current Status of Kidney Transplant Outcomes: Dying to Survive. *Adv. Chronic Kidney Dis.* **23**, 281–286 (2016).

254. Wilhelm, M. J. Long-term outcome following heart transplantation: current perspective. *J. Thorac. Dis.* **7**, 549–551 (2015).
255. Stacy, A. & Belkaid, Y. Microbial guardians of skin health. *Science* **363**, 227–228 (2019).
256. Weiner, J. *et al.* Long-term Persistence of Innate Lymphoid Cells in the Gut After Intestinal Transplantation. *Transplantation* **101**, 2449 (2017).
257. Snyder, M. E. & Farber, D. L. Human lung tissue resident memory T cells in health and disease. *Curr. Opin. Immunol.* **59**, 101–108 (2019).
258. Snyder, M. E. *et al.* Generation and persistence of human tissue-resident memory T cells in lung transplantation. *Sci. Immunol.* **4**, eaav5581 (2019).
259. Belheouane, M. *et al.* Assessing similarities and disparities in the skin microbiota between wild and laboratory populations of house mice. *ISME J.* **14**, 2367–2380 (2020).
260. Hirai, T. *et al.* Competition for Active TGFβ Cytokine Allows for Selective Retention of Antigen-Specific Tissue- Resident Memory T Cells in the Epidermal Niche. *Immunity* **54**, 84-98.e5 (2021).
261. Masopust, D. & Soerens, A. G. Tissue-Resident T Cells and Other Resident Leukocytes. *Annu. Rev. Immunol.* **37**, 521–546 (2019).
262. Hobbs, S. J. & Nolz, J. C. Targeted Expansion of Tissue-Resident CD8+ T Cells to Boost Cellular Immunity in the Skin. *Cell Rep.* **29**, 2990-2997.e2 (2019).
263. Lai, J. C. Y. *et al.* Topical Adjuvant Application during Subcutaneous Vaccination Promotes Resident Memory T Cell Generation. *J. Immunol.* **203**, 2443–2450 (2019).
264. Sun, Y. *et al.* Staphylococcal Protein A Contributes to Persistent Colonization of Mice with Staphylococcus aureus. *J. Bacteriol.* **200**, e00735-17 (2018).
265. Chun, J. & Hartung, H.-P. Mechanism of Action of Oral Fingolimod (FTY720) in Multiple Sclerosis. *Clin. Neuropharmacol.* **33**, 91 (2010).
266. Suthanthiran, M., Morris, R. E. & Strom, T. B. Immunosuppressants: Cellular and molecular mechanisms of action. *Am. J. Kidney Dis.* **28**, 159–172 (1996).
267. Jiang, X. *et al.* Skin infection generates non-migratory memory CD8+ TRM cells providing global skin immunity. *Nature* **483**, 227–231 (2012).
268. Dijkgraaf, F. E. *et al.* Tissue patrol by resident memory CD8+ T cells in human skin. *Nat. Immunol.* **20**, 756–764 (2019).
269. Zaid, A. *et al.* Chemokine Receptor–Dependent Control of Skin Tissue–Resident Memory T Cell Formation. *J. Immunol.* **199**, 2451–2459 (2017).
270. Menares, E. *et al.* Tissue-resident memory CD8+ T cells amplify anti-tumor immunity by triggering antigen spreading through dendritic cells. *Nat. Commun.* **10**, 4401 (2019).
271. Klicznik, M. M. *et al.* Human CD4+CD103+ cutaneous resident memory T cells are found in the circulation of healthy individuals. *Sci. Immunol.* **4**, eaav8995 (2019).
272. Bromley, S. K., Yan, S., Tomura, M., Kanagawa, O. & Luster, A. D. Recirculating Memory T Cells Are a Unique Subset of CD4+ T Cells with a Distinct Phenotype and Migratory Pattern. *J. Immunol.* **190**, 970–976 (2013).
273. Schreiner, D. & King, C. G. CD4+ Memory T Cells at Home in the Tissue: Mechanisms for Health and Disease. *Front. Immunol.* **9**, 2394 (2018).
274. Burnet, F. M. "Self-recognition" in Colonial Marine Forms and Flowering Plants in relation to the Evolution of Immunity. *Nature* **232**, 230–235 (1971).
275. Hildemann, W. H. Some new concepts in immunological phylogeny. *Nature* **250**, 116–120 (1974).
276. Klein, J. Self-nonself discrimination, histoincompatibility, and the concept of immunology. *Immunogenetics* **50**, 116–123 (1999).
277. Oberbarnscheidt, M. H. *et al.* Non-self recognition by monocytes initiates allograft rejection. *J. Clin. Invest.* **124**, 3579–3589 (2014).
278. Zecher, D., van Rooijen, N., Rothstein, D. M., Shlomchik, W. D. & Lakkis, F. G. An Innate Response to Allogeneic Nonself Mediated by Monocytes1. *J. Immunol.* **183**, 7810–7816 (2009).
279. Chu, Z. *et al.* Primed macrophages directly and specifically reject allografts. *Cell. Mol. Immunol.* **17**, 237–246 (2020).

280. Lakkis, F. G. & Li, X. C. Innate allorecognition by monocytic cells and its role in graft rejection. *Am. J. Transplant.* **18**, 289–292 (2018).
281. Atarashi, K. *et al.* Treg induction by a rationally selected mixture of Clostridia strains from the human microbiota. *Nature* **500**, 232–236 (2013).
282. Tanoue, T. *et al.* A defined commensal consortium elicits CD8 T cells and anti-cancer immunity. *Nature* **565**, 600–605 (2019).
283. Stefka, A. T. *et al.* Commensal bacteria protect against food allergen sensitization. *Proc. Natl. Acad. Sci.* **111**, 13145–13150 (2014).
284. Xie, Y. *et al.* Effect of intestinal microbiota alteration on hepatic damage in rats with acute rejection after liver transplantation. *Microb. Ecol.* **68**, 871–880 (2014).
285. Jimenez, M., Langer, R. & Traverso, G. Microbial therapeutics: New opportunities for drug delivery. *J. Exp. Med.* **216**, 1005–1009 (2019).
286. Nagler, C. R. Drugging the microbiome. *J. Exp. Med.* **217**, e20191642 (2020).
287. Aggarwal, S. *et al.* Postbiotics: From emerging concept to application. *Front. Sustain. Food Syst.* **6**, (2022).
288. Koh, A., De Vadder, F., Kovatcheva-Datchary, P. & Bäckhed, F. From Dietary Fiber to Host Physiology: Short-Chain Fatty Acids as Key Bacterial Metabolites. *Cell* **165**, 1332–1345 (2016).
289. Shapiro, H., Thaiss, C. A., Levy, M. & Elinav, E. The cross talk between microbiota and the immune system: metabolites take center stage. *Curr. Opin. Immunol.* **30**, 54–62 (2014).
290. Donohoe, D. R. *et al.* The Microbiome and Butyrate Regulate Energy Metabolism and Autophagy in the Mammalian Colon. *Cell Metab.* **13**, 517–526 (2011).
291. Arpaia, N. *et al.* Metabolites produced by commensal bacteria promote peripheral regulatory T-cell generation. *Nature* **504**, 451–455 (2013).
292. Singh, N. *et al.* Activation of Gpr109a, Receptor for Niacin and the Commensal Metabolite Butyrate, Suppresses Colonic Inflammation and Carcinogenesis. *Immunity* **40**, 128–139 (2014).
293. Chang, P. V., Hao, L., Offermanns, S. & Medzhitov, R. The microbial metabolite butyrate regulates intestinal macrophage function via histone deacetylase inhibition. *Proc. Natl. Acad. Sci.* **111**, 2247–2252 (2014).
294. Feehley, T. *et al.* Healthy infants harbor intestinal bacteria that protect against food allergy. *Nat. Med.* **25**, 448–453 (2019).
295. Cait, A. *et al.* Reduced genetic potential for butyrate fermentation in the gut microbiome of infants who develop allergic sensitization. *J. Allergy Clin. Immunol.* **144**, 1638-1647.e3 (2019).
296. Wang, W. *et al.* Increased proportions of Bifidobacterium and the Lactobacillus group and loss of butyrate-producing bacteria in inflammatory bowel disease. *J. Clin. Microbiol.* **52**, 398–406 (2014).
297. Machiels, K. *et al.* A decrease of the butyrate-producing species Roseburia hominis and Faecalibacterium prausnitzii defines dysbiosis in patients with ulcerative colitis. *Gut* **63**, 1275–1283 (2014).
298. Luceri, C. *et al.* Effect of butyrate enemas on gene expression profiles and endoscopic/histopathological scores of diverted colorectal mucosa: A randomized trial. *Dig. Liver Dis. Off. J. Ital. Soc. Gastroenterol. Ital. Assoc. Study Liver* **48**, 27–33 (2016).
299. Italiani, P. & Boraschi, D. From Monocytes to M1/M2 Macrophages: Phenotypical vs. Functional Differentiation. *Front. Immunol.* **5**, (2014).
300. Sheu, K. M. & Hoffmann, A. Functional Hallmarks of Healthy Macrophage Responses: Their Regulatory Basis and Disease Relevance. *Annu. Rev. Immunol.* **40**, 295–321 (2022).
301. Mack, M. *et al.* Expression and characterization of the chemokine receptors CCR2 and CCR5 in mice. *J. Immunol. Baltim. Md 1950* **166**, 4697–4704 (2001).
302. Tan, J. *et al.* Chapter Three - The Role of Short-Chain Fatty Acids in Health and Disease. in *Advances in Immunology* (ed. Alt, F. W.) vol. 121 91–119 (Academic Press, 2014).
303. Byndloss, M. X. *et al.* Microbiota-activated PPAR-γ signaling inhibits dysbiotic Enterobacteriaceae expansion. *Science* **357**, 570–575 (2017).

304. Freemerman, A. J. *et al.* Metabolic Reprogramming of Macrophages: GLUCOSE TRANSPORTER 1 (GLUT1)-MEDIATED GLUCOSE METABOLISM DRIVES A PROINFLAMMATORY PHENOTYPE*. *J. Biol. Chem.* **289**, 7884–7896 (2014).
305. Ji, J. *et al.* Microbial metabolite butyrate facilitates M2 macrophage polarization and function. *Sci. Rep.* **6**, 24838 (2016).
306. Goldstein, D. R., Tesar, B. M., Akira, S. & Lakkis, F. G. Critical role of the Toll-like receptor signal adaptor protein MyD88 in acute allograft rejection. *J. Clin. Invest.* **111**, 9 (2003).
307. McCallum, G. & Tropini, C. The gut microbiota and its biogeography. *Nat. Rev. Microbiol.* 1–14 (2023) doi:10.1038/s41579-023-00969-0.
308. Kaper, J. B., Nataro, J. P. & Mobley, H. L. T. Pathogenic Escherichia coli. *Nat. Rev. Microbiol.* **2**, 123–140 (2004).
309. Schlee, M. *et al.* Induction of human beta-defensin 2 by the probiotic Escherichia coli Nissle 1917 is mediated through flagellin. *Infect. Immun.* **75**, 2399–2407 (2007).
310. Ukena, S. N. *et al.* Probiotic Escherichia coli Nissle 1917 Inhibits Leaky Gut by Enhancing Mucosal Integrity. *PLoS ONE* **2**, e1308 (2007).
311. Ju, T., Kong, J. Y., Stothard, P. & Willing, B. P. Defining the role of Parasutterella, a previously uncharacterized member of the core gut microbiota. *ISME J.* **13**, 1520–1534 (2019).
312. Kreutzer, C. *et al.* Hypothalamic Inflammation in Human Obesity Is Mediated by Environmental and Genetic Factors. *Diabetes* **66**, 2407–2415 (2017).
313. Cani, P. D., Depommier, C., Derrien, M., Everard, A. & de Vos, W. M. Akkermansia muciniphila: paradigm for next-generation beneficial microorganisms. *Nat. Rev. Gastroenterol. Hepatol.* **19**, 625–637 (2022).
314. Everard, A. *et al.* Cross-talk between Akkermansia muciniphila and intestinal epithelium controls diet-induced obesity. *Proc. Natl. Acad. Sci. U. S. A.* **110**, 9066–9071 (2013).
315. Shin, N.-R. *et al.* An increase in the Akkermansia spp. population induced by metformin treatment improves glucose homeostasis in diet-induced obese mice. *Gut* **63**, 727–735 (2014).
316. Grander, C. *et al.* Recovery of ethanol-induced Akkermansia muciniphila depletion ameliorates alcoholic liver disease. *Gut* **67**, 891–901 (2018).
317. Li, J., Lin, S., Vanhoutte, P. M., Woo, C. W. & Xu, A. Akkermansia Muciniphila Protects Against Atherosclerosis by Preventing Metabolic Endotoxemia-Induced Inflammation in Apoe-/- Mice. *Circulation* **133**, 2434–2446 (2016).
318. Sandoval-Mosqueda, I. L. *et al.* Ligilactobacillus murinus Strains Isolated from Mice Intestinal Tract: Molecular Characterization and Antagonistic Activity against Food-Borne Pathogens. *Microorganisms* **11**, 942 (2023).
319. Mukohda, M. *et al.* Treatment with Ligilactobacillus murinus lowers blood pressure and intestinal permeability in spontaneously hypertensive rats. *Sci. Rep.* **13**, 15197 (2023).
320. Forster, S. C. *et al.* Identification of gut microbial species linked with disease variability in a widely used mouse model of colitis. *Nat. Microbiol.* **7**, 590–599 (2022).
321. Bang, S. *et al.* A Cardiolipin from Muribaculum intestinale Induces Antigen-Specific Cytokine Responses. *J. Am. Chem. Soc.* **145**, 23422–23426 (2023).
322. Yaeshima, T., Fujisawa, T. & Mitsuoka, T. Bifidobacterium globosum, Subjective Synonym of Bifidobacterium pseudolongum, and Description of Bifidobacterium pseudolongum subsp. pseudolongum comb. nov. and Bifidobacterium pseudolongum subsp. globosum comb. nov. *Syst. Appl. Microbiol.* **15**, 380–385 (1992).
323. Dery, K. J., Górski, A., Międzybrodzki, R., Farmer, D. G. & Kupiec-Weglinski, J. W. Therapeutic Perspectives and Mechanistic Insights of Phage Therapy in Allotransplantation. *Transplantation* **105**, 1449–1458 (2021).
324. Lee, J. R. *et al.* Butyrate-producing gut bacteria and viral infections in kidney transplant recipients: A pilot study. *Transpl. Infect. Dis.* **21**, (2019).
325. Kim, S. G. *et al.* Microbiota-derived lantibiotic restores resistance against vancomycin-resistant Enterococcus. *Nature* **572**, 665–669 (2019).

326. Woodworth, M. H. *et al.* Fecal microbiota transplantation promotes reduction of antimicrobial resistance by strain replacement. *Sci. Transl. Med.* **15**, eabo2750 (2023).
327. Xie, D. *et al.* Systematic Metabolic Profiling of Mice with Dextran Sulfate Sodium-Induced Colitis. *J. Inflamm. Res.* **14**, 2941–2953 (2021).
328. Notararigo, S. *et al.* Targeted 1H NMR metabolomics and immunological phenotyping of human fresh blood and serum samples discriminate between healthy individuals and inflammatory bowel disease patients treated with anti-TNF. *J. Mol. Med.* **99**, 1251–1264 (2021).
329. Wu, D. *et al.* Proline uptake promotes activation of lymphoid tissue inducer cells to maintain gut homeostasis. *Nat. Metab.* 1–16 (2023) doi:10.1038/s42255-023-00908-6.
330. Rinschen, M. M. *et al.* Accelerated lysine metabolism conveys kidney protection in salt-sensitive hypertension. *Nat. Commun.* **13**, 4099 (2022).
331. Ma, E. H. *et al.* Serine Is an Essential Metabolite for Effector T Cell Expansion. *Cell Metab.* **25**, 345–357 (2017).
332. Girlanda, R. *et al.* Metabolomics of Human Intestinal Transplant Rejection. *Am. J. Transplant.* **12**, S18–S26 (2012).
333. Mikkelsen, K. & Apostolopoulos, V. Vitamin B1, B2, B3, B5, and B6 and the Immune System. in *Nutrition and Immunity* (eds. Mahmoudi, M. & Rezaei, N.) 115–125 (Springer International Publishing, Cham, 2019). doi:10.1007/978-3-030-16073-9_7.
334. Wang, Z. *et al.* Mucosal-associated invariant T cells predict increased acute graft-versus-host-disease incidence in patients receiving allogeneic hematopoietic stem cell transplantation. *Cancer Cell Int.* **22**, 297 (2022).
335. St. Paul, M. *et al.* Coenzyme A fuels T cell anti-tumor immunity. *Cell Metab.* **33**, 2415-2427.e6 (2021).
336. Yuzefpolskaya, M. Gut microbiota, endotoxemia, inflammation, and oxidative stress in patients with heart failure, left ventricular assist device, and transplant. *J. Heart Lung Transplant.* **39**, 880–890 (2020).
337. Watanabe, T. *et al.* Repeated LPS Exposure Augments Alloimmune-Dependent and Airway-Targeted Chronic Lung Allograft Fibrosis in a Mouse Model. *Transplantation* **101**, S27 (2017).
338. Sakamoto, M. & Benno, Y. Reclassification of Bacteroides distasonis, Bacteroides goldsteinii and Bacteroides merdae as Parabacteroides distasonis gen. nov., comb. nov., Parabacteroides goldsteinii comb. nov. and Parabacteroides merdae comb. nov. *Int. J. Syst. Evol. Microbiol.* **56**, 1599–1605 (2006).
339. Sato, Y. *et al.* Novel bile acid biosynthetic pathways are enriched in the microbiome of centenarians. *Nature* **599**, 458–464 (2021).
340. Verdam, F. J. *et al.* Human intestinal microbiota composition is associated with local and systemic inflammation in obesity. *Obesity* **21**, E607–E615 (2013).
341. Del Chierico, F. *et al.* Gut microbiota profiling of pediatric nonalcoholic fatty liver disease and obese patients unveiled by an integrated meta-omics-based approach. *Hepatology* **65**, 451 (2017).
342. Cekanaviciute, E. *et al.* Gut bacteria from multiple sclerosis patients modulate human T cells and exacerbate symptoms in mouse models. *Proc. Natl. Acad. Sci.* **114**, 10713–10718 (2017).
343. Collins, S. L., Stine, J. G., Bisanz, J. E., Okafor, C. D. & Patterson, A. D. Bile acids and the gut microbiota: metabolic interactions and impacts on disease. *Nat. Rev. Microbiol.* **21**, 236–247 (2023).
344. Pulendran, B. *et al.* Lipopolysaccharides from Distinct Pathogens Induce Different Classes of Immune Responses In Vivo. *J. Immunol. Baltim. Md 1950* **167**, 5067–5076 (2001).
345. Ostanin, D. V. *et al.* T cell transfer model of chronic colitis: concepts, considerations, and tricks of the trade. *Am. J. Physiol. Gastrointest. Liver Physiol.* **296**, G135-146 (2009).
346. Lefferts, A. R., Norman, E., Claypool, D. J., Kantheti, U. & Kuhn, K. A. Cytokine competent gut-joint migratory T Cells contribute to inflammation in the joint. *Front. Immunol.* **13**, (2022).
347. Chen, Y. E. *et al.* Engineered skin bacteria induce antitumor T cell responses against melanoma. *Science* **380**, 203–210 (2023).

348. Pedroza-Dávila, U. *et al.* Metabolism, ATP production and biofilm generation by Staphylococcus epidermidis in either respiratory or fermentative conditions. *AMB Express* **10**, 31 (2020).
349. Møller, S. H., Wang, L. & Ho, P.-C. Metabolic programming in dendritic cells tailors immune responses and homeostasis. *Cell. Mol. Immunol.* **19**, 370–383 (2022).
350. Miller, M. L. *et al.* Distinct Graft-Specific TCR Avidity Profiles during Acute Rejection and Tolerance. *Cell Rep.* **24**, 2112–2126 (2018).
351. Canfora, E. E., Jocken, J. W. & Blaak, E. E. Short-chain fatty acids in control of body weight and insulin sensitivity. *Nat. Rev. Endocrinol.* **11**, 577–591 (2015).
352. Lynch, J. B. *et al.* Gut microbiota Turicibacter strains differentially modify bile acids and host lipids. *Nat. Commun.* **14**, 3669 (2023).
353. Bernard, K. *et al.* Characterization of isolates of *Eisenbergiella tayi*, a strictly anaerobic Gram-stain variable bacillus recovered from human clinical materials in Canada. *Anaerobe* **44**, 128–132 (2017).
354. Trompette, A. *et al.* Gut-derived short-chain fatty acids modulate skin barrier integrity by promoting keratinocyte metabolism and differentiation. *Mucosal Immunol.* **15**, 908–926 (2022).
355. Lauterbach, A. L. *et al.* Mannose-Decorated Co-Polymer Facilitates Controlled Release of Butyrate to Accelerate Chronic Wound Healing. *Adv. Healthc. Mater.* **12**, 2300515 (2023).
356. Wu, H. *et al.* Gut Microbial Metabolites Induce Donor-Specific Tolerance of Kidney Allografts through Induction of T Regulatory Cells by Short-Chain Fatty Acids. *J. Am. Soc. Nephrol.* **31**, 1445 (2020).
357. Schulthess, J. *et al.* The Short Chain Fatty Acid Butyrate Imprints an Antimicrobial Program in Macrophages. *Immunity* **50**, 432-445.e7 (2019).
358. DeBerge, M., Chaudhary, R., Schroth, S. & Thorp, E. B. Immunometabolism at the Heart of Cardiovascular Disease. *JACC Basic Transl. Sci.* **8**, 884–904 (2023).
359. Ip, W. K. E., Hoshi, N., Shouval, D. S., Snapper, S. & Medzhitov, R. Anti-inflammatory effect of IL-10 mediated by metabolic reprogramming of macrophages. *Science* **356**, 513–519 (2017).
360. Cui, H. *et al.* Long noncoding RNA Malat1 regulates differential activation of macrophages and response to lung injury. *JCI Insight* **4**, e124522.
361. Gao, Y. *et al.* LncRNA lncLy6C induced by microbiota metabolite butyrate promotes differentiation of Ly6Chigh to Ly6Cint/neg macrophages through lncLy6C/C/EBPβ/Nr4A1 axis. *Cell Discov.* **6**, 1–14 (2020).
362. Nguyen, K. T. *et al.* The MARCHF6 E3 ubiquitin ligase acts as an NADPH sensor for the regulation of ferroptosis. *Nat. Cell Biol.* **24**, 1239–1251 (2022).
363. Lan, W., Yang, L. & Tan, X. Crosstalk between ferroptosis and macrophages: potential value for targeted treatment in diseases. *Mol. Cell. Biochem.* (2023) doi:10.1007/s11010-023-04871-4.
364. Schaefer, B., Effenberger, M. & Zoller, H. Iron metabolism in transplantation. *Transpl. Int.* **27**, 1109–1117 (2014).
365. Zhou, X. *et al.* Dusp6 deficiency attenuates neutrophil-mediated cardiac damage in the acute inflammatory phase of myocardial infarction. *Nat. Commun.* **13**, 6672 (2022).
366. Meyer, K. C. The Role of Neutrophils in Transplantation. in *Immunobiology of Organ Transplantation* (eds. Wilkes, D. S. & Burlingham, W. J.) 493–507 (Springer US, Boston, MA, 2004). doi:10.1007/978-1-4419-8999-4_27.
367. Lau, A. *et al.* Dipeptidase-1 governs renal inflammation during ischemia reperfusion injury. *Sci. Adv.* **8**, eabm0142.
368. Qu, L. *et al.* Histone demethylases in the regulation of immunity and inflammation. *Cell Death Discov.* **9**, 1–15 (2023).
369. Higashijima, Y. *et al.* Coordinated demethylation of H3K9 and H3K27 is required for rapid inflammatory responses of endothelial cells. *EMBO J.* **39**, e103949 (2020).
370. Maslowski, K. M. *et al.* Regulation of inflammatory responses by gut microbiota and chemoattractant receptor GPR43. *Nature* **461**, 1282–1286 (2009).
371. Tao, R. *et al.* Deacetylase inhibition promotes the generation and function of regulatory T cells. *Nat. Med.* **13**, 1299–1307 (2007).

372. de Zoeten, E. F., Wang, L., Sai, H., Dillmann, W. H. & Hancock, W. W. Inhibition of HDAC9 increases T regulatory cell function and prevents colitis in mice. *Gastroenterology* **138**, 583–594 (2010).
373. Raqib, R. *et al.* Improved outcome in shigellosis associated with butyrate induction of an endogenous peptide antibiotic. *Proc. Natl. Acad. Sci.* **103**, 9178–9183 (2006).
374. Eshleman, E. M. *et al.* Microbiota-derived butyrate restricts tuft cell differentiation via histone deacetylase 3 to modulate intestinal type 2 immunity. *Immunity* **57**, 319-332.e6 (2024).
375. Kaiko, G. E. *et al.* The Colonic Crypt Protects Stem Cells from Microbiota-Derived Metabolites. *Cell* **167**, 1137 (2016).
376. Kopecky, B. J. *et al.* Donor Macrophages Modulate Rejection After Heart Transplantation. *Circulation* **146**, 623–638 (2022).
377. Fan, H. *et al.* Trans-vaccenic acid reprograms CD8+ T cells and anti-tumour immunity. *Nature* **623**, 1034–1043 (2023).